UQÀM

UNIVERSITÉ DU QUÉBEC À MONTRÉAL

RÉPONSES DES COMMUNAUTÉS VÉGÉTALES AU CHANGEMENT CLIMATIQUE, À L'URBANISATION ET AUX DIFFÉRENCES BIOGÉOGRAPHIQUES

THÈSE
PRÉSENTÉE COMME EXIGENCE PARTIELLE
DU DOCTORAT EN BIOLOGIE

PAR
JOHANNA ANDREA MARTINEZ VILLA

AVRIL 2024

UNIVERSITÉ DU QUÉBEC À MONTRÉAL

PLANT COMMUNITY RESPONSES TO CLIMATE CHANGE, URBANIZATION AND BIOGEOGRAPHIC DIFFERENCES

THESIS
PRESENTED AS A PARTIAL REQUIREMENT
OF THE DOCTORATE IN BIOLOGY

BY
JOHANNA ANDREA MARTINEZ VILLA

APRIL 2024

ACKNOWLEDGMENTS

I would like to express my sincere gratitude to my research director, Christian Messier, and my co-director, Sandra M. Durán, for their mentoring, guidance, and steadfast support during my Ph.D. I want to highlight the support not just in the academic rigor but also the guidance they extended for life and personal growth. They have my deepest gratitude for their patience and understanding in all the different moments of my doctoral journey. Thanks for encouragement to give the best of myself and for the holistic support that actively and sincerely helped me achieve my goals. I am very grateful to them for not only being my academic guides but also as sources of inspiration and emotional support.

I am also very grateful to the many people who helped me during this journey. The following paragraphs are intended to offer my deepest gratitude to each and every one of the people who have helped me in one way or another in the achievement of this dissertation.

Special thanks to my Master's advisor, Professor Alvaro Duque, who has always been a huge support and a guide both academically and personally. I am tremendously grateful for the opportunity to coordinate the Andean plot network "Expedición Antioquia". This project has taught me valuable lessons in my professional career and personal life and has shown me the beauty of the Andean Forest. Certainly, Professor Duque has been an inspiration and a fundamental pillar during my academic career; I will always be grateful for his support over so many years. To Pprofessor Brian Enquist and the Enquist lab, thank you for the warm hospitality during my academic internship. Professor Enquist gave me very valuable supervision for the first chapter. He is not just a great person; he is a great scientist who is always happy to teach and help. I really learned a lot from him. To Professor Kenneth Feeley, whom I have known a long time and who continued supporting me during my Ph.D, taught me a lot about plant physiology and was very supportive and motivating during the writing of my second chapter. To Paula Morales, who was my

assistant in the field and lab, and during the analytical process in the urban project. I am very happy to have met her and to now call her my friend.

To my friends and colleagues Daniel Zuleta, Sebastián González, Miguel Peña, and Sebastián Ramirez, for their time discussing research ideas with me, reviewing papers, or just giving me motivation to continue, I am very fortunate to have people like you in my life. To Rita Sousa-Silva for her support during the Ph.D. exam and Eric Sandler for his statistical advice. To my friends Ilse Esparza and Ximea Florez for being my family and adventure gang in Montreal.

I also want to thank the BESS program for their scholarship, for the immersive training experience in tropical ecology and the great and friendly environment they provided during the program. Thanks to Mitacs Globalink for their financial support and for their continued academic and personal training. To the program, Women in Science, at UQAM, thanks for motivating, encouraging, and visualizing women in STEM. Thanks to the Botanical Garden of Montreal for the collaborative effort measuring tree physiology within the installations. To all the staff from CEF and UQAM thank you for the administrative support at the university.

Last but not least, thanks to my mom for always encouraging me to be strong and perseverant. To my husband Jhon, who was always there to encourage me and motivate me in the most difficult moments of my Ph.D, thanks for being with me in the good and bad moments and for coming with me on this adventure in Canada. I am so lucky to have meet you in a world with 8.000 billions of people.

DEDICATION

To my husband Jhon and my beautiful daughter Juana
To my mom

In memory of
My father Juan Martínez, who taught me the most important lesson of my life.
My brother Felipe Martínez, who is always in my mind and my heart.
My grandfather Alfonso Villa, who is my model of life always.

SUMMARY

Forest diversity and function can be influenced by environmental variations driven by natural factors, such as environmental gradients, as well as environmental variations created by human activities, including climate change and urbanization, and their interactions. Understanding the ecological mechanisms behind these natural factors is crucial, as they illuminate the extent to which tree communities and species adapt to environmental shifts. Conversely, human-induced factors are disrupting and altering the natural balance, with the precise effects of these anthropogenic forces on forest diversity and function remaining largely uncharted. Given the importance of both natural and anthropogenic environmental variation on forest diversity and functioning, my research investigated how diversity patterns and the ecological mechanisms behind species variation change along an elevational gradient (Andean forest) (**Chapter I**) and across contrasting biogeographic areas (Andes and Amazon) (**Chapter II**). Furthermore, I examined the impact of climate change on Andean Forest functional composition (**Chapter III**) and investigated the influence of increased urban temperatures on tree physiology in Montreal trees (**Chapter IV**).

Through my research, I analyzed the natural factors driving species variation and found that ecological mechanisms exert a stronger influence at higher elevations within Andean gradients. As elevation increases, environmental filtering becomes more important in shaping species composition. However, my comparative study of lowland (Amazon) and highland (Andes) forests revealed that the pronounced impact of ecological mechanisms on species variation is not solely attributable to environmental filtering. In the species-rich lowland forests, intense niche partitioning occurs to mitigate competition. Therefore, in these lowland ecosystems, the ecological mechanisms fostering species variation are more tied to competition avoidance rather than niche specialization. This highlights the roles of ecological mechanisms in different environmental contexts, shaping biodiversity across various ecosystems.

Regarding environmental variation created by anthropogenic activities, climate change significantly impacts the functional composition of Andean forests, primarily due to increases in temperature and vapor pressure deficit, especially at higher elevations. These environmental shifts prompt forest communities to adapt by favoring the recruitment and abundance of species equipped with traits resilient to the new conditions. Consequently, there is a notable trend towards species with more conservative traits at various elevations within the Andean forest. This change in functional composition could directly influence ecosystem services, such as carbon sequestration. In the last chapter, I found that temperature is also a crucial factor affecting the functioning of urban trees. Elevated urban temperatures (urban heat island effect -UHI-) diminish the capacity for carbon capture through photosynthesis in some tree species that are particularly susceptible to heat and lack the ability to acclimate to increased temperatures. However, some species demonstrate high plasticity by adjusting key morphological leaf traits, which aids in increasing transpiration and stomatal conductance. Nevertheless, the morphological and physiological changes did not result in complete acclimation. Therefore, the impact of the urban heat island effect is highly dependent on the species, underscoring the importance of assessing tree species' vulnerability to heat in urban planning to preserve ecosystem services.

This work has major implications for natural and urban forest management and conservation, as it provides crucial information to guide more effective management in the long term and ensure ecosystem services.

Key words: Climate change, Urban Heat Island, functional composition, species variation, elevated temperature, tree functioning.

RÉSUMÉ

La diversité et la fonction des forêts peuvent être influencées par des variations environnementales induites par des facteurs naturels, tels que les gradients environnementaux, ainsi que par des variations environnementales créées par les activités humaines, y compris le changement climatique et l'urbanisation, et leurs interactions. Comprendre les mécanismes écologiques derrière ces facteurs naturels est crucial, car ils éclairent dans quelle mesure les communautés d'arbres et les espèces s'adaptent aux changements environnementaux. En revanche, les facteurs d'origine humaine perturbent et modifient l'équilibre naturel, les effets précis de ces forces anthropiques sur la diversité et la fonction des forêts restant largement inexplorés. Compte tenu de l'importance des variations environnementales naturelles et anthropiques sur la diversité et le fonctionnement des forêts, mes recherches ont examiné comment les modèles de diversité et les mécanismes écologiques derrière la variation des espèces changent le long d'un gradient altitudinal (forêt andine) (Chapitre I) et à travers des zones biogéographiques contrastées (Andes et Amazonie) (Chapitre II). De plus, j'ai examiné l'impact du changement climatique sur la composition fonctionnelle de la forêt andine (Chapitre III) et étudié l'influence des températures urbaines élevées sur la physiologie des arbres à Montréal (Chapitre IV).

À travers mes recherches, j'ai analysé les facteurs naturels qui influent sur la variation des espèces et j'ai constaté que les mécanismes écologiques exercent une influence plus forte à des altitudes plus élevées dans les gradients andins. À mesure que l'altitude augmente, le filtrage environnemental devient plus important dans la formation de la composition des espèces. Cependant, mon étude comparative des forêts de basse altitude (Amazonie) et de haute altitude (Andes) a révélé que l'impact prononcé des mécanismes écologiques sur la variation des espèces n'est pas uniquement attribuable au filtrage environnemental. Dans les forêts riches en espèces de basse altitude, un partitionnement des niches intense se produit pour atténuer la concurrence. Par conséquent, dans ces écosystèmes de basse altitude, les mécanismes écologiques favorisant la variation des espèces sont davantage liés à

l'évitement de la compétition qu'à la spécialisation des niches. Cela met en évidence les rôles des mécanismes écologiques dans différents contextes environnementaux, façonnant la biodiversité à travers divers écosystèmes.

En ce qui concerne les variations environnementales créées par les activités anthropiques, le changement climatique impacte significativement la composition fonctionnelle des forêts andines, principalement en raison de l'augmentation des températures et du déficit de pression de vapeur, surtout à des altitudes plus élevées. Ces changements environnementaux incitent les communautés forestières à s'adapter en favorisant le recrutement et l'abondance d'espèces dotées de traits résilients aux nouvelles conditions. Par conséquent, on observe une tendance notable vers des espèces avec des traits plus conservateurs à différentes altitudes dans la forêt andine. Ce changement dans la composition fonctionnelle pourrait influencer directement les services écosystémiques, tels que la séquestration du carbone. Dans le dernier chapitre, j'ai constaté que la température est également un facteur crucial affectant le fonctionnement des arbres urbains. Les températures urbaines élevées (effet d'îlot de chaleur urbain -ICU-) réduisent la capacité de capture du carbone par la photosynthèse dans certaines espèces d'arbres particulièrement sensibles à la chaleur et incapables de s'acclimater aux températures élevées. Cependant, certaines espèces montrent une grande plasticité en ajustant des traits morphologiques clés des feuilles, ce qui aide à augmenter la transpiration et la conductance stomatique. Néanmoins, les changements morphologiques et physiologiques n'ont pas abouti à une acclimatation complète. Par conséquent, l'impact de l'effet d'îlot de chaleur urbain dépend fortement de l'espèce, soulignant l'importance d'évaluer la vulnérabilité des espèces d'arbres à la chaleur dans la planification urbaine pour préserver les services écosystémiques.

Ce travail a des implications majeures pour la gestion et la conservation des forêts naturelles et urbaines, car il fournit des informations cruciales pour orienter une gestion plus efficace à long terme et garantir les services écosystémiques.

Mots-clés: Changement climatique, Îlot de Chaleur Urbain, composition fonctionnelle, variation des espèces, température élevée, fonctionnement des arbres.

Preface

The findings from this research are the result of collaborative work, thus it contains journal articles co-authored by researchers from other universities than Universite du Quebec a Montreal:

Chapter I of this thesis has been published as Martínez-Villa, J. A., González-Caro, S., & Duque, A. (2020). The importance of grain and cut-off size in shaping tree beta diversity along an elevational gradient in the northwest of Colombia. *Forest Ecosystems*, *7*(1), 1-12.

Chapter II will be submitted for publication as Martínez-Villa, J. A., González-Caro, S., Messier C., Durán S.M & Duque, A.

Chapter III of this thesis has been published as Martínez-Villa, J. A., Durán, S. M., Enquist, B. J., Duque, A., Messier, C., & Paquette, A. (2023). Temporal shifts in the functional composition of Andean forests at different elevations are driven by climate change. *Global Ecology and Biogeography*, *33*(1), 85-99.

Chapter IV of this thesis has been published as Martínez-Villa, J. A., Paquette, A., Feeley, K.J., Morales-Morales, P.A., Messier, C & Durán, S. M (2024). Changes in morphological and physiological traits of urban trees in response to elevated temperatures within an Urban Heat Island. *Tree Physiology*, tpae145, *https://doi.org/10.1093/treephys/tpae145*

TABLE OF CONTENT

LIST OF FIGURES

CHAPTER I

CHAPTER II

CHAPTER III

CHAPTER IV

LIST OF TABLES

CHAPTER I

CHAPTER II

CHAPTER III

CHAPTER IV

LIST OF APPENDICES

INTRODUCTION

Understanding the drivers of forest diversity and functioning has long been a central pursuit in ecology (Zhang et al., 2014). Environmental variation, whether produced by natural factors such as **environmental gradients** and **biogeographic differences** or by anthropogenic factors such as **climate change** and **urbanization,** are the main drivers of diversity and functional changes in forests (Faulkner & Gov, 2004; Fine, 2015; Martínez-Villa et al., 2024; Melliger et al., 2018; Mitchell & Devisscher, 2022; Morin et al., 2018; Rahbek, 1995). On the one hand, natural changes associated with environmental gradients and biogeographic differences have been recognized as fundamental drivers of plant diversity, abundance, distribution, and functioning (Fine, 2015, Rahbek, 1995). On the other hand, anthropogenic changes are creating unprecedented pressures on forests, potentially precipitating profound transformations in terrestrial ecosystems as we know them (Nolan et al., 2018). Currently, the study of how environmental variation affects forest diversity and functioning is garnering even more attention since i) this topic is crucial for understanding how plants respond to natural environmental variation and how ecological assemblages change as a function of the environment, and ii) there is a growing evidence of forest directional shifts associated with human-induced environmental variation (e.g., **climate change and urbanization**) (Lewis et al., 2009). This topic is critical for anticipating how forest will react to environmental changes in the future.

Natural filters that shape forest diversity and composition.

Diversity across environmental gradients and Biogeographic differences

Since 1805, after the "*Essay on the Geography of Plants*" written by Alexander Von Humboldt and Aimé Bompland, scientists and nature lovers have been fascinated by how plants respond to environmental gradients. Elevational gradients have been recognized as one of the main gradients in biogeography since they have the particularity to have large environmental variation in short distances, making them the perfect natural laboratory to study plant responses to environmental changes (Sanders & Rahbek, 2012). Thus, changes

in different factors such as soils, topography, and VPD, but mainly temperature, determine forest diversity, structure, dynamics, and functioning (Barkhordarian et al., 2019; Pabón-Caicedo et al., 2020). The correlation between these primary environmental variables and elevation has helped use elevation as a surrogate to test hypotheses in community ecology directly (Gómez-Diaz et al., 2023). In the tropics, due to the steep mountains such as the Andes, the biogeographic differences created by elevation and the exuberant diversity have made the study of responses of tree communities to environmental changes a cornerstone in tropical ecology.

Elevational gradients of diversity are dependent on a combination of historical, geographic, biotic, abiotic, and stochastic forces shaping species distribution and community structure, forces known as ecological mechanisms (Laiolo et al., 2018). Understanding the relative importance of ecological mechanisms, such as deterministic and stochastic processes, in shaping community assembly at different elevations is crucial for effective conservation (Tello et al., 2015). β-diversity, a metric commonly used to assess species variation, provides mechanistic insights into the ecological forces driving species turnover along environmental gradients (Legendre 2014). Traditionally, β-diversity analysis has focused on environmental gradients, such as elevation and biogeographical differences (Lomolino, 2001; Rahbek, 1995; Sanders & Rahbek, 2012; Dick & Heuertz, 2008; Droissart et al., 2018). These studies have elucidated the drivers of species variability, trait divergence, and the strength of local community assembly mechanisms (Martínez-Villa et al., 2020; Mori et al., 2013). Research conducted along elevational gradients consistently indicates a decline in species richness and β-diversity with increasing elevation (Martínez-Villa et al., 2020; Mori et al., 2013). Furthermore, environmental filtering mechanisms become more pronounced in these challenging conditions, shaping community composition (Tello et al., 2015).

Species diversity and their variation (β-diversity) are closely related to the scale because detecting patterns and identifying ecological mechanisms critically depend on it (Levin et al. 1992). The concept of scale has long been acknowledged as pivotal in ecology, given that ecological processes operate across diverse spatial scales, each likely producing

distinct patterns (Levin, 1992). Studying a system at an inappropriate scale can lead to a misinterpretation of its actual dynamics, as patterns observed may merely be artifacts of the chosen scale (Wiens, 1989). The study of scale is gaining attention due to the erosion of diversity at different scales. It has been considered a problem in the modern era, and conservation research, including scale, is paramount to define adequate conservation plants. Similarly, the size of sampled individuals and the species pool can impact results related to diversity and composition, depending on whether they include a broader or narrower range of species (Lessard et al., 2012). It is also probable that different ecological mechanisms influence small and large trees, resulting in distinct diversity patterns. Therefore, the effects of spatial scale and tree size should be carefully considered to enhance precision in ecological studies.

Anthropogenic filters influencing forest diversity, composition, and tree function.

Climate change, forest functional composition and structure

Climate has always shaped the world's forests (Bhatti et al., 2006), but human activities have significantly impacted Earth's climate since the late 1800s, altering mean climatic patterns (Salinger 2005). Global warming, the increase in global mean temperature, is one of the main characteristics of climate change. Forecasting scenarios, including those from the Intergovernmental Panel on Climate Change (IPCC, 2022), predict an average temperature increase of 1.5 to 5.8 $°C$ by the mid-21st century. Although global warming is one of the most important and broadly studied models, climate change also involves global changes in precipitation, vapor pressure deficit (VPD), and cloud cover, among other important variables for forest composition and functioning (Barkhordarian et al., 2019; Pabón-Caicedo et al., 2020). Consequently, shifts in the climatic variables to which plants have adapted may trigger profound transformations in plant ecosystems as we currently understand them (Turner et al., 2020). Studies have reported changes in species distribution ranges (Chen et al., 2011; Duque et al., 2015; Feeley et al., 2011, 2012; Santini et al., 2021), species diversity (Esquivel-Muelbert et al., 2019), carbon storage (Duque et

al., 2021; Sullivan et al., 2020), and forest dynamics (Peña et al., 2018) due to climate change. However, many questions remain regarding how forests will respond to long-term climate change, particularly in less studied aspects such as functional structure and composition and in less studied forests such as hyper-diverse tropical forests.

Although climate change has widespread global impacts, species responses are not uniform (Fadrique et al., 2018). The way plants react to climate change depends on their vulnerability and sensitivity, influenced by their physiological limits and ranges, functional traits, evolutionary adaptations to climate, and the extent of regional climate change (Ahrens et al., 2020; Andrew et al., 2022; Crous, 2019). In tropical elevational gradients, for example, studies have reported an upward migration of dominant genera at a specific rate, primarily in heat-tolerant genera (Feeley et al., 2011). Consequently, shifts in species abundance and distribution are reorganizing terrestrial ecosystems, thereby altering their functional composition (Duque et al., 2015). In this context, important questions arise, such as whether climate change is driving broad changes in the functional composition of local communities along large elevational gradients. If so, what are the key factors determining the direction and magnitude of these changes?

This question is challenging, partly due to the complexity of collecting trait data and long-term demographic information in species-rich forests. With the recognized impact of climate change on forest species composition, the next step is to discern shifts in functional composition and their consequences for forest functionality (Aguirre-Gutiérrez et al., 2022). While studies have observed changes in species composition changes and upward migrations along elevational gradients (Feeley et al., 2011), suggesting a potential shift towards species with acquisitive strategies at higher elevations, empirical data to support this hypothesis is lacking. Conversely, research in dry and lowland Amazon forests indicates that climate change—marked by rising temperatures and droughts—is prompting a shift towards more conservative, drought-tolerant species (Enquist & Enquist, 2011; Esquivel-Muelbert et al., 2019). However, the lack of information on the impact of climate change on functional composition at different elevations is a critical gap that must be

addressed to conserve mountain forests and safeguard their ecosystem services for future generations.

Urbanization, Urban Heat Islands (UHI), and the effect on tree functioning.

In parallel with climate change, urbanization is expanding at a rapid pace, creating unique environments and posing challenges for urban forests (Lüttge & Buckeridge, 2023). One of the main characteristics of urban areas is the temperature variation, commonly increasing from natural and rural areas to the most urbanized city core (Mclean et al., 2005). This pattern, known as urban heat island (UHI), is one of the most important selective pressures for urban trees (Mclean et al., 2005; Wang et al., 2016). Since the environmental conditions created and modified by humans are significantly different from the conditions required by trees in nature, it may alter tree functioning (Lüttge & Buckeridge, 2023). For example, due to the combination of climate change and urbanization, temperatures reached within UHI can exacerbate thermal stress and can even exceed the natural physiological limits of tree species (Esperon-Rodriguez et al., 2021; Hara et al., 2021). If this occurs, important services and functions that trees provide to the human population can be diminished by the stress responses of urban forests to extreme environmental conditions. Due to harsh urban environments, studies have reported decreases in carbon storage (Meineke et al., 2016) and in photosynthetic rates (Hara et al., 2021), and changes in thermal tolerances (Hara et al., 2021; Wang et al., 2016) and functional traits (Esperon-Rodriguez et al., 2020; Zhu et al., 2020). Cities are becoming the main places where people live worldwide. Therefore, to understand and mitigate the effects of UHI and urbanization, we must first understand the effects of environmental variation created by cities on tree functioning and thereby increase our potential to manage urban forests.

The intense heat associated with UHI can significantly impair tree functions. Trees react to heat stress through mechanisms such as crown defoliation, early wilting, shedding of branches, and ultimately lowered resistance to pests (Haase & Hellwig, 2022). These symptoms typically manifest only after substantial internal damage from the heat. Initially, heat affects critical physiological processes, such as photosynthesis, transpiration, and

stomatal conductance, leading to reduced chlorophyll variability and inhibited photosystem II (PSII) functionality (Allakhverdiev et al., 2008; Percival, 2023). Additionally, metabolic processes such as electron transport and the activation of rubisco are reduced, and heat can deactivate enzymes crucial for photosynthesis and respiration, among other effects (Scafaro et al., 2023). These heat-induced responses can culminate in stunted or halted growth, diminished carbon sequestration, and a reduced cooling effect, which in turn lessens the ecological benefits that plants provide in urban settings (Meineke et al., 2016).

Comprehending the physiological thresholds of urban tree species is crucial for integrating future climate variability into urban planning. Recent research indicates that a significant portion of urban tree species are already enduring conditions that exceed their physiological tolerances. For example, Esperon-Rodriguez et al (2022) found that about 15% of these species are subjected to maximum temperatures beyond what they are evolutionarily accustomed to. The IPCC forecasts that cities near the equator will face substantial reductions in rainfall, whereas cities in temperate zones will encounter the most pronounced temperature rises. By coupling these climate projections with data on species' vulnerabilities, we can gain critical insights essential for enhancing ecosystem services. The sustainability of urban trees and the array of benefits they furnish hinge on the selection and cultivation of species with the highest resilience to climate change.

Understanding the influences of natural environmental variation (such as temperature, topography, soils) and the human-induced environmental variation (including climate change, urbanization, and the urban heat island effect) on tree community structure and function is critical for devising effective conservation strategies and managing both natural and urban forests. By adopting this integrative approach, we can more accurately forecast the repercussions of environmental shifts, devise robust forest conservation initiatives, and bolster biodiversity and ecosystem services across various landscapes amidst the challenges of global environmental changes.

Thesis overview

The central objective of my dissertation is to examine the influence of environmental variations, both those occurring naturally and those resulting from anthropogenic activities, on the diversity of tree species, their functional traits composition, and tree functioning. In pursuit of this. In pursuit of this, i) I have explored the impacts of climate change on functional composition of Andean Forest over time along an elevational gradient. ii) I analyzed how species composition variation changes along an Andean altitudinal gradient and across scales, iii) I investigated the effect of biogeographic differences and scale on species composition variation. Additionally, I examined which ecological mechanisms play a predominant role in each region and how sampling methods affect these diversity outcomes. Finally iv) I investigated the effect of Urban Heat Islands (UHI) on the functioning of urban trees, specifically the effect of heat on photosynthetic performance of tree species. From these objectives, the following chapters have been delineated.

Chapter I. *The importance of grain and cut-off size in shaping tree diversity along an elevational gradient in the northwest of Colombia.* The goal of this chapter was to assess the main drivers of tree β-diversity at local scales in a hyper-diverse forest, as well as how the sampling effect alters β-diversity estimations. For running the analysis, I used data from 15 1-ha permanent plots spread out along a 3000 m elevational gradient. I used standardized β-deviation to assess the extent to which either sampling effects or the community assembly mechanisms determine the changes in species composition at local scales.

Chapter II*. Sampling dependence of local β-diversity in two Neotropical forests located at contrasting elevations.* Using two 25-hectare permanent plots in biogeographically contrasting regions (Amazon and Andes), we compared how tree species variation differs between these areas and identified the ecological mechanisms at work in each. Similar to Chapter 4, we also investigated how sampling effects influence diversity outcomes in these two regions that are critical to ecological research.

Chapter III. *Temporal shifts in the functional composition of Andean forests at different elevations are driven by climate change.* In this chapter, I evaluated the impact of climate change on the functional composition of the Andean Forest, focusing on variations along an elevational gradient over time. I have integrated data pertaining to climate change,

functional characteristics, and forest dynamics collected across a decade. The objective was to determine how fluctuations in minimum, maximum, and average temperatures, precipitation, and vapor pressure deficit (VPD) influence the suite of traits within Andean communities. To carry out this project, I measured for two years leaf traits on 1,200 tree species on nine 1-ha permanent plots.

Chapter IV*. Thermal tolerance and photosynthetic responses of urban trees to Urban Heat Island in a temperate city.* Utilizing temperature data from urban areas and physiological performance metrics of key urban tree species from Montreal's forest inventory, I investigated how Urban Heat Island (UHI) temperatures impact tree photosynthesis and thermal tolerance. These findings also have implications for the ecosystem services that urban plants provide to city dwellers. The results of this research were also shared with the municipality of Montreal to inform and enhance urban planning strategies.

Synthesis

REFERENCES

Aguirre-Gutiérrez, J., Berenguer, E., Menor, I. O., Bauman, D., Corral-Rivas, J. J., Nava-Miranda, M. G., Both, S., Ndong, J. E., Ondo, E., N'ssi Bengone, N., Shenkin, A., Riutta, T., Girardin, C. A. J., Moore, S., Abernethy, K., Asner, G. P., Bentley, L. P., Burslem, D. F. R. P., Cernusak, L. A., … Malhi, Y. (2022). Functional susceptibility of tropical forests to climate change. Nature Ecology & Evolution, 6(7), 878–889. https://doi.org/10.1038/s41559-022-01747-6

Ahrens, C. W., Andrew, M. E., Mazanec, R. A., Ruthrof, K. X., Challis, A., Hardy, G., Byrne, M., Tissue, D. T., & Rymer, P. D. (2020). Plant functional traits differ in adaptability and are predicted to be differentially affected by climate change. *Ecology and Evolution*, *10*(1), 232–248. https://doi.org/10.1002/ece3.5890

Allakhverdiev, S. I., Kreslavski, V. D., Klimov, V. V., Los, D. A., Carpentier, R., & Mohanty, P. (2008). Heat stress: An overview of molecular responses in photosynthesis. In *Photosynthesis Research* (Vol. 98, Issues 1–3, pp. 541–550). https://doi.org/10.1007/s11120-008-9331-0

Andrew, S. C., Gallagher, R. V., Wright, I. J., & Mokany, K. (2022). Assessing the vulnerability of plant functional trait strategies to climate change. *Global Ecology and Biogeography*, *31*(6), 1194–1206. https://doi.org/10.1111/geb.13501

Barkhordarian, A., Saatchi, S. S., Behrangi, A., Loikith, P. C., & Mechoso, C. R. (2019). A Recent Systematic increase in Vapor Pressure Deficit over Tropical South America. *Scientific Reports*, *9*(15331), 1–12. https://doi.org/10.1038/s41598-019-51857-8

Bhatti J.S, Lal R, Apps M.J, Price M.A, (2006). Climate Change and Managed Ecosystems. Boca Raton, FL, USA: CRC Press.

Chen, I. C., Hill, J. K., Ohlemüller, R., Roy, D. B., & Thomas, C. D. (2011). Rapid range shifts of species associated with high levels of climate warming. *Science*, *333*(6045), 1024–1026. https://doi.org/10.1126/science.1206432

Crous, K. Y. (2019). Plant responses to climate warming: physiological adjustments and implications for plant functioning in a future, warmer world. In *American Journal of Botany*. Wiley-Blackwell. https://doi.org/10.1002/ajb2.1329

Dick, C. W., & Heuertz, M. (2008). The complex biogeographic history of a widespread tropical tree species. *Evolution*, *62*(11), 2760–2774. https://doi.org/10.1111/j.1558-5646.2008.00506.x

Droissart, V., Dauby, G., Hardy, O. J., Deblauwe, V., Harris, D. J., Janssens, S., Mackinder, B. A., Blach-Overgaard, A., Sonké, B., Sosef, M. S. M., Stévart, T., Svenning, J. C., Wieringa, J. J., & Couvreur, T. L. P. (2018). Beyond trees: Biogeographical regionalization of tropical Africa. *Journal of Biogeography*, *45*(5), 1153–1167. https://doi.org/10.1111/jbi.13190

Duque, A., Peña, M. A., Cuesta, F., González-Caro, S., Kennedy, P., Phillips, O. L., Calderón-Loor, M., Blundo, C., Carilla, J., Cayola, L., Farfán-Ríos, W., Fuentes, A., Grau, R., Homeier, J., Loza-Rivera, M. I., Malhi, Y., Malizia, A., Malizia, L., Martínez-Villa, J. A., … Feeley, K. J. (2021). Mature Andean forests as globally important carbon sinks and future carbon refuges. *Nature Communications*, *12*(1), 1–5. https://doi.org/10.1038/s41467-021-22459-8

Duque, A., Stevenson, P. R., & Feeley, K. J. (2015). Thermophilization of adult and juvenile tree communities in the northern tropical Andes. *Proceedings of the National Academy of Sciences of the United States of America*, *112*(34), 10744–10749. https://doi.org/10.1073/pnas.1506570112

Enquist, B. J., & Enquist, C. A. F. (2011). Long-term change within a Neotropical forest: Assessing differential functional and floristic responses to disturbance and drought. *Global Change Biology*, *17*(3), 1408–1424. https://doi.org/10.1111/j.1365-2486.2010.02326.x

Esperon-Rodriguez, M., Tjoelker, M. G., Lenoir, J., Baumgartner, J. B., Beaumont, L. J., Nipperess, D. A., ... & Gallagher, R. V. (2022). Climate change increases global risk to urban forests. *Nature Climate Change*, *12*(10), 950-955.

Esperon-Rodriguez, M., Power, S. A., Tjoelker, M. G., Marchin, R. M., & Rymer, P. D. (2021). Contrasting heat tolerance of urban trees to extreme temperatures during heatwaves. *Urban Forestry and Urban Greening*, *66*. https://doi.org/10.1016/j.ufug.2021.127387

Esperon-Rodriguez, M., Rymer, P. D., Power, S. A., Challis, A., Marchin, R. M., & Tjoelker, M. G. (2020). Functional adaptations and trait plasticity of urban trees along a climatic gradient. *Urban Forestry and Urban Greening*, *54*. https://doi.org/10.1016/j.ufug.2020.126771

Esquivel-Muelbert, A., Baker, T. R., Dexter, K. G., Lewis, S. L., Brienen, R. J. W., Feldpausch, T. R., Lloyd, J., Monteagudo-Mendoza, A., Arroyo, L., Álvarez-Dávila, E., Higuchi, N., Marimon, B. S., Marimon-Junior, B. H., Silveira, M., Vilanova, E., Gloor, E., Malhi, Y., Chave, J., Barlow, J., … Phillips, O. L. (2019). Compositional response of Amazon forests to climate change. *Global Change Biology*, *25*(1), 39–56. https://doi.org/10.1111/gcb.14413

Fadrique, B., Báez, S., Duque, Á., Malizia, A., Blundo, C., Carilla, J., Osinaga-Acosta, O., Malizia, L., Silman, M., Farfán-Ríos, W., Malhi, Y., Young, K. R., Cuesta C, F., Homeier, J., Peralvo, M., Pinto, E., Jadan, O., Aguirre, N., Aguirre, Z., & Feeley, K. J. (2018). Widespread but heterogeneous responses of Andean forests to climate change. *Nature*, *564*(7735), 207–212. https://doi.org/10.1038/s41586-018-0715-9

Faulkner, S., & Gov, S. (2004). *Urbanization impacts on the structure and function of forested wetlands* (Vol. 7).

Feeley, K. J., Rehm, E. M., & Machovina, B. (2012). The responses of tropical forest species to global climate change: acclimate , adapt , migrate or go extinct? *Frontiers of Biology*, *4*, 69–84. https://doi.org/10.21425/F5FBG12621

Feeley, K. J., Silman, M. R., Bush, M. B., Farfan, W., Cabrera, K. G., Malhi, Y., Meir, P., Revilla, N. S., Quisiyupanqui, M. N. R., & Saatchi, S. (2011). Upslope migration of Andean trees. *Journal of Biogeography*, *38*(4), 783–791. https://doi.org/10.1111/j.1365-2699.2010.02444.x

Fine, P. V. A. (2015). Ecological and Evolutionary Drivers of Geographic Variation in Species Diversity. *Annual Review of Ecology, Evolution, and Systematics*, *46*, 369–392. https://doi.org/10.1146/annurev-ecolsys-112414-054102

Gómez-Díaz, J. A., Carvajal-Hernández, C. I., Bautista-Bello, A. P., Monge-González, M. L., Guzmán-Jacob, V., Kreft, H., ... & Villalobos, F. (2023). Humboldt's legacy: explaining the influence of environmental factors on the taxonomic and phylogenetic diversity of angiosperms along a Neotropical elevational gradient. AoB Plants, 15(1), plac056.

Haase, D., & Hellwig, R. (2022). Effects of heat and drought stress on the health status of six urban street tree species in Leipzig, Germany. *Trees, Forests and People*, *8*. https://doi.org/10.1016/j.tfp.2022.100252

Hara, C., Inoue, S., Ishii, H. R., Okabe, M., Nakagaki, M., & Kobayashi, H. (2021). Tolerance and acclimation of photosynthesis of nine urban tree species to warmer growing conditions. *Trees*. https://doi.org/10.1007/s00468-021-02119-6

IPCC, Pörtner, Hans-Otto, et al., (2022) Summary for policymakers. 3-33.

Laiolo, P., Pato, J., & Obeso, J. R. (2018). Ecological and evolutionary drivers of the elevational gradient of diversity. Ecology letters, 21(7), 1022-1032

Legendre, P. (2014). Interpreting the replacement and richness difference components of beta diversity. Global Ecology and Biogeography, 23(11), 1324-1334.

Lessard, J. P., Belmaker, J., Myers, J. A., Chase, J. M., & Rahbek, C. (2012). Inferring local ecological processes amid species pool influences. *Trends in Ecology and Evolution*, *27*(11), 600–607. https://doi.org/10.1016/j.tree.2012.07.006

Levin, S. A. (1992). The problem of pattern and scale in ecology. *Ecology*, *73*(6), 1943–1967. https://doi.org/10.2307/1941447

Lewis, S. L., Lloyd, J., Sitch, S., Mitchard, E. T. A., & Laurance, W. F. (2009). Changing ecology of tropical forests: Evidence and drivers. *Annual Review of Ecology, Evolution, and Systematics*, *40*, 529–549. https://doi.org/10.1146/annurev.ecolsys.39.110707.173345

Lomolino, M. (2001). Elevation gradients of species-density : historical and prospective views. *Global Ecology and Biogeography*, *10*(1), 3–13. https://doi.org/10.1046/j.1466-822x.2001.00229.x

Lüttge, U., & Buckeridge, M. (2023). Trees: structure and function and the challenges of urbanization. In *Trees - Structure and Function* (Vol. 37, Issue 1, pp. 9–16). Springer Science and Business Media Deutschland GmbH. https://doi.org/10.1007/s00468-020-01964-1

Martínez-Villa, J. A., Durán, S. M., Enquist, B. J., Duque, A., Messier, C., & Paquette, A. (2024). Temporal shifts in the functional composition of Andean forests at different elevations are driven by climate change. *Global Ecology and Biogeography*, *33*(1), 85–99. https://doi.org/10.1111/geb.13774

Martínez-Villa, J. A., González-Caro, S., & Duque, Á. (2020). The importance of grain and cut-off size in shaping tree beta diversity along an elevational gradient in the northwest of Colombia. *Forest Ecosystems*, *7*(1). https://doi.org/10.1186/s40663-020-0214-y

Mclean, M. A., Jr, M. J. A., & Williams, K. S. (2005). If you can ' t stand the heat , stay out of the city : Thermal reaction norms of chitinolytic fungi in an urban heat island. *Journal of Thermal Biology*, *30*, 384–391. https://doi.org/10.1016/j.jtherbio.2005.03.002

Meineke, E., Youngsteadt, E., Dunn, R. R., & Frank, S. D. (2016). Urban warming reduces aboveground carbon storage. *Proceedings of the Royal Society B: Biological Sciences*, *283*(1840). https://doi.org/10.1098/rspb.2016.1574

Melliger, R. L., Braschler, B., Rusterholz, H. P., & Baur, B. (2018). Diverse effects of degree of urbanisation and forest size on species richness and functional diversity of plants, and ground surface-active ants and spiders. *PLoS ONE*, *13*(6). https://doi.org/10.1371/journal.pone.0199245

Mitchell, M. G. E., & Devisscher, T. (2022). Strong relationships between urbanization, landscape structure, and ecosystem service multifunctionality in urban forest fragments. *Landscape and Urban Planning*, *228*. https://doi.org/10.1016/j.landurbplan.2022.104548

Mori, A. S., Shiono, T., Koide, D., Kitagawa, R., Ota, A. T., & Mizumachi, E. (2013). Community assembly processes shape an altitudinal gradient of forest biodiversity. *Global Ecology and Biogeography*, *22*(7), 878–888. https://doi.org/10.1111/geb.12058

Morin, X., Fahse, L., Jactel, H., Scherer-Lorenzen, M., García-Valdés, R., & Bugmann, H. (2018). Long-term response of forest productivity to climate change is mostly driven by change in tree species composition. *Scientific Reports*, *8*(1). https://doi.org/10.1038/s41598-018-23763-y

Nolan, C., Overpeck, J. T., Allen, J. R. M., Anderson, P. M., Betancourt, J. L., Binney, H. A., Brewer, S., Bush, M. B., Chase, B. M., Cheddadi, R., Djamali, M., Dodson, J., Edwards, M. E., Gosling, W. D., Haberle, S., Hotchkiss, S. C., Huntley, B., Ivory, S. J., Kershaw, A. P., … Jackson, S. T. (2018). *Past and future global transformation of terrestrial ecosystems under climate change*. https://www.science.org

Pabón-Caicedo, J. D., Arias, P. A., Carril, A. F., Espinoza, J. C., Borrel, L. F., Goubanova, K., Lavado-Casimiro, W., Masiokas, M., Solman, S., & Villalba, R. (2020). Observed and Projected Hydroclimate Changes in the Andes. In *Frontiers in Earth Science* (Vol. 8). Frontiers Media S.A. https://doi.org/10.3389/feart.2020.00061

Peña, M. A., Feeley, K. J., & Duque, A. (2018). Effects of endogenous and exogenous processes on aboveground biomass stocks and dynamics in Andean forests. *Plant Ecology*, *219*(12), 1481–1492. https://doi.org/10.1007/s11258-018-0895-2

Percival, G. C. (2023). Heat tolerance of urban trees − A review. In *Urban Forestry and Urban Greening* (Vol. 86). Elsevier GmbH. https://doi.org/10.1016/j.ufug.2023.128021

Rahbek, C. (1995). *The elevational gradient of species richness: a uniform pattern?*

Salinger, M. J.(2005). Climate variability and change: past, present and future–an overview. Climatic change 70.1-2: 9-29.

Sanders, N. J., & Rahbek, C. (2012). The patterns and causes of elevational diversity gradients. *Ecography*, *35*(1), 1–3. https://doi.org/10.1111/j.1600-0587.2011.07338.x

Santini, L., Benítez-López, A., Maiorano, L., Čengić, M., & Huijbregts, M. A. J. (2021). Assessing the reliability of species distribution projections in climate change research. *Diversity and Distributions*, *27*(6), 1035–1050. https://doi.org/10.1111/ddi.13252

Scafaro, A. P., Posch, B. C., Evans, J. R., Farquhar, G. D., & Atkin, O. K. (2023). Rubisco deactivation and chloroplast electron transport rates co-limit photosynthesis above optimal leaf temperature in terrestrial plants. *Nature Communications*, *14*(1). https://doi.org/10.1038/s41467-023-38496-4

Sullivan, M. J., Lewis, S. L., Affum-Baffoe, K., Castilho, C., Costa, F., Cuni Sanchez, A., N Ewango, C. E., Hubau, W., Marimon, B., Monteagudo-Mendoza, A., Qie, L., Sonké, B., Vasquez Martinez, R., Baker, T. R., W Brienen, R. J., Feldpausch, T. R., Galbraith, D., Gloor, M., Malhi, Y., … Phillips, O. L. (n.d.). *Long-term thermal sensitivity of Earth's tropical forests*. https://www.science.org

Tello, J. S., Myers, J. a., Macía, M. J., Fuentes, A. F., Cayola, L., Arellano, G., Loza, M. I., Torrez, V., Cornejo, M., Miranda, T. B., & J??rgensen, P. M. (2015). Elevational gradients in-diversity reflect variation in the strength of local community assembly mechanisms across spatial scales. *PLoS ONE*, *10*(3), 1–17. https://doi.org/10.1371/journal.pone.0121458

Turner, M. G., Calder, W. J., Cumming, G. S., Hughes, T. P., Jentsch, A., LaDeau, S. L., Lenton, T. M., Shuman, B. N., Turetsky, M. R., Ratajczak, Z., Williams, J. W., Williams, A. P., & Carpenter, S. R. (2020). Climate change, ecosystems and abrupt change: Science priorities. In *Philosophical Transactions of the Royal Society B: Biological Sciences* (Vol. 375, Issue 1794). Royal Society Publishing. https://doi.org/10.1098/rstb.2019.0105

Wang, Y., Berardi, U., & Akbari, H. (2016). Comparing the effects of urban heat island mitigation strategies for Toronto, Canada. *Energy and Buildings*, *114*, 2–19. https://doi.org/10.1016/j.enbuild.2015.06.046

Wiens, J. A. (1989). Spatial scaling in ecology1. In *Source: Functional Ecology* (Vol. 3, Issue 4).

Zhang, Y., Chen, H. Y. H., & Taylor, A. (2014). Multiple drivers of plant diversity in forest ecosystems. *Global Ecology and Biogeography*, *23*(8), 885–893. https://doi.org/10.1111/geb.12188

Zhu, J., Zhu, H., Cao, Y., Li, J., Zhu, Q., Yao, J., & Xu, C. (2020). Effect of simulated warming on leaf functional traits of urban greening plants. *BMC Plant Biology*, *20*(1). https://doi.org/10.1186/s12870-020-02359-7

Appendix 1.1. Glossary.

- **Biodiversity**: the number, abundance, composition, spatial distribution, and interactions of genotypes, populations, species, functional types and traits, and landscape units in a given system (Díaz *et al*., 2006).

- **Functional traits**: the characteristics or attributes of an organism that are considered relevant to its response to the environment or its effect on ecosystem processes, for example, leaf size, longevity, seed size and dispersal mode (Díaz & Cabido, 2001; Hooper *et al*., 2005).

- **Functional composition:** the combination of different functional traits within a community or ecosystem. Functional composition can be described by both the diversity of traits as well as the community weighted trait means (CWM). Thus, it influences the function of ecosystems such as productivity and responses to environmental changes and considers how each species contributes to ecosystem processes and properties. (Garnier et al., 2004; Vile, Shipley & Garnier, 2006)

- **Climate change**: *"a change of climate which is attributed directly or indirectly to human activity that alters the composition of the global atmosphere and which is in addition to natural climate variability observed over comparable time periods."* UNFCC, Article 1 – Paragraph 2, 1994.

- **Ecosystem services**: the benefits that ecosystems provide to humanity either directly or indirectly (Díaz *et al*., 2006). The Millennium Ecosystem Assessment classifies the ecosystem services in supporting (e.g., primary production, nutrient cycling), regulating (e.g., climate regulation, pest control), provisioning (e.g., food, wood, fresh water), and providing cultural services (e.g., recreation and aesthetic values) (MEA, 2005).

- **Urban Heat Island (UHI):** a global phenomenon where urban areas are significantly warmer than surrounding rural areas. This phenomenon occurs when

cities have less vegetation and dense construction resulting in the retention of heat in urban infrastructure (Stewart 2011).

- **Beta-diversity:** the measurement of variation in species composition between different habitats, environments, or sites (Whittaker 1960).

CHAPTER I

THE IMPORTANCE OF GRAIN AND CUT-OFF SIZE IN SHAPING TREE BETA DIVERSITY ALONG AN ELEVATIONAL GRADIENT IN THE NORTHWEST OF COLOMBIA.

ABSTRACT

Species turnover (β-diversity) along elevational gradients is one of the most important concepts in plant ecology. However, there is a lack of consensus about the main driving mechanisms of tree β-diversity at local scales in very diverse ecosystems (e.g., Andean mountains), as well as how the sampling effect can alter β-diversity estimations. Recently, it has been hypothesized that patterns of change in β-diversity at local scales along elevational gradients are driven by sampling effects stemming from differences in the size of the species pool rather than by underlying community assembly mechanisms. Thus, we aim to evaluate the relative extent to which sampling effects, such as species pool size, grain size, and tree size cut-off, determine species sorting, and thus, the variability of β-diversity at local scales along elevational gradients in the northwest of Colombia. Using 15 1-ha permanent plots spread out along a 3000 m elevational gradient, we used standardized β-deviation to assess the extent to which either sampling effects or the community assembly mechanisms determine the changes in species composition at local scales.

Standardized β-deviation was measured as the difference between the observed and null β-diversity divided by the standard deviation of the null β-diversity. We found that the magnitude of change in local β-deviation along the elevational gradient was significant and dependent on the employed spatial grain size and tree size cut-off. However, β-deviation increased with elevation in all sampling designs, which suggests that underlying community assembly mechanisms play a key role in shaping local β-diversity along the elevational gradient. Our findings suggest that grain size enlargement and the inclusion of trees with small diameters will improve our ability to quantify the extent to which the community assembly mechanisms shape patterns of β-diversity along elevational gradients. Overall, we emphasize the scale-dependent nature of the assessment of β-diversity. Likewise, we call for the need of a new generation of enlarged forest inventory plots along gradients of elevation in tropical forests that include small individuals to improve our understanding about the likely response of diversity and function to global change.

Keywords: Andean forests, null models, species pool, species sorting, sampling effect.

INTRODUCTION

Spatial turnover in community composition (β-diversity) along elevational gradients has been one of the most striking and studied patterns in ecology (Lomolino, 2001b; Rahbek, 2005; R. H. Whittaker, 1960). In tropical mountain systems, β-diversity is expected to decrease with elevation (Tello et al., 2015b) due to the influence of different community assembly mechanisms that could vary along the elevational gradient (Laiolo et al., 2018). Overall, different assembly mechanisms, such as dispersal limitation (Condit et al., 2002), species sorting (Qian & Ricklefs, 2007), habitat specialization (Jankowski et al., 2009; Janzen, 1967), and priority effects (Chase, 2010; Fukami, 2015), have been thought to explain the spatial turnover in the composition of plant communities. However, sampling effects associated with the size of the species pools and the regional abundance distributions have recently been proposed as the main cause of the observed decreased in β-diversity along elevational gradients (Kraft et al., 2011). In other words, the observed variation in β-diversity along steep elevational gradients may be primarily driven by differences in the size of the species pools and the number of individuals per specie generated by biogeographical or regional processes (Ricklefs, 1987) rather than by the underlying mechanisms of community assembly described above. Disentangling the relative importance that species pool size, regional abundance distribution (Kraft et al. 2011) or community assembly mechanisms have on determining β-diversity at different

scales along elevation gradients in the tropics is paramount for developing robust forest conservation plans capable of maintaining diversity (Lomolino 2001; Rahbek 2005).

The spatial scale at which vegetation studies are developed is a key factor that can strongly influence β-diversity gradients (Stier et al., 2016). The concept of scale involves two factors: i) extent, the geographical area where comparisons are made; and ii) grain size, the unit of measurement at which data are collected or aggregated for analysis (R. J. Whittaker et al., 2001). In a fixed extent, a variation in grain size implies a variation in a sampled relative species abundances and, subsequently, its spatial patterns of aggregation (Crawley & Harral, 2002). Directly related to β-diversity, when the spatial grain size of local communities increases, species present in the regional species pool will be better represented, generally lending to a decline in β-diversity (Barton et al. 2013). Along an elevational gradient, the use of 0.1-ha plots with grain sizes of 0.01-ha has been widely used to assess and detect fine-grained environmental variation effects on determining β-diversity at a local scale (Kraft et al., 2011; Mori et al., 2013b; Tello et al., 2015b). However, in species-rich communities, smaller grain sizes may lead to the undersampling of individuals, an issue that can artificially enhance β-diversity (Condit et al., 2005). Comparative studies of β-diversity at contrasting grain sizes along elevational gradients are needed to help disentangle the extent to which either sampling effects or community assembly mechanisms shape β-diversity patterns.

Along elevational gradients, another largely unexplored issue pertains to the likely effect that different diameter at breast height (DBH) cut-off sizes can have in β-diversity assessments (Mori et al. 2013). Overall, reducing the minimum size, or DBH, of the sampled individuals increases the community size, potentially increasing floristic diversity measurements as well (Stier et al., 2016). In tropical mountains, the most popular DBH cut-off size utilized to assess changes in β-diversity along elevational gradients are individuals with DBHs varying from ≥ 2.5 cm (Kraft et al., 2011; Myers et al., 2013; Tello et al., 2015b) to ≥ 10 cm DBH (Girardin et al. 2014). However, none of these studies have evaluated the likely comparative effect that tree cut-off size variation can have on shaping β-diversity. The sampling effect of keeping the grain size constant and decreasing the DBH

cut-off will cause a change in species relative abundance; and whereby this difference in abundance may lead to changes in the extent to which underlying ecological mechanisms can explain the overall pattern of diversity (Chase & Knight, 2013; Powell et al., 2011). In other words, sampling not only has a potential effect on the diversity patterns, but also on our ability to identify the underlying community assembly mechanisms that drive these observed patterns. For example, in tropical lowlands, several studies have proposed that enhancing community size by including smaller individuals (e.g. shrubs and juveniles) may lead to a higher influence of deterministic processes, such as soil fertility, on defining species sorting (Comita et al., 2007; Duque et al., 2002). Understanding the effect of different tree cut-off sizes in determining the magnitude of β-deviation at a local scale along elevational gradients will help to distinguish sampling constructs from true ecological signals. This is essential in helping researchers to identify the underlying drivers of species distribution and forest function in the tropical Andean mountains.

In order to identify the likely influence of local community assembly mechanisms on shaping β-diversity along elevational gradients, we first need to determine whether β-diversity deviates from null (stochastic) processes (Kraft et al. 2011). Null models help to disentangle ecological assembly mechanisms by quantifying random processes in the ecological community and making comparisons among regions with different species pool sizes possible (Chase & Myers, 2011). A positive standardized difference between the observed β-diversity and the expected β-diversity obtained from a null model divided by the standard deviation of the null model (defined here as β-deviation), indicates a higher β-diversity than expected by chance due to the influence of local processes that cause an aggregated non-random spatial pattern of species distribution (Mori et al. 2013, Tello et al. 2015). However, a positive and systematic increase of β-deviation along the elevational gradient, after removing sampling effects and differences in the size of species pools among sites, is not enough and fails to identify the underlying community assembly mechanism (e.g species sorting or dispersal limitation) responsible for an aggregated non-random pattern along the whole elevational gradient (i.e. Tello et al. 2015). Mirroring the magnitude of the operating species assembly mechanisms found along the latitudinal gradient (Myers et al., 2013), we might expect the relative importance of biological

processes, such as dispersal limitation, to decrease with elevation; an opposing effect to species sorting, which can be positively correlated with elevation.

In this study, we employed a nested sampling design using a series of 15 1-ha plots scattered in wet forests located in northwestern Colombia, where the Andean mountain ranges end, to examine the role that species pool size, grain size and tree cut-off size played in determining β-diversity along elevational gradients. For this study, we had three main hypotheses: i) under the assumption that local variation in species composition primarily depends on the size of the species pool, we do not expect any significant relationships between β-deviation and elevation to occur after controlling for the species pool (Kraft et al. 2011). In contrast, if ecological mechanisms (e.g. species sorting) determine a non-random spatial species distribution, the variation on β-deviation may show a systematic change with elevation as a result of the harsh conditions imposed by highlands (after Tello et al. 2015). ii) The increase of grain size within a fixed extent increases the floristic similarity among samples (hereafter grain size hypothesis), and thus, decreases β-diversity. We expect the magnitude of the relationship between elevation and β-deviation (the slope of the line) to decrease with the increase of grain size at a local scale along the elevational gradient. iii) The reduction of the selected tree cut-off size will increase the local community size and will reduce the compositional differences between samples. We also would expect a reduction in the β-deviation of each plot along the elevational gradient.

METHODS

Study área

The study area was located in the northwest region of Colombia between 5º50’ and 8º61’ North and 74º61’and 77º33’ West. This region encompasses a highly variable elevational gradient in terms of its topography, climate, and soils. The study was conducted using data collected from 15 permanent 1-ha (100 m × 100 m) forest inventory plots which were established between 2006 and 2010. The permanent plots were established across a large geographic area that covers approximately 64,000 km^2, mostly within the province of Antioquia (Fig. 1) and span an elevational gradient of 50 to 2,950 m asl. The average distance between plots was 160.5 km (ranging = 26.1- 419.5 km). The Andean region in

Colombia contains only approximately 34% of its original natural cover primarily due to historical deforestation (Cabrera et al., 2019; Duque et al., 2014). Thus, at least in some of the surveyed locations, we expected to find some previous human disturbances, specifically inthe El Bagre, Carepa and Necoclí plots (Fig. 1), which were located in small forest fragments (≈ 50 ha). These plotsmay have experienced human disturbance and elevated tree mortality along forest edges (Duque et al., 2015c).

Plot censuses

In each 1-ha plot, all shrubs, trees, palms, and tree ferns with a diameter at breast height (DBH) ≥ 10 cm (hereafter "large trees") were mapped, tagged, and measured. Additionally, all of the plants with a DBH ≥ 1 cm (hereafter "all trees") were also mapped, tagged and measured in a 40 m × 40 m subplot (1600 m^2) located near the center of each plot (Fig. S1). Voucher specimens were collected for each potentially unique species in each plot. We collected vouchers in all cases where there was any doubt as to whether an individual plant was the same species as another individual that was already collected within the same plot. Taxonomic identifications were made by comparing the specimens with herbarium material and with the help of specialists for some plant groups. Vouchers are kept at the University of Antioquia's Herbarium (HUA). The plants that could not be identified to the species level were classified into morphospecies based on differences in the morphology of their vegetative characters. Approximately 3.5% of individuals were excluded from the analysis due to low-quality vouchers resulting from a lack of clear botanical characters, earlier stages of development, or incorrect enumeration. In total, we identified 26,222 individuals, 112 families, 428 genera and 1,707 morphospecies.

Sampling effects

DBH cut-off and species pool size effect

We divided the dataset into three DBH cut-off sizes: i) large trees: represented by all individuals with a DBH ≥ 10 cm tallied in the entire 100 m × 100 m plots (1-ha); ii) small trees: represented by all individuals with a 1 ≤ DBH < 10 cm, which were measured only in the 40 m × 40 m subplot inserted within the 1-ha plot (Fig. S1); iii) all trees: represented by

all individuals with a DBH ≥ 1 cm tallied in the 40 m × 40 m subplot (0.16-ha) described above. In order to assess the effect of species pool size for each one of the tree DBH cut-off sizes employed to generate our three sampling communities (large, small and all trees), we used the species richness corresponding to each data set. For large trees, we used the species richness from each 1-ha plot but only including trees with a DBH ≥ 10 cm. For the small and all trees categories, we used their respective species richness from each 0.16-ha plot (40 m × 40 m) (see Table 1).

Grain size effect

The grain size hypothesis was assessed by employing three different grain sizes. For large trees, we used 10 m × 10 m (0.01-ha), 20 m × 20 m (0.04-ha) and 50 m × 50 m (0.25-ha). The grain size used to analyze the influence of the spatial scale for small and all trees were 5 m × 5 m (0.0025-ha), 10 m × 10 m (0.01-ha) and 20 m × 20 m (0.04-ha). The differences in the spatial grain size among large versus small and all trees are due to individuals with a DBH ≥ 1 cm were only measured in the 40 m × 40 m subplot.

Environmental features

The elevation of each plot was calculated using a GPS. Each elevation point corresponds to the 0,0 point located in the lower-left corner of each plot along the gradient (Fig. S1). Samples of the soil A horizon (mineral soil after removing the organic layer) from five points in each 20 m × 20 m quadrat were collected (N = 25 composite samples per 1-ha plot). At each point, a 500 g soil sample was taken from a depth of 10-30 cm; the five samples from each quadrat were then combined, and a 500 g composite sample was taken and air-dried after removing macroscopic organic matter. pH, Ca, Mg and K concentrations were analyzed at the Biogeochemical Analysis Laboratory at the National University of Colombia in Medellín. Exchangeable Ca, Mg, and K were extracted with 1 M ammonium acetate and analyzed using atomic-absorption. Soil pH was measured in water as one-part soil to two parts water. Other soil cations, such as N and P, were not measured due to logistical constraints of sampling at this spatial resolution and scale.

We used geostatistical methods to obtain spatial predictions of soil variables at spatial scales smaller than 20 m × 20 m (5 m × 5 m and 10 m × 10 m). We first computed empirical variograms to test the likely spatial structure of each soil variable (pH, Ca, Mg, and K) within the 1-ha plot. The variograms for the four variables did not show any spatial significant trend. Therefore, we used a bilinear interpolation method based on resampled soil data to obtain values of soil variables at different grain sizes in each plot. This method employs the distance-weighted average of the nearest pixel values to estimate the values of no measured points (Hijmans et al. 2016). We calculated soil variables at the 50 m × 50 m grain size using the mean of the soil variables at the 20 m × 20 m scale. Spatial analyses were conducted using the geoR (Ribeiro and Diggle 2001) and raster (Hijmans et al. 2016) packages.

Estimations of β-diversity

We calculated the observed β-diversity (BD_{obs}) based on abundance data (Legendre and Gallagher 2001b; De Cáceres et al. 2012). Taking into account all living trees by species in each one of the plots, for every grain size, we built a matrix ($X= [x_{ij}]$) with dimension n × p (quadrat × species), where X is the community matrix of each plot and x_{ij} contains the number of individuals of species *j* in the quadrat (grain) *i* (De Cáceres et al. 2012). For each matrix $X= [x_{ij}]$, β-diversity was estimated in two steps. First, we transformed the abundances of each species by grain size using the Hellinger transformation. This transformation consists in standardize the abundance of each species by rows. It means, to standardize the abundance of each species by the total abundance of the site (in this case, species by grain), in each plot. Then, the square root of these values is taken (Legendre and Gallagher 2001). Thus, data set express species abundance as square-root transformed proportionate abundance in each grain by site (Jones et al., 2008). The Hellinger transformation is given by:

$$Y_{ij} = \sqrt{\frac{x_{ij}}{\sum_{k=1}^{p} x_{ik}}}$$

Where Y*ij* is the transformed matrix. x_{ij} is the value of species *j* in site *i*, *k* is the species index and *p* is the number of species in a given grain with row and column indices *i* and *j* (Tan et al., 2017). The Hellinger transformation standardizes species abundance and reduces the weight of the most abundant species in the analysis. The use of the Hellinger transformation makes community compositional data containing many zeros ("double zero") suitable for analysis by linear methods (Legendre and Gallagher 2001a; Legendre 2007). Secondly, we estimated BD_{obs} as the variance of Y (De Cáceres et al. 2012), which is calculated as follows:

$$BD_{obs} = Var(Y) = \frac{SS(Y)}{(n-1)}$$

Where SS(Y) is the sum of squares and n is the number of quadrats. BD_{obs} is 0 when all quadrants have exactly the same composition and 1 when they do not share any species.

Null model

We used a null model to quantify the extent to which the variation in the size of species pool (different species number due to the DBH cut-off size) and scale (different grain size) account for variation in β-diversity (Kraft et al. 2011). The species pool for large, small and all trees was defined as the observed number of species in either the 1-ha or the 0.16-ha plots (after Kraft et al. 2011). The null model randomizes the location of trees among grains within the plot, creating communities that vary in relation to the location of individuals, but fixing the community size (number of individuals), and thus, the observed relative species abundance of each species pool (Tello et al. 2015). This null model removes the local ecological mechanism that creates non-random patterns, such as aggregation and intraspecific co-occurrence (De Cáceres et al., 2012). The Hellinger transformation is then applied to the randomized matrix and expected β-diversity (BD_{exp}) is calculated using the formula presented above. This process is repeated 1000 times per plot, for each grain size, and for each predefined DBH cut-off size. The BD_{exp} is calculated as the mean of 1000 iterations of the null model.

β-deviation (BD_{dev}) was defined as the standardized effect size (SES) calculated using the difference between BD_{obs} and BD_{exp} divided by the standard deviation of the frequency distribution of the null model (SD_{exp}).

$$BD_{dev} = BD_{obs} - \frac{mean(BD¿¿\exp)}{SD_{\exp}}¿$$

Positive values in the slope of the variation between BD_{dev} along elevational gradients indicate a significant effect of community assembly mechanisms on determining the rate of change in species composition at local scales (Chase & Myers, 2011; Tello et al., 2015b). Contrarily, values of the slope of the variation in BD_{dev} along elevational gradients non-significantly different from zero (0) are primarily due to sampling effects that come up along with the variation in the size of the species pool (Kraft et al. 2011).

Data analysis

We used linear mixed regression models (LMM; Zuur et al. 2009) to identify the main determinants of change in BD_{obs}, BD_{exp}, and BD_{dev} along the elevational gradient. Variables included in the LMM as fixed effects were: grain size, size of the species pool, elevation (m asl) and soil heterogeneity. Soils heterogeneity was assessed for each grain size using the interpolated values from 20 m × 20 m subplots described above. To represent soils heterogeneity at a local scale, we used the variance of the subplot scores on the first axis of a principal component analysis (PCA). PCA was applied to pH, Ca, Mg, and K concentrations. PCA analyses were performed for each grain size and DBH cut-off size (Additional file 1; Methods). Soils heterogeneity was modeled as a continuous variable. Finally, plot identity (or plot name) was included as a random effect to control for particular conditions of each site (Zuur et al., 2009). The interaction term between grain size and elevation was included to directly assess the combined effect of these variables on shaping the β-diversity (BD_{obs}, BD_{exp}, and BD_{dev}).

In LMMs, the marginal explained variation (R^2 marginal) is associated with fixed effects, while the conditional explained variation (R^2 conditional) associated with random effects. Because individuals with DBH ≥ 1 cm and with 1 ≤ DBH < 10 cm were not sampled at the 50 m × 50 m scale, we were unable to include the three tree size categories in the same

model. Therefore, separate models were used for large trees, small and all trees. The best model for each DBH cut-off size was chosen using the backward stepwise model selection based on the Akaike information criterion (AIC) (Crawley, 2007). In order to assess the likely spatial autocorrelation in our models, we extracted the residuals for each model (BD_{obs}, BD_{exp}, and BD_{dev}, for large, small and all trees), separating them by grain size, and assigning the respective spatial coordinate to each one. Then, we estimated a semi-variogram based on 100 draws to define an envelope for the significance of the observed spatial structure of the residuals. This analysis was performed with the geoR package (Ribeiro and Diggle 2001).

All analyses were performed in R 3.3.0 (Core Team 2016).

RESULTS

Elevation and species pool

As we expected, BD_{obs} and BD_{exp} decreased with elevation independent of the grain size and DBH cut-off size (Fig 2). In contrast, BD_{dev} increase with elevation, also in all grain sizes, regardless of the DBH cut-off size (Fig 2). After controlling for the regional species pool effect, BD_{dev} still showed an increase with elevation. Overall, the standardized local BD_{dev} increased from lowlands to highlands, which suggests a differential effect from the underlying species assembly mechanism in accordance to elevation.

Grain size

Both BD_{obs} and BD_{exp} decrease with grain size independent of the tree DBH cut-off size (Fig 2). The slopes among grain size, or the relationship BD_{dev}-elevation, were significantly different for large trees, but small and all trees did not show any significant difference among grains (Fig S2).

Determinants of local scale changes in tree β-diversity along the elevational gradient

According to the LMMs, the BD_{obs} was significantly associated with grain size, the size of the species pool and elevation for the three size-classes employed (large trees, small trees, all trees). The interaction between grain size and elevation was only significant for large

trees. The BD_{exp} was significantly associated with grain size and elevation for the three DBH cut-off size employed, while the size of species pool was significant for large and all the trees but only marginally significant for small trees. The BD_{dev} was significantly associated with grain size for all the three DBH cut-off size. The interaction between grain size and elevation was significant for large and small trees, but not for all the trees. Finally, the marginal explained variation (R^2 marginal) by the models was almost always the same than that explained by the conditional variation (R^2 conditional) for observed and expected β-diversity and for BD_{dev} in large trees. However, the marginal and conditional explained variation for BD_{dev} for small and all trees had differences, which indicates greater relative importance of random effect for the last two tree sizes (Table 2). Model residuals showed no evidence of spatial autocorrelation (Additional file 1; Fig S3, Fig S4, and Fig S5)

DISCUSSION

Sampling effects

In this study, we assessed three hypotheses regarding the influence of sampling effects (size of species pool, grain size, and tree cut-off size) on the variation of local β-diversity along elevational gradients in the northern region of the Andean mountains of Colombia. Overall, we found that observed and expected β-diversity decreased with elevation, but that the standardized β-deviation followed an increasing trend with elevation after controlling for the effect of species pool size. The systematic increase in the β-deviation with elevation was independent of the grain size employed, indicating that alternative underlying community assembly mechanisms had a significant role in shaping tree β-diversity along this elevational gradient. Our finding contradicts the claim of sampling effects due to the species pool size as the key determinant of changes in β-diversity (*sensu* Kraft et al. 2011). Therefore, our results emphasize the importance that different community assembly mechanisms have on shaping the observed decrease in local β-diversity along elevational gradients in tropical forests (Mori et al. 2013; Tello et al. 2015), rejecting our first hypothesis.

Following some studies on tree β-diversity along latitudinal gradients (De Cáceres et al., 2012; Sreekar et al., 2018), our second hypothesis predicted and confirmed a decrease in both the observed and expected tree β-diversity with the increase in grain size along an elevational gradient. Regarding the β-deviation, our findings were dependent on the DBH cut-off tree size as predicted by the third hypothesis, similar to other studies along elevational gradients (Mori et al. 2013). Mori et al. (2013) claimed that the overall β-diversity decreases in response tothe DBH cut-off size, contrary to β-deviation. Therefore, for large trees (DBH ≥ 10 cm), we accept the hypothesis that changes in grain size have a significant effect on the assessment of the standardized β-deviation, and conclude that the larger the grain size, the lower the observed β-diversity, but the higher the β-deviation. In other words, especially for large trees, and along elevational gradients, the probability of detecting the influence of community assembly mechanisms increase positively at larger grain sizes (Fig. 2). A likely explanation for this pattern could be that large trees are those that survived self-thinning and their spatial distribution, at smaller spatial scales (e.g. 0.04-ha), are more random than at larger scales, which indicates that the degree of aggregation does not vary much at such small grain sizes.

When assessing the β-deviation for the small and all individuals size classes (DBH ≥ 1 cm), the interaction between grain size and elevation included in the LMMs was significant for small trees but not for all trees. This contrasting result, stemming from similarly nested datasets (see Table 1), hampers our capacity to make conclusions as to the effect of grain size on the local β-deviation for the small and all individuals along the elevational gradient. In fact, when using an independent Analysis of Covariance (ANCOVA) to evaluate the grain size – elevation interaction term, only large trees were significant (Table S1; Fig. S2). The low sampling size (4) used to assess tree β-diversity at the largest grain size (4) may be a reason for the high variance observed when we included individuals with DBH ≥ 1 cm. In the Andean mountains, the lack of sampling schemes of plots ≥ 1-ha that include individuals with DBHs ≥ 1 cm, such as those available for tropical lowlands (i.e (De Cáceres et al. 2012; Anderson-Teixeira et al. 2015; Sreekar et al. 2018), prevents us from concluding about the expected trend of the β-deviation at larger grain sizes along the elevational gradient in tropical forests.

Tree community assembly mechanisms along the elevational gradient

The increase of β-deviation in relation to elevation indicates that in colder regions, the extent to which species assembly mechanisms operate is higher compared to warmer areas. One important conclusion to note is that low temperatures may impose constraints to plant establishment and functioning, and play a key role in determining species distribution (Girardin et al., 2014; Kitayama & Aiba, 2002). For example, changes in species composition could be associated with changes in species richness along elevational gradients in very diverse understory families, such as Rubiaceae ($r= -0.58$, $p= 0.02$).

Soil variation has been shown to be a key community assembly mechanism which shapes species sorting at local scales in some tropical forests (John et al., 2007; Russo et al., 2005). However, in this study, we did not find soil variation to be significantly associated with the local β-deviation along the elevational gradient. This result did not support the idea of an increase in plant habitat-association of juveniles and shrubs (Comita et al., 2007; Duque et al., 2002; Fortunel et al., 2016). Nonetheless, our soil variation index focuses primarily focuses base content, hindering our ability to understand the likely influence of other very important soil cations, such as P and N, which, in tropical lowland forests (Condit et al., 2013), have been identified as key elements for tree species distribution. Furthermore, soil sampling was only carried out at the 20 m × 20 m scale, which might have obscured processes operating at smaller spatial scales. Additional studies testing the likely influence of topographic and edaphic variables, not considered here, will shed new insights on the still unanswered question about the extent to which environmental filtering locally shapes species sorting, and thus, the gradient of β-diversity at local scales along elevational gradients in tropical forests.

The lack of significance of soil variation on shaping species sorting implies that other community assembly mechanisms, rather than environmental filtering, are likely drivering the observed change in β-diversity at a local scale with elevation. Mirroring the latitudinal gradient (Myers et al. 2013), a systematic decrease in the importance of dispersal limitation (*sensu* (Hubbell 2001)) with elevation seems the first likely alternative assembly

mechanism to explain the increase in β-deviation observed in this study. Another possible explanation for the positive deviations of β-diversity is the hypothetic positive increase of density-dependence with the size of the species pool (Lamanna et al., 2017), which suggests that the stronger the conspecific and heterospecific the negative dependence is, the higher the diversity, but the weaker the influence of environmental filtering and niche partitioning. A decrease of species competition but an increase of species facilitation in highlands, due to the adverse conditions imposed by low temperatures on the ecosystem functioning and survival capacity of plants (Coyle et al., 2014), could also promote the observed increase of β-deviation with elevation observed in our study.

One likely factor not assessed here that could have influenced the pattern of variation in local β-diversity is the expected biotic homogenization caused by forest disturbance (Karp et al., 2012; Solar et al., 2015). The high fragmentation and historical degradation of the tropical Andes (Armenteras et al., 2013), could have caused some of our sites to display a lower local β-diversity than under undisturbed conditions. In mountainous ecosystems, we expect the steep terrain at the highest mountain peaks to limit site access and act as a shield against human disturbances (Spracklen & Righelato, 2014), thus generating a higher biotic homogenization in lowlands than in highlands. Indeed, the plots located in the smallest forest fragments (Carepa, Necoclí and El Bagre; see methods), were all located in lowlands. However, the systematic decline in the observed β-diversity (BD_{obs}) does not support the hypothesis of biotic homogenization as a major cause of the observed pattern. For example, we did not find statistical differences (unpaired *t-test*) when comparing the β-deviation between the three sites located in the smallest forest fragments, which we assumed were exposed to higher disturbances, and the rest of the plots located in lowlands (< 1000 m asl). This result was a generalized outcome for any grain size for both large trees (50 m × 50 m: p=0.79; 20 m × 20 m, p=0.82; 10 m ×10 m, p= 0.42) and small trees (20 m × 20 m: p=0.92; 10 m ×10 m: p=0.78, 5 m × 5 m: p=0.64).

Methodological remarks

First, for large trees, the LMMs selected species pool size (species richness) as a significant variable to explain the variation of the β-deviation with elevation (Table 2). This finding

indicates that the applied null-model did not, in some cases, entirely and effectively remove the influence of the size of the species pool. Understanding the effect that changes in the shape of the species abundance distribution models have on determining the β-diversity along elevational gradients is still under debate (Qian et al. 2013). However, it could be seen as an alternative way to analyze the effect from changes in community size. Second, the absence of plots ≥1-ha that include small individuals in the Andean mountains prevents the use of sampling sizes along the elevational gradient which are large enough to properly assess the grain size and cut-off size hypotheses together in this complex ecosystem. Although our study is the first attempt in the Andean mountains to test the species pool hypothesis using plots ≥ 0.1 ha, our results were based on very few replicates of the largest grain sizes and need to be seen as preliminary evidence of an expected pattern rather than a conclusive view. To truly understand the pattern of β-diversity variation in mountainous tropical forests, it appears we need to transition towards a new generation of larger forest sampling schemes (e.g (Garzon-Lopez et al. 2014; Duque et al. 2017; Sreekar et al. 2018) that goes beyond the valuable heritage left by A.L. Gentry. Such a big challenge should be a priority in the tropical Andes, where the availability of information is much more scarce than in their Amazon lowland counterparts (Feeley, 2015).

CONCLUSION

We determined that the effect of the grain size, species pool size and tree cut-off size, are paramount to identify the underlying processes that shape species assembly of tree communities. Our findings suggest that grain size enlargement and the inclusion of small size classes can help improve our ability to identify the extent to which the species assembly mechanisms shape the patterns of local β-diversity change along elevational gradients in tropical ecosystems. However, in future field campaigns that aim to assess tree local β-diversity along the elevational gradient in tropical forest inventories, we need to evaluate the limitation of the relatively small plot size employed so far. Overall, our study emphasizes the scale-dependent nature of β-diversity assessments. It showcases the advantage to decreasing the tree cut-off size and increasing the plot size in forest inventories (Barton et al., 2013; De Cáceres et al., 2012; Sreekar et al., 2018) to improve

our understanding about the likely response of tree diversity to global change in tropical mountain ecosystems.

Table 1.1. Description and location of the 15 1-ha permanent plots in the northwest of Colombia. Latitude (North) and Longitude (West) are presented in geographical coordinates (degrees). N: total number of individuals. S: species richness. The columns of 0.16-ha contain the information about N (number of individuals) and S (species number) by different DBH cut-off size in the 40 m × 40 m subplot inside the plot. The column of 1-ha has information about N and S for the large trees in the whole plot.

Plot	Elevation	LAT	LONG	0.16 ha (DBH≥ 1 cm)		0.16 ha (1 ≤ DBH < 10 cm)		1 ha (DBH ≥ 10 cm)	
				N	S	N	S	N	S
Carepa	58	7.779	-76.764	855	100	802	89	369	109
Caucasia	64	8.133	-74.942	445	79	364	68	503	72
El Bagre	67	7.656	-74.815	973	174	900	157	497	141
Necoclí	70	8.507	-76.657	981	141	891	127	561	100
Puerto triunfo	180	6.006	-74.610	1050	135	975	123	384	78
Sapzurro	228	8.651	-77.354	747	119	656	108	606	102
Segovia	717	7.111	-74.731	1267	251	1177	234	624	170
Porce	1006	6.776	-75.076	737	107	614	93	834	75
Maceo	1016	6.458	-74.786	1020	113	909	103	820	133
Anorí	1784	6.987	-75.143	1386	215	1261	206	918	158
Ventanas	2080	7.079	-75.475	1733	149	1590	142	938	122
Angelópolis	2118	6.153	-75.695	2173	189	2033	177	868	137
Jardín	2525	5.492	-75.898	1397	82	1238	75	942	76
Caicedo	2635	6.378	-76.031	1437	112	1202	107	1244	112
Belmira	2885	6.612	-75.654	1053	60	959	59	541	37

Table 1.2. Results from the best-fit linear mixed models for large (>10 cm DBH), small (1 ≤ BDH < 10 cm) and all trees (DBH > 1 cm). BDobs: observed β-diversity. BDexp: expected β-diversity. BDdev: β-deviation (BDobs – BDexp)/SDexp. Conditional R2 takes into account both fixed and random effects to measure the goodness of adjustment and prediction power, while marginal R2 only has the fixed effects part. · p=0.05, *p<0.05, **p<0.01, ***p< 0.001.

	Dependent variable	Variable	Parameter	Standard Error	p-value	Marginal R^2	Conditional R^2

		10x10	0.80	0.016	***		
		20x20	0.65	0.016	***		
	BD_{obs}	50x50	0.39	0.016	***		
		elevation	-0.07	0.017	**	0.89	0.94
		richness	0.06	0.013	**		
		20x20*elevation	0.01	0.018	NS		
		50x50*elevation	0.05	0.018	**		
		10x10	0.78	0.015	***		
		20x20	0.58	0.015	***		
LARGE TREES	BD_{exp}	50x50	0.30	0.015	***	0.93	0.95
		elevation	-0.08	0.011	***		
		richness	0.05	0.012	***		
		10x10	3.85	0.7	***		
		20x20	6.73	0.7	***		
	BD_{dev}	50x50	6.80	0.7	***		
		elevation	1.07	0.7	NS	0.94	0.95
		richness	0.04	0.6	*		
		20x20*elevation	0.62	0.5	NS		
		50x50*elevation	1.76	0.5	**		
		5x5	0.77	0.011	***		
	BD obs	10x10	0.57	0.013	***	0.94	0.95
		20x20	0.37	0.013	***		
		elevation	-0.03	0.011	*		
		richness	0.02	0.007	*		
		5x5	0.70	0.014	***		
		10x10	0.47	0.014	***		
SMALL TREES	**BD exp**	20x20	0.25	0.014	***	0.92	0.96
		elevation	-0.05	0.013	*		
		richness	0.02	0.012	·		
		5x5	9.80	1.0	***		
		10x10	10.5	0.6	***		
		20x20	9.71	0.6	***		
	BD_{dev}	elevation	22.53	1.0	*	0.25	0.85
		10x10*elevation	0.03	0.6	NS		
		20x20*elevation	1.6	0.6	*		
ALL	BD_{obs}						

		5x5	0.76	0.009	***		
		10x10	0.56	0.009	***		
		20x20	0.35	0.009	***	0.93	0.97
		elevación	-0.04	0.007	***		
		richness	0.03	0.007	*		
		5x5	0.69	0.012	***		
		10x10	0.46	0.012	***		
TREES	**BD_{exp}**	20x20	0.25	0.012	***	0.95	0.97
		elevación	-0.06	0.010	***		
		richness	0.03	0.010	**		
		5x5	10.1	1.2	***		
		10x10	10.6	1.2	***	0.30	0.80
	BD_{dev}	20x20	10.0	1.2	***		
		elevation	2.65	1.7	*		

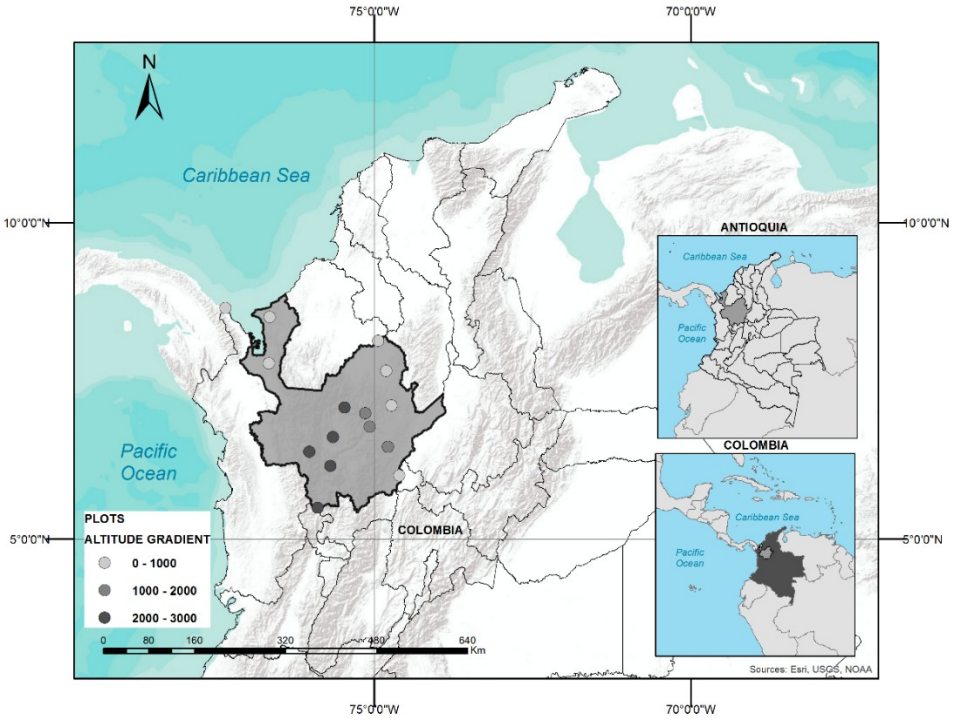

Figure 1.1) Location of 15 1-ha plots in Antioquia on a regional map (inset) to show its location within Colombia. The elevation range of the plots are presented in grayscale. white color for plots located between 0-1000 m asl. Gray for plots located between 1000-2000 m asl, and black for those located between 2000-3000 m asl.

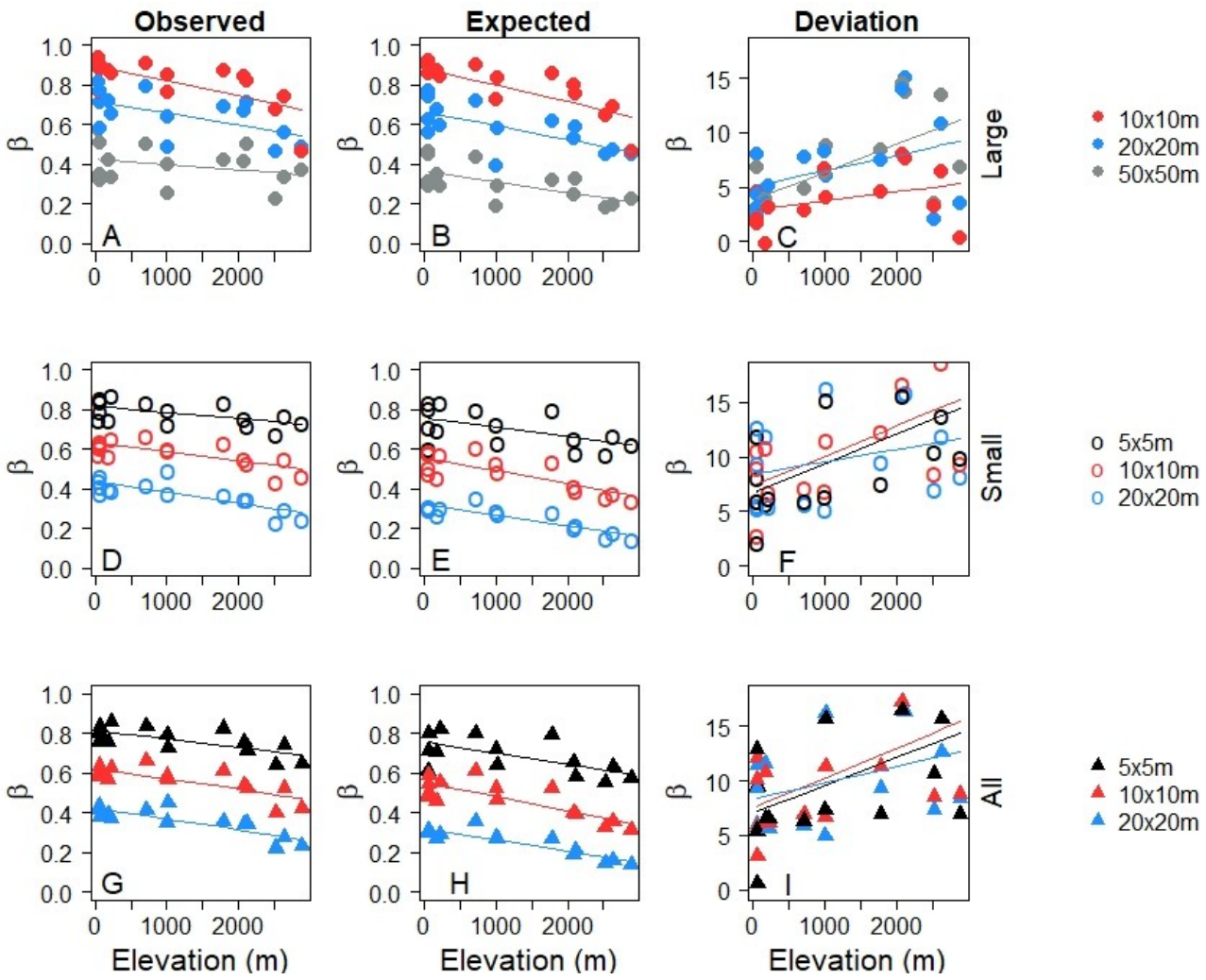

Figure 1.2) Observed (BD_{obs}), expected (BD_{exp}), and standardized (BD_{dev}) patterns of variatio of β-diversity along the elevational gradient. β-deviation (BD_{dev}) is taken as (BD_{obs} – BD_{exp}) /SD_{exp}. Upper panel (A, B, C): large trees (DBH ≥ 10 cm). Middle panel (D, E, F): small trees (1≤ BDH<10 cm) and Lower panel (G, H, I): all trees (DBH ≥ 1 cm). Large trees are taken into account in an area of 1-ha. Small and all the trees are taken into account in 0.16-ha plot.

APPENDIX S1.1: Supplementary methods

Schematic representation of the analytical procedure employed to generate the soil data sets. A) Data input consist of the available environmental variables at the 20 m × 20 m quadrat scale. B) Bilinear interpolation procedure based on samples at 20 m × 20 m scale. Each variable is interpolated at 10 m × 10 m and 5 m × 5 m; for 50 m × 50 m quadrat scale we use the mean of the soil variables at 20 m × 20 m. C) With each interpolated data set was run a PCA analysis, in all cases the first PC explained >70% of the multivariate variation, then was extracted the standard deviation of each PCA done with each data set by grain size. The value of standard deviation was used as a measure of environmental heterogeneity in the mixed linear models.

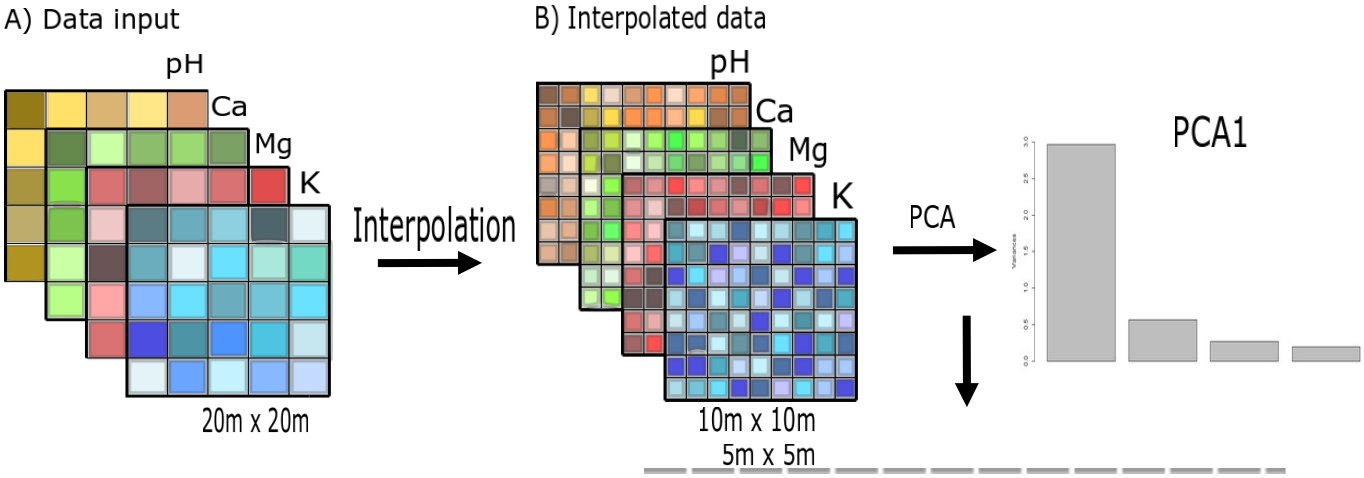

	Standard deviation			
Plot	**5m x 5m**	**10m x 10m**	**20m x 20m**	**50m x 50m**
Caicedo	-0,5297	-0,5321	-0,4751	-0,5140
Jardín	0,2724	0,2770	-0,3431	-0,2174
Maceo	-0,3511	-0,3593	-0,2030	-0,0852
Ventanas	-0,5921	-0,5894	-0,4949	-0,3450
Caucasia	-0,7132	-0,7137	-0,6071	-0,5438
El Bagre	-0,3295	-0,3346	-0,2138	-0,4286
Puerto Triunfo	-0,3295	-0,3346	-0,2138	-0,4286
Carepa	0,6038	0,6105	0,6310	0,1942
Necoclí	-0,4199	-0,4138	-0,4423	-0,2762
Sapzurro	0,7819	0,7570	0,9277	0,2283
Anorí	-0,0533	-0,0353	-0,3244	0,0757
Belmira	-0,1775	-0,1750	-0,3181	-0,0962
Angelopolis	3,2116	3,2155	3,2498	3,4879
Porce	-0,7074	-0,7059	-0,6026	-0,5178
Segovia	-0,6666	-0,6663	-0,5704	-0,5334

SUPLLEMENTARY FIGURES

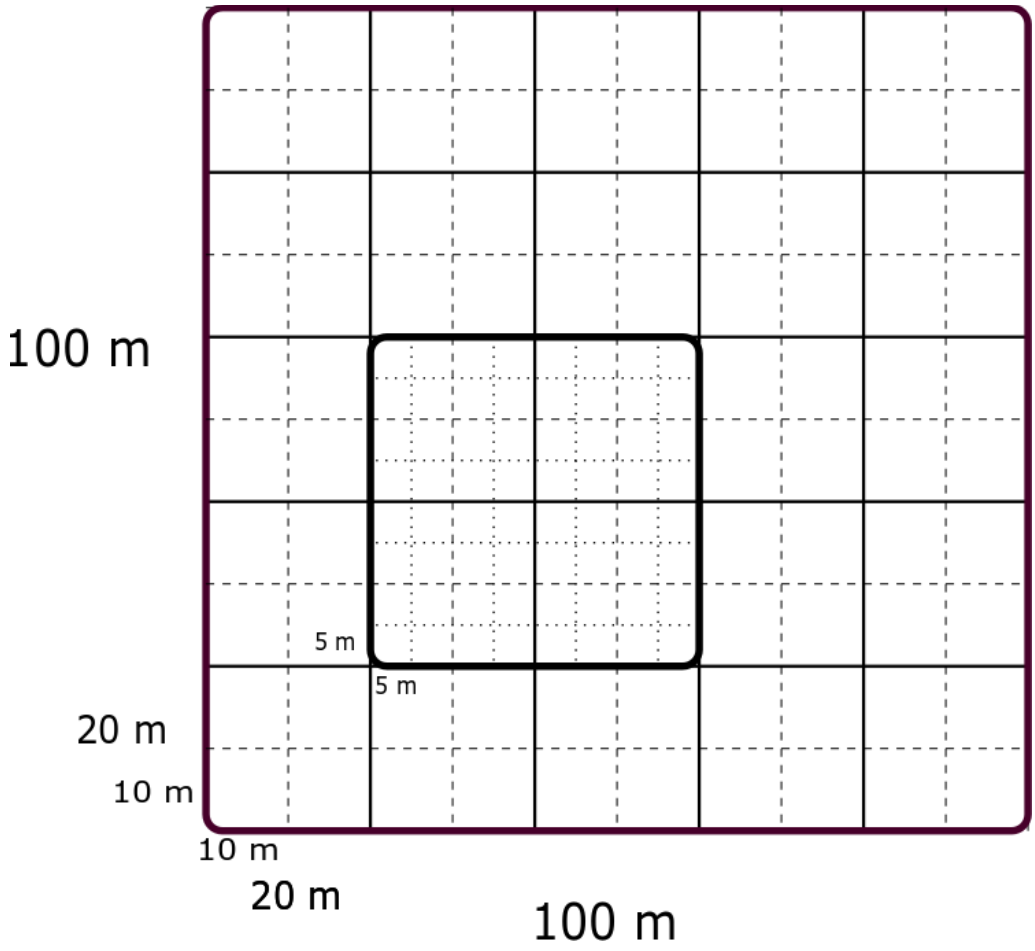

Figure S1.1. Graphical representation of each one of the plots. Continuous lines represent the design of the plot in reality. In the terrain, each plot has 100 m × 100 m, divided by subplots of 20 m × 20 m. Inside the plot, there is a subplot of 40 m × 40 m, subdivided into smaller subplots of 10 m × 10 m. Discontinuous lines in gray represent an imaginary grille composed of 10 m × 10 m subplots, in the whole plot. Dotted lines represent an imaginary division of 5 m × 5 m within the 40 m × 40 m subplot. In the 1-ha plot, all trees, shrubs and tree ferns with DBH ≥ 10 cm are measured and mapped. In the 40 m × 40 m subplot, all the individuals with DBH ≥ 1 cm are measured.

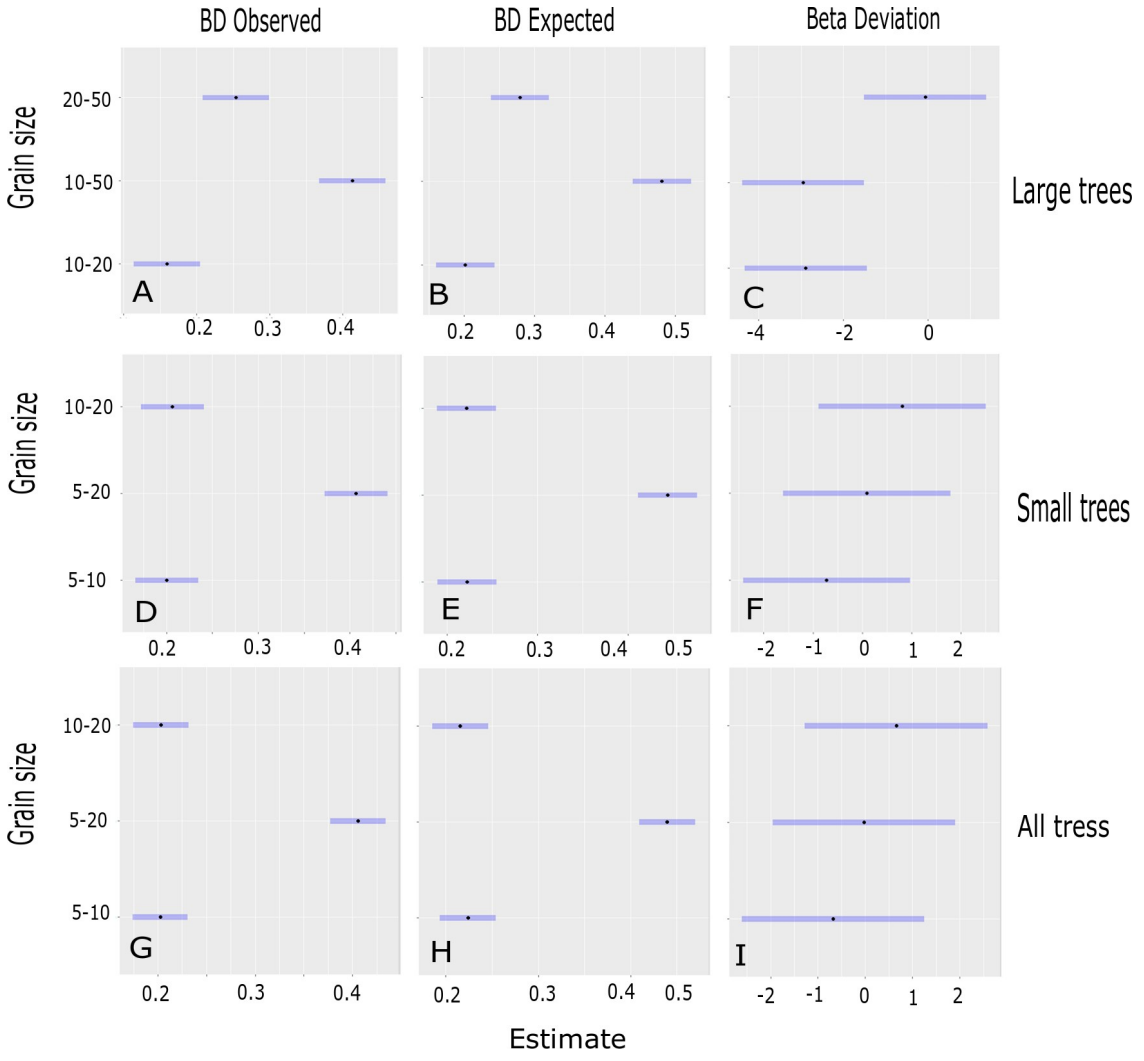

Figure S1.2) Post hoc analysis for ANCOVA. Multiple comparisons with interaction terms across groups for each one of the linear mixed model previously fitted. Comparisons among the relationship (slopes) grain-size and elevation were done with "Tukey" test. A pairwise analysis was run for conducting comparisons among all possible pairs of combinations. *X*-axes show the comparison between the slopes in each grain size. The overlap between lines means that there are no significant differences among slopes.

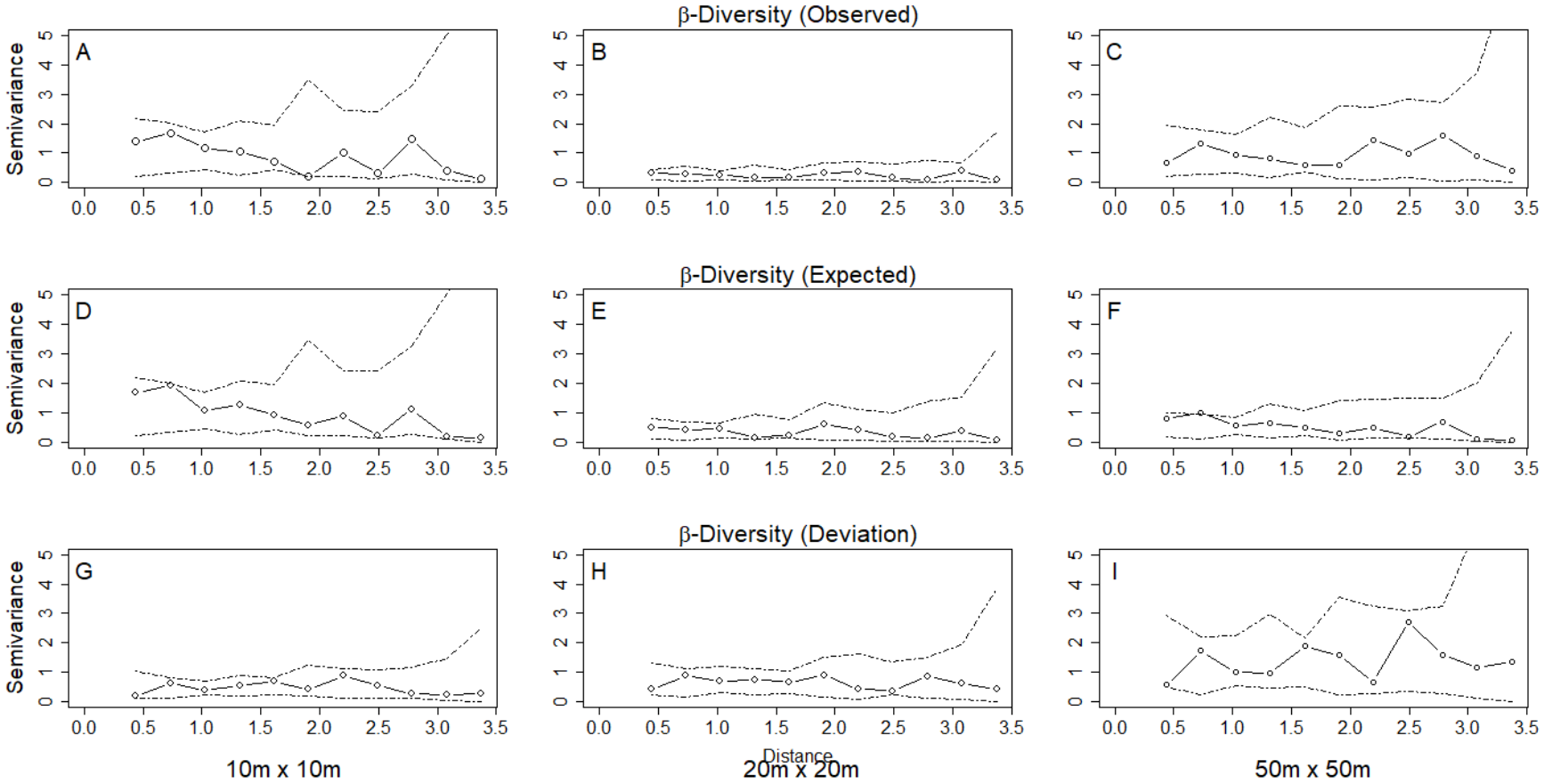

Figure S1.3) Mixed linear model validation for large trees using variograms with model residuals using Pearson method and geographical coordinates of the plots. DBobs by grain size (A: 10 m × 10 m, B: 20 m × 20 m and C: 50 m × 50 m). DBexp by grain (D: 10 m × 10 m, E: 20 m × 20 m and F: 50 m × 50 m) and DBdev by grain size (G: 10 m × 10 m, H: 20 m × 20 m and I: 50 m ×50 m).

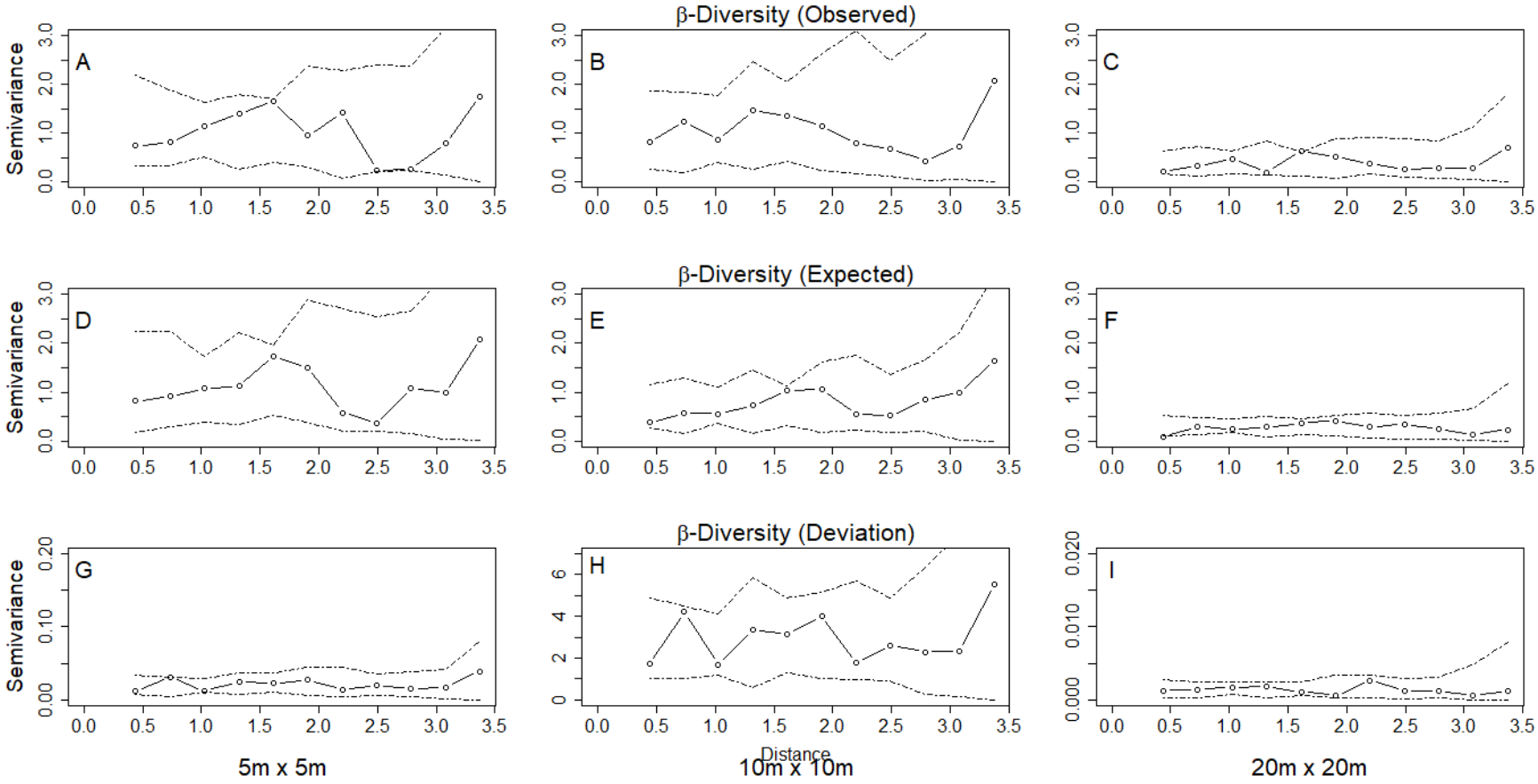
β-Diversity (Observed)
β-Diversity (Expected)
β-Diversity (Deviation)
Semivariance
Distance
A
B
C
D
E
F
G
H
I
5m x 5m
10m x 10m
20m x 20m

Figure S1.4) Mixed linear model validation for small trees using variograms with model residuals using Pearson method and geographical coordinates of the plots. DBobs by grain size of (A: 5 m × 5 m, B: 10 m × 10 m and C: 20 m × 20 m). DBexp by grain size of (D: 5 m × 5 m, E: 10 m × 10 m and F: 20 m ×20 m) and DBdev by grain size of (G: 5 m × 5 m, H: 10 m ×10 m and I: 20 m ×20 m).

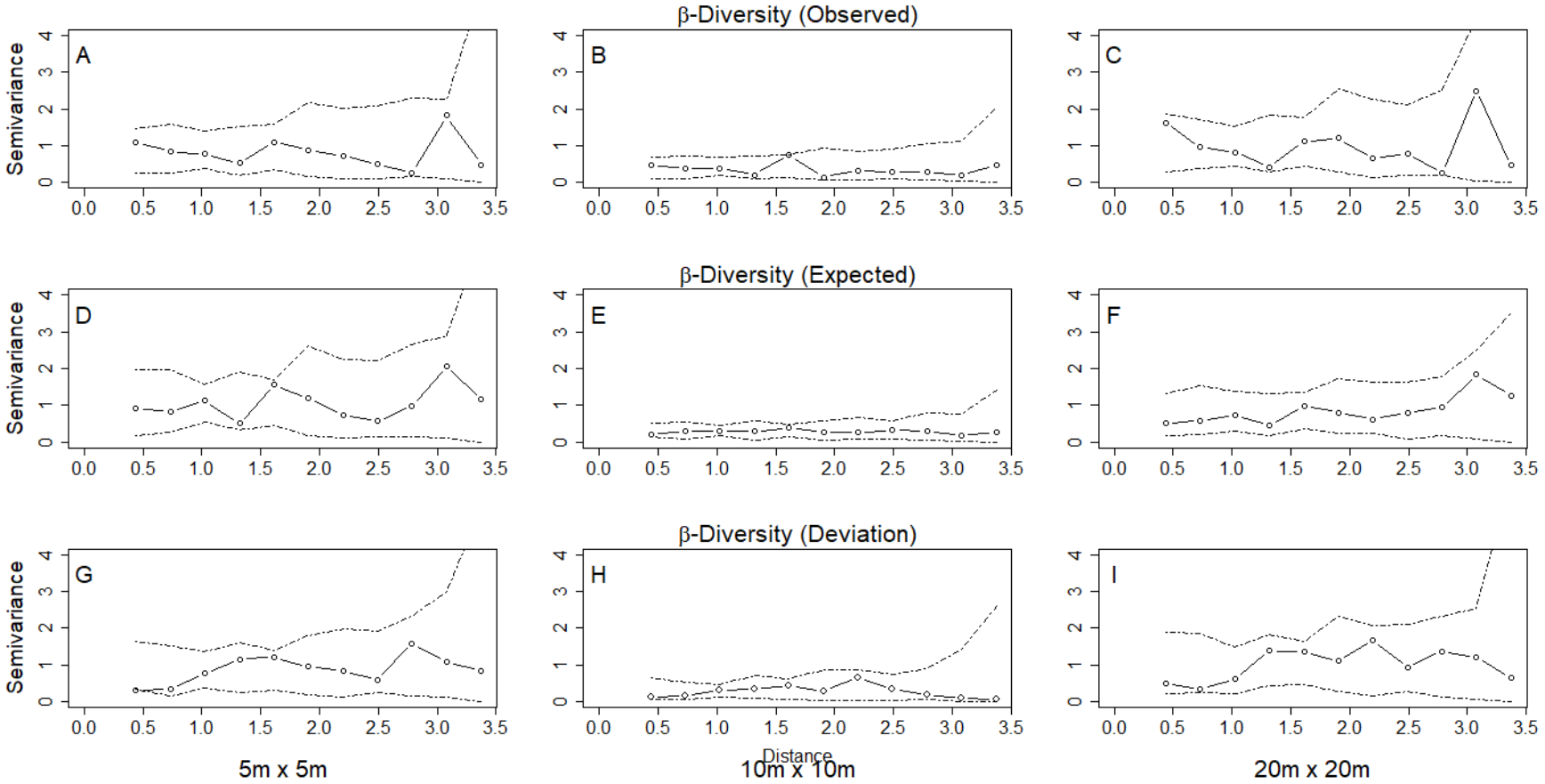

Figure S1.5) Mixed linear model validation for all trees using variograms with model residuals using Pearson method and geographical coordinates of the plots. DBobs by grain size of (A: 5 m × 5 m, B: 10 m × 10 m and C: 20 m × 20 m). DBexp by grain size of (D: 5 m × 5 m, E: 10 m × 10 m and F: 20 m ×20 m) and DBdev by grain size of (G: 5 m × 5 m, H: 10 m ×10 m and I: 20 m ×20 m).

Table S1.1. Analysis of covariance (ANCOVA). Comparison of slopes between grain-size and elevation for the β-deviation and for all of the DBH cut-off sizes. Post hoc analysis was done using a Tukey Honestly Significant test.

	Comparisons between slopes	***p*-value**
Large trees	10–20	0.0001
	10–50	0.0001
	20–50	0.1
Small trees		
	5–10	0.54
	5–20	0.1
	10–20	0.46
All trees	5–10	0.66
	5–20	0.99
	10–20	0.67

CHAPTER II

ECOLOGICAL MECHANIMS AND SAMPLING DEPENDENCE OF LOCAL β-DIVERSITY IN TWO NEOTROPICAL FORESTS AT CONTRASTING BIOGEOGRAPHIC REGIONS.

ABSTRACT

β-diversity has been a focal point in community ecology. However, little is known about the ecological mechanisms and factors governing locally in different biogeographic regions in tropical forests, and how the sampling effort may affect our estimations. Different hypotheses suggest that β-diversity is driven by main processes such as niche selection, environmental filtering, and dispersal limitation. Other hypotheses suggest that β-diversity is driven just by variation in species pool, rather than different ecological mechanisms. These hypotheses have been studied through latitudinal comparisons but comparing different biogeographic regions at similar latitudes is scarce. Using two 25-ha plots in contrasting biogeographic regions in Colombia (Amazonas and Andes), we compare β-diversity and β-deviation (standardized differences from null values) to measure the effect of local community assembly mechanism after removing the effect of species pool. To calculate the sampling effect, we compare the same metrics using different grain-sizes and tree cut-off sizes in both regions. We found that β-diversity was higher in the region with the highest diversity at lowlands. After controlling the species pool effect, β-deviation was also higher in lowlands than highlands. Moreover, β-deviation change when grain-size and cut-off tree category changed. We suggest that by increasing the sampling effort both, the representation of the species pool and environmental heterogeneity is better captured. And that deterministic processes may have equal or higher influences in highly diverse regions than low-diverse regions, which can be masked by the regional sampling effect and the differences in species pool.

Kewords: Beta-diversity, species variation, Andean forest, Amazon forest, ecological mechanism, Beta-deviation.

INTRODUCTION

The variation in species composition within tree communities (local β-diversity) is considered a paramount measure to advance our understanding of the mechanisms that maintain species coexistence in plant communities (Anderson et al., 2011; Bergamin et al., 2017; Socolar et al., 2015). In the tropics, it has been widely proposed that tree local β-diversity decreases from lowlands to highlands (Kraft et al., 2011; Mori et al., 2013; Tello et al., 2015). Nevertheless, the mechanism that drives this pattern is still under debate. On the one hand, previous studies have shown that the strength of community assembly mechanisms, such as habitat filtering or dispersal limitation, change alongside elevation. The extent to which the underlying mechanisms of community assembly determine local species turnover seem to be greater in (cold) highlands than in (warm) lowlands (Martínez-Villa et al., 2020; Tello et al., 2015). Thus, compositional turnover of local community assemblage at different elevations can be attributed to environmental heterogeneity (Stein et al., 2014), topography, and edaphic variation (Baldeck et al., 2013). On the other hand, other authors argue that the tree local β-diversity shifts along an elevational gradient is an artifact of the change in the species pool, rather than changes in the ecological mechanisms (Kraft et al., 2011). Thus, after controlling for the size of the species pool, the difference in local β-diversity alongside elevation should disappear. This debate suggests that it still is unclear if the pattern of variation in tree local β-diversity in the elevational gradient in tropical forests is due to differences in the underlying mechanisms or simply due to sampling effects associated with the size of the species pool (Chase & Myers 2011).

An additional factor to the underlying mechanisms or the species pool on local β-diversity estimates, and that plays a key role is the sampling dependence, such as grain-size. The implicit scale-dependence of local β-diversity is highly related to the representativeness of species included in the grain compared to the total number of species at the regional scale (Tan et al., 2017). According to the theoretical framework proposed by Barton et al. (2013),

we expect an increase of local β-diversity with grain-size reduction (negative relationship) because the probability of finding shared species between grains diminishes. Recently, the interest in studying the effect of grain-size on shaping tree local β-diversity has increased because it can lead to different conclusions on factors such as the degree of either species aggregation (Bar-Massada et al., 2018) or the relative species abundance (Chase & Knight, 2013). However, the relatively small area used in many studies limits the possibility of estimating tree local β-diversity at multiple grain-sizes on the same site. Therefore, studies that shed light on an appropriate grain-size to analyze local β-diversity in different forest types are scarce. The vast majority of the studies that focus on local species variation at different elevations in the tropics use plots of 0.1-ha (e.g., Kraft et al., 2011; Mori et al., 2013; Tello et al., 2015), and just one study has used 1-ha plots and multiple grain-sizes (Martínez-Villa et al., 2020). Other studies have used large plots (>20-ha) but focused on the latitudinal gradient (De Caceres et al., 2013, Baldeck et al., 2013; Tan et al., 2018) rather than on the elevational one. Comparative studies using large plots located at contrasting elevations are needed to inform about the consistency of the former reported patterns found using smaller plots (0.1-ha to 1-ha plots) along the elevational gradient, and thus, begin to consider which grain-size are most appropriate for studying local β-diversity in different forest types.

Sampling dependence on local β-diversity estimations is not related solely to grain-size, but also to the tree cut-off size (i.e., tree size). The most common diameter at breast height (DBH) employed in β-diversity studies are either 2.5 cm (e.g., Kraft et al., 2011, Tello et al., 2015) or 10 cm (Mori et al., 2013), but there exist few studies comparing the ontogenetic effects or the inclusion of different tree cut-off size (Chao et al., 2006; Stier et al., 2016; Martinez-Villa et al., 2020). In most forest inventories used to analyze variation in species composition, regardless of the cut-off size, the data are assumed as a complete representation of the community, an assumption that can lead to empirical errors due to the possible numerical undersampling (Chao et al., 2005; 2006). For example, just including large trees (DBH>10 cm), many understories and/or rare species are excluded from the analyses leading to underestimating observed local β-diversity, since there are fewer unshared species considering mature trees (Chao et al., 2006). Thus, local β-diversity

differences should emerge simply due to the (sub-) sampling effect rather than by ecological effects (Stier et al., 2016). Additionally, with including different tree cut-off sizes, we include different aspects of community variation, which may result in different ecological conclusions. In the tropics, some authors have demonstrated that small individuals are strongly associated with habitat type (Duque et al. 2002; Comita et al., 2007) and soil nutrients (Holste et al., 2011), while large trees with topography (Zuleta et al., 2018, Muscarella et al., 2019). The tree cut-off size and the undersampling effect on β-diversity have been recently analyzed using simulations (Beck et al., 2013; Schroeder & Jenkins, 2018; Zou & Axmacher, 2021), and only a few empirical studies (Beck et al., 2013; Tello et al., 2015). This lack of conclusions based on empirical data highlights the importance of large and complete inventoried plots as the ideal scenario to test the sampling effect on local β-diversity estimations (Sreekar et al., 2018).

Both the variation in grain-size and the inclusion of different tree-cut off sizes may affect local β-diversity estimates in ways largely unknown and that has been little studied by field sampling. In this study, we used two 25-ha plots located at contrasting elevations and biogeographic regions in the Neotropics (Amazon and Andean regions), which have differences in total species richness and size of the species pool, to assess the relative importance of ecological process and sampling effects (grain-size and cut-off tree size) on determining local β-diversity in tropical forests. We use null models with different grain-sizes and including different tree cut-off sizes to quantify the relative importance of both deterministic and stochastic processes at sampling sizes on shaping the variation of β-diversity at a local scale (Chase & Myers, 2011, Catano et al., 2017). Specifically, we want to answer the following questions: i) Are the extent of ecological mechanisms different between contrasting elevations in determining the community assembly? We hypothesize that β-diversity correlates with environmental heterogeneity (soils and topographic variables) more strongly in cold highlands than in warm lowlands, as a consequence of strong deterministic processes; therefore, we expected more deviation from a null model in highlands. ii) How do different grain-sizes or tree cut-off sizes affect local β-diversity estimates in different types of forest at contrasting elevations? Due to the higher spices diversity in lowlands, smaller sampling size (by smaller grain-size or including less

individuals) will have greater effect in lowlands than in highlands, overestimating local β-diversity. With this study, we hope to provide information about the appropriate sampling size in different types of forest for monitoring local β-diversity in the tropics.

Methods

Study area

The study area comprises two long-term tropical forest plots of 25-ha, each one (500 m × 500 m), established in highly diverse forests in Colombia. These two plots belong to the ForestGEO network (Davies et al. 2020), a monitoring network including more than 60 forest plots established worldwide and monitored under the same protocol (Condit, 1998). The first plot is the Amacayacu Forest Dynamics Plot (hereafter AFDP), located in the Amacayacu National Park in the Colombian Amazon Forest (3°48′02′′S-70°16′04.29′′W). The life zone corresponds to a Tropical wet forest (Holdridge, 1978) on terra firme. The elevation is 93 m asl, but the plot is not subjected to flooding by the Amazon River. The mean annual temperature (MAT) is 25.8ºC, mean relative humidity is ca. 86%, and the mean annual precipitation (MAP) is 3,216 mm (climate statistics for the weather station at the airport at Leticia, 55.39 km away from the plot; Prieto 1994). Soils are dominated by Ultisols, characterized by high acidity, low base saturation, and poor nutrients (Chamorro 1989).

The second study site is La Planada Forest Dynamic Plot (hereafter LPFDP), located in the department of Nariño, in La Planada Natural Reserve in southwestern Colombia (1°17′ N-78°15′ W), on the western slope of the Andean Forest (Vallejo et al., 2004). This Pacific flank of the Andes is characterized by a dense fog with periods of low cloud cover (Grubb and Whitmore 1966). The elevation is 1797, and the life zone is defined as pluvial premontane forest (Holdridge, 1978). The MAT is 19°C, and the MAP is 4,087 mm (Anderson-Teixeira et al., 2015). Soils are dominated by Andisols (Anderson-Teixeira et al., 2015), developed from volcanic ash, characterized by slow decomposition of organic matter and high fertility (Vallejo et al., 2004). Sites were deliberately chosen to span a contrasting biogeographic region to assess the different mechanisms that raise local β-diversity on Colombian highlands and lowlands regions.

Plot census

Within each 25-ha plot, all shrubs, trees, palms, and tree ferns with a diameter at breast height (DBH) ≥ 1 cm were mapped, tagged, and measured according to Condit, 1998. Voucher collections were made for each potentially unique species in each plot. For AFDP, voucher specimens were deposited and identified in Herbario Amazónico Colombiano (COAH) of the Instituto Amazónico de Investigaciones Científicas (SINCHI). For LPFDP, voucher specimens were deposited in the Instituto de Investigaciones Biológicas Alexander Von Humboldt (AvH). We used the Baseline information (Table 1, S1) of each 25-ha plot.

Sampling effect

Grain size effect

To assess the grain-size effect on local β-diversity, we first divided each 25-ha plot into 25 1-ha plots (our sample unit). Then, each 1-ha plot was divided into three different grain-sizes:10 m × 10 m (0.01-ha), 20 m × 20 m (0.04-ha), and 50 m × 50 m (0.25-ha). The number of grains decreases when increasing the grain size (100, 25, 4, respectively; Figure. S1).

Cut-off size category and species pool effect

We also divided the dataset for each plot into three cut-off categories. All individuals with DBH ≥ 1 cm (hereafter all trees), 1<DBH<10 cm (hereafter small trees), and DBH ≥ 10 cm (large trees). These cut-off size categories are present in all grain-sizes, allowing analyze the the effect of the species pool (number of species included) on local β-diversity estimates.

Environmental data

Soil samples

Soil samples were taken in the first 10 cm horizon (mineral soil after removing the organic layer), at the intersection of a 40 or 50 m grid across the plots, with additional point samples taken near the alternate grid to estimate fine-scale variation soils (Baldeck et al., 2013). Soil variables concentration was extracted with Mehlich-III solution and analyzed

on an atomic emission-inductivel couple plasma (AE-ICP, Perkin ElmerInc., Massachusetts, USA) (Baldeck et al., 2013). The common variables between the two plots were selected to build the soil dataset: P, pH, Al, Ca, Fe, K, Mg, and Mn. To obtain the soil samples at each 20 m × 20 m, 10 m × 10 m, and 50 m × 50 m for each 1-ha plot (within each 25-ha plot), we used a bilinear interpolation method based on soils resampled data. This method employs the distance-weighted average of the nearest pixel values to estimate samples that were not measured directly at fine-scale (Hijmans et al., 2016). Spatial analyses were run employing geoR (Ribeiro & Diggle 2001) and raster (Hijmans et al. 2016) packages in R software.

Topographic data

Topographic variables correspond to elevation, slope, and convexity calculated throughout each 1-ha plot at the 10 × 10 m, 20 × 20 m, and 50 × 50 m grain-size using the CTFS fgo.analyze R package (http://ctfs.si.edu/) (Lepore et al., 2020). The database contains elevation data for each 5 × 5 m used to estimate the mean elevation of each 10 m quadrant. The slope is the average slope of the four planes formed by connecting three corners of a quadrant at a time. And finally, convexity is estimated as the center point's elevation minus the mean elevation of the four corners (Fig S2).

Ecological assembly mechanism (β-diversity and β-deviation)

β-diversity

For each 1-ha plot (within each 25-ha plot), we built a matrix X_{ij} with n × p (grain by species), where x_{ij} is the number of individuals of each species *j* in the grain *i* (De Cáceres et al., 2012). This matrix was built for each grain-size/cut-off category combination separately. After that, each matrix X_{ij} was transformed using the Hellinger method. The ecological matrices are characterized by a large number of zeros, which bias the distributions, this transformation reduce the weight of zeros and dominant species and increases the weight of rare species (Pierre Legendre & Gallagher, 2001).

$$Y_{ij} = \sqrt{\frac{x_{ij}}{\sum_{k=1}^{p} x_{ik}}}$$

Where Y*ij* is the transformed X*ij* matrix. x_{ij} is the value of species *j* in the grain *i*, *k* is the species index, and *p* is the number of species in a given grain with row and column indixes *i* and *j* (Legendre and Legendre, 2012, De Caceres et al., 2012). Once we have the Hellinger transformed matrix (Y), the observed β-diversity is estimated as the variance of Y (De Cáceres et al., 2012; Legendre et al., 2005), which is calculated as follows:

$$Observed\ \beta-diversity = Var(Y) = \frac{SS(Y)}{(n-1)}$$

Where SS(Y) is the sum of squares, and n is the number of quadrats employed. Observed β-diversity is 0 when all quadrats have the same composition and 1 when they do not share any species (De Cáceres et al., 2012).

β-deviation

To disentangle the sampling effects associated with the size of species pool and grain-size, we used a null model following Kraft et al. (2011) (but see Mori et al., 2013; Tello et al., 2015). This method is proposed as a statistical control of the variation in the species pool from one region to another and quantifies how the variation of scale accounts for variation in β-diversity (Kraft et al., 2011; Bennett & Gilbert, 2015). The species pool for the three cut-off size categories (all trees, large and small trees) was defined as the total species richness in each one of the 1-ha plot within each 25-ha plot in both regions (after Kraft et al. 2011) (Table S1). To estimate expected β-diversity, we generate a null model for randomizing individuals' location among grains within each 1-ha plot, fixing the number of individuals and relative abundance (Tello et al., 2015). Our null model removes the local processes that determine the species distribution or species clumping in the local assemblages (De Caceres et al., 2012, Tello et al., 2015). In each randomized matrix, we applied the Hellinger transformation and expected β-diversity was estimated as the variance of the transformed matrix (De Caceres et al., 2012). This process is repeated 1000 times in each one of the 1- for each grain size / cut-off category combination. The total expected β-

diversity is the mean of the distribution of β-diversity values under the null model (De Caceres et al., 2012).

Finally, β-deviation is defined as the difference between observed β-diversity and null mean β-diversity value, divided by the standard deviation of the null β-diversity distribution (i.e., standardized effect size). This value indicates the deviation of the observed from a null distribution (De Cáceres et al., 2012; Qian et al., 2013). Therefore, positive and negative β-deviation values indicate higher or lower β-diversity than expected by chance, respectively, while a value of zero means a β-diversity expected under the null model (Myers et al., 2013). However, according to Kraft et al. (2011), a constant β-deviation in the elevational gradient may be due to the observed β-diversity resulting from differences in the size of the species pool. Comparisons between observed β-diversity and β-deviation help assess how β-diversity deviates from a stochastic community and whether the stochasticity or deterministic processes determine to a greater extent the local species assemblage. Similarly, comparisons between elevations help to clarify which process predominates at different elevations.

Data analysis

To quantify the effect of grain size (categorical factor, represented by the length of the side of the reference quadrant (m^2)), species pool, soils heterogeneity, elevation and topography (fixed quantitative factors), on local β-diversity, we used a linear mixed regression model (LMM; Zuur et al., 2009). Soil heterogeneity was calculated as the variation of the interpolated values at each grain size for P, pH, Al, Ca, Fe, K, Mg, and Mn. A principal component analysis (PCA) was run with the soil elements and then we use the standard deviation of each 1-ha plot score on the first axis in the PCA as heterogeneity soil values. We performed a PCA for each grain size and each cut-off size category. All response variables were standardized before being included in the model. Finally, the random effect in the model was defined as a nested random effect with each 1-ha in each 25-ha plot to control particular characteristics in each plot and accounting the hierarchical data (Zuur et al., 2009). The models' random effect was selected, comparing models with the same fixed effect structure and varying random effects. The model with the lowest Akaike Information

Criterion (AIC) presented the best random effect. Model selection was done following (Zuur et al. 2009), starting with a saturated model (including interactions). The best-fixed effects were chosen with the backward stepwise model selection based on the AIC. Models validation for spatial autocorrelation was tested using the semi-variograms of the model residuals for each 25-ha plot, based on 100 draws to define the envelope for the observed significance spatial structure of the residuals. Semi-variograms were done with the geoR package (Ribeiro and Diggle 2001). All the analyses were performed in R 4.0.0 (Core Team 2020).

Results

We sampled 1,299 species in AFDP represented by 90 families and 359 genera. In LPFDP, were sampled 222 species represented by 59 families and 135 genera. The average species richness by 1-ha plot in AFDP was 604 ± 49 and 152 ± 8.2 at LPFDP (Table 1).

Overall, we found that observed and expected β-diversity was higher at AFDP plot (Amazon) compared to LPFDP (Andes), as we expected (Figure 1A-1F). On the other hand, the standardized β-deviation did not follow our expectations of higher values at higher elevations (LPFDP - Andean plot) for all grain-sized and cut-off categories. In fact, β-deviation was similar for AFDP and LPFDP for large trees and was lower for LPFDP (high elevation) for small and all the trees (Figure 1G-1I). This pattern means that after controlling for differences in species pool for large trees, the β-deviation is similar for both regions (Amazon and Andes). It is important to note that, even β-deviation was consistent for both regions, values were always positive (except large trees at 10 m × 10 m), indicating higher species variation than expected by chance. In general, β-deviation was different for each species pool (large, small, and all the trees), suggesting that the β-diversity patterns in our results depend of the sampling design.

Regarding the spatial scale, the observed β-diversity increases when decreasing the grain sizes for all the cut-off size categories, as we expected (Figure 1A-1F). On the other hand, β-deviation increases when the grain-size increases for large trees, but the pattern is reversed for small and all the trees, where the β-deviation decreases when the grain size

increases. Observed β-diversity and expected β-diversity show significant differences among grain-size for all cut-off sizes. β-deviation in AFDP showed significant differences among all grain-sizes for large trees (p-value <0.05), while small and all the trees showed differences between the 10 m × 10 m and 20 m × 20 m. LPFDP had differences between 10 m × 10 m and 20 m × 20 m for large trees, but these grain sizes had no differences for small and all the trees (Figure 1G-1I).

Linear mix effect models indicate a strong effect of grain size on observed, expected β-diversity, and β-deviation. Elevation has a significant impact on determining the shift in all the β-diversity metrics and the species pool's size (species richness). Concerning environmental variables, the slope was significant for observed β-diversity, and soil heterogeneity was related to β-deviation. The interaction between grain size and elevation was one of the determinant variables for the shift in β-diversity and β-deviation in all the cut-off sizes, suggesting that we could obtain different β-diversity estimations at different elevations depending on the grain-size used (spatial scale). Finally, the marginal explained variation values (R2 marginal) presented in the models were higher than 0.8 and always close to conditional variation (R2 conditional), which implies very low relative importance of the random effect (Table 2).

DISCUSSION

β-deviation, grain-size, and cut-off category

There is a debate about if β-diversity variation between regions with different elevations is an effect of the differences in species pool or is the result of varying community assembly mechanisms (Kraft et al., 2011; Qian et al., 2012). Here we analyzed the effect of the species pool on β-diversity variation and different sampling efforts (grain-size and cut-off size). Our first hypothesis predicts that after controlling the size of the species pool, the β-diversity differences between regions disappear, presenting the same β-deviation (Kraft et al., 2011). Our results partially support this hypothesis presented by Kraft et al. (2011). This pattern was only applied for one combination grain-size (10 m × 10 m) and cut-off size (large trees). These results strongly suggest that an essential part of the debate can be

attributed to the variation in the spatial scale (grain-size) across studies or the characteristic of sampling intensity to failure to account for a complete representation of the community, as we did here.

Observed β-diversity was higher in the lowlands than in the highlands (Figure 1A-1F), as we expected. This observed pattern may correspond to the high differences in the total species pool (species richness). This is because, in highly diverse ecosystems, a small fraction of the regional species pool can potentially belong to any given local community, increasing β-diversity, a feature of non-saturated communities, as it is, in this case, the AFDP (Figure S3 A) (Shurin & Srivastava, 2005, Harrison & Howard, 2008). On the other hand, saturated communities such as LPFDP (Fig S3 B) rise faster the asymptote in the relationship regional-local richness and found shared species among local communities increase, thus decreasing β-diversity (Harrison and Howard 2008). To disentangle the deterministic and stochastic processes that shape β-diversity, we used the standardized effect size of β-diversity (β-deviation). Our study's main result is that β-deviation was similar for different biogeographic regions for large trees and was lower in highlands for small and all trees, which contrasts with other tropical studies (Martínez-Villa et al 2020, Tello et al 2015).

The β-deviation pattern for large trees supports the hypothesis presented by Kraft et al. 2011. β-deviation was constant and close to zero between the regions for the combination of 10 m × 10 m and large trees, which means a β-diversity expected by chance. However, for the same cut-off size, the grain-size augmentation increased β-deviation (Figure 1G). Therefore, deterministic processes are more likely to be found with increasing grain-size, highlighting the role of the spatial scale of the sampling unit (Chase 2014; Chase & Myers, 2011; Garzon-Lopez et al., 2014). Other authors have attributed the importance of grain-size to detecting different processes that structure species variation (Legendre et al., 2009; Chase, 2014; Garzon-Lopez, 2014). At very smaller grain-sizes, the unobserved environmental (e.g., topography or soil variation) and even neutral variables (e.g., death and recruitment) will result in a purely spatial process (Legendre et al., 2009). And when the spatial grain-size increases, the relative importance of environmental factors increases

because of the higher probability of finding habitat associations and heterogeneity. Thus, we perceive a more structured system (Chase, 2014; Garzon-Lopez et al., 2014).

It is worth noting that β-deviation in AFDP shows significant differences among the three grain-sizes (P-value < 0.005) (Figure 1G), suggesting that by increasing grain-size, the probability of finding more deterministic processes increases too. But when we increased the grain-sized for LPFDP, β-deviation did not show differences (Figure 1G). This means that the detection of deterministic processes depends on grain-size and the environmental and topographic conditions of the area (Figure S2). For example, Baldeck et al. (2013) found in the same plot (LPFDP) that 13% of the explained variation of β-diversity was dependent on the environment, while in lowland and more diverse plots such as BCI, this percentage was 25%.

The fact that we found lower β-deviation in LPFDP (1800 m asl) than in AFDP (100 m asl) did not follow our hypothesis. In contradiction to other studies, we found a higher magnitude of deterministic processes in the lowland region (with the highest diversity). By including lower tree sizes (DBH ≥ 1cm), a higher representative portion of the species pool is better captured, and so, we also capture distribution patterns of juveniles and understory species. Chase & Myers (2011) and Siqueira et al. (2020) explained that in some ecosystems, the deterministic process might have even more importance in highly diverse regions than in low diverse regions when density-dependence processes are overriding for niche selection or by the presence of strong environmental gradients. The positive relationship between high diversity and high β-deviation indicates that in AFDP, the species aggregation was stronger to cause non-random variation than in LPFDP. To test this idea, we calculated the relative conspecific Omega (Ω) neighborhood density index (sensu Condit et al., 2000) at five scales (10, 20, 30, 40, and 50 m), for those species with more than 50 individuals per 25-ha, as a function of the abundance of each species on log-log scale. Aggregation is indicated when Ω > 1, random dispersion when Ω = 1 and spacing at some scale or hyperdispersion when Ω < 1. The Ω was always higher in AFDP than in LPFDP (Figure 2A, Table S2). When we compared the Ω for small and all the trees, within the region, the pattern was similar. Therefore, including lower size categories, small trees

can gain higher importance in shaping the species variation. Although we do not have mortality metrics, by the Janzen (1979)-Connel (1971) theory, we can assume that communities with higher aggregation present higher density-dependent processes, which are more important in the highest-diverse region.

The influence of assembly processes

Although β-deviation was greater in the lowlands (Amazonas) than in the highlands (Andes), the value was always positive, indicating that both regions exist deterministic processes to a greater or lesser extent structuring species variation. In highly diverse forests, such as the Amazon or Andes, it has been shown that soil nutrients influence species' spatial distribution (John et al., 2007; Baldeck et al., 2013). Our models' results corroborate these findings since β-deviation presented a significant relationship with soil variation (P-value 0.02, Table 2). The significant relationship can be interpreted as a direct response to variation in soil properties, reflected in the own species' variation. Even though soil variation appears as an essential component for niche structuring, different soil components can operate differentially in each forest type. In LPFDP, for example, have been shown that K, P, Fe, and N have particular importance, while in lowland forests, such as BCI, B, K, Ca, and Mg have a robust priority on community structure (John et al., 2007). The slope was only significant for observed β-diversity (Table 2) but not for β-deviation. The lack of significance for topography, considering that we have a mountain region in the analysis, can be related to the relatively flat plateaus in both plots (AFDP=20 m and LPFDP=40 m, Fig S2), showing more significance in soil variation than in the topography. Previous studies have shown higher importance of soil resources than topography, explaining species variation (Baldeck et al., 2013).

The similarity between the β-diversity and β-deviation patterns for the cut-off categories of small trees and all the trees, implies that small tree cut-off categories may drive a large extent of the species variation pattern. Comita et al. (2007) documented that in early life stages, a strong habitat association exists that gradually changes in mature stages. The habitat specialization at early life stages can strongly influence our estimations when we

include small trees. If habitat association increases, β-deviation too, and stronger deterministic processes can be found. On the other hand, just analyzing large trees, the β-diversity pattern was completely different. Underlying mechanisms that shape β-diversity change with varying life stages, and mechanisms detected just for large trees could be rarely seen for small trees and vice-versa. For example, the neighborhood competition changes depending on the tree size and life stage (Zhang et al., 2017; Zhu et al., 2018). Therefore, density dependence processes must be found strongly in small trees or including small trees in the community.

We show the extent of ecological mechanism change between regions at different elevations, as reported by other studies (De Cáceres et al., 2012; Qian et al., 2013), making elevation a key factor (Table 2). (Tello et al., 2015) In the tropics, it is widely recognized that the extent of deterministic processes increases with elevation because harsh conditions can impose stronger filters (Mori et al., 2013; Tello et al., 2015; Martinez-Villa et al., 2020). Nevertheless, higher β-deviation in lowlands and highly diverse ecosystems has been reported (Sabatini et al., 2018; Siqueira et al., 2020). The high diversity and productive regions can also impose harsh conditions in terms of species interactions, such as higher competition, priority effects (Chase, 2010), or density dependence (Condit et al., 2000; Lamanna et al., 2017). Mechanisms that are often overlooked just by analyzing environmental conditions and that highlight the importance of analyzing different biogeographic areas separately (Qian et al., 2013). Another important point is that because of high diversity, niche-partitioning should be narrower and, thus, narrower ecological ranges (Giles Egbert et al., 2004). Although we must be cautious when extrapolating this hypothesis directly to lowlands vs. highlands, assuming wider ecological ranges for highlands species, just for chance, higher species homogenization can be expected and, therefore, less steep β-deviation change (Sabatini et al., 2018). Further analysis in large and complete survey plots, including other factors such as light gradient or gap dynamic, should be done to disentangle mechanisms in different regions. So far, we have shown that highly diverse lowlands regions also present high determinism, and including more than environmental factors is required to understand better what shapes the species variation.

Conclusions

We have shown a strong sampling effect (in terms of grain-size and cut-off tree categories) on β-diversity and β-deviation estimations. β-deviation always varies with the grain-size, corroborating the critical importance of the sampling unit in diversity analysis. Regarding the cut-off tree categories, small (1<DBH<10 cm) and all the trees (DBH>1cm) presented high similarity in the β-diversity patterns. This indicates that a high proportion of the species variation patterns is driven by the smaller trees, mainly because of an accurate quantification of spatial aggregation, including a better representation of the species pool. Finally, high β-deviation was found in lowland and highly diverse regions compared to the highland regions. These results evidence, first, the community size's role in β-diversity analysis and the importance of accounting for its effect. Second, in highly diverse ecosystems, deterministic processes can be equal to or more important than in less diverse ecosystems. In these regions, niche selection can be driven mainly by dispersal processes and differences in aggregation patterns.

REFERENCES

Anderson-Teixeira, K. J., Davies, S. J., Bennett, A. C., Gonzalez-Akre, E. B., Muller-Landau, H. C., Joseph Wright, S., … Zimmerman, J. (2015). CTFS-ForestGEO: A worldwide network monitoring forests in an era of global change. *Global Change Biology*, *21*(2), 528–549. https://doi.org/10.1111/gcb.12712

Anderson, M. J., Crist, T. O., Chase, J. M., Vellend, M., Inouye, B. D., Freestone, A. L., … Swenson, N. G. (2011). Navigating the multiple meanings of β diversity: A roadmap for the practicing ecologist. *Ecology Letters*, *14*(1), 19–28. https://doi.org/10.1111/j.1461-0248.2010.01552.x

Baldeck, C. A., Harms, K. E., Yavitt, J. B., John, R., Turner, B. L., Navarrete, H., … Thomas, D. W. (2013). Soil resources and topography shape local tree community structure in tropical forests Soil resources and topography shape local tree community structure in tropical forests. *Proceedings of the Royal Society of London B: Biological Sciences*, *280*, 20122532. https://doi.org/10.1098/rspb.2012.2532

Bar-Massada, A., Yang, Q., Shen, G., & Xihua, W. (2018). Tree species co-occurrence patterns change across grains : insights from a subtropical forest. *Echosphere*, *9*(May),

1–12.

Barton, P. S., Cunningham, S. A., Manning, A. D., Gibb, H., Lindenmayer, D. B., & Didham, R. K. (2013). The spatial scaling of beta diversity. *Global Ecology and Biogeography*, *22*(6), 639–647. https://doi.org/10.1111/geb.12031

Beck, J., Holloway, J. D., & Schwanghart, W. (2013). Undersampling and the measurement of beta diversity. *Methods in Ecology and Evolution*, *4*, 370–382. https://doi.org/10.1111/2041-210x.12023

Bennett, J. R., & Gilbert, B. (2015). Contrasting beta diversity among regions : how do classical and multivariate approaches compare ? *Global Ecology and Biogeography*, *25*(3), 368–377. https://doi.org/10.1111/geb.12413

Bergamin, R. S., Bastazini, V. A. G., Vélez-Martin, E., Debastiani, V., Zanini, K. J., Loyola, R., & Müller, S. C. (2017). Linking beta diversity patterns to protected areas: lessons from the Brazilian Atlantic Rainforest. *Biodiversity and Conservation*, *26*(7), 1557–1568. https://doi.org/10.1007/s10531-017-1315-y

Chao, A., Chazdon, R. L., Colwell, R. K., & Shen, T.-J. (2005). A new statistical approach for assessing similarity of species composition with incidence and abundance data. *Ecology Letters*, *8*, 148–159. https://doi.org/10.1111/j.1461-0248.2004.00707.x

Chase, J. M. (2014). Spatial scale resolves the niche versus neutral theory debate. *Journal of Vegetation Science*, *25*(2), 319–322. https://doi.org/10.1111/jvs.12159

Chase, J. M., & Knight, T. M. (2013). Scale-dependent effect sizes of ecological drivers on biodiversity: Why standardised sampling is not enough. *Ecology Letters*, *16*(SUPPL.1), 17–26. https://doi.org/10.1111/ele.12112

Chase, J. M., & Myers, J. A. (2011). Disentangling the importance of ecological niches from stochastic processes across scales. *Philosophical Transactions of the Royal Society B: Biological Sciences*, *366*(1576), 2351–2363. https://doi.org/10.1098/rstb.2011.0063

Comita, L. S., Condit, R., & Hubbell, S. P. (2007). Developmental changes in habitat associations of tropical trees. *Journal of Ecology*, *95*, 482–492. https://doi.org/10.1111/j.1365-2745.2007.01229.x

Condit, R. Ashton, P. Sarayudh, PB. Gunatilleke, S. Gunatilleke, N. Hubbel, P, Foster, R. Itoh, A. LaFrankie, J. Hua, S. Losos, E. Manokaran, N. Sukumar, R. Yamakura, T.

(2000). Spatial Patterns in the Distribution of Tropical Tree Species. *Science*. https://doi.org/10.1126/science.288.5470.1414

Condit, R. (1998). *Tropical forest census plots: methods and results from Barro colorado Island, Panama and a comparison with other Plots*. *Tropical forest census plots*. Tokyo, Japan: Springer. https://doi.org/10.1007/978-3-662-03664-8

Condit, R. S., Ashton, P. S., Baker, P. J., Bunyavejchewin, S., Gunatilleke, S., Gunatilleke, N., … Yamakura, T. (2000). Spatial patterns in the distribution of tropical tree species. *Science*, *288*(5470), 1414–1418. https://doi.org/10.1126/science.288.5470.1414

De Cáceres, M., Legendre, P., Valencia, R., Cao, M., Chang, L. W., Chuyong, G., … He, F. (2012). The variation of tree beta diversity across a global network of forest plots. *Global Ecology and Biogeography*, *21*(12), 1191–1202. https://doi.org/10.1111/j.1466-8238.2012.00770.x

Garzon-Lopez, C. X., Jansen, P. A., Bohlman, S. A., Ordonez, A., & Olff, H. (2014). Effects of sampling scale on patterns of habitat association in tropical trees. *Journal of Vegetation Science*, *25*(2), 349–362. https://doi.org/10.1111/jvs.12090

Giles Egbert, L. J., Davidar, P., Dick, C. W., Puyravaud, J.-P., Terborgh, J., ter Steege, H., & Wright, S. J. (2004). Why Do Some Tropical Forests Have so Many Species of Trees ? *Biotropica*, *36*(4), 447–473.

Holste, E. K., Kobe, R. K., & Vriesendorp, C. F. (2011). Seedling growth responses to soil resources in the understory of a wet tropical forest. *Ecology*, *92*(9), 1828–1838.

John, R., Dalling, J. W., Harms, K. E., Yavitt, J. B., Robert, F., Mirabello, M., … Foster, R. B. (2007). Soil nutrients influence spatial distributions of tropical tree species. *PNAS*, *3*, 864–869. https://doi.org/10.1073/pnas.0604666104

Kraft, N. J. B., Comita, L. S., Chase, J. M., Sanders, N. J., Swenson, N. G., Crist, T. O., … Myers, J. A. (2011). Disentangling the drivers of β diversity along latitudinal and elevational gradients. *Science*, *333*(2011), 1755–1758. https://doi.org/10.1126/science.1208584

Kraft, N. J., Comita, L. S., Chase, J. M., Sanders, N. J., Swenson, N. G., Crist, T. O., … Myers, J. a. (2011). Disentangling the Drivers of Beta Diversity Along Latidunial and Elevational Gradients. *Science*, *333*(September), 1755–1758. https://doi.org/10.1007/s13398-014-0173-7.2

Lamanna, J. A., Mangan, S. A., Alonso, A., Bourg, N. A., Brockelman, W. Y., Bunyavejchewin, S., … Memiaghe, H. R. (2017). Plant diversity increases with the strength of negative density dependence at the global scale. *Science*, *1392*(June), 1389–1392.

Legendre, P., Borcard, D., & Peres-Neto, P. R. (2005). Analyzing beta diversity: Partitioning the spatial variation of cummunity composition data. *Ecological Monographs*, *75*(4), 435–450.

Legendre, Pierre, & Gallagher, E. D. (2001). Ecologically meaningful transformations for ordination of species data. *Oecologia*, *129*(September 2000), 271–280. https://doi.org/10.1007/s004420100716

Legendre, Pierre, & Legendre, L. (2012). *Numerical Ecology*.

Legendre, Pierre, Mi, X., Ren, H., Ma, K., Yu, M., Sun, I. F., & He, F. (2009). Partitioning beta diversity in a subtropical broad-leaved forest of China. *Ecology*, *90*(3), 663–674. https://doi.org/10.1890/07-1880.1

Levin, S. A. (1992). The problem of pattern and scale in ecology. *Ecology*. https://doi.org/10.2307/1941447

Liancourt, P., & Dolezal, J. (2020). Community-scale effects and strain : Facilitation beyond conspicuous patterns. *Journal of Ecology*, *00*, 1–7. https://doi.org/10.1111/1365-2745.13458

Martínez-Villa, J. A., González-caro, S., & Duque, Á. (2020). The importance of grain and cut-off size in shaping tree beta diversity along an elevational gradient in the northwest of Colombia. *Forest Ecosystems*, *7*(2), 1–12. https://doi.org/10.1186/s40663-020-0214-y

Mori, A. S., Shiono, T., Koide, D., Kitagawa, R., Ota, A. T., & Mizumachi, E. (2013). Community assembly processes shape an altitudinal gradient of forest biodiversity. *Global Ecology and Biogeography*, *22*(7), 878–888. https://doi.org/10.1111/geb.12058

Muscarella, R., Kolyaie, S., Morton, D. C., Zimmerman, J. K., & Uriarte, M. (2019). Effects of topography on tropical forest structure depend on climate context. *Journal of Ecology*, (00), 1–15. https://doi.org/10.1111/1365-2745.13261

Myers, J. A., Chase, J. M., Jiménez, I., Jørgensen, P. M., Araujo-Murakami, A., Paniagua-Zambrana, N., & Seidel, R. (2013). Beta-diversity in temperate and tropical forests

reflects dissimilar mechanisms of community assembly. *Ecology Letters*, *16*(2), 151–157. https://doi.org/10.1111/ele.12021

Qian, H., Chen, S., Mao, L., & Ouyang, Z. (2013). Drivers of ??-diversity along latitudinal gradients revisited. *Global Ecology and Biogeography*, *22*(6), 659–670. https://doi.org/10.1111/geb.12020

Qian, H., Wang, X., & Zhang, Y. (2012). Comment on "disentangling the drivers of β diversity along latitudinal and elevational gradients." *Science*, *335*(6076). https://doi.org/10.1126/science.1216450

Sabatini, F. M., Jiménez-alfaro, B., Burrascano, S., Lora, A., Chytrý, M., & Fitzpatrick, M. (2018). Beta-diversity of central European forests decreases along an elevational gradient due to the variation in local community assembly processes. *Ecography*, *41*, 1038–1048. https://doi.org/10.1111/ecog.02809

Segre, H., Ron, R., Malach, N. De, Henkin, Z., Mandel, M., & Kadmon, R. (2014). Competitive exclusion , beta diversity , and deterministic vs . stochastic drivers of community assembly. *Ecology Letters*, *14*(11), 1400–1408. https://doi.org/10.1111/ele.12343

Siqueira, T., Saito, V. S., Bini, L. M., Melo, A. S., Petsch, D. K., Landeiro, V. L., … Heino, J. (2020). Community size can affect the signals of ecological drift and niche selection on biodiversity. *Ecology*, *101*(6), 1–10. https://doi.org/10.1002/ecy.3014

Socolar, J. B., Gilroy, J. J., Kunin, W. E., & Edwards, D. P. (2015). How Should Beta-Diversity Inform Biodiversity Conservation ? *Trends in Ecology & Evolution*, *31*(1), 1–14.

Sreekar, R., Katabuchi, M., Nakamura, A., Corlett, R. T., Slik, J. W. F., Fletcher, C., … Tan, S. (2018). Spatial scale changes the relationship between beta diversity , species richness and latitude. *Royal Society*, *5*. https://doi.org/10.1098/rsos.181168

Stein, A., Gerstner, K., & Kreft, H. (2014). Environmental heterogeneity as a universal driver of species richness across taxa, biomes and spatial scales. *Ecology Letters*, *17*(7), 866–880. https://doi.org/10.1111/ele.12277

Stier, A. C., Bolker, B. M., & Osenberg, C. W. (2016). Using rarefaction to isolate the effects of patch size and sampling effort on beta diversity. *Ecosphere*, *7*(12), 1–15. https://doi.org/10.1002/ecs2.1612

Tan, L., Fan, C., Zhang, C., Gadow, K. Von, & Fan, X. (2017). How beta diversity and the underlying causes vary with sampling scales in the Changbai mountain forests. *Ecology and Evolution*, (March), 1–8. https://doi.org/10.1002/ece3.3493

Tello, J. S., Myers, J. a., Macía, M. J., Fuentes, A. F., Cayola, L., Arellano, G., … Jorgensen, P. M. (2015). Elevational gradients in-diversity reflect variation in the strength of local community assembly mechanisms across spatial scales. *PLoS ONE*, *10*(3), 1–17. https://doi.org/10.1371/journal.pone.0121458

Thang, T. H., Thu, A. M., & Thang, T. H. (2020). Microsite Preferences and Determinants for Recruitment of Keystone Tree Species in a Tropical Montane Forest of Myanmar Microsite Preferences and Determinants for Recruitment of Keystone Tree Species in a Tropical Montane Forest of Myanmar. *Journal of Sustainable Forestry*, *00*(00), 1–16. https://doi.org/10.1080/10549811.2020.1841005

Tucker, C. M., Shoemaker, L. G., Davies, K. F., Nemergut, D. R., & Melbourne, B. A. (2016). Differentiating between niche and neutral assembly in metacommunities using null models of b -diversity. *Oikos*, *125*(6), 778–789. https://doi.org/10.1111/oik.02803

Wiens, J. A. (1989). Spatial Scaling in Ecology. *Functional Ecology*, *3*(4), 385–397. https://doi.org/10.2307/2389612

Zhang, Z., Papaik, M. J., Wang, X., Hao, Z., Ye, J., Lin, F., & Yuan, Z. (2017). The effect of tree size , neighborhood competition and environment on tree growth in an old-growth temperate forest. *Journal of Plant Ecology*, *10*(6), 970–980. https://doi.org/10.1093/jpe/rtw126

Zhu, Y., Queenborough, S. A., Condit, R., Hubbell, S. P., Ma, K. P., & Comita, L. S. (2018). Density-dependent survival varies with species life-history strategy in a tropical forest. *Ecology Letters*, *21*(4), 506–515. https://doi.org/10.1111/ele.12915

Zuur, A. F., Ieno, E. N., Walker, N. J., Savaliev, A. A., & Smith, G. M. (2009). *Mixed Effects Models and Extension in Ecology with R*.

Table 2.1) Baseline descriptive values for each 25-ha plot. All trees: DBH ≥ 1 cm, small trees: 1 cm ≤ DBH < 10 cm, All the trees: DBH ≥ 10 cm. Numbers in parentheses indicate standard deviations (SD).

	25 ha Plot	
	AFDP	**LPFDP**
Total species richness	1,299	222
Species richness (Small trees)	1191	218
Species richness (Large trees)	836	174
Total number of stems	117,041	113,447
Number of stems (Small trees)	102,69	98,792
Number of stems (Large trees)	14,351	14,655
Total number of genus	395	135
Total number of families	90	59
Average number of species per hectare	604(±49.8)	152(±8.2)
Average number of stems per hectare	4680(±495)	4536 (±804)

Table 2.2. Results from the best-fit linear mixed model between observed and expected β-diversity and β-deviation and the explanatory variables. β-deviation is defined as (observed β-diversity – expected β-diversity)/expected SD from the null model. Conditional R2 involves random and fixed effects. Marginal R2 just involved the fixed effect in measuring the goodness of the adjustment and prediction power.

Dependent variable	Variable	Parameter	p-Value	Marginal	Condicional
Observed β-diversity	Intercept	0.54	<0.0001	0.97	0.98
	20x20	-0.81	<0.0001		
	50x50	-1.70	<0.0001		
	Size (Large)	0.80	<0.0001		
	Size (Small)	0.05	0.03		
	Elevation	-0.46	<0.0001		
	Slope	0.02	0.047		
	20x20: Large	0.04	0.003		
	20x20:Elev	-0.16	<0.0001		
	50x50:Elev	-0.10	<0.0001		

	Size (Large): Elev	0.14	<0.0001		
β-deviation	Intercept	0.52	<0.0001	0.86	0.91
	20x20	0.34	<0.0001		
	50x50	-0.23	0.0001		
	Size (Large)	-1.79	<0.0001		
	Size (Small)	0.01	0.7		
	Elevación	-2.54	<0.0001		
	sd soils	0.12	0.02		
	20x20: Large	-0.18	0.02		
	50x50: Large	0.48	0.0001		
	50x50: richness	-2.454	0.0001		
	20x20:Elev	-2.790	0.01		
	50x50:Elev	-2.667	0.007		
	Size (Large): Elev	0.41	<0.0001		

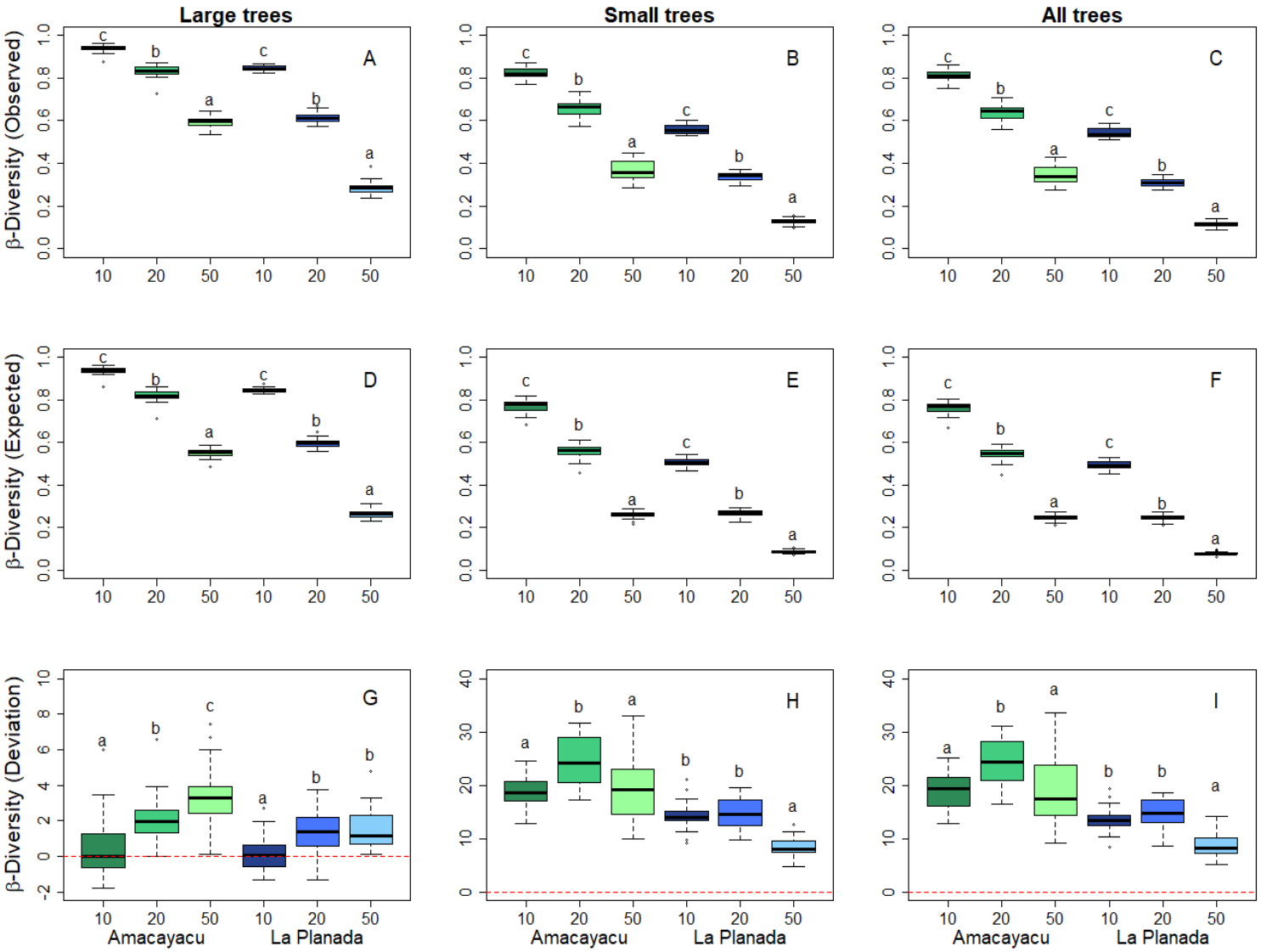

Figure 2.1) Observed ß-diversity for large (A), small (B) and all trees (C). Expected ß-diversity diversity under the null model for large (D), small (E), and all trees (F). And ß-deviation [(BD0bs-BDexp)/SDexp] for large (G), small (H) and all trees (I). For both plots the 25-ha plot was divided in 25 1-ha plots, which were divided in turn in grids of 10 x 10 m, 20 x 20 and 50 x 50 m.

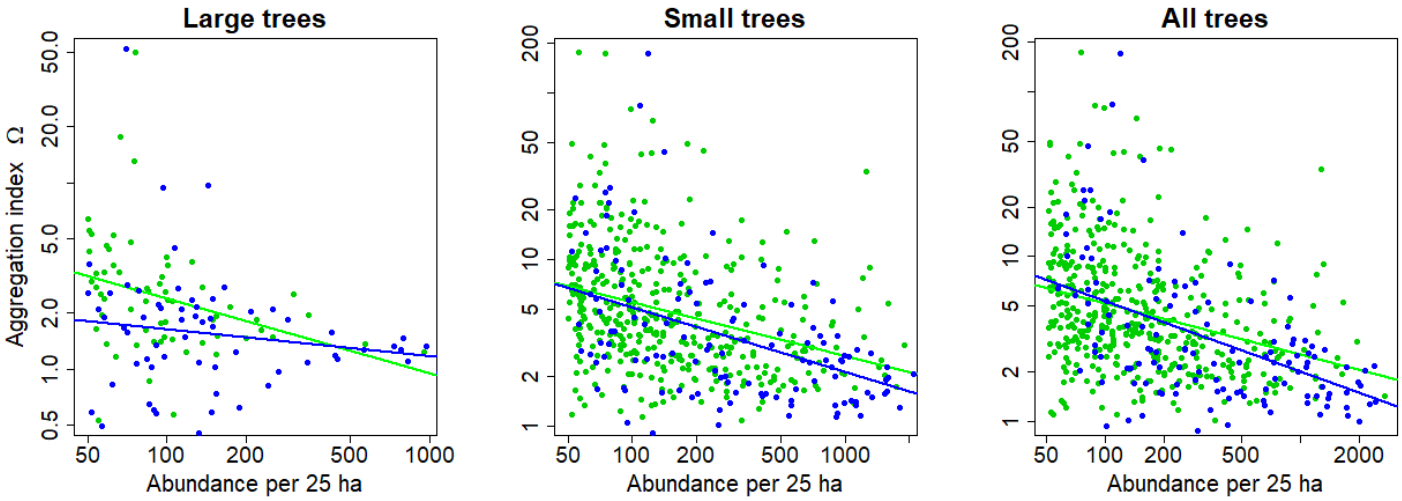

Figure 2.2) Aggregation index (Ω0-10) for species with more than 50 individuals per 25-ha, as a function of the abundance of each species on log-log scale. Each green point represents one species in AFDP and each blue point represents one species in LFDP.

Table S2.1. Species number by each 1-ha plot within the 25-ha plot. All trees: DBH ≥ 1 cm, Small trees: 1 cm ≤ DBH < 10 cm, All the trees: DBH ≥ 10 cm. R: Species richness and N: total number of individuals.

Plot	Amacayacu						La Planada					
Sub-Plot (1ha)	All trees		Small trees		Large trees		All trees		Small trees		Large trees	
	R	N	R	N	R	N	R	N	R	N	R	N
		481		416		65		569		429		
0-0	643	3	592	3	251	0	159	6	146	4	79	571
		497		442		55		607		441		
0-100	673	3	630	0	225	3	169	9	151	2	91	675
		548		490		58		542		401		
0-200	644	9	595	5	213	4	179	1	158	5	90	593
		470		415		54		557		419		
0-300	621	0	589	8	199	2	157	6	145	3	89	665
		378		323		55		490		366	10	
0-400	572	4	519	3	198	1	177	2	158	3	3	586
		476		418		58		547		398		
100-0	615	7	569	5	233	2	157	1	146	7	74	513
100-		472		418		54		659		524		
100	624	7	581	0	208	7	162	3	148	9	86	659
100-		485		421		63		505		371		
200	625	8	563	9	254	9	170	4	154	6	88	591
100-		442		384		57		568		402		
300	597	0	557	5	223	5	167	7	144	8	95	616
100-		468		404		63		539		418		
400	618	4	568	9	247	5	160	9	151	7	82	538
		481		423		58		543		407		
200-0	624	4	580	0	222	4	154	7	142	2	77	544
200-		421		367		54		573		412		
100	608	0	563	0	209	0	167	6	154	2	89	571
200-		518		458		60		537		477		
200	664	9	619	9	247	0	170	1	150	9	99	634
200-		469		414		54		514		390		
300	629	5	582	8	213	7	163	0	146	4	92	606
200-		563		503		59		469		314		
400	663	0	599	4	254	6	153	3	134	0	84	563
		467		408		58		550		419		
300-0	589	5	545	7	219	8	148	4	132	9	78	532

300-100	422	4247	385	3690	164	557	168	5414	147	3731	84	600
300-200	596	4748	553	4214	202	534	169	5271	154	3983	93	607
300-300	568	4223	534	3744	174	479	172	5215	153	4070	81	478
300-400	643	5921	586	5326	248	595	172	5105	148	3651	89	516
400-0	567	4333	516	3778	213	555	157	5096	141	3771	87	630
400-100	596	4234	544	3654	222	580	150	4774	136	3629	77	560
400-200	570	4453	528	3842	224	611	157	5136	137	3832	86	588
400-300	564	4440	522	3860	227	580	156	4748	136	3588	92	605
400-400	575	4014	519	3467	212	547	150	4792	130	3578	82	614

Table S2.2. Spatial aggregation index Omega (Ω) for 10, 20, 30, 40 and 50 m from the focal tree. Median, mean and max index Ω value by distance. P-value and R2 correspond to the linear regression between Ω and their forest-wide abundance.

	Mega-plot	Omega	Median	Mean	Max	P-value	R^2	spp	Abundance
LARGE TREES DBH≥10 cm	AFDP	10	2.32	3.63	50.1	0.007	0.11	64	7.885
		20	1.73	2.67	40.7	0.02	0.1		
		30	1.56	2.20	31.4	0.05	0.05		
		40	1.40	1.87	22.2	0.06	0.05		
		50	1.3	1.6	15.3	0.1	0.05		
	LPFDP	10	1.48	2.63	52.5	0.23	0.02	63	13.530
		20	1.38	1.81	23.7	0.19	0.02		
		30	1.22	1.48	12.7	0.15	0.03		
		40	1.14	1.30	7.81	0.20	0.02		
		50	1.11	1.18	5.2	0.25	0.02		
	AFDP	10	4.38	8.00	174.5	<0.001	0.10	413	92.378

		20	2.68	4.21	88.7	<0.001	0.06		
		30	2.00	2.99	48.4	<0.001	0.05		
SMALL TREES		40	1.76	2.42	27.9	<0.001	0.04		
1 ≥DBH <10		50	1.55	2.07	18.1	0.003	0.04		
								12	
	LPFDP	10	2.61	6.6	171	<0.001	0.25	9	97.501
		20	1.81	3.49	70.2	<0.001	0.22		
		30	1.50	2.40	33.9	<0.001	0.20		
		40	1.33	1.90	19.1	<0.001	0.18		
		50	1.19	1.63	12.4	<0.001	0.16		
								44	
	AFDP	10	3.9	7.3	173.1	<0.001	0.1	4	105.909
		20	2.48	3.9	88.7	<0.001	0.05		
		30	1.97	2.8	48.4	<0.001	0.04		
ALL TREES		40	1.70	2.3	27.9	0.004	0.03		
DBH≥1 cm		50	1.53	2.0	18.1	0.001	0.03		
								13	
	LPFDP	10	2.3	6.5	171.9	<0.001	0.29	2	112.052
		20	1.7	3.4	70.2	<0.001	0.26		
		30	1.3	2.3	33.9	<0.001	0.24		
		40	1.2	1.8	19.1	<0.001	0.22		
		50	1.1	1.6	12.4	<0.001	0.21		

Note: All species with abundances lower than 50 individuals within the 25-ha were remove from the analysis.

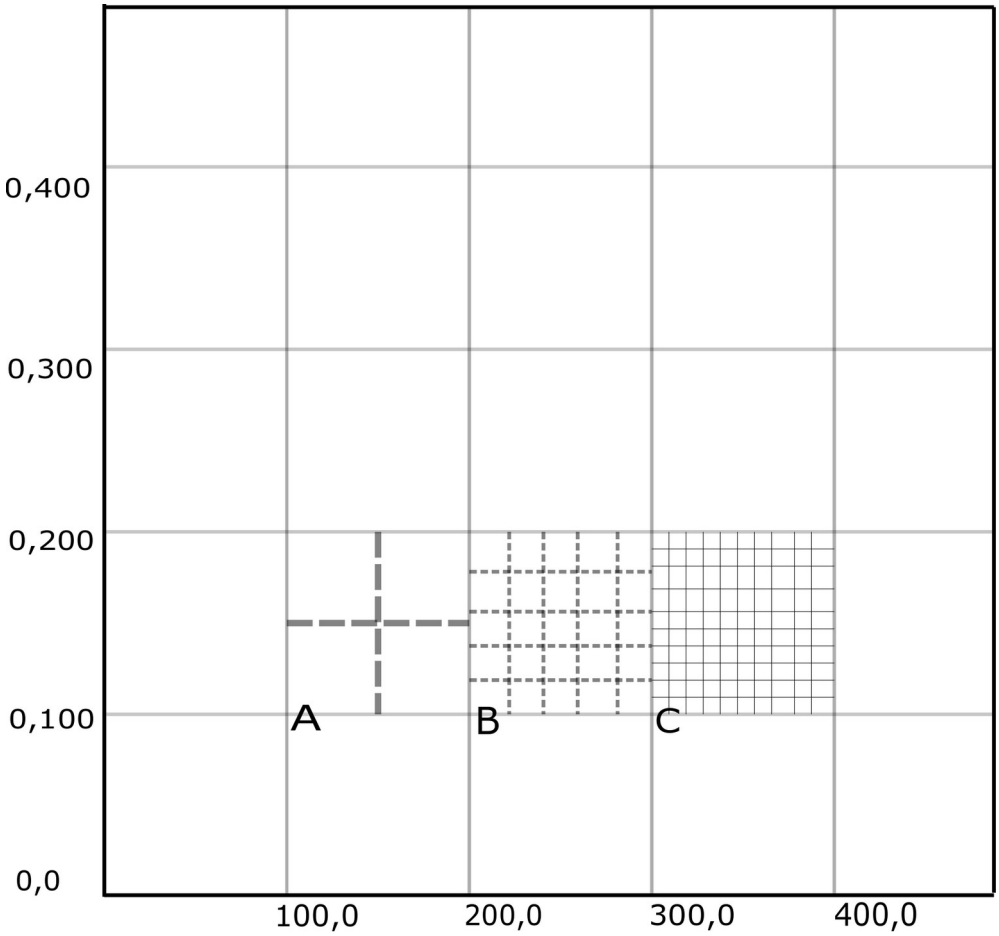

Figure S2.1) Representation of the design for each plot. The total area is 500 m × 500 m. Each square represents a 1-ha plot. A) Grid design for 50 m × 50 m within each 1-ha plot (four grains in total by 1-ha plot). B) Grid design for 20 m × 20 m within each 1-ha plot (25 grains in total by 1-ha plot). C) Grid design for 10 m × 10 m within each 1-ha plot (100 grains in total by 1-ha plot).

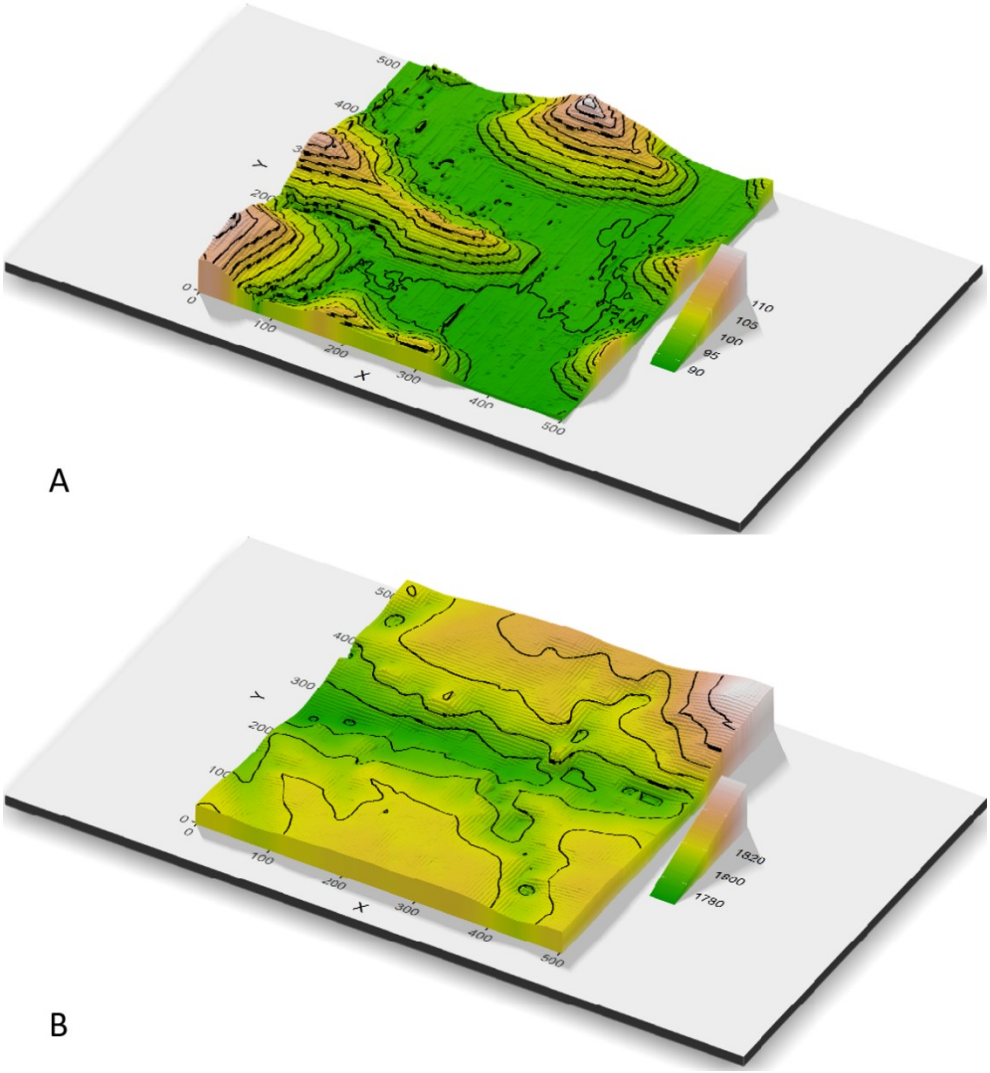

Figure S2.2) Topographic 3D map for each one 25-ha plots. A) Amacayacu Forest Dynamic plot (AFDP) at 100 m asl, representing lowlands region. B) La Planada Forest Dynamic plot (LPFDP) at 1800 m asl, representing highlands region. Colors from green to red represent the elevation within each plot. The color gradient goes from the flat areas (green) to the highest areas within the plot (red).

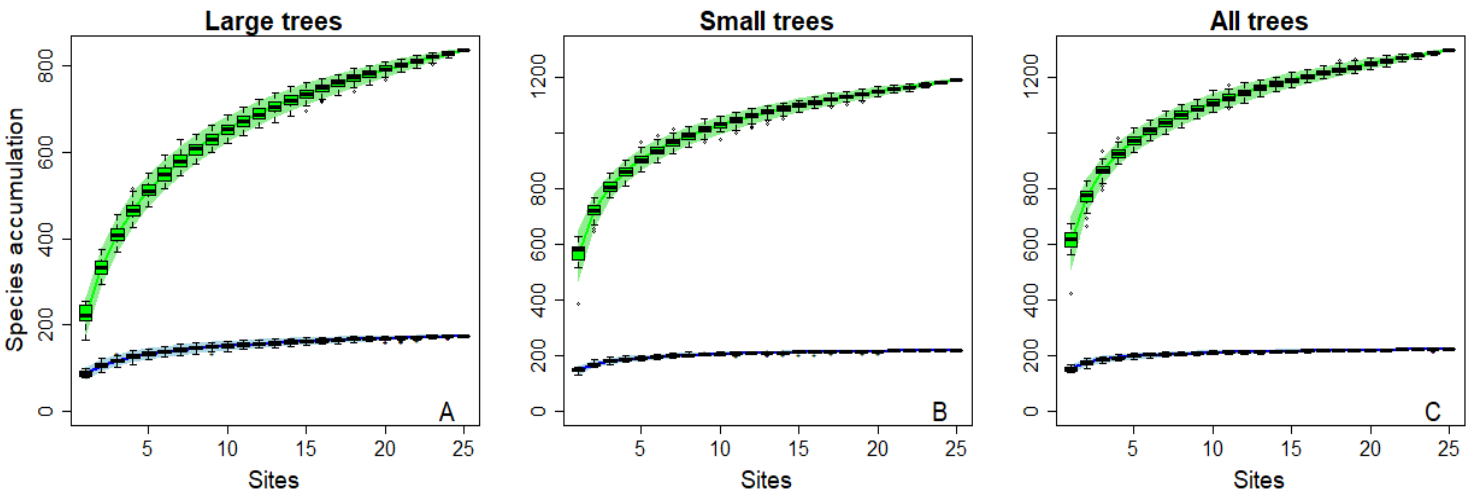

Figure S2.3) Species accumulative curve for AFDP (green) and LPFDP (blue) and different cut off sizes, A) Large trees, B) Small trees and C) All trees. In the curve each site make reference to each 1-ha plot within each 25-ha mega plot.

APPENDIX S2.1: R Code

```
#### assemble.from.pool.randA function was taken from Tello et al., 2015.
x=read.csv2("arb_ama10.csv")
x<-droplevels(subset(x, sp!=""))

x$ab=1
plot=unique(x$Cuadrante.100) # 1-ha plot

names(x)
sub = c (24, 25, 26,27) # Columns containing grain-size as factor
ss = c(50, 20,10) # grain-size


library(foreach)
library(doParallel)
library(vegan)

beta_data <- data.frame ()

for(p in 1:length(plot))
{

 s <- subset(x,Cuadrante.100==plot[p])

 bet2 <- data.frame()

 for(j in 1:length(sub))
 {
  s2 <- table(droplevels(s[,sub[j]]),droplevels(s$sp))
  obs <- beta.div(decostand(s2,method="hellinger"))$SStotal_BDtotal[2]
  w1 <- assemble.from.pool.randA(s2,rand.N=999)[[2]]

  #
  cores <- detectCores()
  cl <- makeCluster(cores[1]-1)
  registerDoParallel(cl)

  random_data <- foreach(i=1:length(w1),.packages="vegan",.combine=rbind) %dopar% {

   temp1 <- beta.div (decostand(w1[[i]], method="hellinger"))$SStotal_BDtotal[2]
   temp1
  }
```

```
    stopCluster(cl)

    #

    sdrandom <- sd(random_data)
    meanrandom <- mean(random_data)
    ses <- (obs - meanrandom)/sdrandom
    p.value <- (rank(c(obs,random_data))[1])/1000
    bet <- data.frame(plot=plot[p],sub=ss[j],obs,meanrandom,sdrandom,ses,p.value)
    bet2 <- rbind(bet2,bet)

  }

  beta_data <- rbind(beta_data,bet2)
  print(c(p,j))

}

print (beta_data)
```

CHAPTER III

TEMPORAL SHIFTS IN THE FUNCTIONAL COMPOSITION OF ANDEAN FORESTS AT DIFFERENT ELEVATIONS ARE DRIVEN BY CLIMATE CHANGE

ABSTRACT

Aim: Andean forests are a global biodiversity hotspot. They harbor many species living within narrow climate ranges and a high functional diversity of trees. It is still unclear how such hotspots respond to climatic changes over time. We investigated whether Andean forests are changing their functional composition over time along an elevational gradient by assessing changes in species composition, abundance, and functional traits.

Location: An elevational gradient in Colombia's northern Andes.

Time period: Species composition changes were studied 2 to 4 times from 2006 to 2017, and functional composition from 2016-2017

Major taxa studied: 1,104 tropical tree species with *in situ* traits characterization.

Methods: We used seven morphological leaf traits and wood density values to analyze the functional trait dynamic over ten years along an elevational gradient. By analyzing changes in species composition, abundance, and trait representation, we inferred the magnitude and direction of changes in functional composition. Then, we assessed if the functional change was related to climate change and demography.

Results: With increased minimum temperature and vapor-pressure deficit, we found a decrease over time in mean values for leaf area and specific leaf area and increases in leaf thickness and leaf dry matter content. Long-term temperature increases are smaller with increasing elevation, but the magnitude of trait changes is greater than in lowlands.

Main conclusions: The functional composition is changing towards more conservative strategies over time across the elevation gradient, with the strongest changes observed at the highest elevations. This pattern is explained by the change in species turnover within

communities due to higher recruitment rates of species with high leaf dry matter content values and low leaf area values. These shifts may be related to communities' responses to higher evapotranspiration demand and thermal stress, mainly at higher elevations.

Keywords: Andean forests, Climate change, Elevational gradient, Functional turnover, Forest plots, Trait-based ecology, Trait Driver Theory, Trait distributions.

INTRODUCTION

Andean forests, one of the most important global hotspots of diversity (Orme et al., 2005), are facing unprecedented climatic changes, but our understanding of how these changes will impact the functioning of their tree communities remains unclear (Payne, Spehn, Snethlage, Fischer, 2017). One plausible way to improve our knowledge of how forests respond to environmental changes is through the Trait Driver Theory (TDT) (Enquist et al., 2015). The TDT provides a theoretical framework focused on the shape of organismal trait distributions, which are expected to underlie the response of plant communities to environmental changes at the local scale (Enquist et al., 2017; Wieczynski et al., 2018). By quantifying the central moments of trait distribution, such as mean, variance, kurtosis, and skewness, we can infer
the local predominant phenotype (optimum), functional dispersion, evenness, and trait abundance (distribution bias), respectively (Figure 1, details in the method section) (Enquist et al., 2015). Therefore, the shape of the distribution of phenotypes can give us insights into the ecological dynamic of the community.

In mountain systems, the variation in functional composition has been studied primarily by evaluating how functional traits change along a natural gradient of temperature with elevation increase (Homeier, Seeler, Pierick & Leuschner, 2021; Ochoa-Beltrán, Martínez-Villa, Kennedy, Salgado-Negret, Duque, 2021). These studies have found that tree communities along elevational gradients tend to vary from acquisitive strategies (plants with fast-growth rates and low constructions costs) in lowlands to conservative strategies (plants with high construction costs) in highlands (Maharjan et al., 2021; Ochoa-Beltrán et

al., 2021). However, the temporal change in the functional composition of plant communities in response to changes in climatic conditions remains poorly understood. Thus, assessing trends in species composition, demographic rates, and trait characterization over time will improve our understanding of the mechanisms that control climate change-driven community trait shift.

In the past six decades, the temperature in the tropical Andes has increased between 0.03-0.04ºC/year, exceeding global average warming rates (Pabón-Caicedo et al., 2020). Species have responded to these increases by migrating up slopes but at a rate much slower than warming (Feeley et al., 2011). Therefore, there may exist an expansion in the distribution range of lowland species in the highlands. Nevertheless, as the climate warms and precipitation becomes more variable in the tropical Andes, vapor-pressure deficit (VPD) also increases (Barkhordarian, Saatchi, Behrangi, Loikith, Mechoso, 2019; Pabón-Caicedo et al., 2020), which may exacerbate plant thermal and water stress due to water loss through evapotranspiration (Grossiord et al., 2020). Studies have shown that plants with acquisitive strategies have low-stress tolerances (Reich, 2014) and high sensitivity to increased temperature and VPD. If so, those species within the community with high-stress tolerances and conservative traits will tend to be maintained in the face of climate change (in this study defined as the rate of change in temperature [mean, minimum and maximum], and VPD in the elevational gradient over 30 years in the study area). In any case, we expect that species responses to climate change will also change trait distributions by shifting the relative abundances of phenotypic frequencies in local communities. If climate change leaves a fingerprint on the functional composition of trees, increases in temperature and VPD will show the most detectable changes in the communities (Wieczynski et al., 2018). For example, a reduction in both leaf area (LA) and specific leaf area (SLA) will lead plant communities towards more conservative strategies over time.

Additionally, shifts in the trait composition of the community might depend on the demographic species' response (Violle et al., 2007). Previous studies have reported increased mortality rates of heat-sensitive species and increased recruitment rates of heat-adapted species (Duque, Stevenson, Feeley, 2015; Fadrique et al., 2018). If climate-induced

alterations in species composition and population dynamics are occurring, they may also entail modifications in functional composition. Recent studies suggest that increases in tree mortality risk in the tropics are driven mainly by the long-term increase in VPD and temperature (Bauman et al., 2022). The negative effects of these changes are exacerbated in species with acquisitive strategies such as low wood density and high SLA (Bauman et al., 2021). With climate change, it is likely that remaining and recruited species in the communities will have more stress-tolerant conservative traits. Overall, we expect the alteration of dominant plant traits in space and time to represent changes in forest functioning (Ruiz-Benito et al., 2017; Violle, Reich, Pacala, Enquist, Kattge, 2014). Nevertheless, the direction of this alteration is still unclear, and thus longitudinal studies across large environmental gradients are imperative.

In this study, we use nine 1-ha permanent plots to evaluate shifts in the functional composition of tree communities along an elevation gradient of more than 2500 m in the Andean forest. We use the TDT framework to assess changes in the trait distributions and their dynamics using seven plant morphological traits of 1,104 tree species. First, we evaluated how trait distribution changes along the elevational gradient and how climatic conditions affected these changes. Due to the considerable decrease in temperature with increasing elevation, we expect a higher abundance of species with conservative traits at higher elevations. This implies progressive changes in the value of local predominant traits (mean) with temperature decreases, such as lower leaf area (LA) and specific leaf area (SLA), but higher leaf dry matter content (LDMC), leaf thickness (LT), toughness (LTh), density (LD), and wood density (WD). With elevation, we also expect an overall decrease in the variance and an increase in kurtosis values of all the traits, indicating high environmental filtering promoting convergence of traits around the predominant local phenotype (Figure 1a, b). Second, we tested whether trait compositions in the nine communities along the elevational gradient shifted in the last decade (Fig. 1c, d). We expect shifts in trait distributions and central moments. For example, for those traits related to the temperature showing decreases in mean values over time (e.g., LA or SLA), a positive skew distribution is expected because of changes in trait dominance within the community (Figure 1c). If our hypothesis is correct, these traits will have a higher rate of

change in functional composition at higher elevations where species are cold adapted. Third, we assessed the climatic and demographic drivers associated with temporal changes in trait composition. Here, we expect that if increases in temperatures and VPD are modulating the changes in functional composition, higher mortality rates would be found in fast-growth species than species with more conservative strategies. On the other hand, increased temperature and upward migration could lead communities to more acquisitive strategies over time along elevation (Figure 1d).

1. METHODS

2.1 Study Area

The study area is located in the northwest region of Colombia between 5º50' and 8º61' North and 74º61' and 77º33' West (Supporting Information Figure S1). We used nine permanent plots of 1-ha (100 m × 100 m) belonging to the Red de Bosques Andinos, which have been monitored for the last decade (Duque et al., 2021; Malizia et al., 2020). The plots were established in Andean tropical forests along an elevation gradient from 50 to 2850 m with an average distance among plots of 146.9 km. All plots were established in areas showing minimal evidence of human disturbance where no fires had been recorded (except Carepa [~58 m], established in a small forest fragment [~50 ha]). The plots range in temperature from 27.7 ˚C to 13 ˚C from the lowest to the highest elevation. Along the elevational gradient, the plots vary significantly in solar radiation, VPD, and potential evapotranspiration (Supporting Information Table S1).

2.2 Abundance data set and censuses

In each of the nine plots, all shrubs and trees (hereafter trees) with a diameter at breast height (DBH) ≥ 10 cm were mapped, tagged, and measured. Near the center of each plot, all trees with a DBH ≥ 1cm were inventoried in a 40 m × 40 m subplot (0.16-ha). Voucher specimens were collected for potentially unique species in each plot, and identification was confirmed by consulting taxonomy specialists and comparing the specimens with herbarium material. The specimens that could not be identified at the species level were classified as morphospecies (hereafter species). All plots were established between 2006

and 2009 and were censused 2 to 4 times between 2016 and 2019 (Supporting Information Table S2).

2.3 Climate data collection

We retrieved mean climate data for each plot using climatic layers at high resolution (30 arcsec) available in WorldClim 2.1 (Fick & Hijmans, 2017) and CGIAR-CSI 2.0 (Zomer, Trabucco & Verchot, 2008). The following variables were obtained: mean annual temperature (MAT), mean annual precipitation (MAP), isothermality (ISO), temperature seasonality (TS), precipitation seasonality (PS), saturated vapor pressure (SVP), potential evapotranspiration (PET), wind speed, and solar radiation (Solar rad) (Table S1). Vapor pressure deficit (VPD) was calculated as saturated vapor pressure minus vapor air pressure**.** To evaluate whether there was climate change in the study area, we retrieved historical climate data from the last 38 years, from 1980 to 2017, for MAT, maximal temperature (T_{max}), minimal temperature (T_{min}), and MAP from the Worldwide Energy Resource database (POWER-NASA) (https://power.larc.nasa.gov) with a resolution of 0.5º. Historical VPD was calculated using the long-term record of vapor air pressure (VAP) of the last 38 years retrieved from the Climate Research Unit (CRU-TS) version 4.04 (Harris, Osborn, Jones & Lister, 2020). We then used these historical climate data to calculate the annual rate of climatic variables in the last four decades (Supporting Information Figure S7, S8). We acknowledge that the choice of 38 years is arbitrary, but our criteria for choosing this time period was mainly related to the data availability. Although undisturbed forests such as those sampled in this study may take longer to show responses to climate changes, 38 years have been enough to find directional shifts in composition in some tree species located in the same study area (Fadrique et al., 2018).

2.4 Trait sampling

We focused on six leaf morphological traits that capture the essential leaf economics: leaf area: LA (mm2), specific leaf area: SLA (mm/mg), leaf density: LD (g/cm 3), leaf dry matter content: LDMC (mg/g), leaf toughness: LTh (Newton/mm), leaf thickness: LT (mm), and wood density: WD (g/cm3) (Supporting Information Appendix S1). Size-related plant traits with power-law growth rates of the form $Y = ax^b$, such as LA and LT, were $\log_{10}$

transformed to normalize trait distributions and reduce the influence of outliers (Kerkhoff & Enquist, 2009).

We measured plant traits during 2016-2017 following standard protocols (Pérez-Harguindeguy et al., 2016). In each plot, we collected five leaves from five healthy individuals per species (three individuals in Angelópolis, Anorí, and Segovia plots, due to the high number of species) for the most abundant species contributing to 80% or more of total species abundance. In addition, we sampled one to two individuals for those remaining species that contribute to less than 80% of the total species abundance (remaining species). Thus, nearly all species were sampled within each plot (Table S2). Shared species among plots were measured in each local community. We analyzed 1,104 species (of which 60% [610] were identified at the species level) distributed over 361 genera and 103 families. We sampled ~10,470 individual leaves belonging to ~2,297 individuals. To collect WD, we took one sample of ~3 cm in diameter and ~10 cm long from one mature branch per individual. Due to some species being presented just in small size individuals (~18%), it was not possible to measure WD directly. Thus, we filled in the missing values hierarchically. First, the missing WD values per individual were assigned based on the average value of the same species in other plots. If the value was not available at the species level, the value by either genus or family was used.

2.5 Trait distributions and central distribution moments

Using the TDT framework, we focused on the four central moments of trait distribution. The community-weighted mean (CWM) represents the distribution's average (predominant) trait value. Community-weighted variance (CWV) reflects the dispersion of trait values and can be interpreted as a measure of functional diversity. Community-weighted kurtosis (CWK) reflects the peakedness of the trait distribution; the higher the peakedness, the higher the dominance of specific traits. High positive kurtosis reflects more peaked distributions relative to a normal distribution due to reduced outliers and the high abundance of functionally similar species (Huang, Xu, Zang, 2021). Low or negative kurtosis reflects platykurtic distributions resulting from a wide range of trait values due to contrasting ecological strategies within the community. Values equal to -1.2 represent a

complete evenness. Finally, negative or positive community-weighted skewness (CWS) reflects a strong right- or left-skewed distribution, which means extreme trait values at the ends of the distribution tails (Enquist et al., 2015; Wieczynski et al., 2018). An asymmetrical distribution results from changes in the frequency of trait values as a response to rapid environmental changes or rare species advantages within communities; this could be interpreted as a fingerprint of climate change (Enquist et al., 2015).

Based on the abundance-weighted kernel density distributions estimated for each trait and community, we quantified the four central moments weighted by species abundance. To calculate density distributions that better represent the community and the variation in trait values, we incorporated intra-specific variability for those species with the largest numbers of sampled individuals. We ran statistical non-parametric bootstrapping to resample (with replacement) individuals' trait values in proportion to the species abundance to generate a set of new distributions (Maitner et al., 2023) (Appendix S1). The following equations define the central abundance-weighted moments:

$$CWM = \frac{\sum w_i x_i}{\sum w_i}$$

$$CWV = \sum w_i \frac{(x¿¿i - CWM)^2}{\sum w_i} ¿$$

$$CWK = \frac{\sum w_{i\times} \frac{x_{i-CWM}}{\sqrt{CWM}}^4}{\sum w_i} - 3$$

$$CWS = \frac{\sum w_{i\times} \frac{x_{i-CWM}}{\sqrt{CWM}}^3}{\sum w_i}$$

Where *wi* is the abundance of species *i* in the local community and *xi* is the local mean trait value for species *i* (Huang et al., 2021; Wieczynski et al., 2018).

2.6 Patterns of change in functional composition over time along the elevational gradient

To analyze community changes in trait composition, we initially plotted the abundance-weighted density estimates for each trait for each plot and census. Next, we quantified the abundance-weighted moments (CWM, CWV, CWK, CWS) corresponding to the trait distribution of the first and the last census. To do this, we used the traits measured and matched trait values with species composition and abundance in the first and last census (8-10 years on average) (Table S2). Finally, to quantify the shift and the direction in functional composition over time, we calculated the Trait Velocity index (TV) (which represents the annual rate of change for each trait moment) (Trugman et al., 2020) as the difference between the last and the first community-weighted moment, divided by the length of the census period (TV_CWM, TV_CWV, TV_CWK, TV_CWS). Because these data do not involve repeated measures of traits over time, we could not assess functional plasticity, so we assumed that trait values were stable over time. Consequently, we focus on the effect of demographic responses on the communities' functional structure. Pairing trait data with species abundance by censuses provides insights into understanding temporal changes based on shifts in community composition and abundance (Aguirre-Gutiérrez et al., 2019; Swenson, Hulshof, Katabuchi, Enquist, 2020).

2.7 Potential drivers of temporal changes in forest functional composition

Climatic changes:

We calculated the annual rate of change of MAP (ΔMAP in mm y^{-1}), MAT (ΔMAT in °C y^{-1}), Tmax (ΔT_{max} in °C y^{-1}), Tmin (ΔT_{min} in °C y^{-1}), and VPD (ΔVPD in Kpa y^{-1}) as the slope of the linear least-square regression between the values of each climatic variable and time (Figure S7). To estimate climate change, we first used two different regressions to estimate the slopes as a measurement of the annual rate of change for the different variables. The first one used the 1980-2017 dataset (data availability at power.larc.nasa.gov). The second one used the 1995-2017 dataset following Fadrique et al., 2018, who used a similar timeframe to calculate the climatic rate in the Andes. We did a t-test for comparing slopes between the two periods, as slopes remain similar ($P>0.05$ for all variables and plots), we

considered climate change from 1980 because, although arbitrary, we believe that in mature forests the lag between climate change and community response can be decades (Alexander et al., 2018; Block et al., 2022). It is important to remark that we refer to climate change as the long-term changes mainly in temperature (mean, minimum and maximum) and VPD.

Demographic tree rates:

We calculated annual mortality and recruitment rates by plot following Phillips et al. (1994) as:

$$Mortality\ rate\,(\%) = \ln\left[\left(\frac{No}{Ns}\right)\right] / \Delta time$$

$$Recruitment\ rate\,(\%) = \ln\left[\left(\frac{Nf}{Ns}\right)\right] / \Delta time$$

Where *No* is the initial number of individuals in the first census, *Nf* is the final number of individuals in the last census, and *Ns* is the number of original individuals surviving until the final inventory. Mortality and recruitment rates were calculated for canopy individuals with DBH ≥ 10 cm in the plots and understory individuals with 1 cm ≤ DBH < 10 cm in the 0.16-ha subplots.

2.8 Data analyses

Changes in trait distribution along the elevational gradient:

To address our first aim of how trait distribution moments change along elevation and what climatic variables are involved, we regressed the central weighted moments of each trait for each plot and the climate conditions at each site for the last census. To reduce the number of climatic variables to two main axes, we ran a principal component analysis (PCA) with all the climate data using the princomp function in R. All variables were standardized to a mean of zero and standard deviation of one before conducting the PCA. The first and second PCA axes explained 47.7% and 23% of the climatic variance, respectively (Supporting Information Figure S2). The $PC1_{\_climate}$ axis was primarily determined by MAT, solar radiation, VPD, and PET (Supporting Information Table S3). Notably, $PC1_{\_climate}$ is primarily negatively correlated with MAT ($p<0.05$, $R= -0.87$) (Figure S3b) and positively

correlated with elevation (Figure S3a). Precipitation seasonality (PS) determined the $PC2_{\_climate}$ axis ($r = 0.69$, $p < 0.05$) (Table S3) and was used as a surrogate of seasonality (Figure S3g). We then built simple linear models between the trait moment values and the $PC1_{\_climate}$ and $PC2_{\_climate}$ separately to quantify the relationship between climatic variation and community-weighted moments.

Changes in trait distribution over time:

To assess our second aim of whether functional composition of each local community changes over time, we first performed a Kolmogorov-Smirnov test between the distributions of the first and last census of each trait for each plot to test significant differences. To evaluate differences in central moments between the first and last census, we used a linear mixed model, with the census as a fixed factor and the plot as a random factor to account for the repeated censuses per plot (van der Sande et al., 2016). Finally, we performed a least-squares linear model between each TV trait and elevation to examine whether there are directional changes in the functional composition along the elevation.

Assessing potential drivers of change in functional composition over time

To address the potential impact of climate change and species demography on functional changes over time (third question), we tested whether shifts in the community trait composition were related to temporal climatic variations and mortality/recruitment. We ran ordinary least-squares regressions between the TV per moment and trait (response variable) and changes in climate and demographic rates (ΔMAP, ΔMAT, ΔTmax, ΔTmin, ΔVPD, Mortality, and Recruitment rate). To control significant false p-values when comparing multiple hypothesis tests, we adjusted the p-value of each regression using the false discovery rate (type I error) (Benjamini & Hochberg, 1995) with the function FDR in the fuzzySim R package (Barbosa, 2015). Due to the statistical restrictions of the small sample size, our models test the effect on one independent variable at a time in order to keep the statistical power of the data. All analyses were performed using R version 4.0.0 (R Development Core Team 2020).

RESULTS

3.1 Variation in trait distribution along the elevational gradient

All the distributions showed a unimodal trend, reflecting one predominant phenotype or mean trait value for the community, except for the distribution of WD, which reflects two peaks in plots located at low elevations, suggesting two possible prevailing phenotypes (Supporting Information Figure S4).

As expected, the central moments showed that functional composition varies from strategies of fast resource acquisition to high construction costs along the climatic/elevational gradient ($PC1_{\_climate}$). Changes in CWM are primarily associated with a significant decrease in traits related to photosynthetic capacity (reduction in leaf area and specific leaf area) and an increase in leaf structural components for protection, such as thickness (Figure 2a). CWM of LDMC showed a humped-shaped relationship with the $PC1_{\_climate}$ (Figure 2a). Contrary to our expectations, CWV (which reflects functional diversity) did not decrease significantly for all traits along the $PC1_{\_climate}$. The CWV of wood density decreased with $PC1_{\_climate}$, and conversely, leaf thickness increased, indicating a broader spectrum of trait values at higher elevations (Figure 2b).

The analysis of the trait distribution shape (CWK) showed that all traits, except LDMC, were characterized by kurtosis values greater than zero, indicating a distribution with a reduction of more variable trait values and more peaked than expected from a normal distribution (Figure 2d). Only the CWK of the leaf toughness showed a significant increase with $PC1_{\_climate}$. None of the moments were significantly related to $PCA2_{\_climate}$ (Figure S5).

3.2 Changes in trait composition over time

The Kolmogorov-Smirnov test showed significant shifts in trait distribution per plot between the first and the last census, particularly in plots located at high elevations (Figure 3). The fourth moment (CWS), which analyzes the bias of the trait distribution and can be interpreted as a fingerprint of climate change, showed that photosynthetic traits such as leaf area and specific leaf area had a CWS greater than zero. This reflects a dynamic change in trait distribution towards lower values of the predominant phenotype. These results support

our hypothesis that if the mean community trait increases across a temperature gradient (e.g., LA and SLA, negatively correlated with $PC1_{\_climate}$), warming would lead to communities characterized by positive skewness (Figure 1 and Figure 2c). Leaf thickness, positively correlated with $PC1_{\_climate}$, showed some communities with negative skewness. Thus, it may be a trait with a slower response to heating than those related to the area.

According to the linear mixed model, which quantifies changes in time, leaf area showed significant differences between the first and the last census for the mean and variance, indicating that functional composition and diversity varied over time (Table 1). In comparison, thickness had changes in skewness values; specific leaf area, and LDMC in the kurtosis (Table 1). Our analyses found a directional shift of functional composition along elevation for one trait. The changes over time in mean values (TV_CWM) of LDMC and the strong tendency of change for leaf area presented a positive and negative relationship with elevation, respectively (Figure 4), indicating an increment in the magnitude of the change in functional composition when elevation increases. Remarkably, nearly all the plots showed decreases over time in mean values of leaf area (negative values) and increased LDMC regardless of elevation (Figure 4). Furthermore, the changes over time in variance (TV_CWV) had a positive relationship with elevation for WD **(**Supporting Information Figure S6**)**. Thus, communities have a broader spectrum of trait values for this trait over time. Finally, changes over time in skewness (TV_CWS) of WD and leaf area significantly decreased along the elevational gradient (Figure S6c). This result indicates that the bias of the trait distribution decreases over time, probably because communities are achieving new values of predominant phenotypes.

3.3 Potential drivers of change in functional composition over time

Over the last 38 years, the temperature and VPD have increased significantly in the nine plots. The ΔT_{min} and ΔVPD have a negative relationship with elevation, which means that lowlands are experiencing more significant warming and more water stress (Figures S7 and S8). We found that negative changes over time for traits associated with photosynthesis (leaf area and specific leaf area) and positive changes for traits associated with leaf structure (leaf thickness and LDMC) had a relationship with increases in minimum

temperature and VPD at high elevations (Figure 5a, b). Climatic changes in the mean, maximal temperature, and precipitation were unrelated to mean trait changes over time (Supporting Information Figure S9). Overall, temperature changes significantly affect changes over time for the variance of leaf area and specific leaf area (Figure S10), indicating that this factor affects the functional diversity over time. Significant changes over time in skewness were present mainly in WD and leaf thickness and were modulated specifically by ΔT_{min} (Figure S12). Finally, the potential climatic drivers did little to explain the changes over time for kurtosis values (TV_CWK) (Figure S11).

Regarding species demography, the recruitment rate of individuals increased with elevation (Figure S8g). The analyses of demographic rates related to changes over time in trait composition of LDMC and leaf area indicated that the higher the recruitment, the higher the LDMC and the lower the leaf area (Figure 5c). Similarly, recruitment also affected the changes over time for mean trait values and variance of WD (Figure S10e) and the changes in the skewness of leaf thickness (Figure S12e). Mortality was not significant with changes over time in mean values (Figure 5d).

4. DISCUSSION

Previous studies have suggested a functional shift over time along elevation in the Andean forests related to climate change (Duque et al., 2021; Fadrique et al., 2018). However, few have evaluated this hypothesis by integrating plant traits and species demography (see Báez, Fadrique, Feeley & Homeier. 2022). Here, we assessed how functional composition changes along elevation and over time and investigated what environmental variables drive these changes. Our results show that shifts in trait composition along elevation and over time are related mainly to changes in temperature and vapor-pressure deficit (VPD). Over time, functional changes show a decline in mean community values of leaf area and specific leaf area and an increase in LDMC and thickness, mainly at higher elevations (Figure 5). Our results agree with previous studies identifying changes in VPD and temperature as drivers of change in species composition (Feeley et al., 2011; Bauman et al., 2021), community plant traits (Fadrique et al., 2018), and plant abundance (Duque et al., 2021; Peña, Feeley, & Duque, 2018) in the tropical forest. Thus, our trait-based approach

can help to understand the potential direction of future changes in Andean forest dynamics with continuous climate change.

4.1 Variation in functional composition along the elevational gradient

Changes in the functional composition along the $PC1_{\_climate}$ were defined by the variation in community mean values from high to low values of leaf area and specific leaf area and from low to high values of leaf thickness. The reduction of leaf area and specific leaf area and the increase in leaf thickness towards higher elevation seems to be related to the marked decrease in temperature and high levels of solar radiation since this morphology allows plants to maximize water use efficiency and conserve heat in cold environments with high radiation (Llerena-Zambrano et al., 2021). These changes reveal a shift from communities characterized by acquisitive strategies in the lowlands to conservative strategies in the highlands. These trends are widely reported in tropical mountain forests (Homeier et al., 2021; Maharjan et al., 2021; Ochoa-Beltrán et al., 2021) and are related to a gradient of the leaf resource investment and return (Wright et al., 2004).

We hypothesized a decrease in the variance of all traits (narrow range of trait values) and an increase in kurtosis along the climatic/elevation gradient (represented by $PC1_{\_climate}$) related to strong environmental filtering. Contrary to our expectations, the variance of leaf thickness increases in high elevations (low temperatures), a pattern that has also been reported by other studies (Homier et al., 2021). Furthermore, we only find a strong positive kurtosis (a more peaked distribution reflecting biotic exclusion) along the climatic/elevation gradient for leaf area and toughness. One possible explanation for this apparent lack of variance reduction and environmental filtering along elevation is the complex mountain topography, which at a small scale, creates different niches that enhance trait variability at high elevations (Homier et al., 2021). A complementary explanation is given that high thickness and toughness confer advantages in low temperatures (Llerena-Zambrano et al., 2021). The high variance suggests the presence of multiple adaptative strategies within the community, such as diverse morphological responses to the specific environmental stress, which result in the over-dispersion of phenotypes (Enquist et al., 2015). These results show that it is critical to evaluate not just community mean values but other moments of trait

distribution, such as variance and kurtosis, which give us information about ecological mechanisms shaping trait distribution along environmental gradients.

4.2 Temporal patterns of change in functional composition

Historical increases in VPD, minimum temperature, and recruitment rate mainly drive shifts in trait composition over time, particularly at high elevations (Figures 3-5). Temperature-related traits presented high positive skewness, such as leaf area and specific leaf area. These patterns are consistent with expected community directional shifts with an increase in VPD and temperature and have been reported in previous tropical mountain studies (Enquist et al., 2017; Wieczynski et al., 2018). The decline in mean values of leaf area and increase in LDMC at higher elevations indicates a potential shift in community functional composition towards more conservative and stress-tolerant strategies, partially supporting our hypothesis. Although this study did not assess the shift in trait plasticity, changes in species composition and dominance may indicate how increases in temperature and VPD modulate and filter species with certain traits, thus shaping the future functional composition.

(Konings, Williams & Gentine, 2017), as shown in our results. In the same way, increased VPD is a risk factor that can increase mortality in species with more acquisitive strategies (Bauman et al., 2022) such as large leaf areas and high values of SLA. Considering that water vapor is a key factor for forest functioning (Yuan et al., 2019), mainly in mountain forests, increases in VPD substantially increase the water demand and decrease the photosynthetic rate (Grossiord et al., 2020). Thus, the effects of higher VPD and decreased cloud cover (Los et al., 2019) should filter species with traits more tolerant to higher solar radiation and with better water-use efficiency. Overall, selecting species with smaller and thicker leaves contributes to increased leaf lifespan, nutrient retention, and water-use efficiency under higher temperatures and VPD (Ackerly et al., 2002). The decreases of mean values over time in leaf areas and increases in LDMC could also prevent leaf overheating (Meng et al., 2015) and water loss in cold-adapted species.

Many studies assessing the effects of climate change on tree communities focused mostly on temperature changes, and VPD tended to be neglected (Báez et al., 2022; Feeley et al., 2011). Nevertheless, in humid regions and cloud forests, changes in VPD may significantly impact the species' physiology and functioning, affecting their demographic responses and, subsequently, community functional composition. This factor, in addition to temperature, helps us to understand more mechanistically the effects of climate change on forest functioning. Although we recognize that our time framework to evaluate changes in the functional composition is short and could be arbitrary due to the data availability (e.g., 10 years), we found recruitment rates and functional shifts over time in four traits related to VPD and minimum temperature changes. We believe it is a matter of time before other traits show changes in functional composition mainly due to the lag between climate change and the community response.

Changes in species composition are long-term accumulative responses (Alexander et al., 2018), and previous studies have shown increases in the recruitment of heat-tolerant species in the Andes (Duque et al., 2015). In our study, increases over time in LDMC and decreases in leaf area were related to higher recruitment rates at high elevations, which could reflect higher recruitment of species with conservative resource-use strategies and a higher capacity to avoid overheating (Reich, 2014). If only warming occurs, we would expect a change toward more acquisitive traits. Nevertheless, increments in VPD and solar radiation (Los et al., 2019) are factors that may filter species with conservative traits. Studies have shown that the upslope migration of tree species in the Andes is significantly slower than the warming rate, which reduces the tracking of environmental changes (Feeley et al., 2011). Furthermore, the habitat loss and subsequent fragmentation of the forest and hence the loss of animals for seed dispersal could further limit tree species migration. Species with conservative traits exhibit higher tolerance to environmental changes, resulting in a slower migration rate compared to acquisitive species. Due to their ability to withstand climatic variations in their current habitats, conservative species have a greater likelihood of successful juvenile recruitment; thus, establishing and recruiting juvenile trees with more conservative traits may be strongly associated with local environmental and soil conditions that promote germination (Block et al., 2022).

Although Andean forests are one of the ecosystems most vulnerable to climate change, they remain an important carbon sink (Duque et al., 2021). The observed filtered traits over this short temporal window are those with the greatest ability to persist under climate change and more stressful environmental conditions (Reich, 2014). Through species demography (recruitment/mortality), those species would be expected to survive and recruit, leading communities towards more conservative strategies, mainly at high elevations.

5. CONCLUSIONS

Our findings emphasize the relationship between shifts in functional composition over time along an elevational gradient in the Andean mountains and the responses of tree communities related to increases over time in vapor-pressure deficit and minimum temperature. Observed changes in functional composition suggest a shift in the community towards promoting species with conservative strategies such as decreases in mean community values of leaf area and specific leaf area and increases in LDMC and leaf thickness. This was also supported by our results of higher recruitment rates of individuals with more stress-tolerant traits. Although we found shifts in trait composition in four of the seven traits, if minimum temperature and vapor-pressure deficit continue increasing at the current rate, we could expect shifts in other plant traits as well with potential consequences for forest functioning. Longitudinal monitoring of permanent plots and *in situ* functional traits is needed to fully understand the effect of climate change on species' demographic and plastic responses to new conditions. Ongoing studies must include dispersal traits to quantify species' migration capacity along elevation and include an analysis of species mortality risk as a function of their traits.

REFERENCES

Ackerly, D. D., Knight, C. A., Weiss, S. B., Barton, D., & Starmer, K. P. (2002). Leaf size, specific leaf area and microhabitat distribution of chaparral woody plants: contrasting patterns in species level and community level analyses. *Oecologia*, *130*, 449–457. https://doi.org/10.1007/s004420100805

Aguirre-Gutiérrez, J., Oliveras, I., Rifai, S., Fauset, S., Adu-Bredu, S., Affum-Baffoe, K., Baker, T. R., Feldpausch, T. R., Gvozdevaite, A., Hubau, W., Kraft, N. J. B., Lewis, S. L.,

Moore, S., Niinemets, Ü., Peprah, T., Phillips, O. L., Ziemińska, K., Enquist, B., & Malhi, Y. (2019). Drier tropical forests are susceptible to functional changes in response to a long-term drought. *Ecology Letters*, *22*(5), 855–865. https://doi.org/10.1111/ele.13243

Alexander, J. M., Chalmandrier, L., Lenoir, J., Burgess, T. I., Essl, F., Haider, S., Kueffer, C., McDougall, K., Milbau, A., Nuñez, M. A., Pauchard, A., Rabitsch, W., Rew, L. J., Sanders, N. J., & Pellissier, L. (2018). Lags in the response of mountain plant communities to climate change. *Global Change Biology*, *24*(2), 563–579. https://doi.org/10.1111/gcb.13976

Barkhordarian, A., Saatchi, S. S., Behrangi, A., Loikith, P. C., & Mechoso, C. R. (2019). A Recent Systematic increase in Vapor Pressure Deficit over Tropical South America. *Scientific Reports*, *9*(15331), 1–12. https://doi.org/10.1038/s41598-019-51857-8

Báez, S., Fadrique, B., Feeley, K., & Homeier, J. (2022). Changes in tree functional composition across topographic gradients and through time in a tropical montane forest. *PLoS ONE*, *17*(4 April). https://doi.org/10.1371/journal.pone.0263508

Barbosa, M.A. (2015). fuzzySim: applying fuzzy logic to binary similarity indices in ecology. Methods in Ecology and Evolution, 6(7), 853-858. doi:10.1111/2041-21X.12372.

Bauman, D., Fortunel, C., Cernusak, L. A., Bentley, L. P., McMahon, S. M., Rifai, S. W., Aguirre-Gutiérrez, J., Oliveras, I., Bradford, M., Laurance, S. G. W., Delhaye, G., Hutchinson, M. F., Dempsey, R., McNellis, B. E., Santos-Andrade, P. E., Ninantay-Rivera, H. R., Chambi Paucar, J. R., Phillips, O. L., & Malhi, Y. (2021). Tropical tree growth sensitivity to climate is driven by species intrinsic growth rate and leaf traits. *Global Change Biology*, *28*(4), 1414–1432. https://doi.org/10.1111/gcb.15982

Bauman, D., Fortunel, C., Delhaye, G., Malhi, Y., Cernusak, L. A., Bentley, L. P., Rifai, S. W., Aguirre-Gutiérrez, J., Menor, I. O., Phillips, O. L., McNellis, B. E., Bradford, M., Laurance, S. G. W., Hutchinson, M. F., Dempsey, R., Santos-Andrade, P. E., Ninantay-Rivera, H. R., Chambi Paucar, J. R., & McMahon, S. M. (2022). Tropical tree mortality has increased with rising atmospheric water stress. *Nature*, *608*(7923), 528–533. https://doi.org/10.1038/s41586-022-04737-7

Benjamini, Y., & Hochberg, Y. (1995). Controlling the False Discovery Rate: A Practical and Powerful Approach to Multiple Testing. *Royal Statistical Society*, *57*(1), 289–300.

Block, S., Maechler, M. J., Levine, J. I., Alexander, J. M., Pellissier, L., & Levine, J. M. (2022). Ecological lags govern the pace and outcome of plant community responses to 21st-century climate change. In *Ecology Letters* (Vol. 25, Issue 10, pp. 2156–2166). John Wiley and Sons Inc. https://doi.org/10.1111/ele.14087

Cuesta, F., Tovar, C., Luis, Llambí, D., William, Gosling, D., Halloy, S., Carilla, J., Muriel, P., Rosa, |, Meneses, I., Beck, S., Carmen, Ulloa, U., Yager, K., Aguirre, | Nikolay, Viñas, P., Jácome, J., David Suárez-Duque, … Pauli, H. (2020). Thermal niche traits of high alpine plant species and communities across the tropical Andes and their vulnerability to global warming. *Journal of Biogeography*, *47*, 408–420. https://doi.org/10.1111/jbi.13759

Duque, A., Peña, M. A., Cuesta, F., González-Caro, S., Kennedy, P., Phillips, O. L., Calderón-Loor, M., Blundo, C., Carilla, J., Cayola, L., Farfán-Ríos, W., Fuentes, A., Grau, R., Homeier, J., Loza-Rivera, M. I., Malhi, Y., Malizia, A., Malizia, L., Martínez-Villa, J. A., … Feeley, K. J. (2021). Mature Andean forests as globally important carbon sinks and future carbon refuges. *Nature Communications*, *12*(1), 1–5. https://doi.org/10.1038/s41467-021-22459-8

Duque, A., Stevenson, P. R., & Feeley, K. J. (2015). Thermophilization of adult and juvenile tree communities in the northern tropical Andes. *Proceedings of the National Academy of Sciences of the United States of America*, *112*(34), 10744–10749. https://doi.org/10.1073/pnas.1506570112

Enquist, B. J., Bentley, L. P., Shenkin, A., Maitner, B., Savage, V., Michaletz, S., Blonder, B., Buzzard, V., Espinoza, T. E. B., Farfan-Rios, W., Doughty, C. E., Goldsmith, G. R., Martin, R. E., Salinas, N., Silman, M., Díaz, S., Asner, G. P., & Malhi, Y. (2017). Assessing trait-based scaling theory in tropical forests spanning a broad temperature gradient. *Global Ecology and Biogeography*, *26*(12), 1357–1373. https://doi.org/10.1111/geb.12645

Enquist, B. J., Norberg, J., Bonser, S. P., Violle, C., Webb, C. T., Henderson, A., Sloat, L. L., & Savage, V. M. (2015). Scaling from Traits to Ecosystems: Developing a General Trait Driver Theory via Integrating Trait-Based and Metabolic Scaling Theories. In *Trait-Based Ecology - From Structure to Function* (1st ed., Vol. 52, Issue October 2017). Elsevier Ltd. https://doi.org/10.1016/bs.aecr.2015.02.001

Fadrique, B., Báez, S., Duque, Á., Malizia, A., Blundo, C., Carilla, J., Osinaga-Acosta, O., Malizia, L., Silman, M., Farfán-Ríos, W., Malhi, Y., Young, K. R., Cuesta C, F., Homeier, J., Peralvo, M., Pinto, E., Jadan, O., Aguirre, N., Aguirre, Z., & Feeley, K. J. (2018). Widespread but heterogeneous responses of Andean forests to climate change. *Nature*, *564*(7735), 207–212. https://doi.org/10.1038/s41586-018-0715-9

Feeley, K. J., Silman, M. R., Bush, M. B., Farfan, W., Cabrera, K. G., Malhi, Y., Meir, P., Revilla, N. S., Quisiyupanqui, M. N. R., & Saatchi, S. (2011). Upslope migration of Andean trees. *Journal of Biogeography*, *38*(4), 783–791. https://doi.org/10.1111/j.1365-2699.2010.02444.x

Feeley, K., Martinez-villa, J., Perez, T., & Duque, A. S. (2020). The Thermal Tolerances , Distributions , and Performances of Tropical Montane Tree Species. *Frontiers in Forest and Global Change*, *3*(March), 1–11. https://doi.org/10.3389/ffgc.2020.00025

Fick, S. E., & Hijmans, R. J. (2017). WorldClim 2: new 1-km spatial resolution climate surfaces for global land areas. *International Journal of Climatology*, *37*(12), 4302–4315. https://doi.org/10.1002/joc.5086

Grossiord, C., Buckley, T. N., Cernusak, L. A., Novick, K. A., Poulter, B., Siegwolf, R. T. W., Sperry, J. S., & McDowell, N. G. (2020). Plant responses to rising vapor pressure deficit. In *New Phytologist* (Vol. 226, Issue 6, pp. 1550–1566). Blackwell Publishing Ltd. https://doi.org/10.1111/nph.16485

Harris, I., Osborn, T. J., Jones, P., & Lister, D. (2020). Version 4 of the CRU TS monthly high-resolution gridded multivariate climate dataset. *Nature*, *7*(109), 1–18.

Homeier, J., Seeler, T., Pierick, K., & Leuschner, C. (2021). Leaf trait variation in species-rich tropical Andean forests. *Scientific Reports*, *11*(1), 1–11. https://doi.org/10.1038/s41598-021-89190-8

Huang, C., Xu, Y., & Zang, R. (2021). Variation Patterns of Functional Trait Moments Along Geographical Gradients and Their Environmental Determinants in the Subtropical Evergreen Broadleaved Forests. *Frontiers in Plant Science*, *12*(July), 1–12. https://doi.org/10.3389/fpls.2021.686965

Kerkhoff, A. J., & Enquist, B. J. (2009). Multiplicative by nature: Why logarithmic transformation is necessary in allometry. *Journal of Theoretical Biology*, *257*(3), 519–521. https://doi.org/10.1016/j.jtbi.2008.12.026

Konings, A. G., Williams, A. P., & Gentine, P. (2017). Sensitivity of grassland productivity to aridity controlled by stomatal and xylem regulation. *Nature*, *10*(4), 284–288. https://doi.org/10.1038/ngeo2903

Llerena-Zambrano, M., Ordoñez, J. C., Llambí, L. D., Van Der Sande, M., Pinto, E., Salazar, L., & Cuesta, F. (2021). Minimum temperature drives community leaf trait variation in secondary montane forests along a 3000-m elevation gradient in the tropical Andes. *Plant Ecology & Diversity*, *14*(1–2), 47–63. https://doi.org/10.1080/17550874.2021.1903604

Los, S. O., Street-Perrott, F. A., Loader, N. J., Froyd, C. A., Cuní-Sanchez, A., & Marchant, R. A. (2019). Sensitivity of a tropical montane cloud forest to climate change, present, past and future: Mt. Marsabit, N. Kenya. *Quaternary Science Reviews*, *218*, 34–48. https://doi.org/10.1016/j.quascirev.2019.06.016

Maharjan, S., Sterck, F. J., Bishnu, |, Dhakal, P., Makri, M., & Lourens Poorter, |. (2021). Functional traits shape tree species distribution in the Himalayas. *Journal of Ecology*, *3818*, 3818–3834. https://doi.org/10.1111/1365-2745.13759

Maitner, B. S., Halbritter, A. H., Telford, R. J., Strydom, T., Chacon, J., Lamanna, C., ... & Enquist, B. J. (2023). Bootstrapping outperforms community-weighted approaches for estimating the shapes of phenotypic distributions. *Methods in Ecology and Evolution*.

Malizia, A. I., Blundo, C., Carilla, J., Osinaga Acosta, O., CuestaID, F., Duque, A., Aguirre, N., Aguirre, Z., Ataroff, M., Baez, S., Calderó n-LoorID, M., Cayola, L., Cayuela, L., Ceballos, S., Cedillo, H., Farfá Ríos, W., Feeley, K. J., Fernando Fuentes, A., Gá mez A, L. E., … Young, K. R. (2020). Elevation and latitude drive structure and tree species composition in Andean forests: Results from a large-scale plot network. *PLoS ONE*, *15*(4). https://doi.org/10.1371/journal.pone.0231553

We found long-term increases in VPD and minimum temperature in the study area, which are associated with high thermal and hydric stress due to high evapotranspiration demand (Grossiord et al., 2020). These long-term changes in climatic conditions may explain some of our results in shifts in trait distribution and species demographic rates. In the most recent communities, the observed increases in LDMC and leaf thickness, along with the corresponding decreases in leaf area and SLA, with rising minimum temperature and VPD at high elevations, likely indicate the heightened susceptibility of tree species to these climatic factors. This susceptibility can be attributed to their lower thermal tolerances, as supported by previous studies (Cuesta et al., 2019; Feeley et al., 2020). Andean forests are highly adapted to low temperatures (Llerena-Zambrano et al., 2021), so they could be more sensitive to changes in minimum temperature than mean, maximum temperatures, or precipitation Meng, T.-T., Wang, H., Harrison, S. P., Prentice, I. C., Ni, J., & Wang, G. (2015). Responses of leaf traits to climatic gradients: adaptive variation versus compositional shifts. Biogeosciences, 12, 5339–5352. https://doi.org/10.5194/bg-12-5339-2015

Ochoa-Beltrán, A., Martínez-Villa, J. A., Kennedy, P. G., Salgado-Negret, B., & Duque, A. (2021). Plant Trait Assembly in Species - Rich Forests at Varying Elevations in the Northwest Andes of Colombia. *Land*, *10*(1057), 1–16.

Orme, C. D. L., Davies, R. G., Burgess, M., Eigenbrod, F., Pickup, N., Olson, V. A., Webster, A. J., Ding, T. S., Rasmussen, P. C., Ridgely, R. S., Stattersfield, A. J., Bennett, P. M., Blackburn, T. M., Gaston, K. J., & Owens, I. P. F. (2005). Global hotspots of species richness are not congruent with endemism or threat. *Nature*, *436*(7053), 1016–1019. https://doi.org/10.1038/nature03850

Pabón-Caicedo, J. D., Arias, P. A., Carril, A. F., Espinoza, J. C., Borrel, L. F., Goubanova, K., Lavado-Casimiro, W., Masiokas, M., Solman, S., & Villalba, R. (2020). Observed and Projected Hydroclimate Changes in the Andes. In *Frontiers in Earth Science* (Vol. 8). Frontiers Media S.A. https://doi.org/10.3389/feart.2020.00061

Payne, D., Spehn, E. M., Snethlage, M., & Fischer, M. (2017). Opportunities for research on mountain biodiversity under global change. *Current Opinion in Environmental Sustainability*, *29*, 40–47. https://doi.org/10.1016/j.cosust.2017.11.001

Peña, M. A., Feeley, K. J., & Duque, A. (2018). Effects of endogenous and exogenous processes on aboveground biomass stocks and dynamics in Andean forests. *Plant Ecology*, *219*(12), 1481–1492. https://doi.org/10.1007/s11258-018-0895-2

Pérez-Harguindeguy, N., Díaz, S., Garnier, E., Lavorel, S., Poorter, H., Jaureguiberry, P., Cornwell, W. K., Craine, J. M., Gurvich, D. E., Urcelay, C., Veneklaas, E. J., Reich, P. B., Poorter, L., Wright, I. J., Ray, P., Enrico, L., Pausas, J. G., de Vos, A. C., Buchmann, N., … Cornelissen, J. H. C. (2013). New handbook for standardised measurement of plant functional traits worldwide. *Australian Journal of Botany*, *64*, 715–716.

Phillips, O. L., Hall, P., Gentry, A. H., Sawyer, S. A., & Vásquez, R. (1994). Dynamics and species richness of tropical rain forests. *Proceedings of the National Academy of Sciences of the United States of America*, *91*(7), 2805–2809. https://doi.org/10.1073/pnas.91.7.2805

R Core Team. R: A language and environment for statistical computing. R Foundation for Statistical Computing, Vienna, Austria. 2010. http://www.R-project.org/.

Reich, P. B. (2014). The world-wide ‘ fast – slow ’ plant economics spectrum : a traits manifesto. *Journal of Ecology*, *102*, 275–301. https://doi.org/10.1111/1365-2745.12211

Ruiz-Benito, P., Ratcliffe, S., Zavala, M. A., Martínez-Vilalta, J., Vilá-Cabrera, A., Lloret, F., Madrigal-González, J., Wirth, Christian, Greenwood, S., Gerald, K, Lehtonen, A., Kattge, J., Dahlgren, J., Alistair, S. Jump. (2017). Climate and successional related changes in functional composition of European forests are strongly driven by tree mortality. *Global*, *23*, 4162–4176. https://doi.org/10.1111/gcb.13728

Swenson, N. G., Hulshof, C. M., Katabuchi, M., & Enquist, B. J. (2020). Long-term shifts in the functional composition and diversity of a tropical dry forest: a 30-yr study. *Ecological Monographs*, *90*(3), 1–16. https://doi.org/10.1002/ecm.1408

Trugman, A. T., Anderegg, L. D. L., Shaw, J. D., & Anderegg, W. R. L. (2020). Trait velocities reveal that mortality has driven widespread coordinated shifts in forest hydraulic trait composition. *Proceedings of the National Academy of Sciences*, *117*(15), 8532–8538. https://doi.org/10.1073/pnas.1917521117

van der Sande, M. T., Arets, E. J. M. M., Peña-Claros, M., de Avila, A. L., Roopsind, A., Mazzei, L., Ascarrunz, N., Finegan, B., Alarcón, A., Cáceres-Siani, Y., Licona, J. C., Ruschel, A., Toledo, M., & Poorter, L. (2016). Old-growth Neotropical forests are shifting in species and trait composition. *Ecological Monographs*, *86*(2), 228–243. https://doi.org/10.1890/15-1815.1

Violle, C., Navas, M.-L., Vile, D., Kazakou, E., Fortunel, C., Hummel, I., & Garnier, E. (2007). Let the concept of trait be functional! *Oikos*, *116*(5), 882–892. https://doi.org/10.1111/j.0030-1299.2007.15559.x

Violle, C., Reich, P. B., Pacala, S. W., Enquist, B. J., & Kattge, J. (2014). The emergence and promise of functional biogeography. *Proceedings of the National Academy of Sciences of the United States of America*, *111*, 13690–13696. https://doi.org/10.1073/pnas.1415442111

Wieczynski, D. J., Boyle, B., Buzzard, V., Duran, S. M., Henderson, A. N., Hulshof, C. M., Kerkhoff, A. J., McCarthy, M. C., Michaletz, S. T., Swenson, N. G., Asner, G. P., Bentley, L. P., Enquist, B. J., & Savage, V. M. (2018). Climate shapes and shifts functional biodiversity in forests worldwide. *Proceedings of the National Academy of Sciences*, *116*(15), 587–592. https://doi.org/10.1073/pnas.1904390116

Wright, I. J., Reich, P. B., Westoby, M., Ackerly, D. D., Baruch, Z., Bongers, F., Cavender-Bares, J., Chapin, T., Cornellssen, J. H. C., Diemer, M., Flexas, J., Garnier, E., Groom, P. K., Gulias, J., Hikosaka, K., Lamont, B. B., Lee, T., Lee, W., Lusk, C., … Villar, R. (2004). The worldwide leaf economics spectrum. *Nature*, *428*(6985), 821–827. https://doi.org/10.1038/nature02403

Yuan, W., Zheng, Y., Piao, S., Ciais, P., Lombardozzi, D., Wang, Y., Ryu, Y., Chen, G., Dong, W., Hu, Z., Jain, A. K., Jiang, C., Kato, E., Li, S., Lienert, S., Liu, S., Nabel, J. E. M. S., Qin, Z., Quine, T., … Yang, S. (2019). Increased atmospheric vapor pressure deficit reduces global vegetation growth. *Science Advances*, *5*, 1–12. https://www.science.org

Zomer, R. J., Trabucco, A., Bossio, D. A., & Verchot, L. v. (2008). Climate change mitigation: A spatial analysis of global land suitability for clean development mechanism afforestation and reforestation. *Agriculture, Ecosystems and Environment*, *126*(1–2), 67–80. https://doi.org/10.1016/j.agee.2008.01.014

Table 3.1. P-values and coefficients (in parenthesis) from the linear mixed effect models between each community-weighted moment and census. The plot was included as a random effect to account for the census as repeated measures per plot.

	CWM	**CWV**	**CWS**	**CWK**
Trait	**Census**	**Census**	**Census**	**Census**
SLA	0.3 (-0.14)	0.1 (-0.36)	0.1 (0.31)	**<0.05 (3.33)**

LogLA	**<0.05 (-0.06)**	**<0.005 (-0.08)**	0.9 (-0.006)	0.3 (0.23)
LDMC	0.1 (0.11)	0.6 (0.01)	0.4 (-0.08)	**<0.05 (0.5)**
LD	0.1 (0.07)	0.2 (0.19)	0.2 (0.46)	0.1 (3.57)
LTh	0.2 (0.14)	0.4 (-0.08)	0.07 (0.49)	0.2 (3.55)
LogLT	0.5 (0.08)	0.1 (-0.23)	**<0.05 (0.30)**	0.2 (0.45)
WD	0.2 (0.01)	0.7 (0.06)	0.6 (0.02)	0.4 (-0.11)

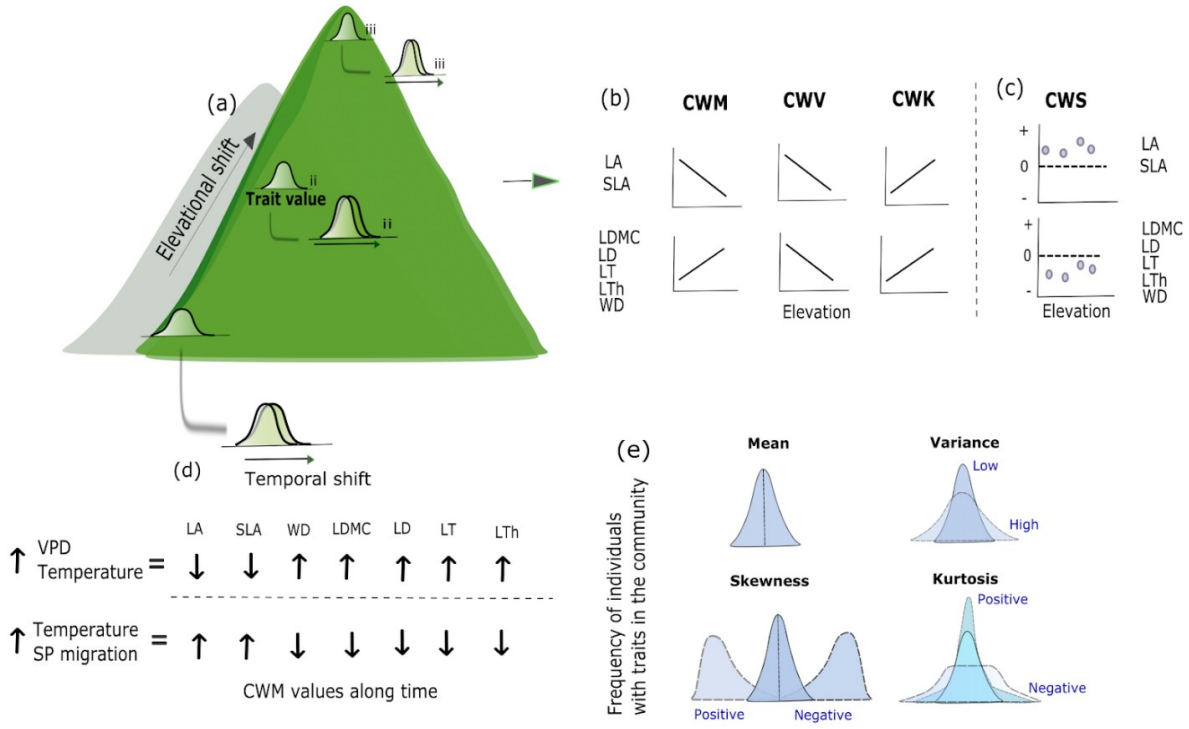

Figure 3.1) Representation of hypothesis on how functional composition would change along elevation and over time. a) Along elevation trait distributions are expected to shift from acquisitive to conservative strategies. This will indicate b) decreases in mean values (CWM) of leaf area (LA) and specific leaf area (SLA), and increases in mean values of leaf dry matter content (LDMC), leaf density (LD), leaf thickness (LT), and leaf toughness (LTh) and wood density (WD). At higher elevations, we expect lower values of trait variance (CWV) and a more peaked distribution with positive CWK related to strong environmental filtering due to lower temperatures at high elevations. c) Community-Weighted Skewness (CWS) indicates the bias of the community trait distribution due to responses to rapid environmental changes in local communities and the dynamic of functional trait distribution over time. For instance, in a community affected by changes in climate, trait distributions will shift to reflect the changing optimal trait value. However, the mean will lag behind, resulting in a distribution bias. Those communities that are shifting in trait mean values, should be characterized by positive or negative skewness. With warming, for those traits increasing across a temperature gradient (LA, SLA), we would predict positive skewness as the community shifts to the new optimal trait value. In contrast, with warming, trait distribution of those traits negatively correlated with temperature will be characterized by negative skewness as the community shifts to the new optimal trait value (Enquist et al. 2015; 2017) (see Figure 4 Wieczynski et al. 2018). d) Hypothesized temporal changes in seven community-weighted mean traits in response to i) increased VPD and temperature and ii) increased temperature and upslope species migration. e) The four central moment distributions; moments are compared with a normal distribution

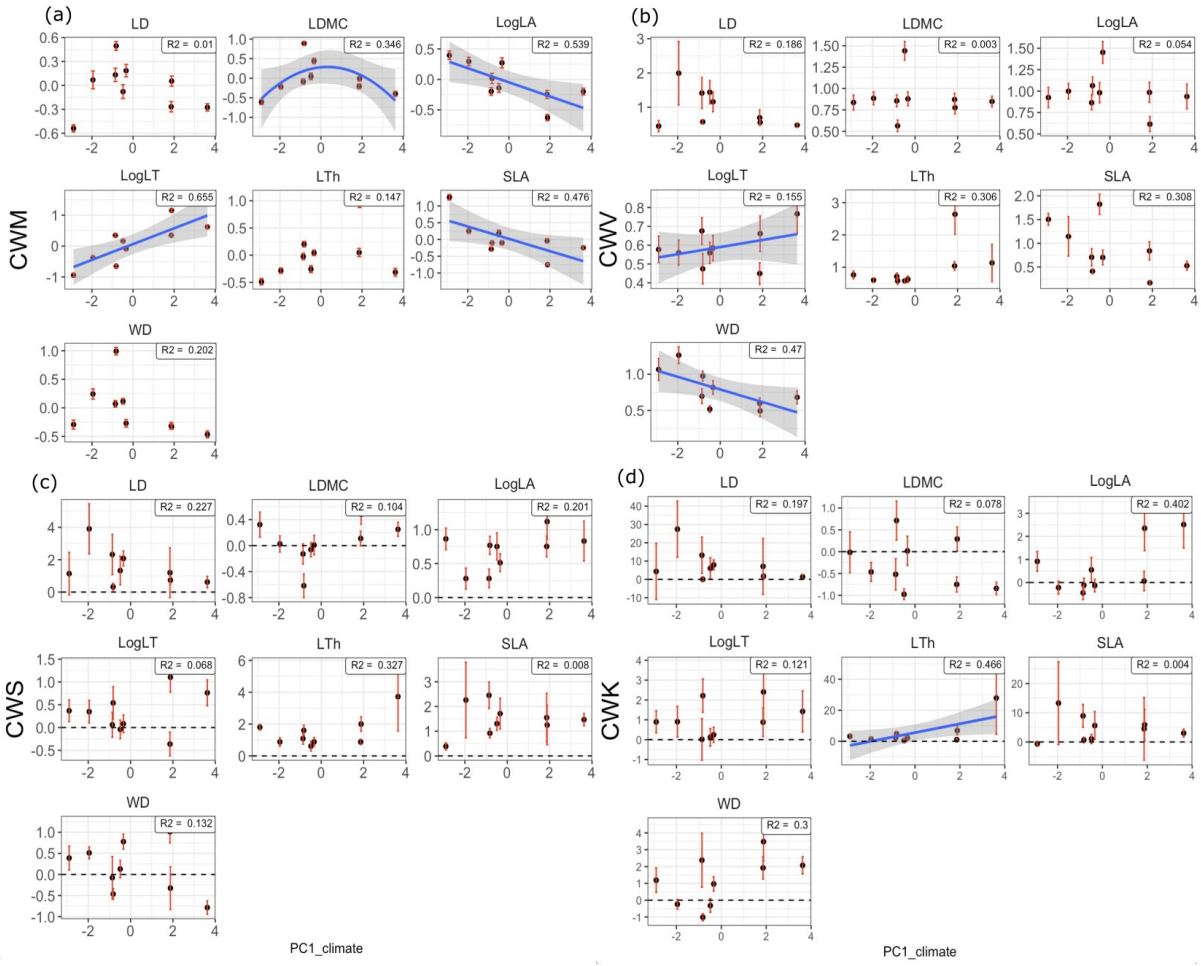

Figure 3.2) Shifts in the abundance-weighted community of a) mean (CWM), b) variance (CWV), c) skewness (CWS), and d) kurtosis (CWK) of each trait along the climatic gradient (PC1_climate, mainly correlated with temperature and elevation) for leaf area (LA), specific leaf area (SLA), and wood density (WD), leaf dry matter content (LDMC), leaf density (LD), leaf thickness (LT), and leaf toughness (LTh). Size-related plant traits with power-law growth rates of the form Y= axb, such as LA and LT, were log10 transformed. CWM and CWV were standardized with mean zero and variance one to compare traits. Significant relationships with PC1_climate axes are shown with the trend line. The 95% confidence intervals (red lines) are reported for each plot and trait per moment. Confidence intervals were calculated based on 1,000 bootstrap replicates for each plot. Values of zero represent a normal distribution. CWS ≠ 0 represents strong left or right tails. CWK = -1.2 represents an even distribution. Note that PC1_climate is negatively correlated with temperature. So, for a CWM trait value that is positively correlated with PC1_climate (negatively correlated with temperature such as SLA and LA) we would predict positive skewness. In contrast, when a CWM trait value is negatively correlated with PC1_climate (positively correlated with temperature, such as LT), we would predict negative skewness. In general, we do see support for these predictions.

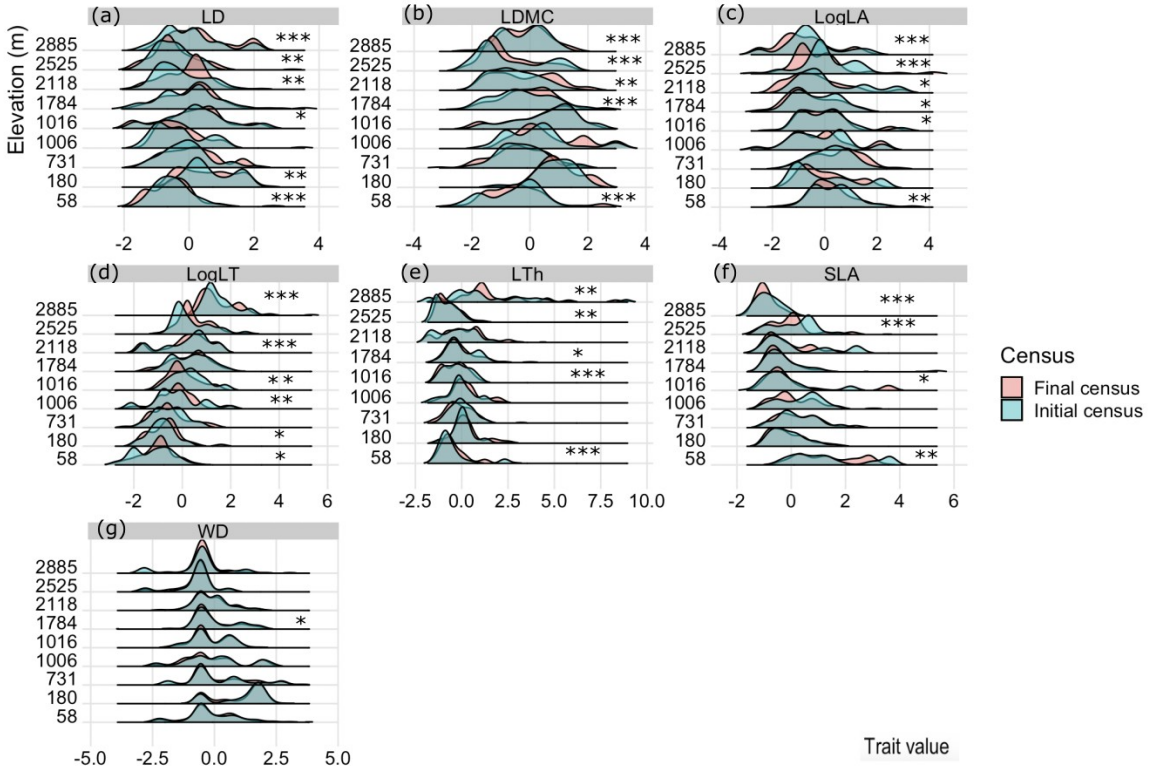

Figure 3.3) Abundance-weighed Kernel density estimates of each trait across the elevational gradient in each census. Each elevation represents a tree community, and each color represents a census. Traits are a) leaf density (LD), b) leaf dry matter content (LDMC), c) leaf area (LogLA), d) leaf thickness (LogLT), e) leaf toughness (LTh), f) specific leaf area (SLA) and g) wood density (WD). Size-related plant traits with power-law growth rates of the form Y= axb, such as LA and LT, were log10 transformed. Results represent P-values from the Kolmogorov-Smirnov test between the trait distribution of the first census and the distribution of the last census (* <0.05, **<0.01, ***<0.001). Data were standardized with mean zero and variance one to compare traits.

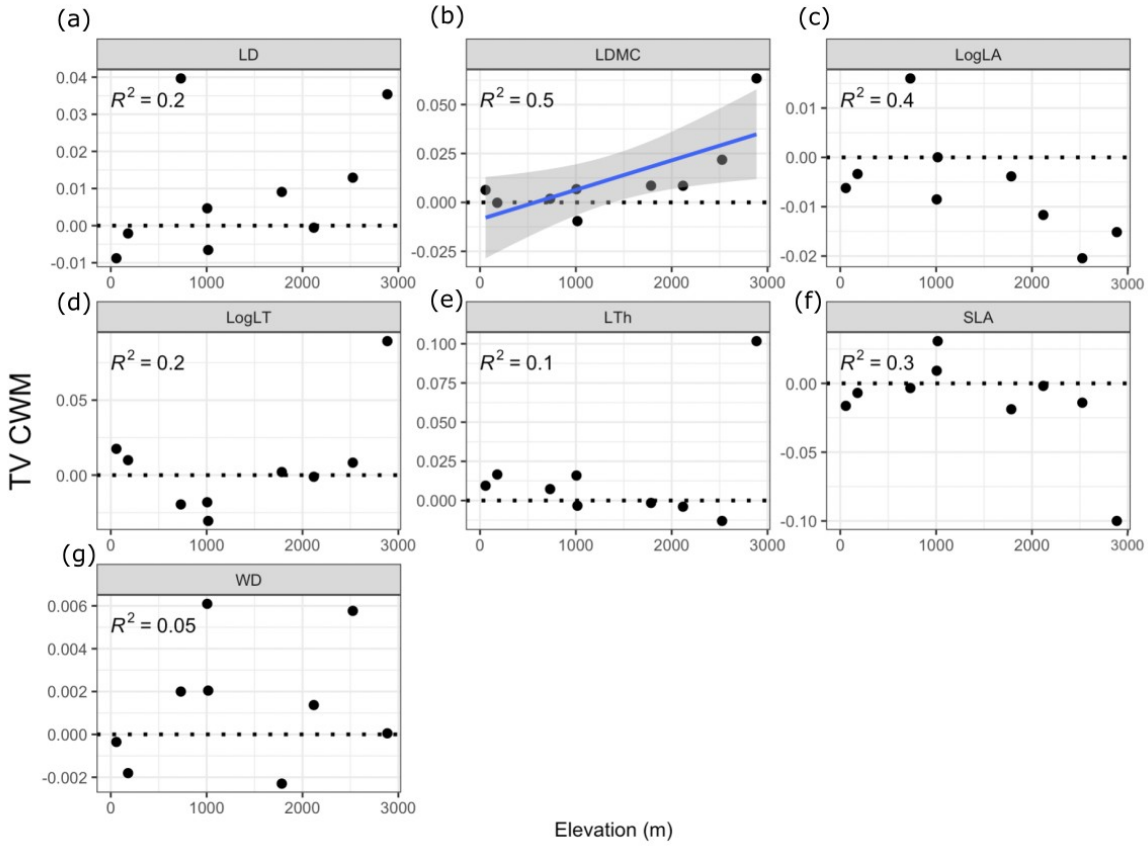

Figure 3.4) Trait Velocity Index of community weighted-mean (TV_CWM) of each trait (y-axis) along the elevational gradient (x-axis). TV_CWM represents the annual rate of change for each trait moment, which indicates the direction and magnitude of the functional change. TV_CWM equal to zero represents no change over time. Positive values mean an increase in the trait community value over time. Negative TV values mean a decrease in community trait value over time. The further the TV value is from zero, the higher the magnitude of the change. A significant relationship between TV_CWM with elevation is presented with the linear regression trend line. Traits are a) leaf density (LD), b) leaf dry matter content (LDMC), c) leaf area (LogLA), d) leaf thickness (LogLT), e) leaf toughness (LTh), f) specific leaf area (SLA) and g) wood density (WD). Size-related plant traits with power-law growth rates of the form Y= axb, such as LA and LT, were log10 transformed.

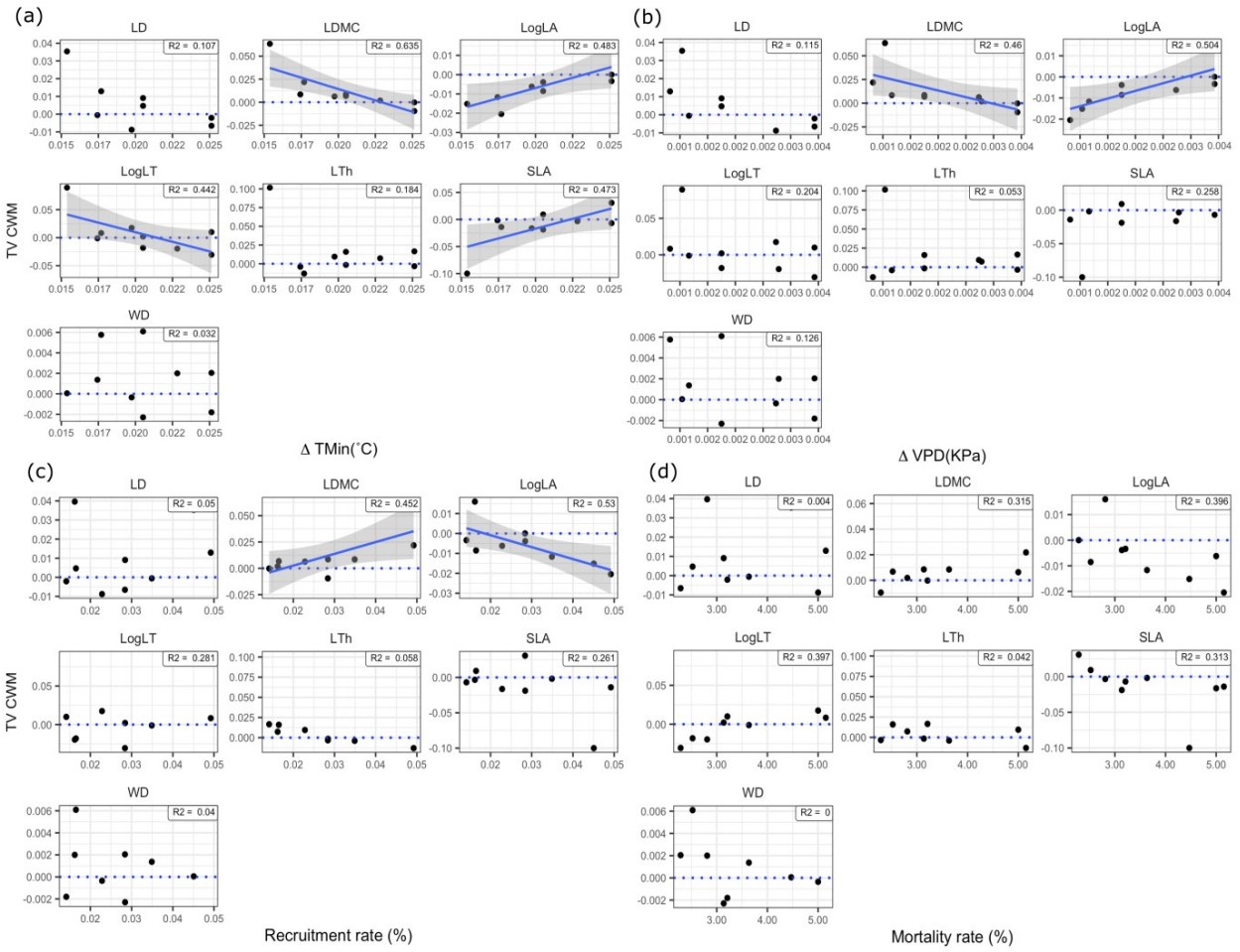

Figure 3.5) Linear regressions between trait velocity of community weighted-mean (TV_CWM) of each trait and the a) annualized rate of change of minimum temperature (ΔT_{min}), b) vapor-pressure deficit (ΔVPD), c) recruitment, and d) mortality of individuals (%). TV_CWM equal to zero represents no change over time. Positive values mean an increase in the trait community value over time. Conversely, negative TV_CWM values mean decreases in community trait value over time. A significant relationship between changes in functional composition and changes in climate or demography is denoted by a linear trend. TV_CWM values were standardized with mean zero and variance one to compare traits. The traits are wood density (WD), leaf dry matter content (LDMC), specific leaf area (SLA), leaf toughness (LTh), leaf density (LD), leaf area (LogLA), and leaf thickness (LogLT). Size-related plant traits with power-law growth rates of the form $Y = ax^b$, such as LA and LT, were $\log_{10}$ transformed. TV values were standardized with mean zero and variance one to compare traits.

APPENDIX S3.1: Supplementary methodology Traits Sampling

Based on the inventory of the most recent census data, we measured five individuals from the species that contribute a minimum of the 80% of the abundance data and at least one individual from the remaining species to characterize as many species as possible. In the plots located at Angelópolis, Anorí, and Segovia, we measured three individuals due to the high number of morpho-species. Shared species between plots were measured in every plot to represent intra-specific variability along the gradient better. Those species inaccessible due to height or those species with small and unique individuals without a sufficient number of leaves were not measured. Five mature and healthy leaves from each tree were collected, making sure to collect leaves with the greatest exposure to light. Due to the plot's arrangement, we sampled leaves from understory species and canopy species, ensuring that canopy species were tested in large trees. With the help of certified climbers, we reached the leaves exposed to the sun in very tall canopy trees. We analyzed 1,104 tree morpho-species distributed in 361 genera and 103 families. The total of trees sampled is 2,297, and 10,470 individual leaves.

We focused on seven leaf morphological traits related to life strategy, resource distribution (Wright et al., 2004), and sensitivity to biotic conditions and environmental changes (Violle et al., 2007). The traits were: Leaf Thickness (LT, mm), reflecting water stress tolerance (Westoby, Falster, Moles, Vesk, & Wright, 2002). Leaf Area (LA, mm^2), Specific Leaf Area (SLA, mm/mg), Leaf Density (LD, g/cm^3), and Leaf Dry Matter Content (LDMC, mg/g), essential for light acquisition, plant growth and nutrient acquisition and allocation (Díaz et al., 2016; Wright et al., 2004). Leaf Toughness (LTh, N/mm) is associated with structural plant defense (Lucas, Turner, Kominy, & Yamashita, 2000), and Wood Density (WD, g/cm^3) is related to hydraulic safety and mechanical and physiological strategies (Díaz et al., 2016; Swenson & Enquist, 2007; Wright et al., 2004).

Using the software ImageJ (http://rsbweb.nih.gov/ij/), we quantified the leaf area (LA) with the petiole. To calculate the specific leaf area (SLA), we placed each leaf in a separate paper bag in the oven for 72 hours (60°C) before measuring dry weight using an analytical

balance with a precision of 0.0001 g. Leaf thickness (LT) was measured with a digital micrometer (Mitutoyo, precision 0.0001 mm), and leaf toughness (LTh) was measured using a Pesola Medio-Line Pressure Set adopted to Spring Scales (300, 600, and 1200 g of capacity, rod diameter 3.16 mm). LT and Lth were measured three times per leaf using fresh leaves and avoiding leaf veins. LT, LTh, and fresh mass were measured immediately when the branch was cut; SLA and leaf dry matter content (LDMC) were conducted at Universidad Nacional de Colombia-Medellín. Additionally, wood density was measured for mature canopy trees using samples from branches. The bark was removed from each sample and rehydrated for 24 hours, and the volume was then estimated through water displacement. Samples were then placed in the oven at 70°C until a constant weight was achieved to measure dry weight.

APPENDIX S1.2: Supplementary methodology: Statistical intra-specific variability

Based on the abundance-weighted kernel density distributions estimated for each trait and community, we quantified the four central moments weighted by species abundance. To calculate density distributions that better represent the community and the variation in trait values, we incorporate intra-specific variability through statistic resampling raw data with a non-parametric bootstrapping (Maitner et al., 2021). This method uses random sampling with replacement from the observed traits in proportion to the species abundance. Thus, the variation of the observed data is used to generate a set of new distributions. In the case that the species just has one trait value, such as in the case of rare species, no variation is incorporated. Distribution and moment values were calculated using the TraitsTrap R package (Maitner et al., 2021).

REFERENCES

Díaz, S., Kattge, J., Cornelissen, J. H. C., Wright, I. J., Lavorel, S., Dray, S., Reu, B., Kleyer, M., Wirth, C., Colin Prentice, I., Garnier, E., Bönisch, G., Westoby, M., Poorter, H., Reich, P. B., Moles, A. T., Dickie, J., Gillison, A. N., Zanne, A. E., … Gorné, L. D. (2016). The global spectrum of plant form and function. *Nature*, *529*(7585), 167–171. https://doi.org/10.1038/nature16489

Lucas, P. W., Turner, I. M., Kominy, N. J., & Yamashita, N. (2000). Mechanical Defences to Herbivory. *Annals of Botany*, *86*, 913–920. https://doi.org/https://doi.org/10.1006/anbo.2000.1261

Maitner, B., Halbritter, A., Telfor, R. et al (2021). On estimating the shape and dynamics of phenotypic distributions in ecology and evolution. Authorea. May 25, 2021

Violle, C., Navas, M. L., Vile, D., Kazakou, E., Fortunel, C., Hummel, I., & Garnier, E. (2007). Let the concept of trait be functional! *Oikos*, *116*(5), 882–892. https://doi.org/10.1111/j.2007.0030-1299.15559.x

Westoby, M., Falster, D. S., Moles, A. T., Vesk, P. A., & Wright, I. J. (2002). Plant ecological strategies: Some leading dimensions of variation between species. *Annual Review of Ecology and Systematics*, *33*, 125–159. https://doi.org/10.1146/annurev.ecolsys.33.010802.150452

Wright, I. J., Reich, P. B., Westoby, M., Ackerly, D. D., Baruch, Z., Bongers, F., Cavender-Bares, J., Chapin, T., Cornellssen, J. H. C., Diemer, M., Flexas, J., Garnier, E., Groom, P. K., Gulias, J., Hikosaka, K., Lamont, B. B., Lee, T., Lee, W., Lusk, C., … Villar, R. (2004). The worldwide leaf economics spectrum. *Nature*, *428*(6985), 821–827. https://doi.org/10.1038/nature02

SUPPLEMENTARY TABLES

Table S3.1 Climatic data for each plot

PLOT	MAT	ISO	Tem seasonality	Max. T	Min. T	MA P	PP. seasonality	dry months	VAP	Wind speed	solar rad	VP D	PET	SVP	Elevation
Carepa	26,8	86	27,2	32	22,3	2585	47,157	1	2,93	1,71	18320,58	0,71	140,17	3,64	**58**
Puerto Triunfo	27,7	91	29,6	33,5	22,3	2535	41,001	0	2,87	0,89	17640,42	0,86	135,08	3,72	**180**
Segovia	24,8	83	58,2	30,7	19	3260	41,437	1	2,52	1,08	17852,58	0,55	129,42	3,08	**717**
Porce	22,6	86	41,3	28,2	16,7	2678	42,036	1	2,28	0,98	17722,67	0,56	127,25	2,84	**1006**
Maceo	23,7	89	39,4	29,1	18,4	2993	33,464	1	2,35	0,93	17739,00	0,61	129,50	2,96	**1016**
Anori	19,8	74	40,9	25,6	13	2830	43,044	0	1,81	1,07	17830,42	0,52	125,58	2,34	**1784**
Angelópolis	16,4	90	30,8	21,7	11,4	2500	38,270	0	1,58	0,98	17488,33	0,41	118,50	1,99	**2118**
Jardin	15	90	22,9	19,5	10,7	2179	35,890	0	1,45	0,96	17354,17	0,21	107,67	1,65	**2525**
Belmira	13,4	87	33,7	19	7,5	2471	48,347	0	1,20	1,17	17624,08	0,26	109,50	1,47	**2885**

Climatic variables were gathered using climate raster layers at high resolution (30 arsec) available in worldClim version 2.0. and Global Aridity Index and Potential Evapo-Transpiration Climate Database V2. CGIAR Consortium for Spatial Information (CGIAR-CSI).

Definitions: **MAT (°C):** mean annual temperature. **ISO (%):** Isothermality calculated as ((max tem-min tem)/tem annual range))*100 quantifies how large the day-to-night temperatures oscillate relative to the annual oscillations, the range is from 0-100, 100 means the diurnal temperature range is equivalent to the annual temperature range, and values less than 100 means a smaller level of temperature variability within an average month relative to the year. **Tem seasonality (°C)**: temperature seasonality is the amount of temperature variation over averaged years based on the monthly temperature average standard deviation. In other words, it is the measure of temperature change over the year by different years. **Max. Tem (°C)**: Maxi temperature of the warmest month. Maximum monthly temperature occurrence over a time series of years. **Min. Tem (°C):** Minimum monthly temperature occurrence over time. **MAP (mm):** mean annual precipitation. **PP. seasonality (%)**: This is a measure of variation in monthly precipitation totals over a range of years. The index is the standard deviation of the monthly total precipitation to the mean monthly total precipitation. It is an index of precipitation variability, and larger values in percent represent greater precipitation variability. **VAP (KPa):** Water vapor pressure. **Wind speed (m/s). Solar rad (KJ m-1 day-1). VPD (KPa)**: Vapor pressure deficit. VPD was calculated as **saturated vapor pressure (Kpa) (SVP)** - VAP. Where SVP=610.7*10^7.5T/ (237.3+T). **PET (mm)**: Potential Evapotranspiration data was taken from Trabucco & Zomer (2019), PET is calculated using FAO Penman-Monteith equation based on WorldClim version 2 data.

Table S3.2. Basic description of the census data of the nine (9) 1-ha Antioquia plot Networks. Total sp: indicates the most recent species richness by the plot. Sp traits: display the number of species with trait data. % Denotes the percentage of species with trait characterization compared with the total species number of the plot. Year refers to the date when the census was performed.

			Census 1			Census 2			Census 3			Census 4		
Plot	**Total sp**	**Elevation (m)**	**sp traits**	**%**	**Year**	**sp traits**	**%**	**Year**	**sp traits**	**%**	**Year**	**sp traits**	**%**	**Year**
Carepa	141	58	120	85	2009	125	89	2013	127	90	2014			
Puerto Triunfo	156	180	124	79	2009	138	88	2014	139	89	2017			
Segovia	323	717	261	81	2008	291	90	2013						
Porce	120	1006	106	88	2008	113	94	2013	113	94	2016			
Maceo	186	1016	146	78	2009	163	88	2013	168	90	2017			
Anori	331	1784	207	63	2006	248	75	2009	278	84	2014	297	90	2016
Angelopolis	256	2118	176	69	2006	207	81	2009	223	87	2014	226	88	2017
Jardin	106	2525	83	78	2009	95	90	2013	95	90	2017			
Belmira	83	2885	49	59	2006	60	72	2009	68	82	2014	68	82	2017

TABLE S3.3. Loadings of the two main axis from the Principal Component Analysis (PCA) run with the climatic data.

Variable	$PC1_{climate}$	$PC2_{climate}$
MAT	-0.4211	-0.1057
ISO	0.1926	0.0316
TS	-0.2286	-0.4392
MAP	-0.3276	-0.4174
PS	-0.1630	0.4804
Wind speed	-0.2343	0.5540
Solar rad	-0.4282	0.2761
VPD	-0.3971	-0.0764
PET	-0.4508	-0.0166

REFERENCES

Trabucco, A., & Zomer, R. (2019). Global Aridity Index and Potential Evapotranspiration Climate Database v2. CGIAR Consortium for Spatial Information (CGIAR-CSI), available at: https://cgiarcsi.community/2019/01/24/global-aridity-index-and-potential-evapotranspiration-climate-database-v2/.

SUPPLEMENTARY FIGURES

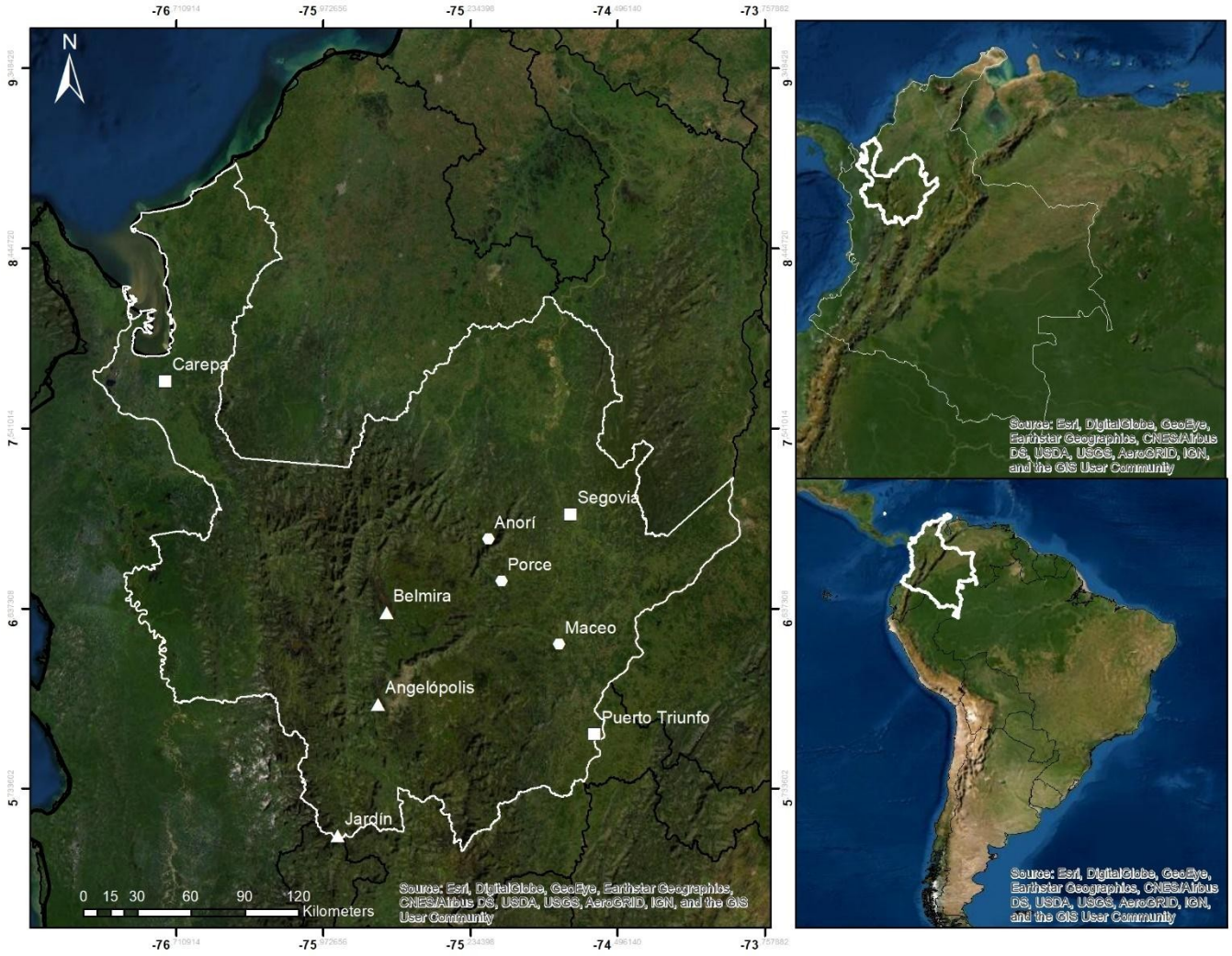

Figure S3.1. Map of the study region showing the location of the nine (9) permanent plots (1-ha each) in the Antioquia department of Colombia. Triangles denote highland plots (2,000-2900 m a.s.l), circles denote mountain forests (1,000-2000 m a..s.l), and squares mean lowland forests (50-1,000 m a.s.l).

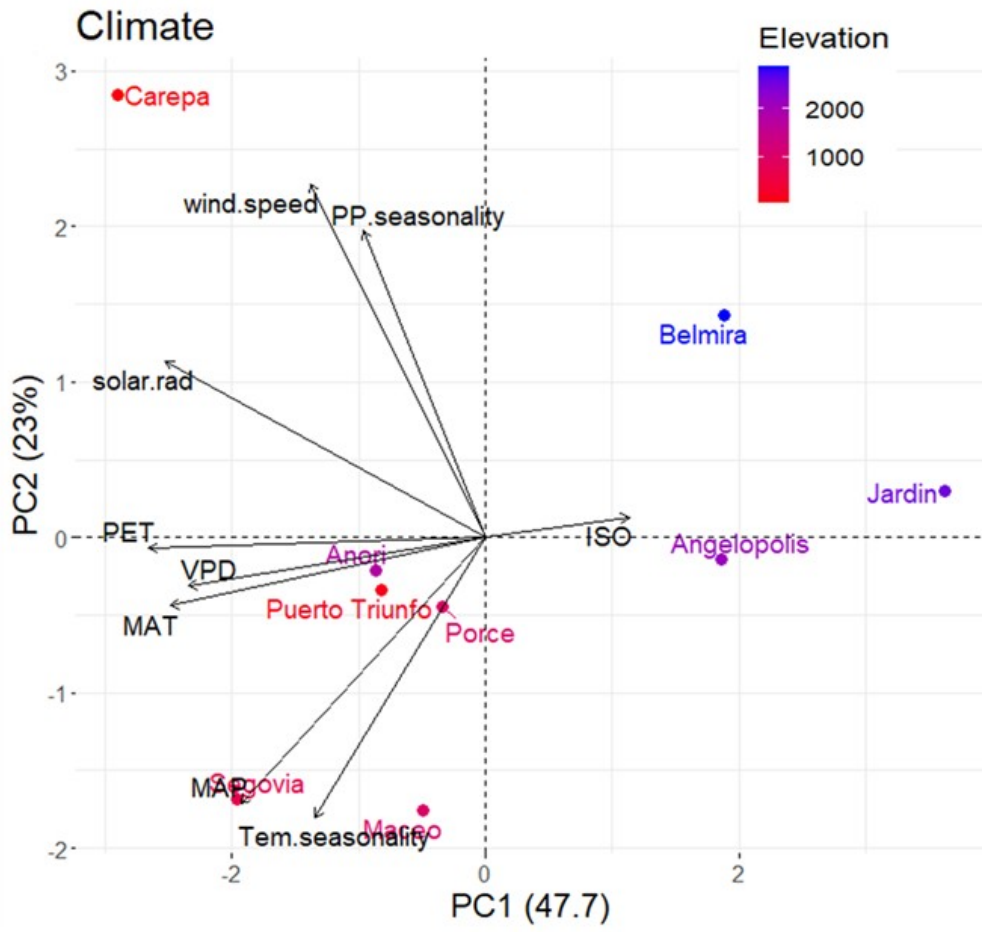

Figure S3.2. Principal Component Analysis (PCA) for climatic data. All variables were standardized and scaled for the analysis. The blue-red color palette represents the elevation of the plot, with blue representing high elevation to red representing low elevation. The climatic variables are mean annual temperature (MAT), isothermality (ISO), temperature seasonality (TS), precipitation seasonality (PS), potential evapotranspiration (PET), wind speed, vapor-pressure deficit (VPD) and solar radiation (Solar.rad) (also see supporting Information Table S1).

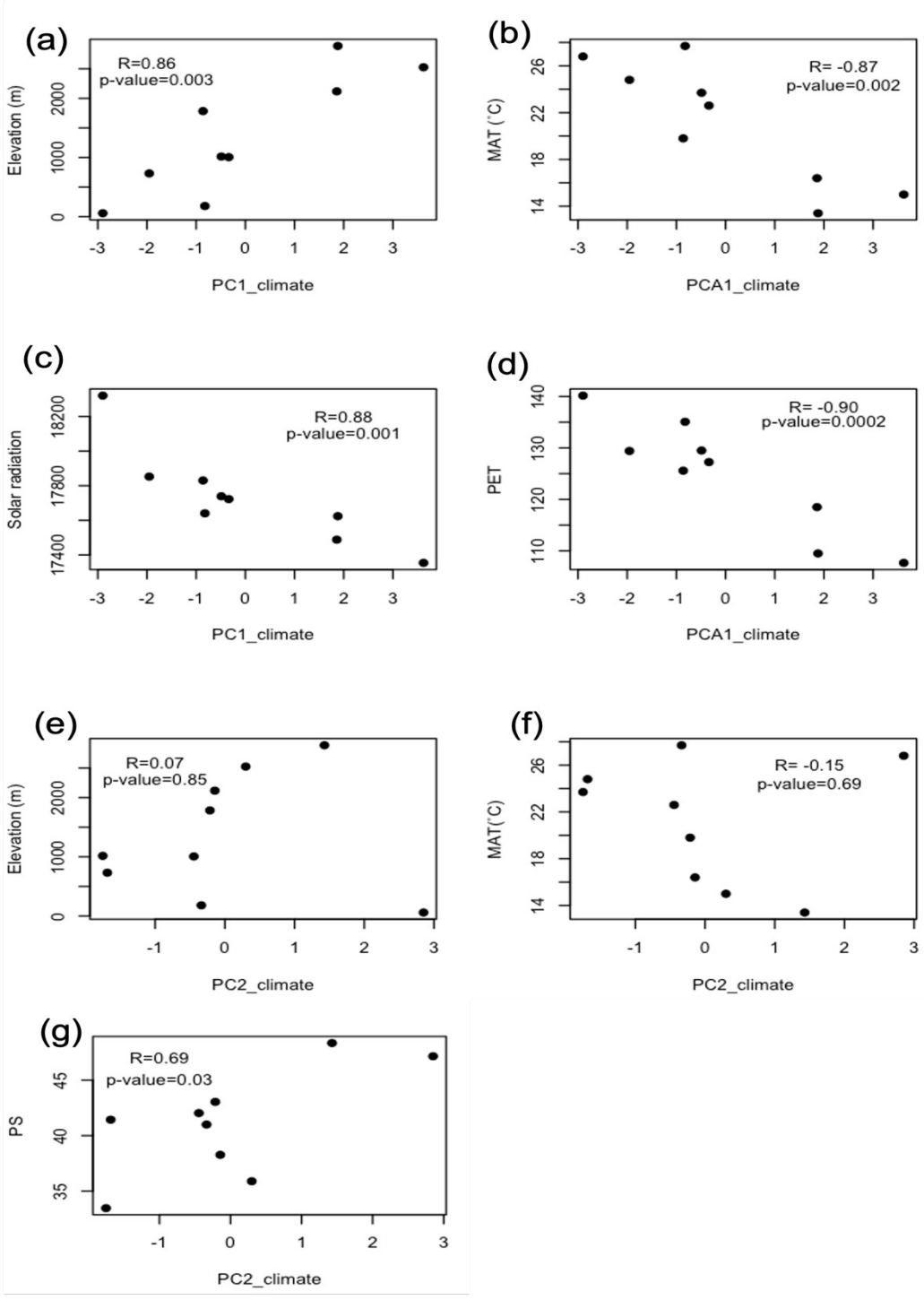
(a)
R=0.86
p-value=0.003
Elevation (m)
PC1_climate
(b)
R= -0.87
p-value=0.002
MAT (°C)
PCA1_climate
(c)
R=0.88
p-value=0.001
Solar radiation
PC1_climate
(d)
R= -0.90
p-value=0.0002
PET
PCA1_climate
(e)
R=0.07
p-value=0.85
Elevation (m)
PC2_climate
(f)
R= -0.15
p-value=0.69
MAT(°C)
PC2_climate
(g)
R=0.69
p-value=0.03
PS
PC2_climate

Figure S3.3. Correlation between $PC1_{\_climate}$ and $PC2_{\_climate}$ with the most related climatic variables of the axis. a) $PC1_{\_climate}$ vs Elevation, b) $PC1_{\_climate}$ vs Mean Annual Temperature (MAT), c) $PC1_{\_climate}$ vs Solar radiation, d) $PC1_{\_climate}$ vs Potential Evapotranspiration (PET), e) $PC2_{\_climate}$ vs Elevation, f) $PC2_{\_climate}$ vs Mean Annual Temperature (MAT), g) $PC2_{\_climate}$ vs Precipitation Seasonality (PS).

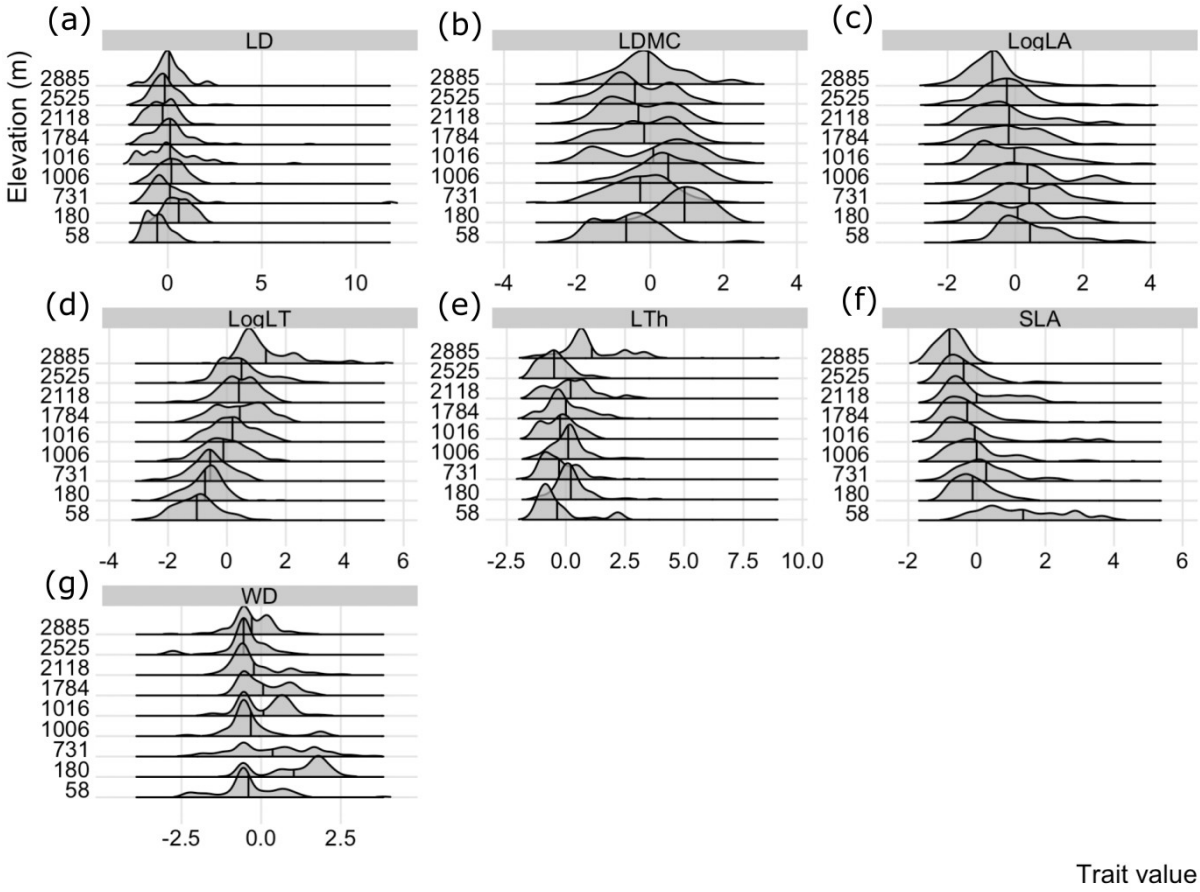

Figure S3.4. Abundance-weighed Kernel estimates of each plant trait and each community along the elevational gradient (each elevation represents one plot). The distributions correspond to the most recent census. The traits plotted are: a) leaf density (LD [g/cm^3]), b) leaf dry matter content (LDMC [mg/g]), c) leaf area (LogLA [mm]), d) leaf Thickness (LogLT [mm]), e) Leaf toughness (LTh [N/mm]), f) specific leaf area (SLA [mm/mg]), g) and wood density (WD [g/ cm^3]). Vertical lines represent the mean of the distribution.

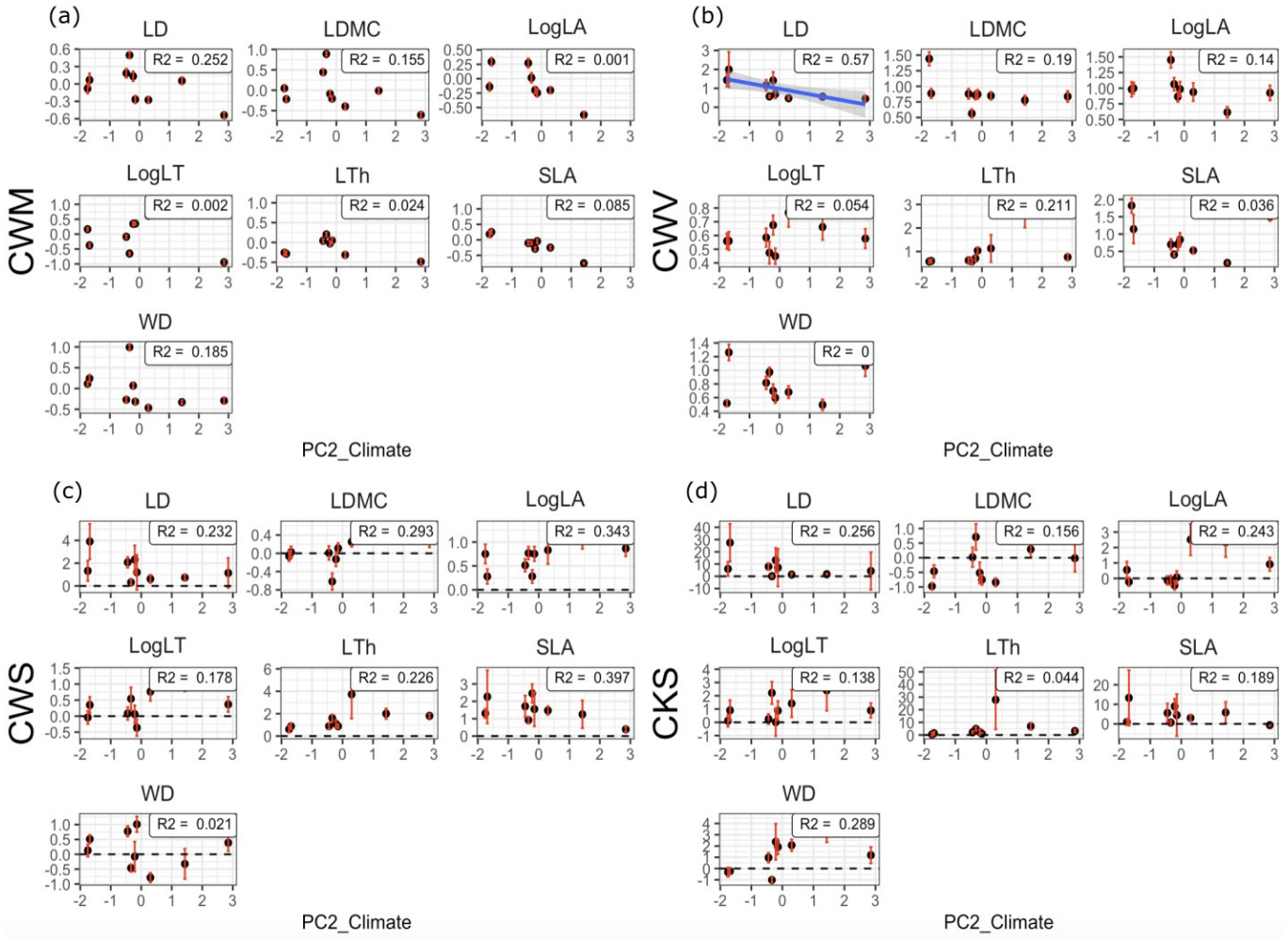
(a)
LD
R2 = 0.252
LDMC
R2 = 0.155
LogLA
R2 = 0.001
CWM
LogLT
R2 = 0.002
LTh
R2 = 0.024
SLA
R2 = 0.085
WD
R2 = 0.185
PC2_Climate
(b)
LD
R2 = 0.57
LDMC
R2 = 0.19
LogLA
R2 = 0.14
CWV
LogLT
R2 = 0.054
LTh
R2 = 0.211
SLA
R2 = 0.036
WD
R2 = 0
PC2_Climate
(c)
LD
R2 = 0.232
LDMC
R2 = 0.293
LogLA
R2 = 0.343
CWS
LogLT
R2 = 0.178
LTh
R2 = 0.226
SLA
R2 = 0.397
WD
R2 = 0.021
PC2_Climate
(d)
LD
R2 = 0.256
LDMC
R2 = 0.156
LogLA
R2 = 0.243
CKS
LogLT
R2 = 0.138
LTh
R2 = 0.044
SLA
R2 = 0.189
WD
R2 = 0.289
PC2_Climate

Figure S3.5. Shifts in the abundance-weighted community a) mean (CWM), b) variance (CWV), c) skewness (CWS), and d) kurtosis (CWK) of each trait along the $PCA2_{\_climate}$ (mainly correlated with Precipitation Seasonality PS, Figure S3). The moments describing the shape of the trait distributions and the 95% confidence intervals (red lines) are reported around each moment and trait. Confidence intervals were calculated based on 1,000 bootstrap replicates for each plot. CWM, CWV, CWS, and CWK values of zero (dashed line) represent a normal distribution. CWM, CWV, CWK, and CWS represent the predominant phenotype in the community, the functional dispersion, evenness, and trait abundance, respectively. CWS $\neq$ 0 represents strong left or right tails. Kurtosis = -1.2 represents an even distribution. Traits are leaf area (LA), specific leaf area (SLA), wood density (WD), high leaf dry matter content (LDMC), Leaf Thickness (LT), Toughness (LTh), and Density (LD). Size-related plant traits reflecting multiplicative processes were Log_{10} transformed (LogLT and LogLA).

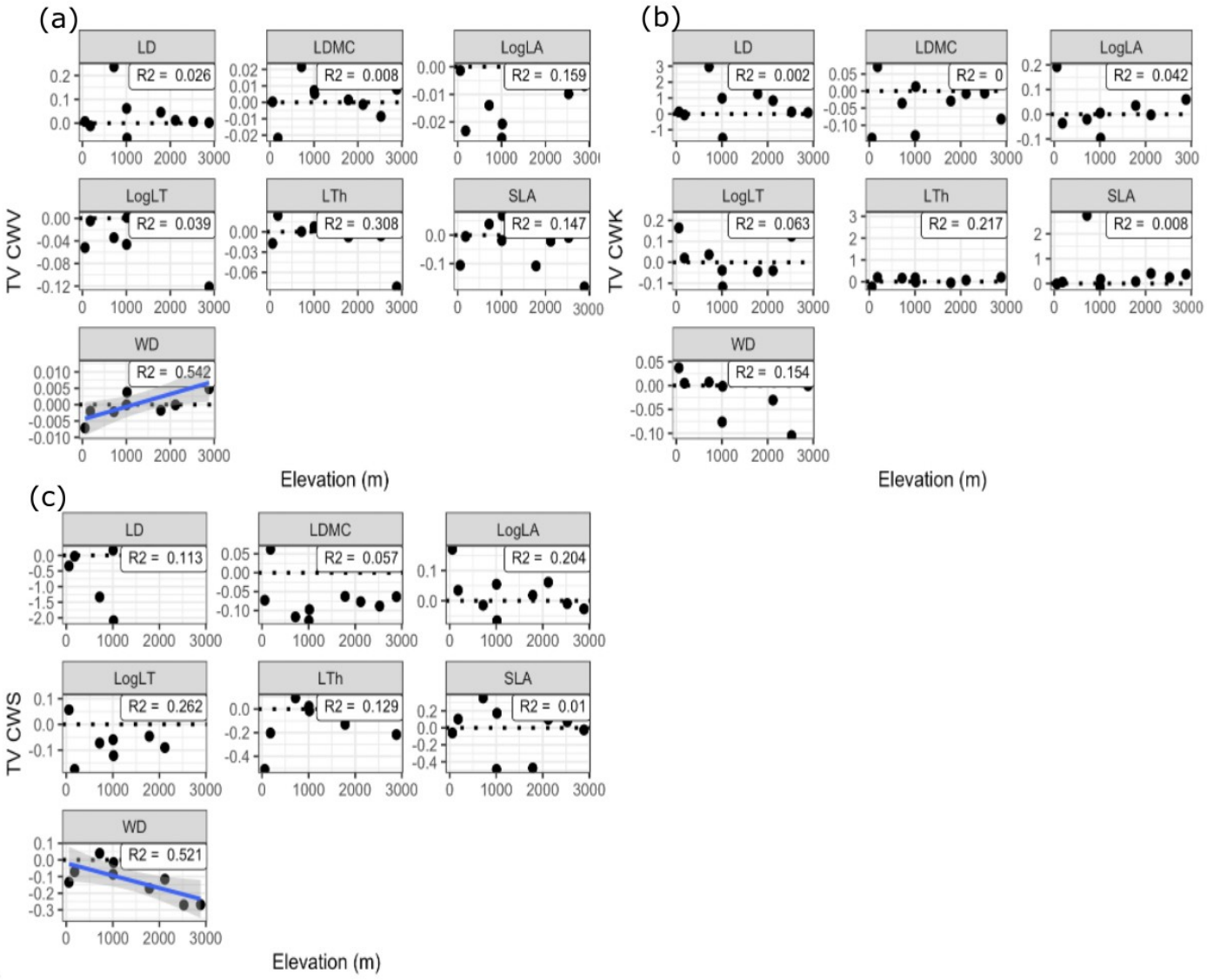

Figure S3.6. Trait Velocity Index of a) community weighted-variance (TV_CWV), b) community weighted-kurtosis (TV_CWK), and c) community weighted-skewness (TV_CWS) of each trait (y-axis) along the elevational gradient (x-axis). TV_CWV, TV_CWK, and TV_CWK represent the annual rate of change of variance, kurtosis, and skewness, respectively, and also indicate the direction and magnitude of the functional change. TV values equal to zero represents no change over time. Positive values mean an increase in the trait community value during the time. Negative TV values mean decreases in community trait value over time. The higher the distance of the TV value from zero, the higher the magnitude of the change. A significant relationship between TV values and elevation is presented with the linear regression trend line. Traits are leaf area (LA), specific leaf area (SLA), and wood density (WD) and increases in mean values of leaf dry matter content (LDMC), leaf density (LD), leaf thickness (LT), and leaf toughness (LTh).

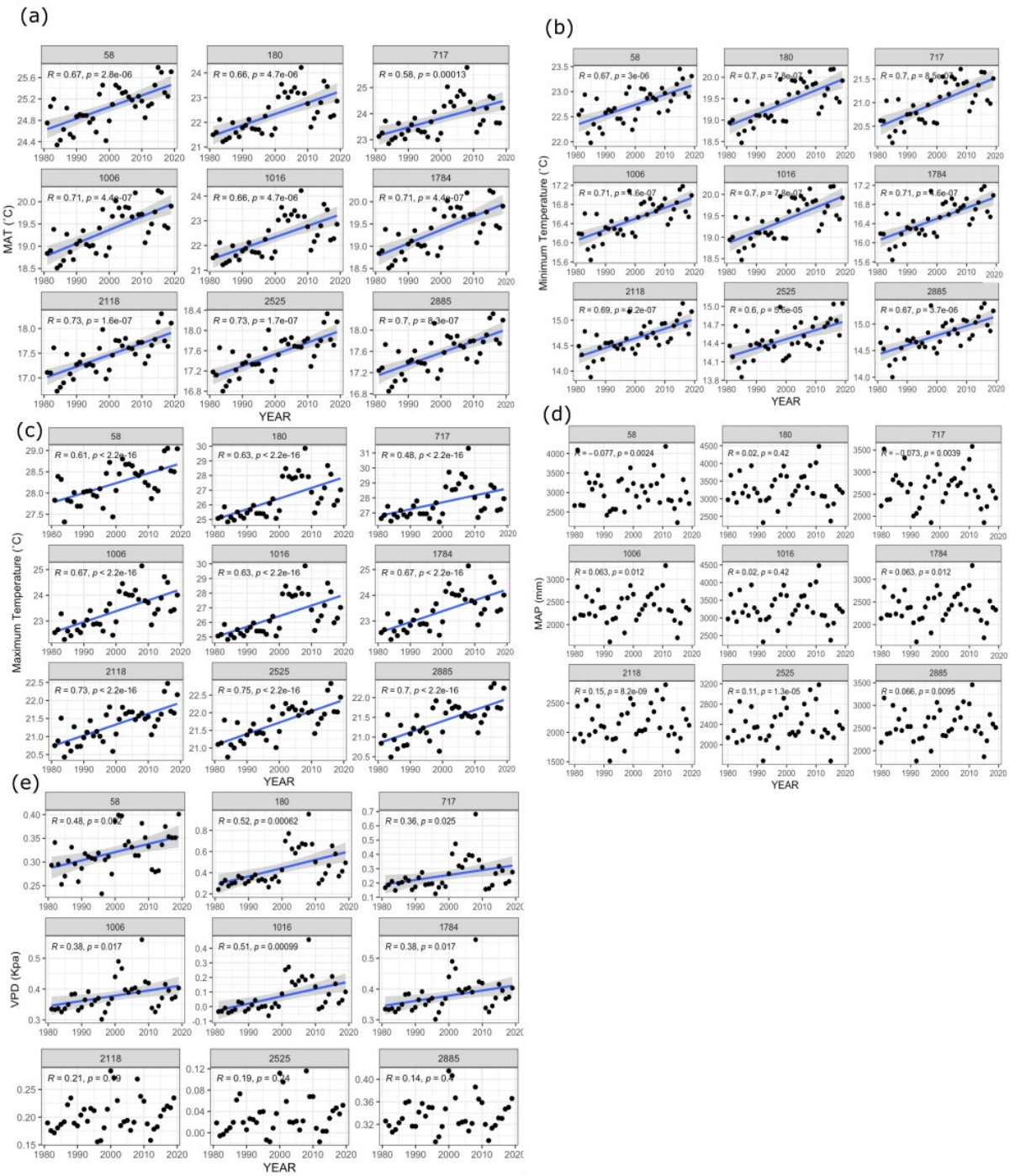

Figure S3.7. Each local community's climate change rate in the last 38 years along the elevational gradient. We calculate the local climate change as the slope of the linear least-square regression for each climatic variable respective to the time period. Each panel represents an elevation (plot), the y-axis represents the climatic variable, and the x-axis is the time in years. a) changes in MAT (ºC) over time by plot (panel), b) changes in minimum temperature (ºC) over

time by plot, c) changes in maximum temperature (ºC) over time by plot, d) changes in mean annual precipitation (mm) over time by plot, e) changes in vapor pressure deficit (Kpa) over time by plot. Then, the figure shows the change in each climatic variable by plot over time. Significant relationships are represented by the regression line trend. The head title per plot panel represents the elevation in m.

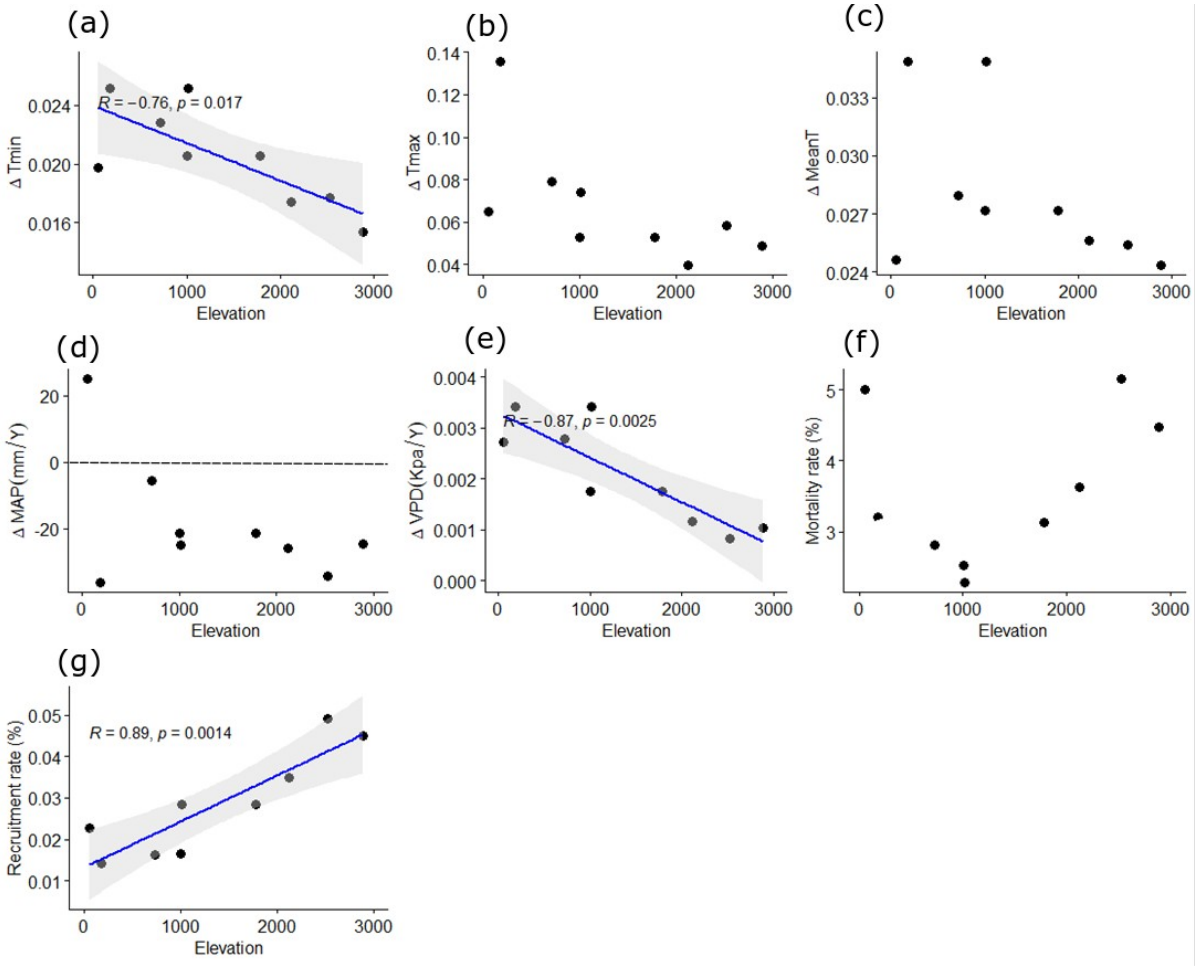

Figure S3.8. Figures from a-e are the average rate of changes during the last 38 years along the elevational gradient in a) minimum temperature (°C Y^{-1}), b) maximum temperature (°C Y^{-1}), c) mean temperature (°C Y^{-1}), d) mean annual precipitation (mm Y^{-1}), and e) vapor pressure deficit (Kpa Y^{-1}). Figures f-g) are the community dynamic based on abundance data across the first and last census. f) annual mortality rate (%) and g) Annual recruitment rate (%).

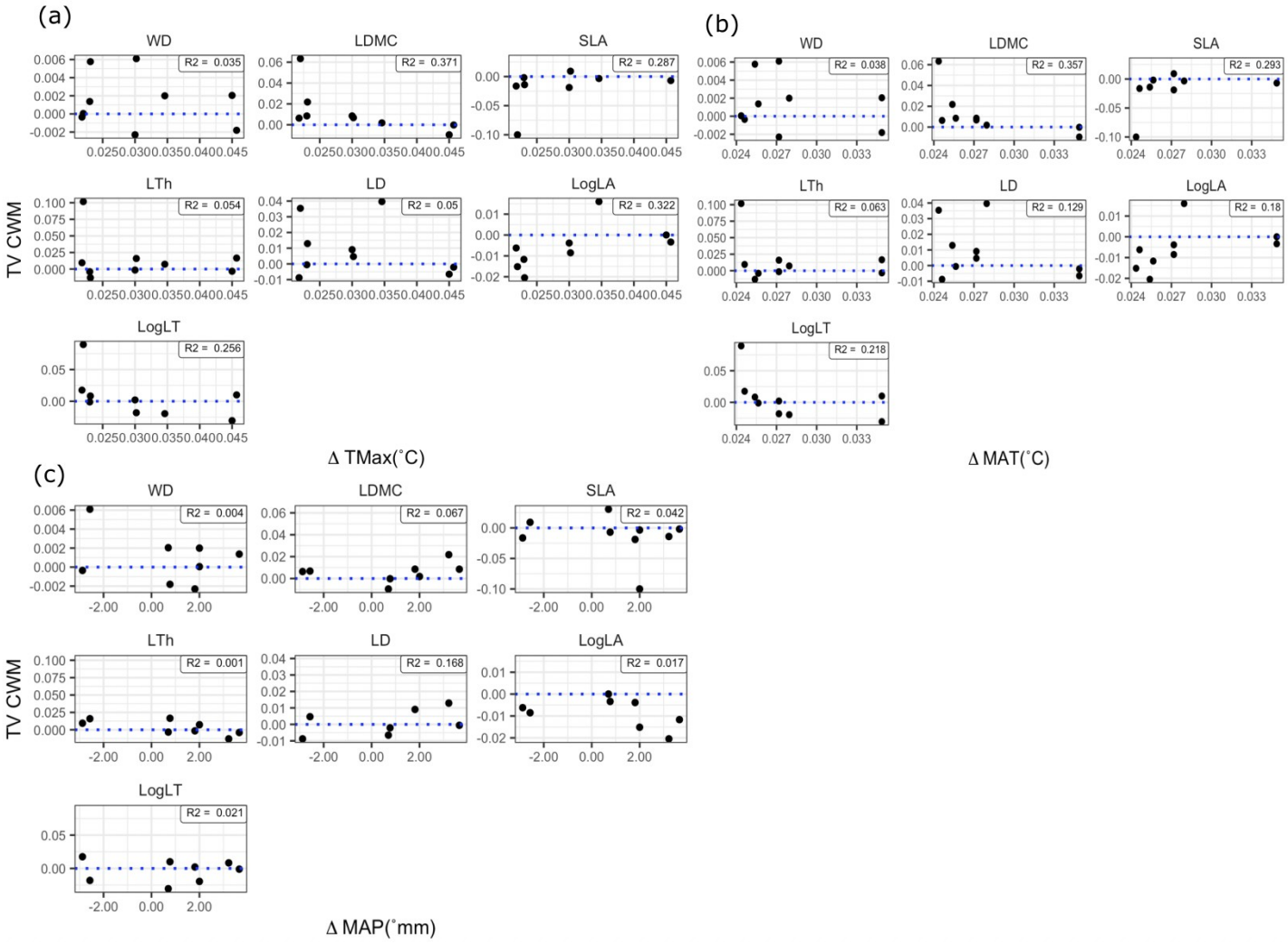

Figure S3.9. Trait Velocity of community weighted mean (TV_CWM) for each trait along changes in a) maximum temperature, b) mean annual temperature, and c) mean annual precipitation. TV represents the rate of change for each trait in each plot. TV equal to zero means no change during time. Positive values mean an increase in the trait community value during the time. Conversely, negative TV values mean decreases in community trait value over time. TV values were standardized with mean zero and variance one to compare traits. Significant relationships with elevation are represented with the regression line.

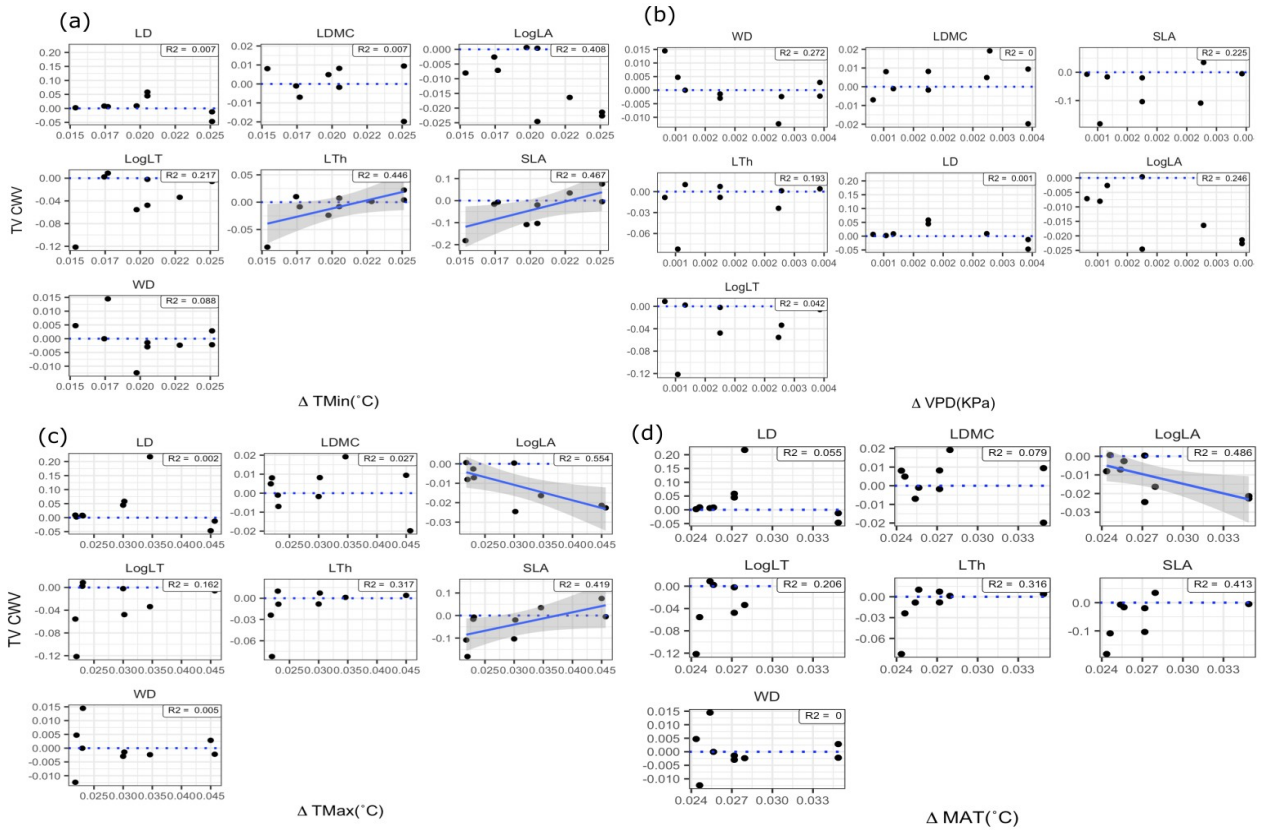

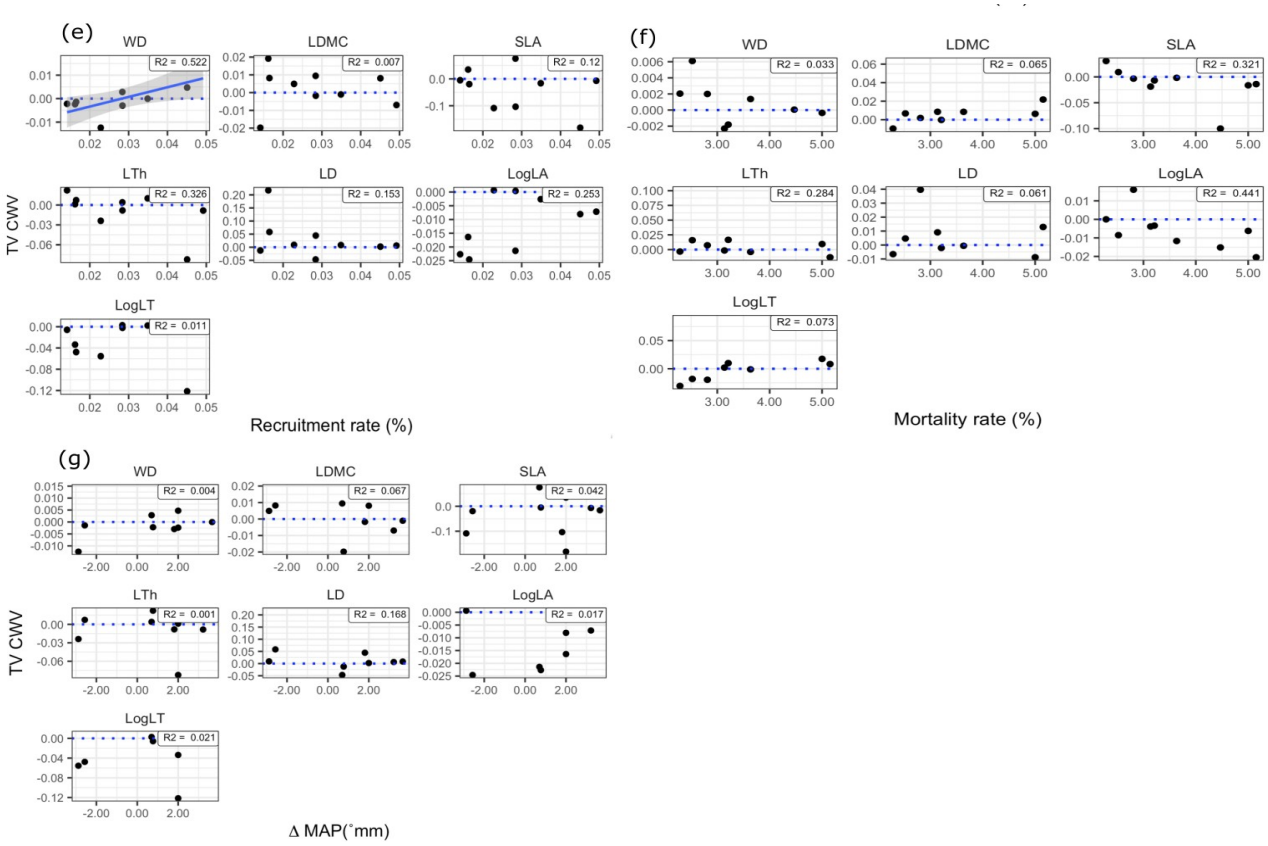

Figure S3.10. Linear regressions between community-weighted variance (TV_CWV) of each trait, the annualized rate of change of each climatic variable, a) minimum temperature, b) vapor-pressure deficit, c) maximum temperature, d) mean annual temperature, g) mean annual precipitation. Units of ΔT_{min}, ΔT_{max}, $\Delta_{Mean}T$ are °C y^{-1}, ΔMAP is mm y^{-1}, ΔVPD (Kpa y^{-1}). And annualized rate of demographic changes by the plot e) recruitment rate, f) mortality rate in %. TV equal to zero represents no change over time. Positive values mean an increase in the trait community value over time. Conversely, negative TV values indicate decreases in community trait value over time. Significant relationships between changes in functional composition and changes in climate or demography are denoted by the linear trend. TV values were standardized with mean zero and variance one to compare traits. Traits are leaf area (LA), specific leaf area (SLA), wood density (WD), high leaf dry matter content (LDMC), Leaf Thickness (LT), Toughness (LTh), and Density (LD). Size-related plant traits reflecting multiplicative processes were Log_{10} transformed (LogLT and LogLA).

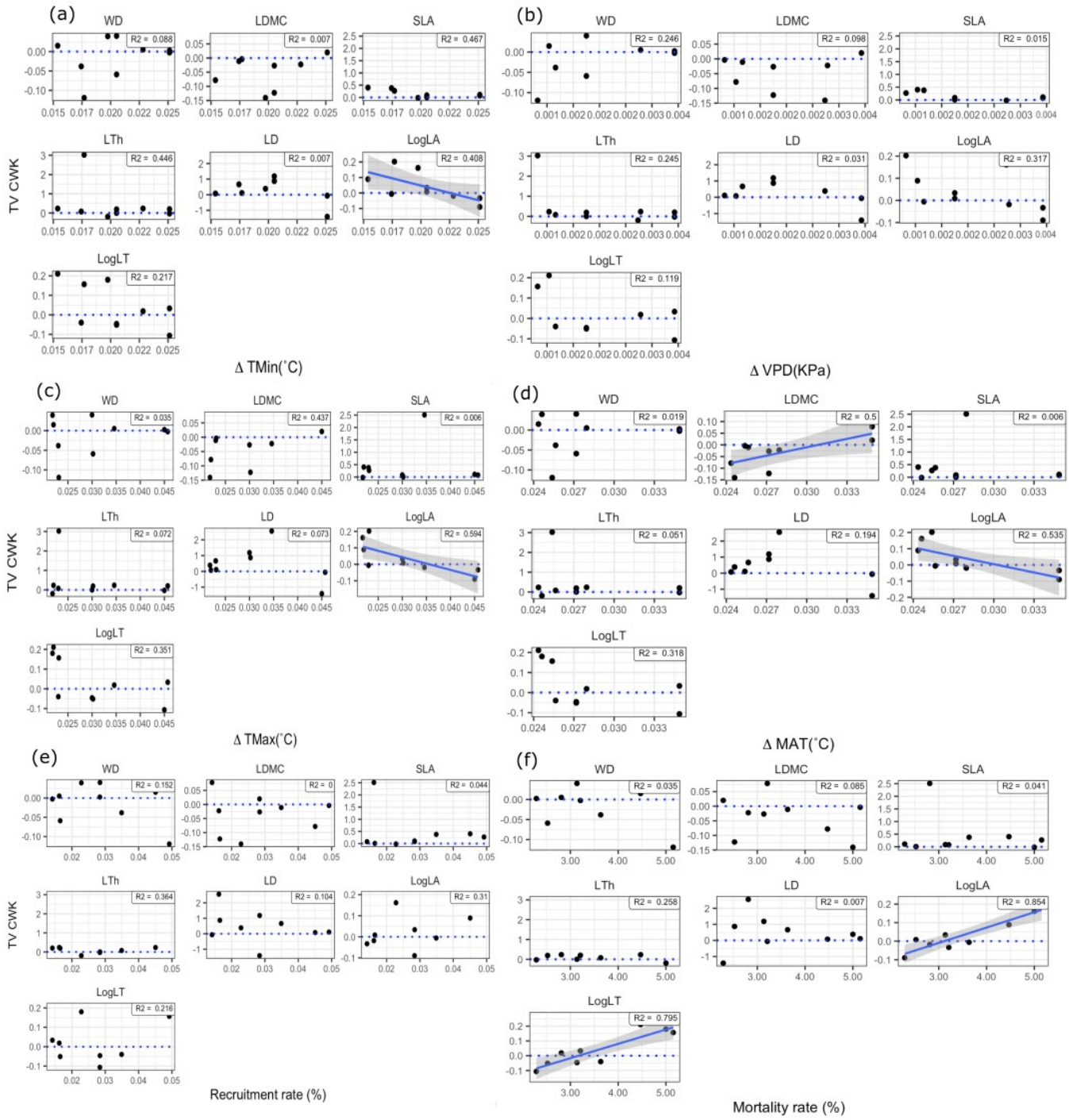
(a)
WD
LDMC
SLA
R2 = 0.088
R2 = 0.007
R2 = 0.467
LTh
LD
LogLA
R2 = 0.446
R2 = 0.007
R2 = 0.408
LogLT
R2 = 0.217
TV CWK
Δ TMin(˚C)
(b)
WD
LDMC
SLA
R2 = 0.246
R2 = 0.098
R2 = 0.015
LTh
LD
LogLA
R2 = 0.245
R2 = 0.031
R2 = 0.317
LogLT
R2 = 0.119
Δ VPD(KPa)
(c)
WD
LDMC
SLA
R2 = 0.035
R2 = 0.437
R2 = 0.006
LTh
LD
LogLA
R2 = 0.072
R2 = 0.073
R2 = 0.594
LogLT
R2 = 0.351
TV CWK
Δ TMax(˚C)
(d)
WD
LDMC
SLA
R2 = 0.019
R2 = 0.5
R2 = 0.006
LTh
LD
LogLA
R2 = 0.051
R2 = 0.194
R2 = 0.535
LogLT
R2 = 0.318
Δ MAT(˚C)
(e)
WD
LDMC
SLA
R2 = 0.152
R2 = 0
R2 = 0.044
LTh
LD
LogLA
R2 = 0.364
R2 = 0.104
R2 = 0.31
LogLT
R2 = 0.216
TV CWK
Recruitment rate (%)
(f)
WD
LDMC
SLA
R2 = 0.035
R2 = 0.085
R2 = 0.041
LTh
LD
LogLA
R2 = 0.258
R2 = 0.007
R2 = 0.854
LogLT
R2 = 0.795
Mortality rate (%)

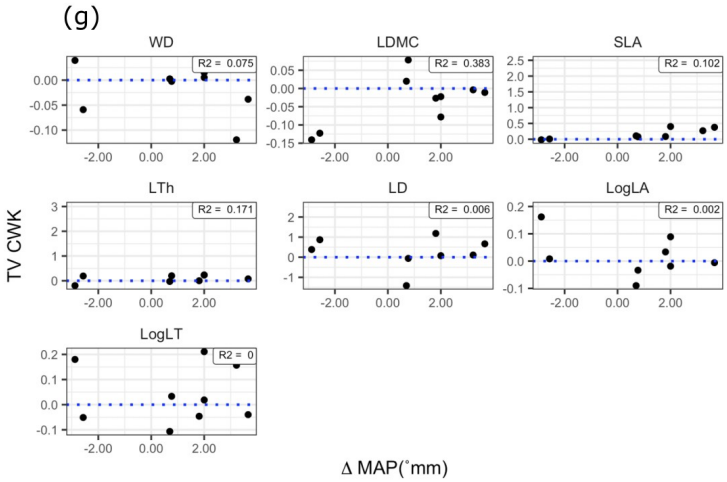

Figure S3.11. Linear regressions between trait velocity community-weighted kurtosis (TV_CWK) of each trait, the annualized rate of change of each climatic variable, a) minimum temperature, b) vapor-pressure deficit, c) maximum temperature, d) mean annual temperature, g) mean annual precipitation. Units of ΔT_{min}, ΔT_{max}, $\Delta_{Mean}T$ are °C y^{-1}, ΔMAP is mm y^{-1}, ΔVPD (Kpa y^{-1}). And annualized rate of demographic changes by the plot e) recruitment rate, f) mortality rate in %. TV equal to zero represents no change over time. Positive values mean an increase in the trait community value over time. Conversely, negative TV values indicate decreases in community trait value over time. Significant relationships between changes in functional composition and changes in climate or demography are denoted by the linear trend. TV values were standardized with mean zero and variance one to compare traits. Traits are leaf area (LA), specific leaf area (SLA), wood density (WD), high leaf dry matter content (LDMC), Leaf Thickness (LT), Toughness (LTh), and Density (LD). Size-related plant traits reflecting multiplicative processes were Log_{10} transformed (LogLT and LogLA).

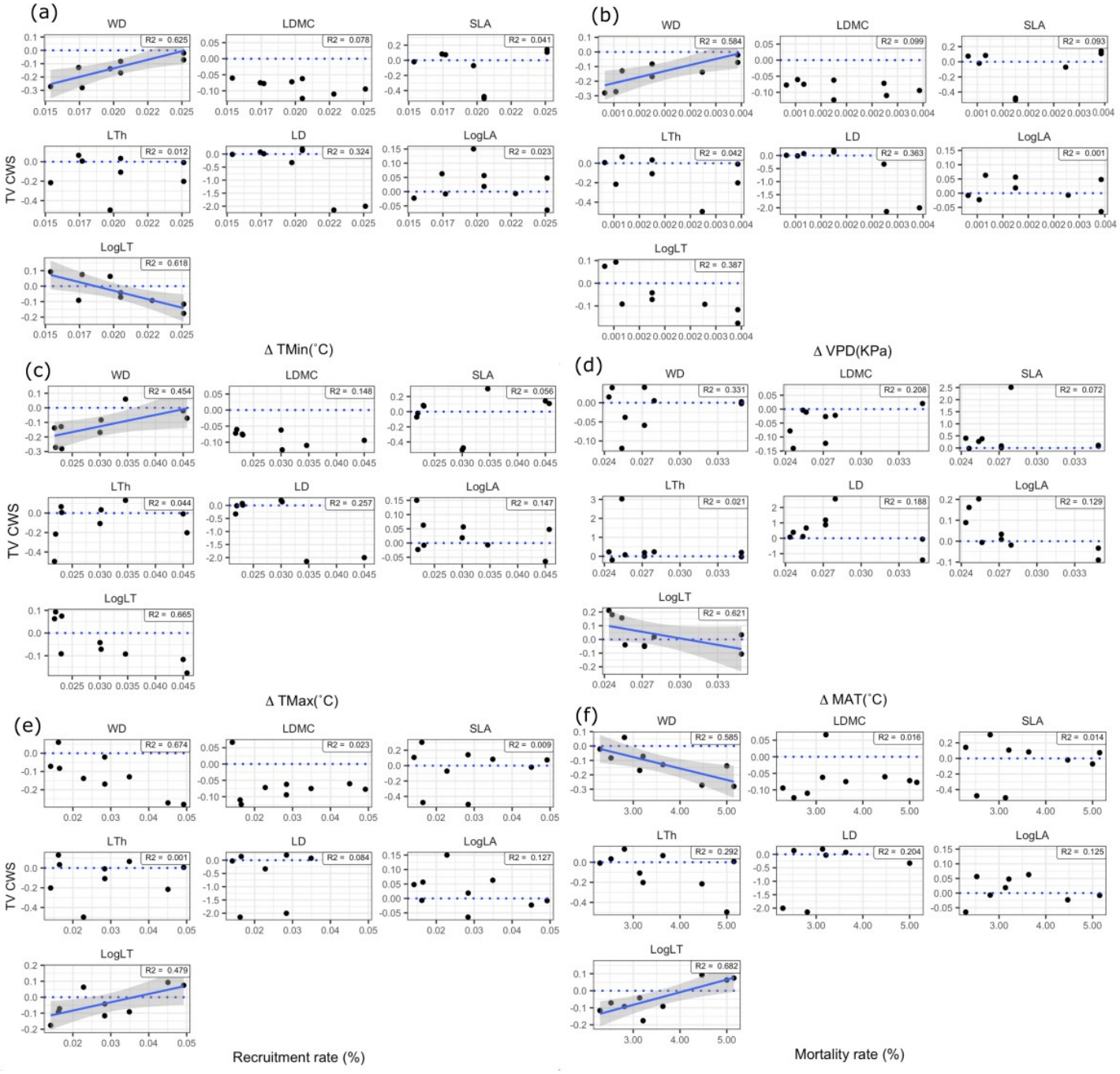
(a)
WD
R2 = 0.625
LDMC
R2 = 0.078
SLA
R2 = 0.041
LTh
R2 = 0.012
LD
R2 = 0.324
LogLA
R2 = 0.023
LogLT
R2 = 0.618
TV CWS
Δ TMin(˚C)
(b)
WD
R2 = 0.584
LDMC
R2 = 0.099
SLA
R2 = 0.093
LTh
R2 = 0.042
LD
R2 = 0.363
LogLA
R2 = 0.001
LogLT
R2 = 0.387
Δ VPD(KPa)
(c)
WD
R2 = 0.454
LDMC
R2 = 0.148
SLA
R2 = 0.056
LTh
R2 = 0.044
LD
R2 = 0.257
LogLA
R2 = 0.147
LogLT
R2 = 0.665
TV CWS
Δ TMax(˚C)
(d)
WD
R2 = 0.331
LDMC
R2 = 0.208
SLA
R2 = 0.072
LTh
R2 = 0.021
LD
R2 = 0.188
LogLA
R2 = 0.129
LogLT
R2 = 0.621
Δ MAT(˚C)
(e)
WD
R2 = 0.674
LDMC
R2 = 0.023
SLA
R2 = 0.009
LTh
R2 = 0.001
LD
R2 = 0.084
LogLA
R2 = 0.127
LogLT
R2 = 0.479
TV CWS
Recruitment rate (%)
(f)
WD
R2 = 0.585
LDMC
R2 = 0.016
SLA
R2 = 0.014
LTh
R2 = 0.292
LD
R2 = 0.204
LogLA
R2 = 0.125
LogLT
R2 = 0.682
Mortality rate (%)

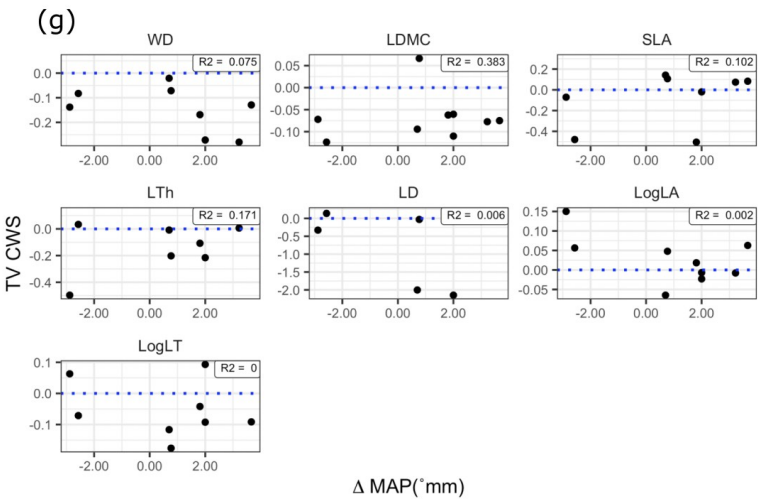

Figure S3.12. Linear regressions between trait velocity community-weighted skewness (TV_CWS) of each trait, the annualized rate of change of each climatic variable, a) minimum temperature, b) vapor-pressure deficit, c) maximum temperature, d) mean annual temperature, g) mean annual precipitation. Units of ΔTmin, ΔTmax, ΔMeanT are °C y-1, ΔMAP is mm y-1, ΔVPD (Kpa y-1). And annualized rate of demographic changes by the plot e) recruitment rate, f) mortality rate in %. TV equal to zero represents no change over time. Positive values mean an increase in the trait community value over time. Conversely, negative TV values indicate decreases in community trait value over time. Significant relationships between changes in functional composition and changes in climate or demography are denoted by the linear trend. TV values were standardized with mean zero and variance one to compare traits. Traits are leaf area (LA), specific leaf area (SLA), wood density (WD), high leaf dry matter content (LDMC), Leaf Thickness (LT), Toughness (LTh), and Density (LD). Size-related plant traits reflecting multiplicative processes were Log10.

CHAPTER IV

CHANGES IN MORPHOLOGICAL AND PHYSIOLOGICAL TRAITS OF URBAN TREES IN RESPONSE TO ELEVATED TEMPERATURES WITHIN AN URBAN HEAT ISLANDS

ABSTRACT

Urban Heat Islands (UHI) are a common phenomenon in metropolitan areas worldwide in which the air temperature is significantly higher in urban areas than in surrounding suburban, rural or natural areas. Mitigation strategies to counteract UHI effects include increasing tree cover and green spaces to reduce heat. The successful application of these approaches necessitates a deep understanding of the thermal tolerances in urban trees and their susceptibility to elevated urban temperatures. We evaluated how the photosynthetic thermal optimum (T_{opt}), photosynthetic heat tolerance (T_{50}), and key leaf morphological traits differ between conspecific trees growing in "hot [UHI]" vs. "cool" parts of Montreal, Canada, to assess the ability of seven common tree species to acclimation to higher temperatures. We hypothesized that individuals with hotter growing temperatures would exhibit higher T_{opt} and T_{50}, as well as leaf thermoregulatory morphological traits aligned with conservative strategies (e.g., reduced leaf area and increased leaf mass) compared to their counterparts in the cooler parts of the city. Contrary to our a priori hypotheses, leaf area increased with growing temperatures and only four of the seven species had higher T_{50} and only three had higher T_{opt} values in the hotter area. These results suggest that many tree species cannot acclimate to elevated temperatures and that the important services they provide, such as carbon capture, can be negatively affected by high temperatures caused by climate change and/or the UHI effect. The ability vs inability of tree species to acclimate to high temperatures should be considered when implementing long term tree planting programs in urban areas.

Keywords: Thermal acclimation, functional traits, urban forest, climate change, physiological responses, photosynthesis, thermal tolerance.

INTRODUCTION

Global warming and urbanization expose organisms to unique environmental conditions (IPCC 2022). Urban areas have high surface and air temperatures, with temperatures generally increasing from rural areas to more densely urbanized city cores. This Urban Heat Island (UHI) effect exacerbates heat stress, risking urban infrastructure and human populations (Tuholske et al. 2021). Mitigation strategies such as the creation of parks and increasing tree cover, have been proposed to counteract the UHI effect (Karimi et al. 2022). Nonetheless, the efficacy of these strategies may be attenuated by the physiological tolerances of trees and their ability to avoid heat stress (Teskey et al. 2015). To avoid heat stress, urban trees must acclimate to higher temperatures through changes in their physiology (e.g., photosynthesis thermal optima or photosynthetic heat tolerance) (Hara et al. 2021) and/or by adjusting leaf traits to reduce leaf surface temperatures (Zhu et al. 2020). Unfortunately, limited information on how trees respond urban temperatures (Kullberg and Feeley 2022), limiting our ability to predict their vulnerability to UHIs in a warming world (Esperon-Rodriguez et al. 2022).

Rather than air temperature, leaf temperature is critical for leaf physiological processes (Cavaleri, 2020). Plants may exhibit plastic responses in leaves to acclimate to warmer environments, maintain leaf temperature below damage thresholds and optimize net photosynthetic CO_2 uptake (A_{net}) (Way and Yamori 2014, Crous et al. 2022). Leaf thermoregulation is mediated, in part, by the morphological leaf traits affecting heat dissipation (Leigh et al. 2017, Fauset et al. 2018). Traits such as leaf area (LA), effective leaf width (LW), leaf thickness (LT), specific leaf area (SLA), and leaf dry matter content (LDMC), determines leaf temperatures and therefore its thermal dynamics (Michaletz et al. 2015). In other words, species with different leaf traits growing under the same air temperature may experience different leaf temperatures. For instance, large, thin leaves typically reach higher temperatures than smaller, thicker leaves due to their thicker boundary layer (which influences the heat transfer) and their low water content (which increases the rate of leaf temperature change) (Leigh et al. 2017, Tserej and Feeley 2021).

Nonetheless, trees can adjust their morphological traits to different air temperatures, as evidenced studies of decreased leaf size with increasing temperatures (Zhu et al. 2020, Manishimwe et al. 2022). These adjustments enables passive thermoregulation, maintaining homeothermy by influencing leaf energy balance and heat dissipation (Michaletz et al. 2015).

Effective acclimation to higher temperatures should lead to a low or even negative difference between leaf and air temperature (ΔT), where leaves remain cooler than the air due to high stomatal conductance to water vapor (g_s) and transpiration (E) at high temperatures (Blonder et al. 2020). The energy balance theory, useful for modeling leaf temperatures, incorporates environmental factors such as solar radiation, wind, relative humidity, and morphological and physiological leaf traits such as g_s, E, and LW (Michaletz et al. 2015), allowing the understanding of how plants adjust and compensate their traits to regulate internal leaf temperature depending on the environment (Varhmmar et al. 2015). For instance, studies have shown that reducing leaf size and increasing E improve ΔT (Varhmmar et al. 2015, Tarvainen et al. 2022). Investigating the ΔT between individuals growing in different urban environments, especially within UHIs, offers valuable insights into the ability of a species to avoid extreme leaf temperatures.

Photosynthesis is especially sensitive to temperature variation, peaking at a species-specific optimum before declining at higher temperatures (Varhmmar et al. 2015, Tarvainen et al. 2022). The optimal temperature for photosynthesis (T_{opt}) align with the local daytime temperatures, suggesting acclimation or local adaptation (Varhmmar et al. 2015). In urban environments, we might expect trees whitin the hotter areas to have both higher T_{opt} and A_{net} (constructive photosynthetic adjustments) if they acclimate effectively to elevated growing temperatures caused by the UHI effect. Similarly, photosystem II (PSII) is highly heat sensitive (Baker 2008). Photosynthetic heat tolerances (P_{HT}), defined as the temperatures causing irrecoverable PSII damage, can be characterized by the leaf critical temperature (T_{crit}) and the leaf thermal tolerance (T_{50} and T_{95}), which indicate the temperatures at which PSII have initial, 50% or 95% of damage, respectively, are commonly used to predict vulnerability to heat damage (Perez and Feeley 2020). Thus,

higher values of T_{crit}, T_{50}, and T_{95} in the UHI shows the P_{HT} acclimation in response to elevated temperatures. Although prior studies in urban settings have demonstrated T_{opt} and P_{HT} acclimation to high temperatures, much of the research has focused on controlled conditions in small trees (Hara et al. 2021) and less is understood about how trees respond to increases in temperature typical of UHI effects. There is therefore a pressing need for further investigation into the long-term acclimation of photosynthetic heat tolerances in mature trees under actual urban conditions.

Here, we evaluated the acclimation capacity of seven urban tree species to higher contrasting environments within a temperate city, representing the hottest (UHI) and coldest temperature extremes. We addressed the following questions: **QI)** is there a response of urban trees to the elevated temperatures within the UHI in their morphological or physiological traits? We hypothesized a priori that **HI:** If urban trees exhibit distinct morphological and physiological acclimation in response to elevated temperatures within UHIs, traits should exhibit significative differences between the UHI and cooler urban environments.

QII) Are changes in leaf morphological traits allowing for passive thermoregulation within UHIs. **HII)** At higher temperatures, we expect smaller, narrower, and thicker leaves (lower specific leaf area (SLA), leaf area (LA) and leaf width (LW)) with high dry matter content (LDMC) and thickness (LT). These changes will enhance cooling due to a smaller boundary layer allowing for increased vapor diffusion. On the other hand, larger LA and LW can be expected when plants are increasing the surface area to increase E and g_s.

QIII) Is the ΔT be lower for individuals grown under higher temperatures? **HIII)** If leaves acclimate their leaf traits as predicted under HI and HII, we expect a smaller difference between leaf and air temperature for trees growing in the UHI vs cooler parts of the city.

QIV) Do trees acclimate to higher temperatures within UHIs through physiological changes in their photosynthetic thermal optimum (T_{opt}) and/or photosynthetic thermal

tolerances (P_{HT})? **HIV)** Since individuals have developed all their life under within the UHI, they will have higher T_{opt} and/or P_{TH} than individuals from cooler parts of the city.

METHODS

We conducted the project in the city of Montreal, Canada from July to September 2021. The city has a warm-summer and humid continental climate (Beck et al. 2018). During the study period, precipitation ranged between 173,1 mm and 364,6 mm, with July being the wettest month (https://climate.weather.gc.ca/). The annual precipitation in 2021 was 811,7 mm; 200 mm less than the multiyear average (https://montreal.weatherstats.ca/charts/precipitation-yearly.html). Furthermore, temperatures record of 37.8 ± 2.3 °C in the UHI and 34.4 ± 2.1 °C in the coldest part, thus, maximum temperatures showed a warming of 3.4 °C in the UHI. Mean temperatures were ~23.3 ± 4.3°C and ~22.0 ± 4.6 °C for the UHI and the coldest part of the city, with a warming of 1.3°C (Table S1). The highest temperatures were recorded in August.

To identify study sites in the city with the greatest temperature disparities, we referred to Montreal's surface temperature map based on satellite images of 2020 (https://open.canada.ca/data/en/dataset/dbdfbdba-0725-470d-a23e-da69dbedc4e6). We selected two distinct environments for study: the downtown area as the hottest part (the UHI) and the Botanical Garden of Montreal as the coldest part in the city (Figure 1). The differences between the two urban environments are 1.3˚C and 3.4˚C in mean and maximum air temperature, respectively. The geographical distance between our two urban environments is ~6.5 km to maintain similar relative humidity and precipitation conditions and focus on temperature contrast. The Urban Heat Island (UHI) effect in Montreal has been extensively studied, primarily using ground surface temperature data (Boulfroy et al. 2012, Touchaei and Wang 2015, Wang and Akbari 2016, Roberge and Sushama 2018). As a result, the hottest areas in the city are well-identified. To capture detailed micro-climatic conditions within each urban environment, we installed five HOBO data loggers (Onset UA-002-64) during field data collection, recording air temperature and solar radiation every 30 minutes.

We deliberately chose public parks in the downtown area and the Botanical Garden due to the absence of management actions (watering or fertilization), enhancing the similarity between these two sites. To further enhance the comparability of habitat conditions between environments, we specifically focused on park trees and excluded street trees in the downtown area.

Thermoregulatory morphological leaf traits

We selected the seven most common tree species across our two urban environments: *Acer platanoides* (ACPL), *Acer saccharinum* (ACSA), *Celtis occidentalis* (CEOC), *Gleditsia triacanthos* (GLTR), *Quercus macrocarpa* (QUMA), *Quercus rubra* (QURU) and *Tilia cordata* (TICO).

We measured six traits important for leaf thermoregulation following the protocol from Pérez-Harguindeguy et al. (2016): leaf area, effective leaf width, leaf thickness, specific leaf area, leaf dry matter content, and leaf absorptance to shortwave radiation.

Leaf area (LA) and effective leaf width (LW) are crucial traits in determining leaf temperature. LA is a robust predictor of temperature range and variation within the leaf (Leigh et al. 2017, Tserej and Feeley 2021), while LW strongly influences the leaf boundary layer size and the photosynthetic surface (Leigh et al. 2017). A larger LW, for instance, leads to increased boundary layer resistance, limiting the exchange of heat and water vapor between the leaf and the environment. Additionally, wider, and larger leaves have a higher capacity to intercept and absorb solar radiation, resulting in an elevated leaf temperature. Nevertheless, wider leaves generally exhibit a larger surface available for transpiration, promoting cooling in species with high transpiration rates (Fauset et al. 2018).

Leaf thickness (LT) is a critical trait for thermal tolerance since it determines the leaf's thermal mass, which plays a vital role in the species' response time to heating (Leigh et al., 2012). Thick leaves with high thermal mass exhibit slower response times to heating, thereby avoiding lethal temperatures, and reducing the temperature range unfavorable for photosynthesis (Leigh et al. 2012).

Specific leaf area (SLA) serves as an indicator of leaf economic strategy associated with photosynthetic capacity. High SLA values indicate a larger surface area available for solar radiation absorption, which can result in increased leaf temperature (Michaletz et al. 2016). However, a higher SLA also allows for greater heat exchange with the atmosphere and increased transpiration (Wright et al. 2001).
Leaf dry matter content (LDMC) and SLA play fundamental mechanistic roles in thermal buffering and net carbon gain of leaves (Michaletz et al. 2016). Leaves with higher LDMC values (high dry mass) exhibit reduced heat transfer permeability but have a higher capacity to store heat energy. Conversely, leaves with low LDMC may heat up more rapidly in response to radiation, leading to greater thermal instability (Michaletz et al. 2015). Consequently, SLA and LDMC contribute to maintaining leaf temperature close to optimal levels for maximizing carbon assimilation (Michaletz et al. 2016).

Additionally, we measured leaf absorptance to shortwave radiation (*a*), which indicates how much radiant thermal energy the leaf can absorb. The higher the absorptance the higher the thermal energy absorbed and thus, the temperature (Lambers et al. 2019). Finally, stomatal conductance (g_s) determines the transpiration capacity of leaves which in turn influences the cooling effect (Fauset et al. 2018).

To measure thermoregulatory morphological traits, we selected ten (10) mature and healthy individuals from each species within the hottest and the coldest part of the city (7 species x 10 individuals by species x 2 environments =140 trees). For each tree, we selected those branches wholly exposed to the sun and accessible from the ground, and we carefully collected five fresh, mature, healthy, and fully expanded leaves exposed to direct sun. Leaves were stored in wet towels in Ziploc bags in a cooler to avoid dehydration while being transported to the laboratory of plant physiology of the Université du Quebec à Montreal to be processed within 24 hours.

We measured LT (mm) using a digital micrometer (Mitutoyo, precision 0.0001 mm). To calculate LA (mm^2) and LW (mm), we used the ImageJ software (http://rsbweb.nih.gov/ij/)

and the LeafArea R package (Katabuchi 2015). LW was calculated as the diameter of the largest circle capable of fitting within a leaf margin (Leigh et al. 2017). To calculate SLA ($mm^2\ mg^{-1}$) and LDMC ($mg\ g^{-1}$), we placed each leaf in a separate paper bag in the oven at 70°C for 72 hours before measuring dry weight using an analytical balance with a precision of 0.0001 g. Leaf absorptance to shortwave radiation (*a*) was calculated as *a*=1-leaf reflectance-leaf transmittance.

Leaf reflectance and leaf transmittance were measured with a CI-710 Miniature Leaf Spectrometer (Bioscience) over 400-1000 nm wavebands (Smith and Nobel 1977).

In-situ gas exchange and photosynthesis temperature responses in urban environments

Due to the limited duration of the summer and the time-consuming nature of the measurements, we selected a subset of five species from the seven species listed above to measure temperature responses of the light-saturated photosynthetic rate (A_{net}): ACSA, CEOC, GLTR, QURU, and TICO. We randomly selected five individual trees from each species in each environment (except for CEOC with three individuals). We selected low branches in each tree with leaves reachable from the ground, and one to three sun-exposed mature leaves from each tree to complete the temperature response curve following the general protocol of Slot and Winter (2017) (see Perez and Feeley 2020).

All leaves were measured *in-situ* using a LICOR-6400 XT portable photosynthesis system (Licor, Lincoln, NE, USA). First, we measured leaf temperature with a digital infrared thermometer HT826 (CA, USA) to set the cuvette temperature at the same value, and then the leaf was allowed to acclimate to the chamber environment. All the measurements were done using the same parameters: the reference [CO_2] was fixed at 400 ppm, the irradiance at the leaf surface at 1200 µmol photons $m^{-2}s^{-1}$, the sample chamber's relative humidity ≅ 50-60%, and a temperature treatment ranging from 20 to 40 °C, incremented by 2 °C intervals. Next, we visually inspected stabilization on these parameters to measure carbon assimilation rates (µ mol m-2s-1) and stomata conductance (g_s) when the leaf was wholly acclimated to each target temperature. To increase the range of leaf temperature with the LICOR-6400 XT, we used a combination of ambient daytime temperatures variation

between 9:00 and 15:00 h, and manipulation of block temperature of the Peltier-controlled leaf cuvette (Slot et al. 2019). We always measured photosynthesis on sunny days; in addition, while measuring photosynthesis, we also measured g_s and transpiration (E) *in situ*.

The temperature response of the light-saturated photosynthetic rate was fitted according to the model presented in June et al. (2004) and adapted by Slot and Winter (2017).

$$P(T) = P\,Opt * e^{-\left(\frac{TLeaf - TOpt}{\Omega}\right)^2}$$

Where P(T) is the net photosynthesis per unit leaf area, $P\,Opt$ is the optimal carbon assimilation. T_{Leaf} is the leaf temperature. Ω describes the width of the curve's peak and is the difference between $T\,Opt$ and the temperature at which $P\,Opt$ drops by about 37% of its value at $T_{Opt.}$

Photosynthetic Heat Tolerance (P_{HT})

Mature leaves were harvested for focal trees (same 10 individuals chosen for thermoregulatory morphological leaf traits) in the morning and were processed for heat tolerance between 10:00 and 16:00 h local time. We used F_V/F_M values to estimate the P_{HT} following established protocols (Perez and Feeley 2020, Feeley et al. 2020). The temperature at which PSII performance begins to decrease is the critical temperature (T_{crit}), the temperature at which ≥ 50% irrecoverable damage is $T_{50,}$ and the temperatures that leads to 95% irreversible and nearly complete heat damage to PSII is T_{95} (Perez et al. 2021).

To ensure the health of the samples, we measured the initial status of each individual leaf using the handheld fluorometer OS30P$^+$ Opti-Science, (Hudson, NH, USA). Five leaves from each individual tree were dark-adapted for 20 min. In the case of compound leaves, a random leaflet was chosen. After dark adaptation, we measured initial fluorescence emission (F_0) and maximum total fluorescence (F_M) to calculate the ratio of variable fluorescence (F_V) as F_M- F_0 to maximum leaf fluorescence as F_V/F_M. We ensured that F_V/F_M was ~0.8 to continue the process. Subsequently, we cut leaf discs of ~2.0 cm in diameter using a hole punch, avoiding the central veins. For each temperature treatment, we placed three discs from each individual in Miracloth fabric to prevent anaerobiosis during the heat

treatments (Perez and Feeley 2020); one layer of Miracloth covered the adaxial surface and three layers covered the abaxial disc surface. Each Miracloth packet was placed inside a waterproof Ziploc plastic bag (removing the air), and completely submerged for 15 min in preheated circulating water baths fixed at 22.0, 40.0, 42.2, 44.5, 47.0, 49.3, 51.5, 53.2 and 56.5 °C. Overall, we analyzed three discs by temperature per individual from both urban environments for a total of 3,780 leaf discs. After the 15 min temperature treatment, we placed the discs into Petri dishes with moist towel paper to avoid dehydration. We allowed them to recover for precisely 24 hrs. under low light and ambient temperature of ~24˚C. At the end of the recovery period, we dark-adapted the discs for 20 min to measure the final F_V/F_M.

To estimate P_{HT} for each species in UHI and the coldest part of the city, we modeled the relationship of F_V/F_M vs. treatment temperatures for each tree using a logistic non-linear least squares model with the "nls" function in the *stats* R package (Core 2021). We calculated T_{50} by predicting the temperature that caused damage in the 50% of PSII efficiency compared to the control temperature as:

$$T_{50} = \frac{1}{1+\exp(-¿(2+3*Temperature))¿}$$

Where θ_1 is the control treatment ($F_V/F_M \cong 0.8$) and θ_2 and θ_3 are the intercept and slope from the logistic model (Perez and Feeley 2020). We generated bootstrapped means and 95% confidence level intervals of T_{50} by reiterating (with replacement) 100 times the nls model for each tree. Using the same model, we calculated T_{crit} and T_{95} as the temperature value where the F_V/F_M begins to decline with 15% and 95% of PSII efficiency, respectively, compared with the control temperature.

Leaf temperature modeling

We employed the leaf-scale energy balance model (Campbell and Normal 1998) to predict the temperature of a horizontal sun-exposed leaf and quantify how leaf-to-air temperature differences vary in response to urban environments. The model assumes that the leaf's thermal radiation is balanced mainly by latent heat loss, sensible heat loss, and emitted

thermal radiation. Consequently, the leaf temperature can be effectively modeled by considering a combination of environmental factors and thermoregulatory traits.

To parameterize the leaf energy balance model, we used LW, g_s, and leaf absorptance (a). As environmental factors, we used the air temperature, relative humidity (%), and wind speed (ms^{-1}) recorded using a digital anemometer Hyelec MS6252A (UK) when measuring the photosynthesis temperature response curves. Additionally, we used the solar irradiance which was collected with the HOBO data loggers located in the sampled trees in each urban environment. The model to calculate leaf temperature is described as:

$$Tl = Ta + \frac{\gamma * ¿}{s + \gamma * ¿¿¿} ¿$$

Where Tl is the leaf temperature calculated with the model (°C), Ta is air temperature (°C), s is the slope of the saturation pressure curve, Rni is the isothermal net radiation incident upon a leaf (W m^{-2}) (i.e., the net radiation that the surface would receive if it had the same temperature as the air). gHR is the sum of boundary layer conductance ($gHa¿$ and radiative conductance ($gr¿$ (mol m^{-2} s^{-1}), Cp is the heat capacity of dry air at constant pressure (29.3, $Jmol^{-1}C^{-1}$), VPD is vapor pressure deficit (KPa) and $\rho$is the atmospheric pressure ($101.3xe^{(altitude/8200)}, KPa$), $\gamma * ¿$ is the modified psychrometric constant determined from the ratio of combined boundary layer and radiative conductance to stomatal conductance (Campbell and Norman, 1998, Perez and Feeley 2020). For the calculation of the model, $\gamma * ¿$, Cp, ρ were constants. $\gamma * ¿$ can be calculated by multiplying the psychrometric constant ($\gamma = ¿6.66$ x 10^{-4} C^{-1}) by the ratio of the radiative conductance (gHR) to the boundary layer conductance of water vapor (g_{wv}). $gHR = gHa + gr$, where gHa is the boundary layer conductance for heat described as $gHa = 1.4$ x $0.135\sqrt[2]{u/d}$, u being the wind speed and d the effective leaf width in meters; and gr is the radioactive conductance defined as $gr = \frac{4\sigma Ta}{Cp}$, σ being the Stefan-Boltzmann constant in W (5.67 x 10^{-8}). The

boundary layer conductance of water vapor (g_{wv}) is defined as $\frac{0.5*\left(\frac{gs}{2}\right)*gva}{\left(\frac{gs}{2}\right)+gva}$, where the boundary layer conductance for vapor is g_{va} = 1.4 x 0.147 $\sqrt[2]{u/d}$ (Campbell & Norman, 1998, Perez and Feeley 2020).

Data analysis

We ran a correlogram to detect autocorrelation in the time series of air temperature in each urban environment (Figure S1). We then fitted ARIMA models separately to the two-time series (air temperature in the hottest and coldest city areas). Subsequently, we used a Wilcoxon-test for non-normal distribution to compare the residuals between the two models to detect significative differences. We ran the analysis for the mean air temperature (T_{air_Mean} (˚C)), daytime air temperature ($T_{air\_dayMean}$ (˚C)), daytime maximum temperature (T_{air_dayMax} (˚C)), and night temperatures ($T_{air\_nightMean}$ (˚C)).

To assess our first question (QI: is there a response from of urban trees to the elevated temperatures within the UHI in their morphological or physiological traits?), we compared all the measured traits between urban environments. We conducted a nested analysis of variance (nested ANOVA) using mixed effect models through the lmer function from the "lme4 " package in R (Bates et al.2015). In the model, the urban environment (hottest [UHI] and coldest) was treated as a fixed effect, while species were considered a random effect. Size-related plant traits with power-law growth rate of the form $Y = ax^b$ (LA, SLA, LT, LW), were $\log_{10}$ transform to normalize trait distribution. We used the “Anova” function from the “car” R package (Fox 2019) to compute the F-statistic and the degrees of freedom using the Kenward-Roger method. The p-value was calculated using the “lmerTest” R package (Kuznetsova et al. 2017). For mean comparisons, we employed Tukey's test using multcompt package in R (Hothorn et al.2008). ANOVA assumptions were tested to run the model.

Next, we investigated whether the thermal adaptation responses to temperature variations between the urban environments are species-specific (QII). Because we employed a hierarchical sampling design, measuring five leaves from five individuals across seven species in two urban environments, we used a nested ANOVA, with the interaction of species and urban environment as fixed effect and individuals' identity as random effect to account for intra-individual variation. The p-values and the degrees of freedom were calculated using "lmerTest" and "car" packages respectively. This analysis enables us to assess the effect of the urban temperature variation on thermoregulatory morphological traits by species and determine whether trees have developed passive thermoregulatory mechanisms through plastic changes in leaf traits.

To evaluate how much the tree species regulate leaf temperature and how leaf temperature varies from air temperature depending on the urban environment (QIII), we graphically compared the theoretical leaf temperature calculated with the energy balance model versus the observed leaf temperature. After, we ran a mixed analysis of covariance (mixed ANCOVA) using air temperature as covariable and individuals' identity as random component to quantify the difference between the modeled leaf temperature within the hottest and coldest area using air temperature as a covariable. A higher decoupling of leaf temperature from air temperature could suggest difficulty in plant thermoregulation and acclimation.

To address QIV (Do trees acclimate to higher temperatures within UHIs through physiological changes in their photosynthetic thermal optimum (T_{opt}) and/or photosynthetic thermal tolerances (P_{HT})?) we used a two-way ANOVA to assess if tree species are showing physiological acclimation signals to higher temperatures within the UHI. In this case, first, we evaluated the effect of the urban environment and tree species on the variation in thermal tolerance (T_{50}, T_{crit}, and T_{95}). Employing this analysis, we are able to assess the separated effect of each factor, and whether the effect of the urban environment on traits varies depending on the tree species. For post-hoc comparisons between urban environments, we employed the emmeans test. To account for multiple comparisons, we applied the Bonferroni correction using the emmeans R package (Lenth et al. 2019). The

emmeans test is particularly suitable for analyzing imbalanced data by adjusting the standard errors (SE) that arise due to variations in the number of observations. The normality and homoscedasticity assumptions were tested before conducting the analyses.

To analyze if there are signs of physiological acclimation in the photosynthetic thermal optimum (T_{opt}). We used Welch's t-test to evaluate the effect of urban environments on variation in T_{opt}. This analysis calculates the degree of overlap of the SE for T_{opt} and optimal carbon assimilation (P_{opt}) (Tarvainen et al. 2022). This test is appropriate for situations where the variances of the two groups are different, and the sample size between groups is unequal (case of CEOC). The fitted parameters of the model were significantly different when the test was higher than the cero, as described in the following equation.

$$|x1 - x2| - 2.99 \times \sqrt{(SE¿¿1^2 + SE_2^2)¿} > 0$$

Where $x1$ and $x2$ are the two parameters fitted with the model (e.g., $P_{opt,}$ T_{opt}) in each urban environment. The constant 2.99 is the t-score corresponding to P=0.05 after adjustment to account for the multiple comparisons. SE_1 and SE_2 are the standard errors of the values' fit (Tarvainen et al. 2022).

Furthermore, we analyzed the differences in both, stomatal conductance (g_s) and transpiration (E) using a two-way ANOVA and Tukey's test as pos-hoc method.
All the analyses were performed using the R version 4.0.0 (R Development Core Team 2021).

RESULTS

Micro-urban climate

According to the Wilcoxon-test on the residuals of the ARIMA models, all air temperature variables (T_{air_Mean}, $T_{air\_dayMean}$, T_{air_dayMax}, $T_{air\_nightMean}$) exhibited significantly larger values in the hotter part of the city, indicating the effect of temperature variation and the presence of the UHI (Figure S2, Table S1). Particularly, the maximum air temperature, crucial for tree

functioning, exhibited the greatest disparity between environments (Figure 2). With a warming of 3.4 °C in the UHI.

Effects of heat on thermoregulatory traits

The nested ANOVA analysis revealed that temperature significantly influences the LA, SLA and LW of the selected species (Table 1). Showing that thermoregulatory leaf traits related with area were particularly sensitive to temperature variation between the UHI and coldest parts of the city. On the other hand, when we analyzed the effect of the temperature and the species on changes in thermoregulatory morphological traits using the nested ANOVA, our results indicated that the responses to elevated temperatures are highly species-specific (Figure 3). From all the traits, SLA had the highest intra-specific variation between the UHI and coldest areas, where five of the seven species showed significant increases within the UHI (Figure 3b). Regarding other traits, LT presented significant differences between the two environments in four of the seven species, with higher values within the UHI (Figure 3e). The LA showed increases within the UHI in three of the seven species (Figure 3a) but was the trait with the largest variation within the hottest part compared to the same species within the coldest part of the city (Table S2). These results indicate that elevated temperatures highly affect morphological traits related to leaf area and mass. Finally, LDMC and LW were less affected by the temperature differences in the urban environment (Figure 3c, d).

Modeled leaf temperature

We compared modeled leaf temperatures to air temperatures in both the UHI and the coldest parts of the city to evaluate individuals' thermoregulation capabilities. Our analysis revealed that leaf temperatures for individuals in both the UHI and coldest part of the city consistently exceeded air temperatures (Figure 4). Notably, individuals located in the UHI exhibited even higher leaf temperatures than individuals in the coldest part of the city. The slopes of the relationship between leaf temperature differed significantly between the two urban environments (mixed ANCOVA P-value < 0.005). Despite higher rates of transpiration and stomatal conductance observed within the UHI for nearly all species (Figure 5), leaf temperatures remained elevated compared to air temperatures. This

indicates that heightened temperatures necessitate tree species to enhance evaporative cooling (E) and stomatal conductance (gs), yet leaf acclimation to these conditions appears limited.

Photosynthetic Heat Tolerance (P_{HT})

Overall, we anticipated that all species would demonstrate increased P_{HT} as a typical response to elevated temperatures and heat acclimation. However, our nested ANOVA revealed no significant P_{HT} parameters (T_{50}, T_{crit}, and T_{95}) as a general effect of temperature over all species together (Table 1). Upon examining the logistic models of F_v/F_m in relation to temperature for each species between urban environments, we observed physiological acclimation in the T_{50} only in ACPL and ACSA to urban elevated temperatures. Conversely, QUMA and TICO displayed significantly lower heat tolerance in the hottest part of the city, while CEOC and GLTR exhibited nearly identical T_{50} in both environments (Figure 6, S3a, Table S3). Thus, only four of the seven species displayed significant differences between urban environments, with only two showing T_{50} acclimation. Furthermore, the T_{50} values for the seven urban tree species were around ~50°C, suggesting a likely upper limit by in P_{HT} temperature. The significant results at the species level, along with the lack of significance in the nested ANOVA conducted with the mixed model, suggest that certain species exhibit specific adaptations, whereas there may not be a general response across all species to elevated urban temperatures. This underscores the importance of species-level analyses in comprehending the impact of urban environments on tree thermal tolerance.

Temperature responses of *in-situ* gas exchange and photosynthetic thermal optimum (T_{opt})

Although T_{opt} was not statistically significant in our nested ANOVA (P-value = 0.06), the marginal value suggests a trend of change among individuals located in different urban environments (Table 1, Table S3). The Welch's t-test, which analyzed intra-specific differences between urban environments, revealed significant differences among three of the five species selected to measure *in-situ* photosynthetic responses to temperature between the UHI and coldest parts of the city (Figure 7, S4a). Specifically, ACSA, CEOC,

and TICOR exhibited higher T_{opt} values in the UHI compared to the coldest part of the city, indicating photosynthetic thermal acclimation to elevated temperatures. On the other hand, P_{opt} was significantly higher in the UHI for ACSA and CEOC, but significantly lower for QURU and TICOR (Figure 7, S4b). The results, wherein species with higher T_{opt} values showed lower P_{opt} in the UHI, suggest that an increase in T_{opt} by acclimation does not necessarily lead to an increase in carbon assimilation.

Furthermore, significant differences were observed between urban environments for all species in both transpiration (E) and stomatal conductance (g_s), except for E for TICO (Figure 5). ACSA, CEOC, and GLTR exhibited higher E and g_s in the UHI, likely as a mechanism to facilitate cooling and sustain optimal carbon assimilation. Conversely, QURU and TICO displayed a slight decrease in both E and g_s within the UHI, likely, indicating the plants' active response to mitigate dehydration (Figure 5a, b).

DISCUSSION

Urbanization significantly modifies the thermal environment for plants, impacting their physiological adaptation (Zipper et al. 2017). Greenhouse studies have documented plastic changes in leaf traits as a response to increased urban temperatures (Hara et al. 2021, Okubo et al. 2023). Yet, field studies involving mature trees are scarce. This study assessed plants' thermoregulatory strategies and acclimation capacity in mature trees within the UHI and how affect their physiology. Overall, our results using the city of Montreal as scenario, suggest that urban tree species have different ways of thermoregulating. One type of response we observed in our tree species to temperature increases was passive thermoregulation by adjustments in leaf morphology, mainly those related with area such as leaf area (LA), specific leaf area (SLA), but also those involving mass, such as leaf thickness (LT). Another type of response was through an active thermoregulation by acclimating photosynthetic thermal optimum (T_{opt}). Although we did not measure metabolism directly, it is important to note that changes in photosynthesis inevitably imply adjustments in metabolic processes (Yamori et al. 2014). Finally, photosynthetic heat

tolerance (measured as $T_{crit,}$ $T_{50,}$ T_{95}), did not show general trend of changes between UHI and the coldest part of the city. Although, this trait tends to be more conserved and retain its evolutionary climatic affinities (Bennett et al. 2021), it also has high adaptability and can show plastic changes under elevated temperatures (Zhu et al. 2018). We argue that, perhaps, this trait is not yet experiencing sufficient thermal stress to acclimatize across species. In fact, although two species showed increased $T_{50,}$ other species showed a decreased T_{50} in the UHI. Our results also indicate the species-specific nature of thermal acclimation, underscoring the necessity for individualized species assessment in urban planning.

Previous studies show that slight increases in temperature, such as 0.78 to maximum 2.8 °C provoke significant modifications in physiological prosses such as photosynthesis, as well as morphological traits (Zhu et al. 2020, Wei et al. 2023). In our study using actual urban microclimates, the maximum air temperature exhibited a difference of 3.4°C between the urban heat island (UHI) and the coldest parts of the city, which proved to be a critical factor influencing plant functioning. This slight temperature difference was enough to reveal significant physiological and morphological responses in urban trees, similar to those observed in previous studies, but evaluated in the specific context of urban environments.

Changes in morphological leaf traits

Plants may respond to changes in temperature by adjusting their growth strategies and altering association among traits (Reich 2014). Because plant strategies are closely linked to resource acquisition and use, their variation is an important indicator of possible plant acclimation (Li et al. 2018, Wang et al. 2022). Within the UHI, we found significant shifts for traits related to the area (LA, SLA, LW) and leaf thickness as a possible response to warmer urban temperatures, supporting our first hypothesis. However, the pattern of change in morphological leaf traits was contrary to our expectations in the second hypothesis. Instead of exhibiting shifts towards conservative strategies (lower values of area-related traits), plants shifted towards acquisitive strategies within UHI (greater LA, SLA LW, and an increase in thickness).

In our case, larger values of LA, SLA and LW within the UHI may act as a mechanism to enhance the cooling effect through increased transpiration, thereby helping to mitigate leaf overheating (Fauset et al. 2018, Kim et al.2024, Ji-yougn et al. 2024). The increases in traits related with leaf area are supported by increases in stomatal conductance and transpiration values for species with larger leaf areas within the UHI (e.g., *Acer saccharinum, Celtis occidentalis, Gleditsia triacanthos*) (Figure 5). These coordinated increases in leaf traits likely result from an environment with rising temperatures but without water stress (Ibsen et al. 2023). Therefore, larger leaves can stay cooler and lose more heat through transpiration when there is sufficient water and adequate levels of solar radiation creating a unique plasticity pattern (Leigh et al. 2017, Ibsen et al. 2023). While municipal crews manage and water newly planted trees, this is not the case for mature trees, like those in our study. To account for potential differences in water availability, we specifically selected park trees, which are less likely to access supplemental water from nearby infrastructure. Thus, the rainfall in the city, particularly during the wettest months (May-September, totaling ~866 mm of precipitation), likely provides sufficient water to prevent drought stress in these trees (https://climate.weather.gc.ca/).

Leaf thickness, instead of increasing, decreased significantly for the same species with higher SLA within the UHI (Figure 3). SLA, a measure of the light-capturing area relative to biomass investment, tends to increase under elevated temperatures, allowing plants to enhance photosynthesis and cooling through transpiration (Xu et al.2023). Furthermore, thinner leaves with higher SLA values are typically less costly to produce and can dissipate heat more effectively, especially when there is no water limitation (Ibsen et al. 2023). In urban areas with higher temperatures but sufficient water supply (such as through regular precipitation), plants might regulate heat by growing thinner leaves with increased SLA and optimize for light-capture, particularly in areas with taller buildings that create varying light dynamics. These plastic shifts in leaf traits are consistent with findings on urban trees, where trees increasing simultaneously carbon gain and the water transport capacity, indicating that urban trees can alter the water-use strategy meeting atmospheric demands (Ibsen 2023, Yin et al 2024, Rahman et al 2020). While this study focuses on leaf morphological traits, it is important to recognize that other physiological and structural

traits, such as stomatal density, cuticular conductance, turgor loss point, and wood density, may also exhibit plasticity in response to temperature variation in urban environments. Further research into plastic responses of trees should investigate these traits along with a set of other environmental factors, such as humidity, wind speed, solar radiation, and water access, to fully understand the mechanisms plants use to offset high temperatures in urban environments.

Thermal tolerance (P_{HT}) and Photosynthetic thermal optimum (T_{opt})

The relationship between leaf temperature and photosynthesis is pivotal for understanding plant physiological acclimation within UHI and how elevated temperatures affect CO_2 uptake in cities (Meineke et al. 2016, Percival, 2023). Each of the urban tree species we analyzed had a unique photosynthetic acclimation response, highlighting the species-specific nature of physiological acclimations. *A. saccharinum* and *C. occidentalis* showed a significant acclimation on T_{opt}, also reflecting a higher photosynthetic rate at higher temperatures. This aligns with previous findings showing that urban flora can exhibit enhanced photosynthetic capacity at elevated temperatures due to acclimation (Hara et al. 2021). This particular response implies that these species might have an inherently high $T_{opt,}$ making them less sensitive to UHI effects. The photosynthetic acclimation of these species, coupled with higher stomatal conductance and transpiration, reflect higher metabolism in response to warming, such a response ensures better photosynthetic performance within UHI (Drake et al. 2018, Dusenge et al. 2019). However, it may also indicate that these species would not be able to maintain photosynthetic rate if high temperatures join with water deficit (Hara et al. 2021).

T. cordata exhibited a significantly higher optimal temperature for photosynthesis (T_{opt}) within the UHI, but its net photosynthesis (A_{net}) decreased substantially. This suggests either limited acclimation capacity (Kullberg and Feeley 2022) or that acclimation alone cannot fully offset the effects of rising temperatures, as it may not provide additional physiological benefits (Way and Yamori 2014). As a result, T_{opt} acclimation does not always improve A_{net} at elevated temperatures (Dusenge et al. 2019), and some species may even experience reduced growth in warmer environments (Meineke et al. 2016). A similar

pattern was observed for *Q. rubra*; despite showing no acclimation in T_{opt}, Anet was also significantly lower at elevated temperatures within the UHI. Both species demonstrated significantly reduced transpiration and stomatal conductance in the UHI, which can be attributed to their water-use strategy, being both categorized as isohydric species (Leuschner et al. 2019, Di lorio et al. 2024). Species with this water-use strategy exercise strict control over their internal water status by closing stomata in response to high temperatures or limited water availability, which may result in photosynthesis being limited by CO_2 supply. In these cases, rising temperatures can result in increased rates of photorespiratory CO_2 release exceeding the carboxylation rates, causing decreases of A_{net} beyond an optimal temperature to which net photosynthesis is acclimated (Teskey et al. 2015).

Contrary to our hypothesis, we did not find that photosynthetic heat tolerance (P_{HT}), particularly T_{50}, acclimates to higher temperatures within the UHI as a general response for all the species, similar to previous studies developed in urban areas (Kullberg and Feeley 2022). Only *A. platanoides and A. sacharinnum* showed acclimation in their T_{50} within the UHI. On the other hand, the declining of T_{50} for *Q. macrocarpa* and *T. cordata* within the UHI, suggests that these species may be more susceptible to heat stress. It has been proved that P_{HT} acclimates to seasonal temperature variation and to sustained changes in growth temperature, remarking that P_{HT} is highly temperature dependent (Zhu et al. 2018). To assess acclimation, it is crucial to evaluate the upper thermal limits of both leaf and air temperatures. In our study, we observed that the P_{HT} thresholds for nearly all species are close to ~50°C, while summer air temperatures within the UHI rarely surpass 40°C. Given this discrepancy, the prevailing air temperatures do not appear to reach the necessary levels to induce thermal stress to drive acclimation of P_{HT}. As such, the relatively moderate urban warming observed in our case is insufficient to trigger or elucidate plant acclimation in this trait. Further studies in environments with more extreme urban heat or under experimental warming conditions may be necessary to understand the potential for thermal acclimation in these species fully.

Leaf energy balance within UHI

Leaf temperature modeling revealed that the disparity between leaf and air temperature (ΔT) was more pronounced for individuals located within the urban heat island (UHI) compared to those in the coldest part. This observation suggests that trees within the UHI may not be developing the capacity to acclimate to higher temperatures by adjusting their leaf energy balance. Our analysis of variation in morphological and physiological traits demonstrated changes in leaf morphology, such as increased leaf area and width within the UHI, as well as alterations in leaf physiology, including elevated transpiration cooling rates (E) and stomatal conductance (gs). These mechanisms play a crucial role in maintaining cellular homeostasis and metabolic function under heightened thermal conditions (Michaletz et al. 2015, Michaletz et al. 2016). However, the active augmentation of E and gs does not fully offset the elevated temperatures to achieve complete acclimation to local conditions.

Leaf energy balance is governed by sensible and latent heat exchange, with the latter being regulated by plant available water, stomatal conductance, and leaf-to-air vapor pressure deficit (Still et al. 2019). Consequently, in an urban setting such as ours, plants within the UHI will require greater water availability to withstand heat stress and potentially develop acclimation mechanisms. It is conceivable that if heat stress coincides with drought, stress levels in tree species will be exacerbated (Esperon-Rodriguez et al. 2021), and acclimation may not be feasible as drought reduces stomatal conductance and latent heat, thereby increasing leaf temperature. Urban water supply is often provided during establishment, when individuals are most susceptible to water constraints (Roman et al. 2014). Our findings underscore the importance of ensuring adequate water supply for mature trees as well, enhancing their acclimation capacity and cooling effect in warmer locales. This ensures that trees can continue to provide the ecosystem services upon which we rely now and in the foreseeable future.

Conclusion

As cities continue to warm due to climate change, particularly within urban heat islands (UHIs), understanding how urban trees acclimate to these novel conditions is crucial for urban planning (Teskey et al. 2015, Percival 2023). Our study on urban tree acclimation to

elevated temperatures revealed highly species-specific responses, highlighting the complexity of plant adaptation in urban environments. We found that both leaf area and specific leaf area (SLA) increased, while transpiration rates rose, and leaf thickness decreased. Interestingly, only a subset of species showed acclimation in optimal photosynthetic temperature (Topt), associated with an increase in Anet; meanwhile, some species, although acclimating the Topt, show decreases in Anet. This highlights that photosynthetic acclimation to higher temperatures does not necessarily imply an increase in Anet. Species with more conservative water use strategies, such as isohydric species, tend to decrease carbon sequestration significantly due to stomatal control under urban environments with elevated temperatures. Overall, urban tree species exhibited no acclimation in photosynthetic heat tolerance (T50), likely due to the substantial thermal margin between their PHT values and the ambient air temperatures, which remained approximately 10°C lower. This significant buffer suggests that the air temperatures in urban environments do not impose sufficient thermal stress to trigger acclimation in this trait.

These findings together suggest that urban trees may prioritize strategies for leaf cooling, such as expanding leaf area and enhancing transpiration, rather than conserving water or thickening leaves in hotter, more humid climates. While our focus was on temperature, other factors like CO_2 levels, irrigation, and soil conditions could also influence these plastic responses. Future research should explore additional traits related to leaf acclimation —such as stomatal density, cuticular conductance, and water-use efficiency—to develop a more comprehensive understanding of urban plant responses to UHI. Our study offers valuable insights, but we are aware that it was conducted over just one year. Long-term studies are encouraged to assess how plastic responses evolve across different environmental conditions, which would help forecast more accurate tree responses to urban stressors and UHI.

REFERENCES

Baker NR (2008) Chlorophyll Fluorescence : A Probe of Photosynthesis In Vivo. Annu Rev Plant Biol, 59: 89–113. https://doi.org/10.1146/annurev.arplant.59.032607.092759.

Bates D, Mächler M, Bolker B, Walker S (2015). Fitting Linear Mixed-Effects Models Using lme4." Journal of Statistical Software, 67(1), 1–48. doi:10.18637/jss.v067.i01.

Beck HE, Zimmermann NE, McVicar TR, Vergopolan N, Berg A, Wood EF (2018) Present and future Köppen-Geiger climate classification maps at 1-km resolution. Sci Data, 5(1): 1-12.

Bennett JM, Sunday J, Calosi P, Villalobos F, Martínez B, Molina-Venegas R, Araújo MB, Algar AC, Clusella-Trullas S, Hawkins BA, Keith SA, Kühn I, Rahbek C, Rodríguez L, Singer A, Morales-Castilla I, Olalla-Tárraga MÁ (2021) The evolution of critical thermal limits of life on Earth. Nat Commun, 12(1). https://doi.org/10.1038/s41467-021-21263-8.

Blonder B, Escobar S, Kapás RE, Michaletz ST (2020) Low predictability of energy balance traits and leaf temperature metrics in desert, montane and alpine plant communities. https://doi.org/10.1111/1365-2435.13643.

Boulfroy, E. et al., 2012. Priorisation pour la conservation d'îlots de fraîcheur existants et l'implantation de nouveaux îlots de fraîcheur., Québec, Canada.: Centre d'enseignement et de recherche en foresterie de Sainte-Foy inc. (CERFO).

Campbell GS, Norman JM (1998) An Introduction to Environmental Biophysics, 2nd edn. Springer, New York

Cavaleri MA (2020) Cold-blooded forests in a warming world. New Phytol. 228(5):1455–1457. https://doi.org/10.1111/nph.16916.

Crous, K. Y., Uddling, J., & De Kauwe, M. G. (2022). Temperature responses of photosynthesis and respiration in evergreen trees from boreal to tropical latitudes. *New Phytologist*, *234*(2), 353-374.

Di Iorio, A., Caspani, A. C., Beatrice, P., & Montagnoli, A. (2024). Drought-related root morphological traits and non-structural carbohydrates in the seedlings of the alien Quercus rubra and the native Quercus robur: possible implication for invasiveness. Frontiers in Forests and Global Change, *7*, 1307340

Drake JE, Tjoelker MG, Vårhammar A, Medlyn BE, Reich PB, Leigh A, Pfautsch S, Blackman CJ, López R, Aspinwall MJ, Crous KY, Duursma RA, Kumarathunge D, De Kauwe MG, Jiang M, Nicotra AB, Tissue DT, Choat B, Atkin OK, Barton CVM (2018) Trees tolerate an extreme heatwave via sustained transpirational cooling and increased leaf thermal tolerance. Global Change Biology. 224(6):2390–2402. https://doi.org/10.1111/gcb.14037.

Dusenge ME, Duarte AG, Way DA (2019) Plant carbon metabolism and climate change: elevated CO2 and temperature impacts on photosynthesis, photorespiration and respiration. New Phytol. 221(1):32–49. https://doi.org/10.1111/nph.15283.

Esperon-Rodriguez M, Power SA, Tjoelker MG, Marchin RM, Rymer PD (2021) Contrasting heat tolerance of urban trees to extreme temperatures during heatwaves. Urban For Urban Green. 66. https://doi.org/10.1016/j.ufug.2021.127387.

Fauset S, Freitas HC, Galbraith DR, Sullivan MJP, Aidar MPM, Joly CA, Phillips OL, Vieira SA, Gloor MU (2018) Differences in leaf thermoregulation and water use strategies between three co-occurring Atlantic forest tree species. Plant Cell Environ. 41(7):1618–1631. https://doi.org/10.1111/pce.13208.

Feeley K, Martinez-Villa J, Perez T, Silva Duque A, Triviño Gonzalez D, Duque A (2020) The thermal tolerances, distributions, and performances of tropical montane tree species. Front For Glob Change. 3:25.

Fox J, Weisberg S (2019). An R Companion to Applied Regression, Third edition. Sage, Thousand Oaks CA. https://www.john-fox.ca/Companion/.

Hara C, Inoue S, Ishii HR, Okabe M, Nakagaki M, Kobayashi H (2021) Tolerance and acclimation of photosynthesis of nine urban tree species to warmer growing conditions. Trees. 2021. https://doi.org/10.1007/s00468-021-02119-6.

Hothorn T, Bretz F, Westfall P (2008). Simultaneous Inference in General Parametric Models. Biometrical Journal, **50**(3), 346–363.

IPCC. Climate Change (2022): Impacts, Adaptation, and Vulnerability. Contribution of Working Group II to the Sixth Assessment Report of the Intergovernmental Panel on Climate Change. Cambridge University Press; doi:10.1017/9781009325844.

Ibsen, P. C., Santiago, L. S., Shiflett, S. A., Chandler, M., & Jenerette, G. D. (2023). Irrigated urban trees exhibit greater functional trait plasticity compared to natural stands. *Biology Letters*, *19*(1), 20220448.

Karimi A, Mohammad P, García-Martínez A, Moreno-Rangel D, Gachkar D, Gachkar S (2022) New developments and future challenges in reducing and controlling heat island effect in urban areas. Environ Dev Sustain. 1–47. https://doi.org/10.1007/s10668-022-02530-0.

Katabuchi M (2015) LeafArea: an R package for rapid digital image analysis of leaf area. Ecol Res. 2015;30:1073-1077.

Kullberg AT, Feeley KJ (2022) Limited acclimation of leaf traits and leaf temperatures in a subtropical urban heat island. Tree Physiol. 42(11):2266–2281. https://doi.org/10.1093/treephys/tpac066.

Kuznetsova A, Brockhoff PB, Christensen RHB (2017). lmerTest Package: Tests in Linear Mixed Effects Models. Journal of Statistical Software, 82(13), 1–26. doi:10.18637/jss.v082.i13.

Lambers H, Oliveira RS (2019) Scaling-up gas exchange and energy balance from the leaf to the canopy level. Plant Physiol Ecol. 291-300.

Leigh A, Sevanto S, Ball MC, Close JD, Ellsworth DS, Knight CA, Nicotra AB, Vogel S (2012) Do thick leaves avoid thermal damage in critically low wind speeds? New Phytol. 194(2):477–487. https://doi.org/10.1111/j.1469-8137.2012.04058.x.

Leigh A, Sevanto S, Close JD, Nicotra AB (2017) The influence of leaf size and shape on leaf thermal dynamics: does theory hold up under natural conditions? Plant Cell Environ. 40(2):237–248. https://doi.org/10.1111/pce.12857.

Lenth R, Singmann H, Love J, Buerkner P, Herve M (2019) Package 'emmeans'. R package version. 1(3.2).

Leuschner, C., Wedde, P., & Lübbe, T. (2019). The relation between pressure–volume curve traits and stomatal regulation of water potential in five temperate broadleaf tree species. *Annals of Forest Science*, *76*, 1-14.

Manishimwe, A., Ntirugulirwa, B., Zibera, E., Nyirambangutse, B., Mujawamariya, M., Dusenge, M. E., ... & Wallin, G. (2022). Warming responses of leaf morphology are highly variable among tropical tree species. Forests, 13(2), 219.

Meineke E, Youngsteadt E, Dunn RR, Frank SD (2016) Urban warming reduces aboveground carbon storage. Proc R Soc B. 283(1840). https://doi.org/10.1098/rspb.2016.1574.

Michaletz ST, Weiser MD, Mcdowell NG, Zhou J, Kaspari M, Helliker BR, Enquist BJ (2016) The energetic and carbon economic origins of leaf thermoregulation. Nat Plants. 2(9):1–8. https://doi.org/10.1038/nplants.2016.129.

Michaletz ST, Weiser MD, Zhou J, Kaspari M, Helliker BR, Enquist BJ (2015) Plant Thermoregulation: Energetics, Trait-Environment Interactions, and Carbon Economics. Trends Ecol Evol. 2015;30(12):714–724. https://doi.org/10.1016/j.tree.2015.09.006.

Okubo N, Inoue S, Ishii HR (2023) Tolerance and Acclimation of the Leaves of Nine Urban Tree Species to High Temperatures. Forests. 2023;14(8). https://doi.org/10.3390/f14081639.

Roberge, F., & Sushama, L. (2018). Urban heat island in current and future climates for the island of Montreal. Sustainable Cities and Society, 40, 501-512.

Percival GC (2023). Heat tolerance of urban trees − A review. Urban For Urban Green. 86. doi.org/10.1016/j.ufug.2023.128021.

Pérez-Harguindeguy N, Díaz S, Garnier E, Lavorel S, Poorter H, Jaureguiberry P, Cornwell WK, Craine JM, Gurvich DE, Urcelay C, Veneklaas EJ, Reich PB, Poorter L, Wright IJ, Ray P, Enrico L, Pausas JG, de Vos AC, Buchmann N, … Cornelissen JHC (2016) New handbook for standardised measurement of plant functional traits worldwide. Aust J Bot. 64:715–716.

Perez TM, Feeley KJ (2020) Photosynthetic heat tolerances and extreme leaf temperatures. Funct Ecol. 34(11):2236–2245. https://doi.org/10.1111/1365-2435.13658.

Perez TM, Socha A, Tserej O, Feeley KJ (2021). Photosystem II heat tolerances characterize thermal generalists and the upper limit of carbon assimilation. Plant Cell Environ. 44(7):2321–2330. https://doi.org/10.1111/pce.13990.

R core Team. R: A language and environment for statistical computing. R Foundation for statistical computing, Vienna, Austria. www.R-project.org. 2021.

Rahman, M. A., Stratopoulos, L. M., Moser-Reischl, A., Zölch, T., Häberle, K. H., Rötzer, T., ... & Pauleit, S. (2020). Traits of trees for cooling urban heat islands: A meta-analysis. *Building and Environment*, *170*, 106606.

Roman LA, Battles JJ, McBride JR (2014) Determinants of establishment survival for residential trees in Sacramento County, CA. Landsc Urban Plan. 129:22–31. https://doi.org/10.1016/j.landurbplan.2014.05.004.

Slot M, Winter K (2017). In situ temperature response of photosynthesis of 42 tree and liana species in the canopy of two Panamanian lowland tropical forests with contrasting rainfall regimes. New Phytol. 214(3):1103-1117 https://doi.org/10.1111/nph.14469.

Smith WK, Nobel PS (1977). Temperature and water relations for sun and shade leaves of a desert broadleaf, Hyptis emoryi. J Exp Bot. 28(102):169–183.

Still C, Powell R, Aubrecht D, Kim Y, Helliker B, Roberts D, Richardson AD, Goulden M (2019) Thermal imaging in plant and ecosystem ecology: applications and challenges. Ecosphere.10(6). E02768 https://doi.org/10.1002/ecs2.2768.

Tarvainen L, Wittemann M, Mujawamariya M, Manishimwe A, Zibera E, Ntirugulirwa B, Ract C, Manzi OJL, Andersson MX, Spetea C, Nsabimana D, Wallin G, Uddling J (2022) Handling the heat – photosynthetic thermal stress in tropical trees. New Phytol. 233(1):236–250. https://doi.org/10.1111/NPH.17809.

Teskey R, Wertin T, Bauweraerts I, Ameye M, McGuire MA, Steppe K (2015) Responses of tree species to heat waves and extreme heat events. Plant Cell Environ. 38(9):1699–1712. https://doi.org/10.1111/pce.12417

Touchaei AG, Wang Y (2015) Characterizing urban heat island in Montreal (Canada)—Effect of urban morphology. Sustain. Cities Soc. 19:395-402.

Tserej O, Feeley KJ (2021) Variation in leaf temperatures of tropical and subtropical trees are related to leaf thermoregulatory traits and not geographic distributions. Biotropica. 53(3):868–878. https://doi.org/10.1111/btp.12919

Tuholske C, Caylor K, Funk C, Verdin A, Sweeney S, Grace K, Peterson P, Evans T (2021) Global urban population exposure to extreme heat. Proc Natl Acad Sci. 118(41):1–9. https://doi.org/10.1073/pnas.2024792118/-/DCSupplemental

Vårhammar, A., Wallin, G., McLean, C. M., Dusenge, M. E., Medlyn, B. E., Hasper, T. B., ... & Uddling, J. (2015). Photosynthetic temperature responses of tree species in Rwanda: evidence of pronounced negative effects of high temperature in montane rainforest climax species. *New Phytologist*, *206*(3), 1000-1012.

Wang, Y., & Akbari, H. (2016). Analysis of urban heat island phenomenon and mitigation solutions evaluation for Montreal. *Sustainable Cities and Society*, *26*, 438-446

Way DA, Yamori W (2014) Thermal acclimation of photosynthesis: On the importance of adjusting our definitions and accounting for thermal acclimation of respiration. Photosynth Res. 119(1–2):89–100. https://doi.org/10.1007/s11120-013-9873-7

Wei, B., Zhang, D., Wang, G., Liu, Y., Li, Q., Zheng, Z., ... & Yang, Y. (2023). Experimental warming altered plant functional traits and their coordination in a permafrost ecosystem. *New Phytologist*, *240*(5), 1802-1816.

Wright IJ, Reich PB, Westoby M (2001) Strategy shifts in leaf physiology, structure and nutrient content between species of high- and low-rainfall and high- and low-nutrient habitats. Funct Ecol. 15(4):423–434. https://doi.org/10.1046/j.0269-8463.2001.00542.x

Xu, L., Zhang, N., Wei, T., Liu, B., Shen, L., Liu, Y., & Liu, D. (2023). Adaptation strategies of leaf traits and leaf economic spectrum of two urban garden plants in China. *BMC Plant Biology*, *23*(1), 274.

Yamori, W., Hikosaka, K., & Way, D. A. (2014). Temperature response of photosynthesis in C 3, C 4, and CAM plants: temperature acclimation and temperature adaptation. *Photosynthesis research*, *119*, 101-117.

Yin, Y., Li, S., Xing, X., Zhou, X., Kang, Y., Hu, Q., & Li, Y. (2024). Cooling Benefits of Urban Tree Canopy: A Systematic Review. *Sustainability*, *16*(12), 4955.

Zhu J, Zhu H, Cao Y, Li J, Zhu Q, Yao J, Xu C (2020) Effect of simulated warming on leaf functional traits of urban greening plants. BMC Plant Biol. 20(1). https://doi.org/10.1186/s12870-020-02359-7

Zipper SC, Schatz J, Kucharik CJ, Loheide SP (2017) Urban heat island-induced increases in evapotranspirative demand. Geophys Res Lett. 44(2):873–881.

TABLES

Table 4.1. Analysis of variance table for the nested ANOVA of plant functional traits and urban environments (Urban Heat Island [UHI] and the coldest part of the city). In the ANOVA, urban environment (hot-cold) was included as fixed effects and species are included as a random effect. The degrees of freedom (DF) were calculated using Kenward-Roger method. DF_{random} considers the structure of the random effects in the model. DF_{fixed} is 1 for all the models because the fixed effects are two treatments (hot-cold).

Type of trait	Trait	Units	F-statistic	P-value	DF_{random}
Morphologic	**LA**	**mm^2**	**44.7**	**<0.001**	**643.06**
Morphologic	**LW**	**mm**	**21.5**	**<0.001**	**643.02**
Morphologic	**SLA**	**$mm^2 mg^{-1}$**	**5.011**	**0.02**	**643.17**
Morphologic	LDMC	$g\ g^{-1}$	3.20	0.07	643.41
Morphologic	**LT**	**mm**	**4.14**	**0.04**	**643.09**
Photosynthetic	**T_{opt}**	**℃**	**3.55**	**0.06·**	34.7
Photosynthetic	P_{opt}	μmol CO_2 $m^{-2}s^{-1}$	0.03	0.8	34.5
Thermal	T_{crit}	℃	1.0	0.31	127.84
Thermal	T_{50}	℃	0.47	0.40	127.15
Thermal	T_{95}	℃	2.90	0.08	127.12

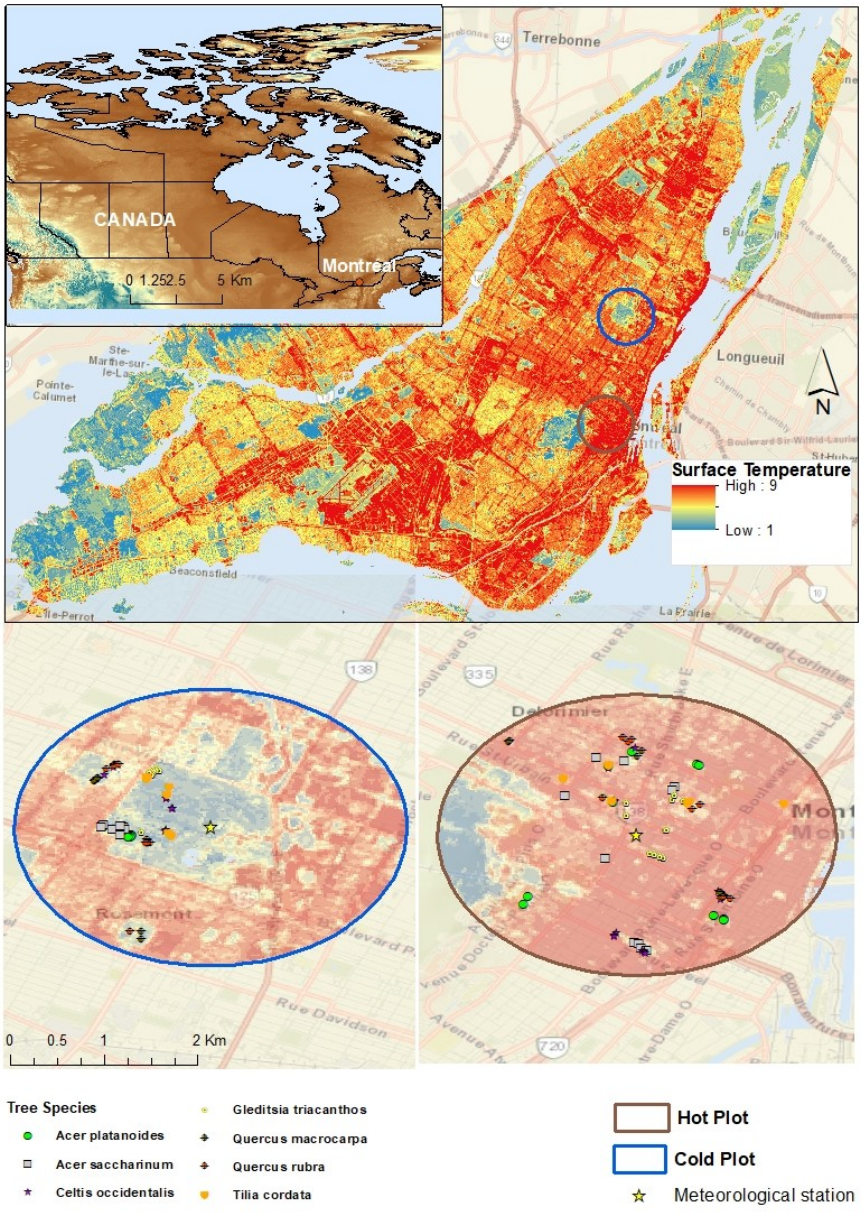

Figure 4.1) Location of the two urban environments within the city of Montreal. The hottest part of the city (UHI) is located in the downtown (brown circle) and the coolest part is located in the Botanical Garden (blue circle). The color scale from blue to red represents the surface temperature, where blue is the coldest temperature and red is the hottest temperature. Tree species are represented by symbols and starts representing the meteorological station from the municipality in each environment

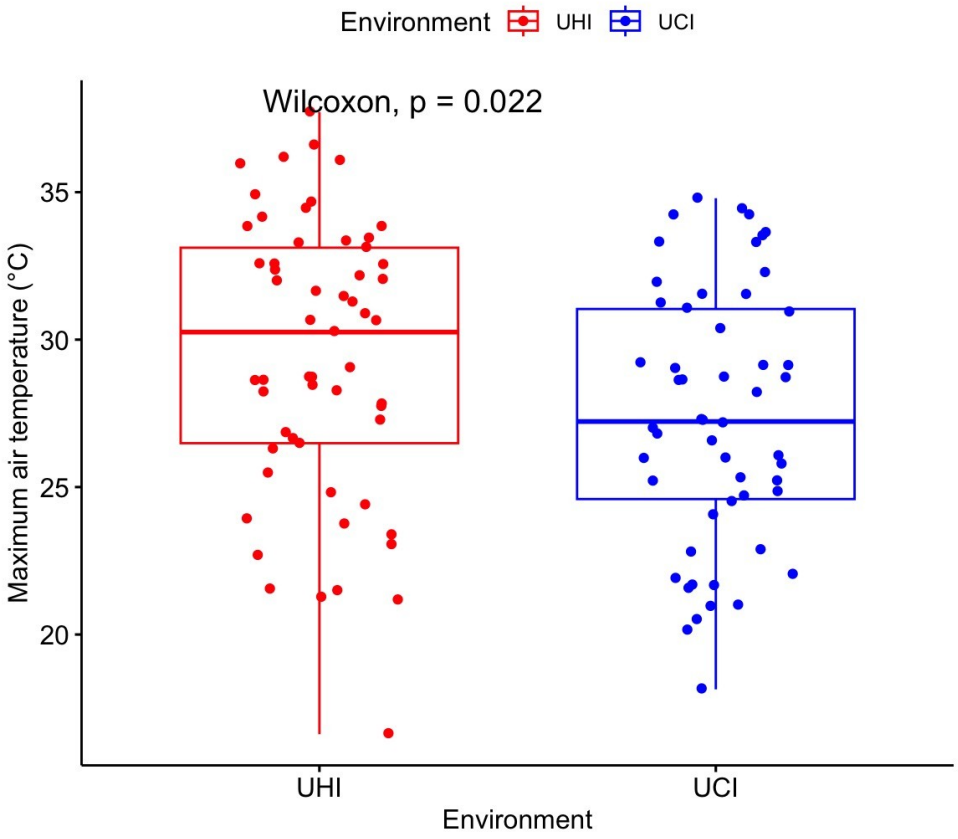

Figure 4.2) Maximum air temperature (ºC) data within the hot vs cold sites in Montreal, Canada, from July to September 2021. Wilcoxon-test is made with the residuals of the ARIMA models.

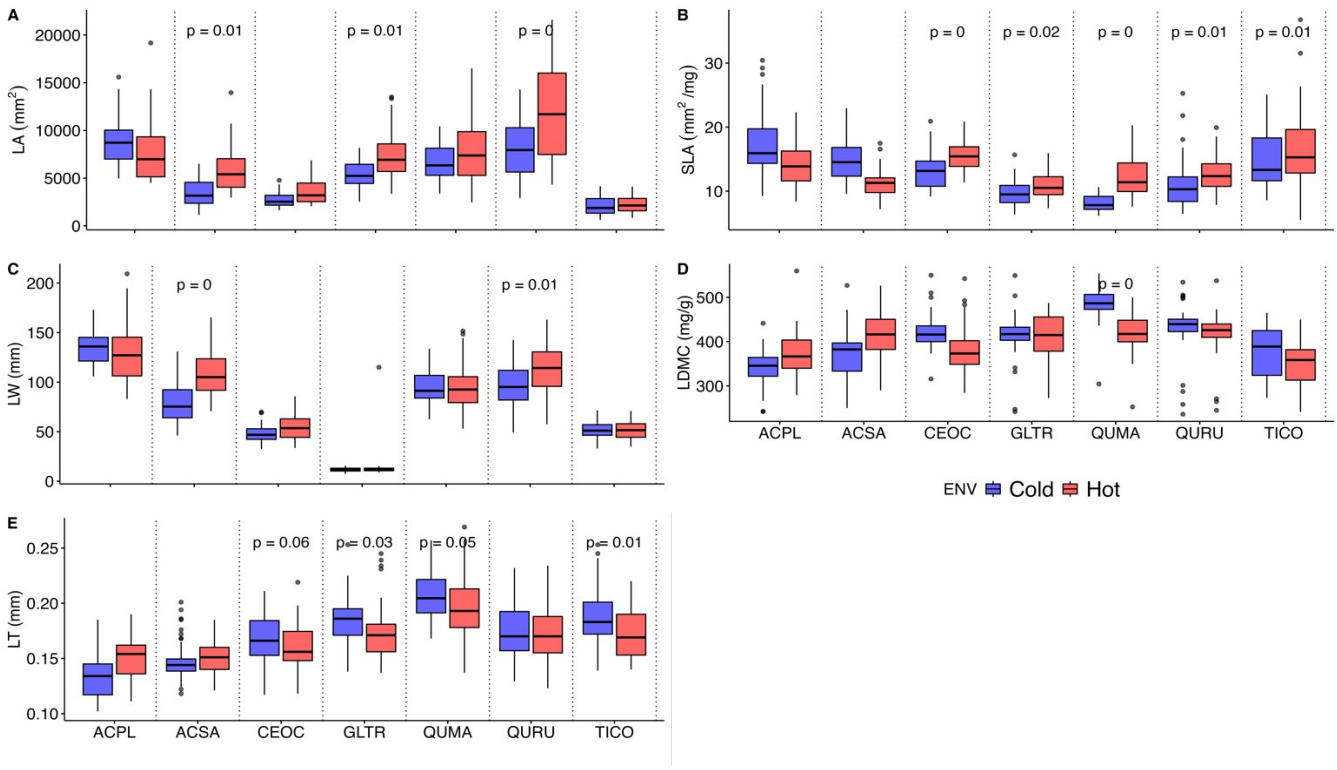

Figure 4.3) Variation in leaf morphological thermoregulatory traits between environments (Hot vs Cold) per specie in A) leaf area (LA), B) specific leaf area (SLA), C) effective leaf width (LW), D) leaf dry matter content (LDMC), and E) leaf thickness (LT). Each box shows one species per environment, the line within each plot represents the median, the upper and lower limit of the boxes represent the 75th and 25th percentile, and the whiskers the 90th and 10th percentiles. Red boxes denote the hottest part of the city (the Urban Heat Island [UHI]), and blue boxes the coldest part of the city. Asterisks between boxes indicate significative differences resulting from the *post hoc* Tukey analysis between urban environments. The species are *Acer platanoides* (ACPL), *Acer saccharinum* (ACSA), *Celtis occidentalis* (CEOC), *Gleditsia triacanthos* (GLTR), *Quercus macrocarpa* (QUMA), *Quercus rubra* (QURU) and *Tilia cordata* (TICO).

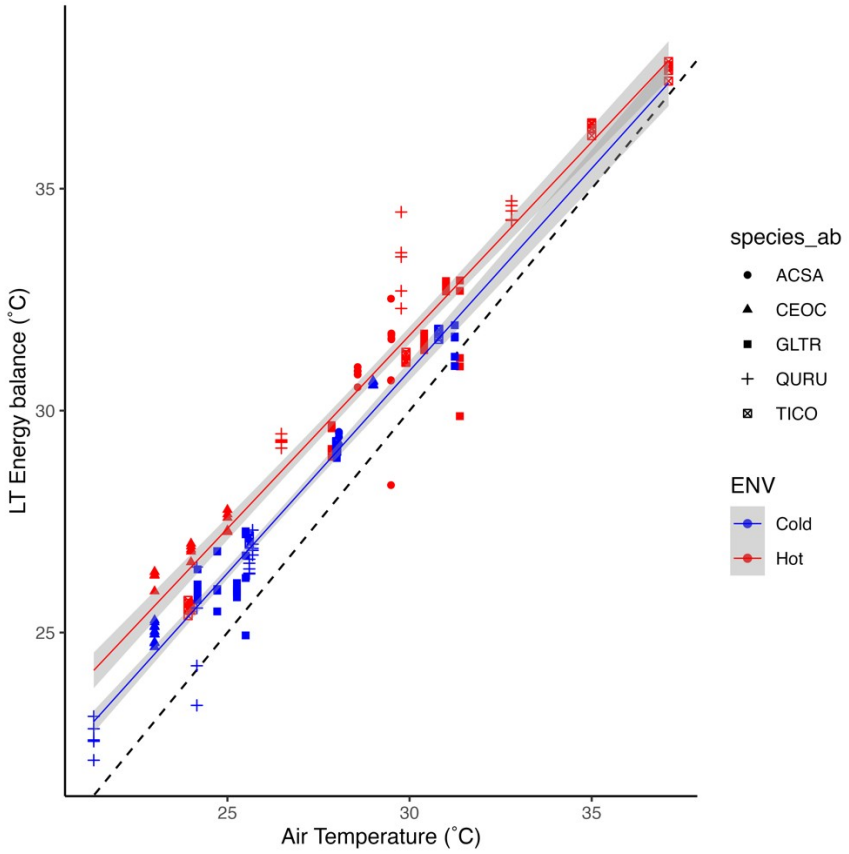

Figure 4.4) Energy balance estimations for leaf temperature (LT Energy balance) vs. air temperature. Colors denote the urban environment. Red figures denotate trees in the hottest part of the city and blue figures are trees in the coldest part of Montreal, Canada. The black dash is the y = x line. The mixed ANCOVA test to assess differences between the two slopes was $P< 0.005$.

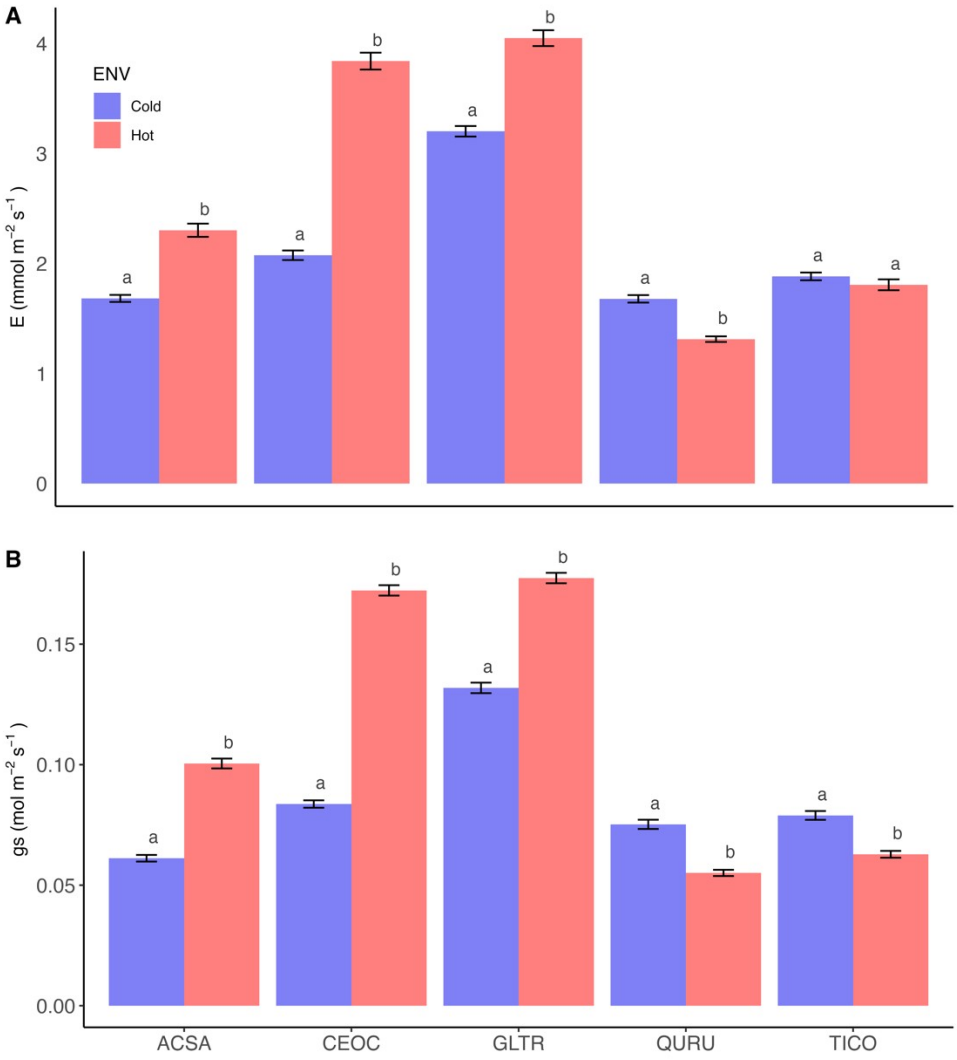

Figure 4.5) Between sites variation in A) Transpiration (E), and B) stomatal conductance (gs). Data are shown as mean ± SE of the values. Asterisks indicates significant differences between urban sites within each specie ($P<0.05$). Statistical comparisons were made using Tukey's honestly test. Abbreviation of species indicates *Acer saccharinum* (ACSA), *Celtis occidentalis* (CEOC), *Gleditsia triacanthos* (GLTR), *Quercus rubra* (QURU) and *Tilia cordata* (TICO).

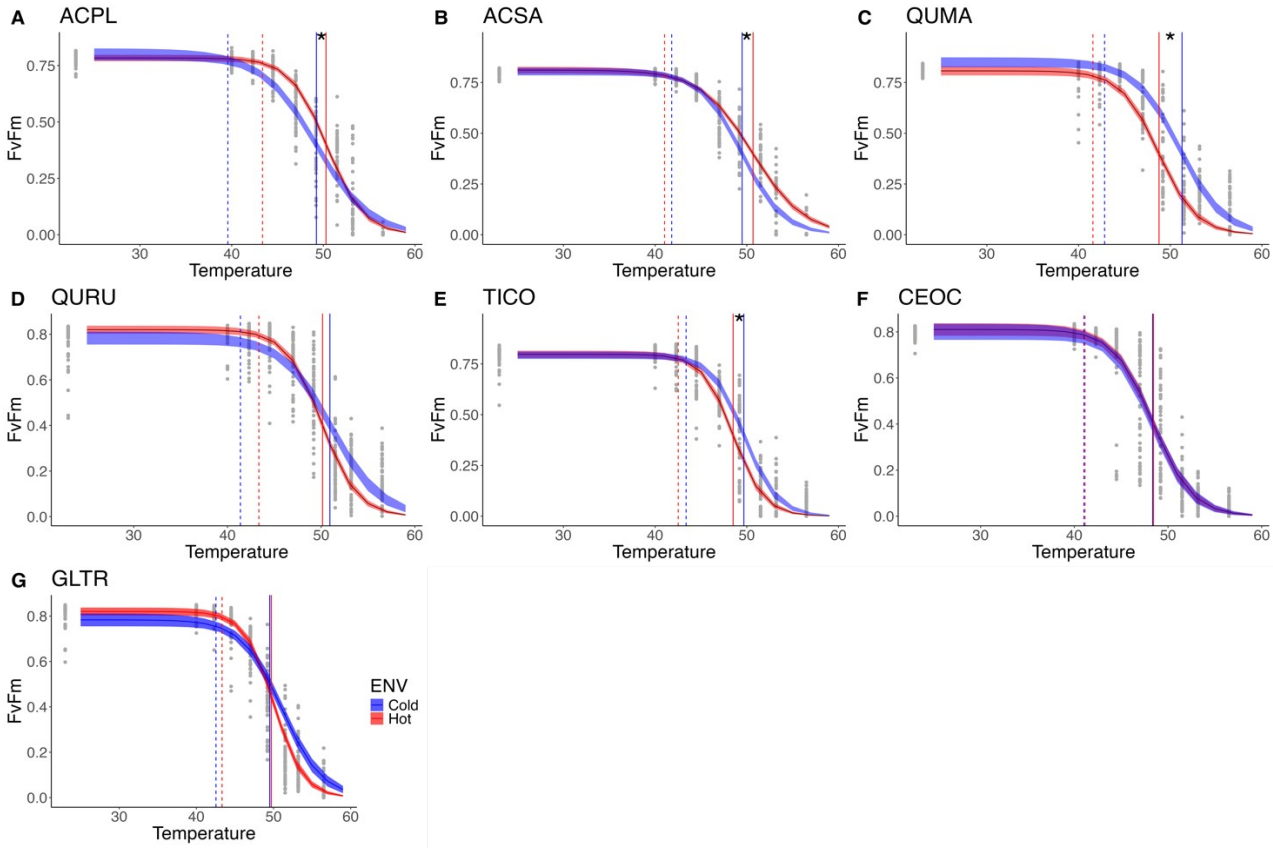

Figure 4.6) Non-linear least square models (nls) between F_V/F_M and temperature to determine photosynthetic heat tolerance (P_{HT}) for each specie by the environment. Grey dots represent individual leaf discs. The Vertical continuous line represents T_{50} and dashes lines $T_{crit.}$ The blue fit denotes the coldest part of the city (cold), and the red fit denotes the urban heat island (UHI). 95% confidence intervals were calculated using 1000 bootstrapped temperature- F_v/F_m nls models. The species are A) *Acer platanoides* (ACPL), B) *Acer saccharinum* (ACSA), C) *Quercus macrocarpa* (QUMA), D) *Quercus rubra* (QURU), E) *Tilia cordata* (TICO), F) *Celtis occidentalis* (CEOC), G) *Gleditsia triacanthos* (GLTR). Asterisk denotes significative differences between urban environments in T_{50} from the two-way ANOVA.

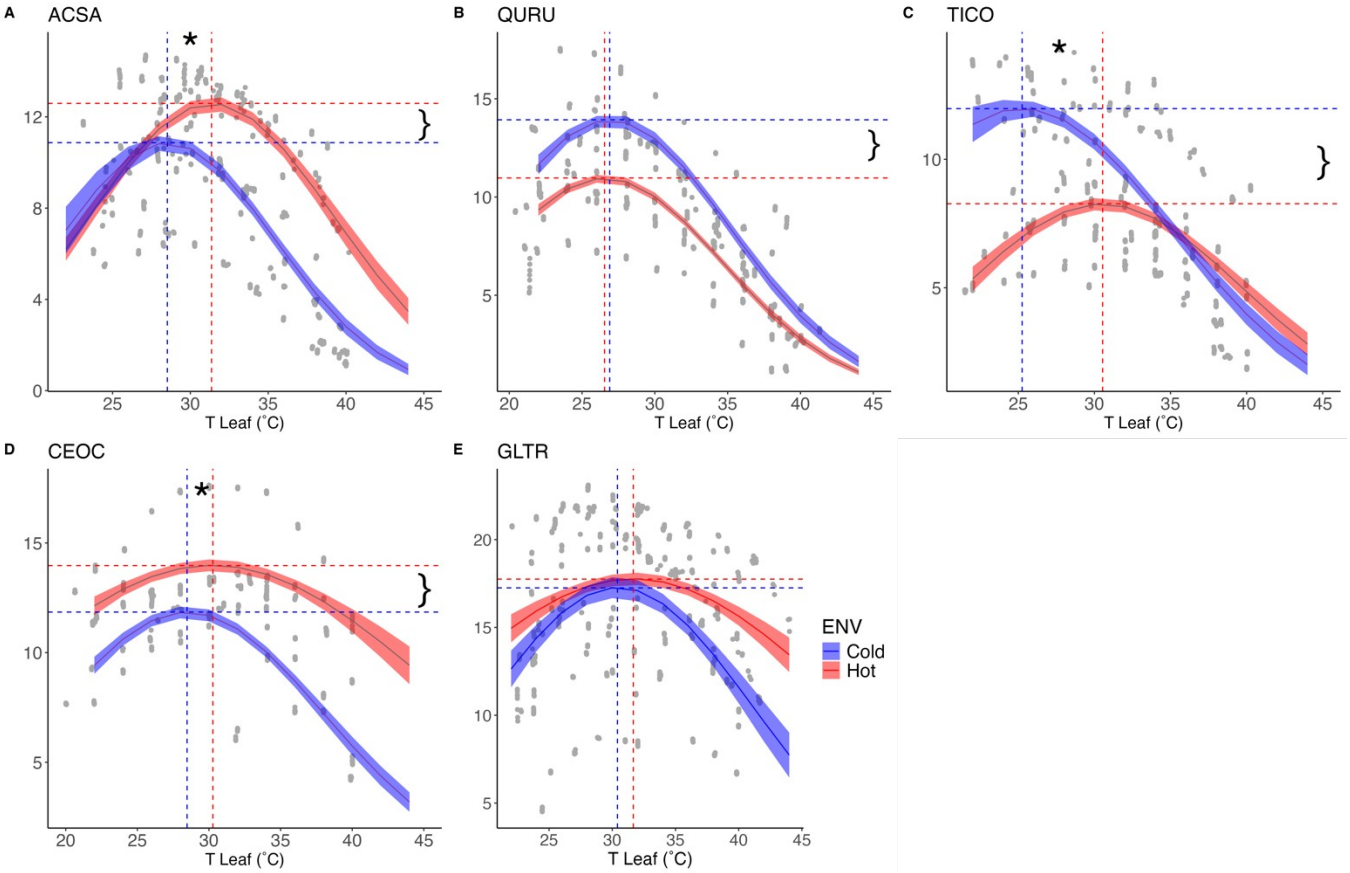

Figure 4.7) Light-saturated photosynthesis as a function of leaf temperature in the hottest part (Urban Heat Island [UHI]) (red) and the coldest part of the city (blue). A) *Acer saccharinum* (ACSA), B) *Quercus rubra* (QURU), C) *Tilia cordata* (TICO), D) *Celtis occidentalis* (CEOC), and E) *Gleditsia triacanthos* (GLTR). Discontinue vertical lines indicate the optimal temperature (T_{opt}), and discontinue horizontal lines indicate optimal photosynthesis (P_{opt}). Asterisks and brackets mean significant differences in T_{opt} and P_{opt}, respectively using the Welch's t-test.

SUPPLEMENTARY TABLES

TABLES

Table S4.1. Air temperature (T_{air_Mean}, °C), daytime air temperature ($T_{air\_dayMean}$, °C), maximum air temperature (T_{air_dayMax}, °C), and air temperature at night ($T_{air\_nightMean}$, °C). Each environment has five HOBBO sensors recording temperature from July to the end of September 2021. The day temperature was calculated from 9 to 17 h. The night temperature was calculated from 17 to 23 h. Values in brackets are standard deviations. In parentheses are the p-values from the Wilcoxon test. Hottest and Coldest denotate the UHI and the coldest part of the city.

Urban Environment	**T_{air_Mean}** (*P-value<0.001*)	**$T_{air\_dayMean}$** (*P-value<0.001*)	**T_{air_dayMax}** (*P-value*=0.02)	**$T_{air\_nightMean}$** (*P-value*<0.001)
Hottest	23.3 [±4.3]	25.9[±4.4]	37.8 [±2.3]	23.0 [±3.8]
Coldest	22.0[±4.6]	24[±4]	34.4 [±2.1]	22.1 [±3]

Table S4.2. Thermoregulatory traits by species in two urban environments, The hottest (UHI) and the coldest part of the city (UCI). Means ± SD are represented. Species are: *Acer platanoides* (ACPL), *Acer saccharinum* (ACSA), *Celtis occidentalis* (CEOC), *Gleditsia triacanthos* (GLTR), *Quercus macrocarpa* (QUMA), *Quercus rubra* (QURU) and *Tilia cordata* (TICO).

Species	ENV	L. Abs	LA (mm^2)	SLA	LW (mm)	LDMC (mg g^{-1})	LT(mm)
ACPL	**UCI**	0.295 +0.02	8833 + 1439	17.5+4.9	135+ 7.17	236+62.9	0.13+0.01
	UHI	0.396 0.01	7682+ 1593	14.2+3	128 + 17	369+57.4	0.15+0.01
ACSA	**UCI**	0.322 +0.02	3570 + 1053	14.5+2	79.5 + 15.8	375+42.3	0.14+0.01
	UHI	0.322 0.01	5669 + 1893	11.1+1.9	106 + 18.2	423+45.1	0.15+0.01
QUMA	**UCI**	0.318+0.02	6695.6+1139	8.08+1.1	94.3+10.6	504.5+22.2	0.20+0.01
	UHI	0.308+0.01	7946+3072	12.3+2.4	97.0+15.8	416.7+66	0.19+0.03
QURU	**UCI**	0.281+0.01	8273.8+2924	11.0+3.1	96.1+16.9	434.5+43.6	0.17+0.02
	UHI	0.271+0.05	11960+4506	12.6+2.5	111.54+22.6	431.1+39.4	0.17+0.02
TICO	**UCI**	0.314+0.01	2084.8+853	14.6+3.9	51.7+8.26	381.3+56.9	0.18+0.02
	UHI	0.274+0.05	2332.2+789	16.6+5.6	51.8+7.6	358.2+57.5	0.17+0.02
CEOC	**UCI**	0.302+0.01	2742.4 +567	12.8+2	48.3+6.3	420.3+27	0.17 +0.02
	UHI	0.297+0.01	3629.3+1081	14.5+2.1	54.9+10.4	387.3+31	0.16 +0.01
GLTR	**UCI**	0.327+0.02	5336.6+901	9.7+1.5	11.7+1.2	418.7+33.8	0.18+0.01
	UHI	0.303+0.05	7477.9+1959	10.9+2	14.0+6.6	419.9+37.1	0.17+0.03

Table S4.3. Parameters (±SE) estimated for thermal tolerance and net photosynthesis in response to temperature for seven urban species in hottest and coldest part of the city. Species are: *Acer platanoides* (ACPL), *Acer saccharinum* (ACSA), *Celtis occidentalis* (CEOC), *Gleditsia triacanthos* (GLTR), *Quercus macrocarpa* (QUMA), *Quercus rubra* (QURU) and *Tilia cordata* (TICO).

Species	F_v/F_m						Photosynthesis			
	UHI			UCI			UHI		UCI	
	T_{crit}	T_{50}	T_{95}	T_{crit}	T_{50}	T_{95}	T_{opt}	P_{opt}	T_{opt}	P_{opt}
ACPL	43.3±0.8	50.4±0.1	56.3±0.7	39.5±0.7	49.4±0.4	57.7±1.1	-	-	-	-
ACSA	41.1±0.7	50.7±0.2	58.9±0.3	41.7±0.6	49.5±0.3	56.1±0.4	31.36±0.1	12.59±0.1	28.52±0.4	10.87±0.1
QUMA	41.6±0.7	48.8±0.1	54.8±0.5	42.9±0.6	51.1±0.4	58.0±0.9	-	-	-	-
QURU	43.3±0.6	50.2±0.2	55.7±0.7	41.3±1.2	51.0±0.3	59.2±0.6	26.55±0.1	10.97±0.1	26.90±0.2	13.93±0.2
TICO	42.6±0.6	48.5±0.2	53.5±0.4	43.4±0.5	49.7±0.1	54.9±0.5	30.54±0.2	8.27±0.1	25.25±0.6	11.97±0.2
CEOC	41.2±0.7	48.5±0.5	54.6±0.6	41.0±0.7	48.4±0.7	54.6±0.5	30.27±0.3	13.97±0.1	28.47±0.1	11.85±0.1
GLTR	43.3±0.5	49.7±0.1	54.8±0.3	42.5±0.3	49.3±0.3	55.1±0.5	31.66±0.4	17.75±0.1	30.41±0.3	17.25±0.3

FIGURES

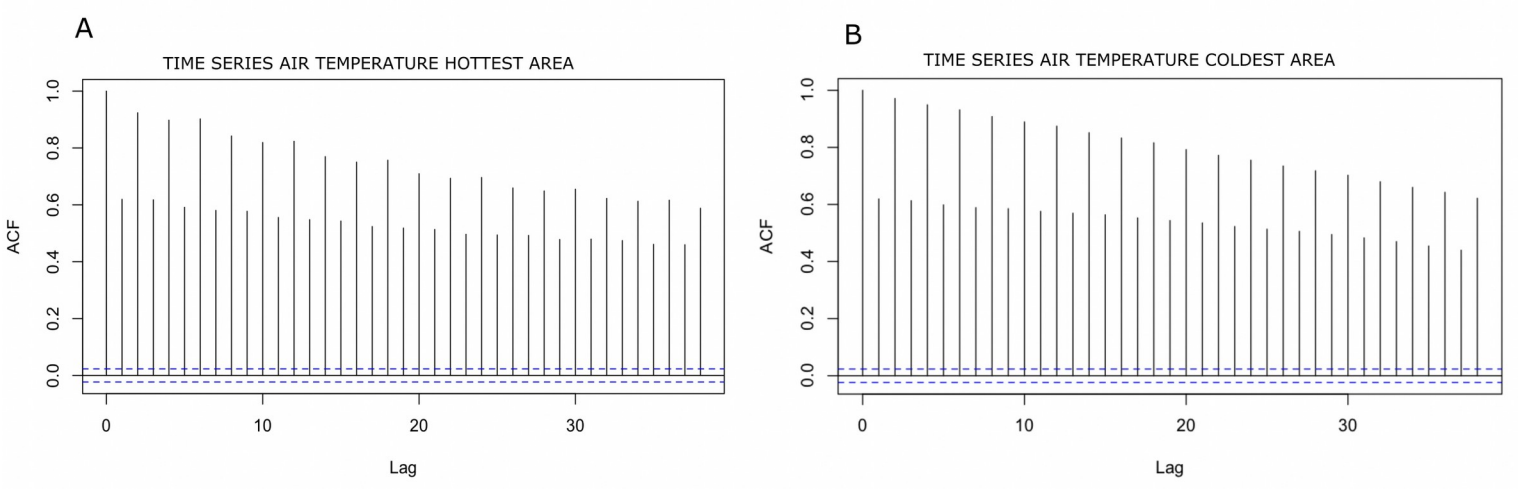

Figure S4.1) Correlogram made with the air temperature time series within the A) hottest part (Urban Heat Island [UHI]) and B) the coldest part of the city. The x-axis represents the lag, and the y-axis represents the autocorrelation. The height of the peaks indicates the strength of the autocorrelation. Blue lines denotates the confidence intervals.

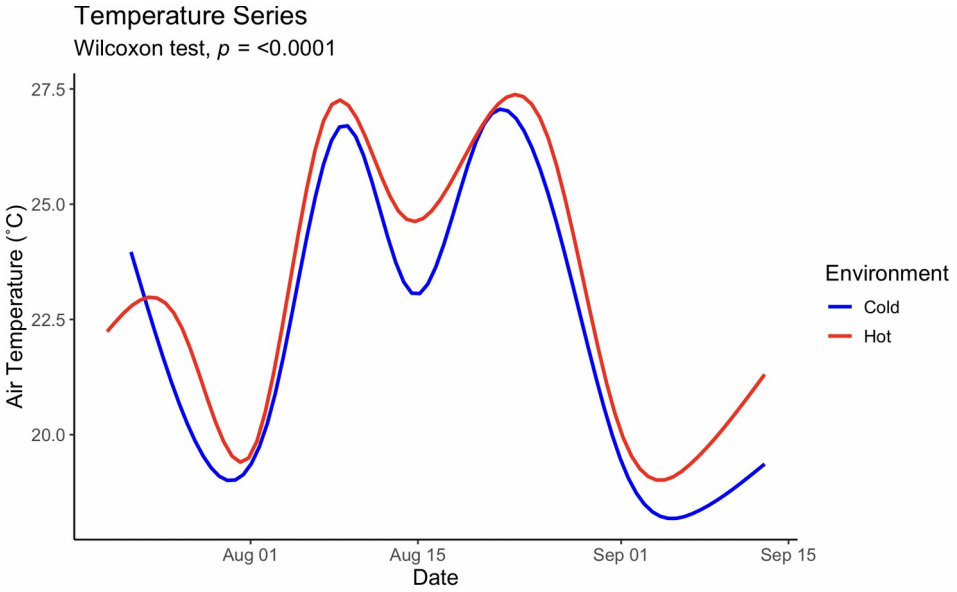

Figure S4.2) Time series variation in air temperature (ºC) (including day and night) from the HOBBO stations within the hottest (red) and coldest (blue) part of the city during the field camping (from July to September 2021). P<0.05 denotes the result from the Wilcoxon-test between urban environments.

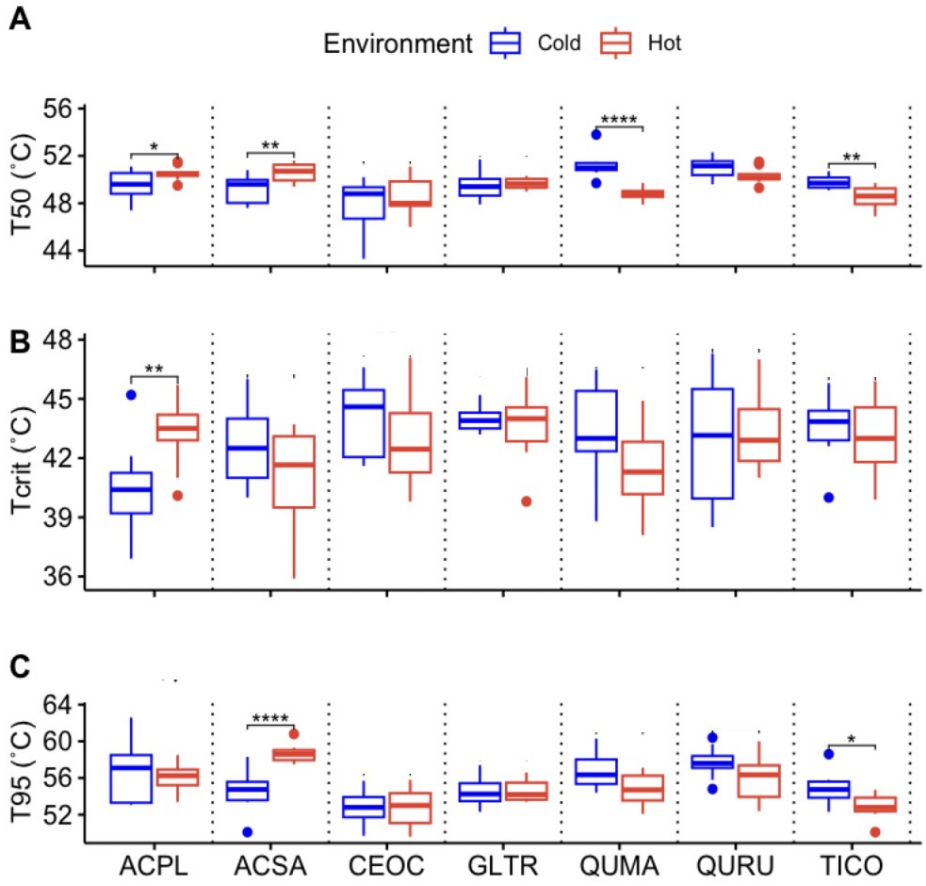

Figure S4.3) Two-way analysis of variance for the photosynthetic thermal tolerance parameters A) T_{50}, B) $T_{crit,}$ and C) T_{95} of seven species in two urban environments. Each panel shows one specie in the two environments and each box shows the median value, the upper and lower limit of the boxes represent the 75th and 25th percentile, and the whiskers the 90 th and 10 th percentiles. Red color denotes the hottest part of the city (Urban Heat Island [UHI]) and blue, coldest part. Asterisks between boxes indicate significative differences resulting from the Tukey *post-hoc* analysis between urban environments. The species are *Acer platanoides* (ACPL), *Acer saccharinum* (ACSA), *Celtis occidentalis* (CEOC), *Gleditsia triacanthos* (GLTR), *Quercus macrocarpa* (QUMA), *Quercus rubra* (QURU) and *Tilia cordata* (TICO).

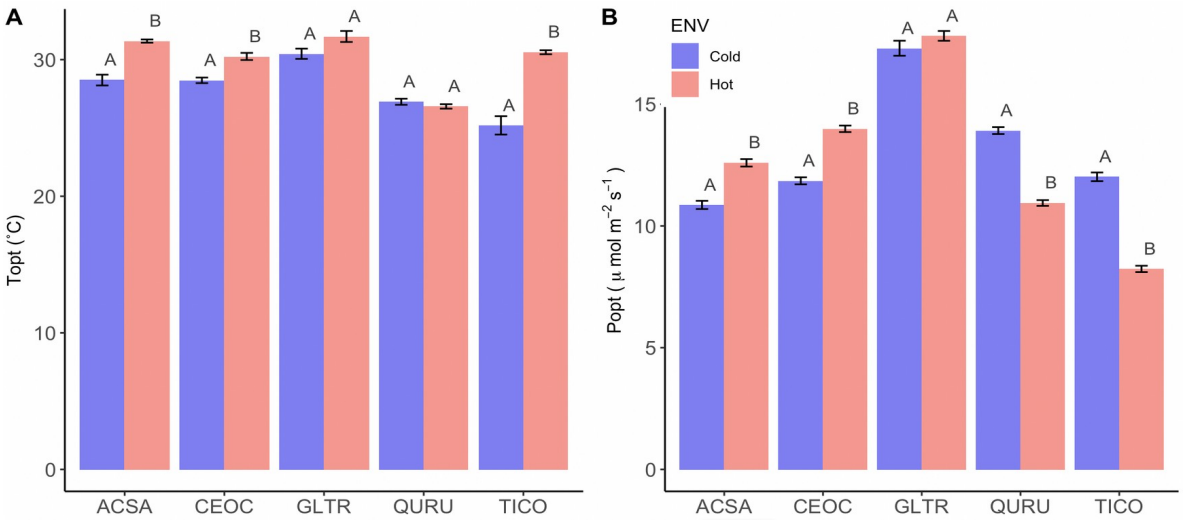

Figure S4.4) Between sites variation in A) T_{opt} and B) $P_{opt.}$ Data are shown as mean ± SE of the fitted temperature and assimilation values. The upper-case letter indicates significant differences urban between sites within each species ($P<0.05$). Welch's t-test was used for statistical comparison among groups. Abbreviation of species indicates *Acer saccharinum (*ACSA), *Celtis occidentalis* (CEOC), *Gleditsia triacanthos* (GLTR), *Quercus rubra* (QURU) and *Tilia cordata* (TICO).

SYNTHESIS

Exploring the drivers of forest diversity and functioning continues to be a critical topic in ecology, with profound implications for both theoretical understanding and conservation strategies (Lindenmayer & Franklin 2002). On one hand, unraveling the environmental factors and ecological mechanisms that shape species diversity is essential for a comprehensive understanding of forest ecosystems and the development of effective forest conservation programs (Zhu & Song 2021). On the other hand, widespread global changes such as climate change and urbanization are altering the very nature of our forests (Linnakoski et al., 2019; McDonald et al., 2014). Examining the effects of these global changes on forest diversity and functioning will provide us with valuable insights into the future trajectory of our forests and guide the development of strategies to strengthen forest resilience. Within this context, the objectives of my thesis were: i) to deepen our understanding of how patterns of diversity change across biogeographic regions and the ecological mechanisms that foster species diversity in highly diverse forests and ii) to evaluate the impact of climate change and urbanization on forest diversity and functioning. The research presented herein is dedicated to a comprehensive understanding of forest community diversity and functioning, as well as to documenting the transformations that forests are undergoing due to human activities. I will succinctly summarize the key findings from each chapter.

Chapter I examines the extent to which changes in the composition of local species are influenced by sampling effects and/or the ecological processes of community assembly. The research has revealed that in highly diverse forests, such as the Andes, expanding the spatial scale and including small trees can reveal more accurately the scope of ecological mechanisms shaping species variation (β-diversity). We can conclude that plots of at least one hectare and including individuals with a DBH $\geq$ 1 cm can better capture the actual ecological processes at play at different stages of tree development (all the community, small trees, large trees, and understory). Although habitat filtering emerged as the most significant ecological mechanism, its impact varies: small trees are more influenced by soil

conditions, whereas large trees are more affected by topography. I also showed that in high-elevation areas, the extent of ecological mechanisms (such as habitant filtering) is larger than in low-elevation plots. To improve our understanding of the drivers of β-diversity, I call for the need for enlarged forest inventory plots along elevational gradients in the tropics.

Chapter II investigates the drivers of beta diversity (β-diversity) in two distinct biogeographic regions, primarily delineated by differences in elevation. We explore the ecological mechanisms and scale that influence species variation. To assess the relative impact of these ecological mechanisms, we compared observed β-diversity with that under a null model. Our analysis revealed that ecological mechanisms had a greater influence in lowland areas (Amazon) compared to highland regions (Andes). This implies that the observed species variation in the Amazon differed more from a null community than in the Andean forest. Despite both the Andean and Amazon forests being highly diverse, species aggregation was more pronounced in the lowlands than in the highlands, suggesting that niche partitioning may play a significant role in species variation. This finding is particularly relevant in non-saturated communities, such as those found in the Amazon Forest.

Chapter III stands out to be the first study to evaluate the impact of climate change on the functional composition of highly diverse Andean forests over time along an elevational gradient of 3.000 m asl, identifying the primary climatic drivers of these shifts. My analysis revealed that increases in minimum temperature and vapor pressure deficit (VPD) are the principal climatic factors influencing functional transitions in Andean forests. These shifts in key climatic variables are causing tree communities to adopt more conservative strategies over time along an elevational gradient, reflected in alterations to species abundance and composition via mortality and recruitment. These insights challenge prevailing hypotheses regarding functional changes along elevational gradients, which predict that as species potentially migrate upslope, more acquisitive strategies would prevail in higher-elevation forests (Anderson & Wadgymar 2020; Feeley et al., 2011). Contrary to this hypothesis, our findings indicate that within tree communities, species

exhibiting more conservative traits are being selected by the new environmental conditions, primarily because such species are better equipped to endure the warmer and drier environments in forests traditionally characterized by cool, cloudy and moist climates.

In **Chapter IV**, I investigated the effects of elevated temperatures within Urban Heat Islands (UHI) on the physiology of trees, focusing on photosynthesis and thermal tolerance. I examined the capacity of urban tree species to acclimate and thermoregulate in response to increased urban temperatures and assessed the implications for ecosystem services, including carbon storage. Positioned at the forefront of urban ecological research, this study addresses the substantial gap in our understanding of urban forests, which have been less studied than their natural counterparts in terms of temperature elevation effects. My findings indicate that urban trees' reactions to elevated temperatures are markedly species-specific, revealing that the impacts of urban warming on physiological processes and ecosystem services are complex and differ among species.

Some species exhibited an increase in photosynthetic thermal optimum (T_{opt}) within UHIs, suggesting thermal acclimation. Yet, changes in T_{opt} were found to either increase or decrease carbon uptake depending on the species, indicating that acclimation to higher temperatures could either enhance or detract from urban ecosystem services. Conversely, other species displayed no thermal acclimation, highlighting their vulnerability to thermal stress. This practical research informs urban forest planning by considering the physiological needs and susceptibilities of each species. By strategically selecting the right species for the appropriate urban locations, we can optimize the provision of ecosystem services.

Contribution and future research

Implications of the study of beta diversity in the conservation of tropical forests

Numerous biodiversity studies prioritize species richness and alpha diversity, forming the foundation of many forest conservation initiatives (Lelli et al., 2019). However, designing

an effective protected network necessitates a deeper exploration of the processes and mechanisms sustaining species variation. Beta diversity (β-diversity) plays a crucial role in this context, as it highlights the variation in community composition across different sites (Socolar et al., 2016). A notable distinction in our research is the emphasis on spatial scale —1 ha in Chapter I and 25 ha in Chapter II, in contrast to the typical 0.25 ha (He et al., 2020) and 0.1 (Tello et al., 2015) scales prevalent in tropical studies. By incorporating larger spatial scales, our study enhances the comprehension of local biodiversity patterns across wider geographic gradients, facilitating the identification of ecological processes impacting species diversity. Another pivotal aspect of our research methodology is the rigorous sampling effort, with tree measurements starting from a diameter at breast height (DBH) of 1 cm. This approach enables the detection of patterns and processes across various tree growth stages, enriching our understanding of biodiversity dynamics.

In Chapter I, we concluded that the influence of ecological assembly mechanisms, which shape species variation, intensifies in highland areas along the elevational gradient in the Andean Forest. This suggests that in higher elevation plots, species configuration is determined by processes such as environmental filtering. These findings align with other studies conducted along tropical elevational gradients (Tello et al., 2015; Mori et al., 2013). However, we observed a contrasting pattern in Chapter II. Contrary to our expectations of a greater influence of ecological assembly mechanisms in highlands, we discovered that the impact of ecological mechanisms on species variation was more pronounced in the Amazonian lowlands than in the Andean highlands. The environmental heterogeneity in the Amazon forest possibly plays a significant role in creating species clumping through niche differentiation, as indicates the results of the clumping index Omega. The results in Chapter II diverge from other studies that analyzed contrasting biogeographic regions using 0.1 ha plots and trees with a diameter of DBH $\geq$ 2.5 cm (Muñoz-Mazón et al., 2021). This discrepancy suggests that β-diversity does not react solely to the size of the species pool but rather to the interplay between species pool size and environmental heterogeneity. Therefore, examining different areas, each with a unique combination of species pool and environmental heterogeneity, will yield distinct β-diversity outcomes. It is imperative to

continue exploring what drives species variation across various regions to unravel the specific mechanisms operating in every site.

β-diversity is crucial for the implementation of forest conservation programs (Socolar et al., 2016). Thus, future research on this topic should investigate how climate change affects β-diversity. For instance, what are the long-term effects of climate change on species turnover along elevational gradients, considering the up-slope migration of species? How has β-diversity changed over time? These questions necessitate the analysis of temporal β-diversity (Legendre 2019) and can provide insightful details about the dynamics of species diversity over time. Moreover, future research on β-diversity should strive to enhance our understanding of how to optimize the delineation of conservation areas. The debate over whether several small reserves are preferable to a single large one should be informed by comprehensive data about environmental heterogeneity and species composition, as elucidated by β-diversity studies.

Climate changes and the future of the hyper diverse tropical Andean forests

Global climate change continues to occur at an alarming rate (Pathak et al., 2022). Several studies show that climate change directly impacts forests worldwide (Pecl et al., 2017; Chen et al., 2011; Feeley et al., 2011). However, the trajectory of functional changes that the different types of forests may experience due to climate change is still largely unknown. In Chapter III, I wanted to investigate this knowledge gap, particularly in the Andes, one of the most vulnerable forests facing climate change (Orme et al., 2005). To date, no studies have evaluated the changes in functional composition in the Andes with empirical data. My research is one of the first studies identifying the functional changes, the trajectory of these changes, and the drivers of change. For that, I used a unique dataset that involved several years of fieldwork for collecting data on nine functional traits measured in situ for 1,200 tree species in nine 1-ha plots. This thesis finds evidence of climate-induced shifts in functional composition over time in response to specific environmental factors associated with the evolution and adaptation of the forest. Here, we highlight the importance to

include different variables in addition to temperatures, such as vapor pressure deficit (VPD). Thus, it is paramount to analyze the specific factors that can impact a certain type of forest to elucidate the patterns of changes. Analysis in Chapter III was done at the community level, showing that recruits are characterized by having more conservative strategies, which is align with other studies (Duque et al., 2015). This indicates that the community traits of the Andean forests could change in a few decades due to climate change.

To better understand Andean Forest responses to climate change, several information gaps need to be filled. For instance, expand the information on estimated ranges and georeferenced locations of native and non-native species, improve climatic information using in situ weather station along the elevational gradient, strengthen long-term vegetation monitoring using permanent plots (e.g., RBA [https:/ /redbosques.condesan.org/] and GLORIA [https://redgloria.condesan.org/] network) and record key information about land use changes, which is the main driver of change in the Andes (Tovar et al., 2022; Mathez-Stiefel et al 2017). Improve this information will help us to better understand the impact of climate change in Andean forest, improve governance and enhance ecosystem services.

Future research focused on the conservation of Andean forests should aim to fill many information gaps, mainly due to this type of forest is poorly explored in comparison to other types of forests, such as the Amazon for example (Pitman et al., 2011). Some of the priorities to address in the tropical Andes are: i) Analyzing demographic processes to improve our understanding of and obtain accurate information about which geographic regions, communities, and species are most vulnerable to climate change (Feeley et al., 2020). ii) Investigating intraspecific adaptations to determine population-level responses to climatic variable variations in different sites with shared species (Razgour et al., 2019). iii) Conducting studies on dispersal traits to identify which species are capable of migrating to higher elevations (Feeley et al., 2011). Enhancing research in these aforementioned areas, along with integrating data on maximum, minimum and mean temperature and drought thresholds, will provide insights into which species and regions are likely to be most affected by climate change. Consequently, this will enable the implementation of effective

conservation programs specifically targeting functionally unique species in forests with the highest number of endemic species (Orme et al., 2005).

Urban forest resilience

In recent years, there has been a growing interest in urban ecology since cities accommodate about 55% of the global population (more than 4.2 billion people) (UN 2018). At the local scale (city), it is paramount to understand how urban trees operate and how climate change and environmental variation generated by urban infrastructure (e.g., Urban Heat Islands [UHI]) impact tree functioning and, thus, ecosystem services. This knowledge is the base for effectively planning the urban forest for future warmer cities. Following this necessity, Chapter IV focused on an applied research question: how do elevated temperatures associated with Urban Heat Islands (UHIs) affect the functioning of urban trees? Important knowledge for the city of Montreal for implementing urban planning.

This work provides detailed information on the physiological performance and photosynthetic thermal limits of each species, identifying those likely to be more resilient to climate change and thus, more suitable for future urban planning. I also highlight the importance of irrigation in mature trees, since, although the summer in Montreal is humid, it was not enough for a complete thermoregulation. Thus, if temperature increases coincide with drought conditions, the vulnerability of urban trees will be exacerbated, and urban trees may not acclimate and diminish their physiological performance (Percival 2023). These findings show the current performance of tree species in Montreal's urban forest under existing urban conditions. With the understanding that climatic conditions will continue to evolve annually, it is crucial to compare current climate variables with future projections for temperature and drought and to model photosynthesis under these forthcoming scenarios.

Future research in urban ecology and urban ecophysiology should prioritize the investigation of critical functional traits, such as thermal thresholds and drought resistance

(Chang et al., 2024). While researchers are starting to tackle this area, the diverse nature of urban planning across cities, variations in climate, soil types, and other factors, poses challenges for generalizing findings. It is essential for studies to examine the behavior of identical species across different urban environments to enhance the universality of the data and its global relevance, particularly in temperate cities that share common species. Beyond examining specific functional traits, which give us a direct indication of ecosystem services, it is important to explore the still poorly understood link between biodiversity and ecosystem services (Percival 2023). This research topic could optimize the selection of tree species in urban planning. For instance, evidence suggests that species diversity positively impacts ecosystem services and boosts forest resilience to climate change (Paquette et al., 2021). Increasing research on functional diversity and functional groups could serve as a foundation for making well-informed urban planning decisions.

Moreover, it is crucial to broaden the study of tropical urban ecology, which remains largely under-researched compared to temperate regions (Dobbs et al., 2021). Tropical cities, with their extensive species diversity—such as Medellín (my home city), which boasts ~1,600 tree species—offer a unique study context (https://www.medellin.gov.co/sau/). The distinct challenges of tropical urban ecology, such as species diversity, climate, and human population density in tropical cities, give us a unique niche for research (Dobbs et al., 2021). The complexity and structure of tropical cities pose the urgent need to expand applied research in tropical urban ecology, aiming to bridge knowledge gaps and apply findings to real-world challenges.

REFERENCES

Anderson, J. T., & Wadgymar, S. M. (2020). Climate change disrupts local adaptation and favours upslope migration. *Ecology letters*, *23*(1), 181-192.

Chang, C. R., Su, M. H., Li, Y. H., & Chen, M. C. (2024). A proposed framework for a social-ecological traits database for studying and managing urban plants and assessing the potential of database development using Floras. *Urban Forestry & Urban Greening*, *91*, 128167.

Chen, I. C., Hill, J. K., Ohlemüller, R., Roy, D. B., & Thomas, C. D. (2011). Rapid range shifts of species associated with high levels of climate warming. *Science*, *333*(6045), 1024-1026.

Dobbs, C., Escobedo, F. J., Clerici, N., de la Barrera, F., Eleuterio, A. A., MacGregor-Fors, I., ... & Hernández, H. J. (2019). Urban ecosystem Services in Latin America: mismatch between global concepts and regional realities?. *Urban ecosystems*, *22*, 173-187.

Duque, A., Stevenson, P. R., & Feeley, K. J. (2015). Thermophilization of adult and juvenile tree communities in the northern tropical Andes. *Proceedings of the National Academy of Sciences*, *112*(34), 10744-10749.

Fadrique, B., Baez, S., Duque, A., Malizia, A., Blundo, C., Carilla, J., ... & Feeley, K. J. (2019). Widespread but heterogeneous responses of Andean forests to climate change (vol 564, pg 207, 2018). *Nature*, *565*(7741), E10-E10.

Feeley, K. J., Silman, M. R., Bush, M. B., Farfan, W., Cabrera, K. G., Malhi, Y., ... & Saatchi, S. (2011). Upslope migration of Andean trees. *Journal of Biogeography*, *38*(4), 783-791.

Feeley, K., Martinez-Villa, J., Perez, T., Silva Duque, A., Triviño Gonzalez, D., & Duque, A. (2020). The thermal tolerances, distributions, and performances of tropical montane tree species. *Frontiers in Forests and Global Change*, *3*, 25

He, J., Lin, S., Kong, F., Yu, J., Zhu, H., & Jiang, H. (2020). Determinants of the beta diversity of tree species in tropical forests: Implications for biodiversity conservation. Science of the Total Environment, 704, 135301.

Legendre, P. (2019). A temporal beta-diversity index to identify sites that have changed in exceptional ways in space–time surveys. *Ecology and Evolution*, *9*(6), 3500-351

Lelli, C., Bruun, H. H., Chiarucci, A., Donati, D., Frascaroli, F., Fritz, O., ... & Heilmann-Clausen, J. (2019). Biodiversity response to forest structure and management: comparing species richness, conservation relevant species and functional diversity as metrics in forest conservation. For. Ecol. Manag. 432, 707–717.

Lindenmayer DB, Franklin JF (2002) Conserving forest biodiversity: a comprehensive multiscaled approach. Island Press, Washington

Linnakoski, R., Kasanen, R., Dounavi, A., & Forbes, K. M. (2019). Forest health under climate change: effects on tree resilience, and pest and pathogen dynamics. *Frontiers in plant science*, *10*, 1157.

Mathez-Stiefel, S. L., Peralvo, M., Báez, S., Rist, S., Buytaert, W., Cuesta, F., ... & Young, K. R. (2017). Research priorities for the conservation and sustainable governance of Andean forest landscapes. *Mountain Research and Development*, *37*(3), 323-339.

McDonald, R., Guneralp, B., Zipperer, W., & Marcotullio, P. (2014). The future of global urbanization and the environment. *Solutions*, *5*(6), 60-69.

Mori, A. S., Shiono, T., Koide, D., Kitagawa, R., Ota, A. T., & Mizumachi, E. (2013). Community assembly processes shape an altitudinal gradient of forest biodiversity. *Global Ecology and Biogeography*, *22*(7), 878-888.

Muñoz Mazón, M., Tello, J. S., Macía, M. J., Myers, J. A., Jørgensen, P. M., Cala, V., ... & Arellano, G. (2021). Mechanisms of community assembly explaining beta-diversity patterns across biogeographic regions. Journal of Vegetation Science, 32(3), e13032.

Orme, C. D. L., Davies, R. G., Burgess, M., Eigenbrod, F., Pickup, N.,Olson, V. A., Webster, A. J., Ding, T. S., Rasmussen, P. C., Ridgely, R.S., Stattersfield, A. J., Bennett, P. M., Blackburn, T. M., Gaston, K. J.,& Owens, I. P. F. (2005). Global hotspots of species richness are not congruent with endemism or threat. Nature, 436(7053), 1016–1019

Paquette, A., Sousa-Silva, R., Maure, F., Cameron, E., Belluau, M., & Messier, C. (2021). Praise for diversity: A functional approach to reduce risks in urban forests. *Urban Forestry & Urban Greening*, *62*, 127157.

Pathak, M., Slade, R., Pichs-Madruga, R., Ürge-Vorsatz, D., Shukla, R., & Skea, J. (2022). Climate Change 2022 Mitigation of Climate Change: Technical Summary.

Pecl, G. T., Araújo, M. B., Bell, J. D., Blanchard, J., Bonebrake, T. C., Chen, I. C., ... & Williams, S. E. (2017). Biodiversity redistribution under climate change: Impacts on ecosystems and human well-being. *Science*, *355*(6332), eaai9214.

Percival, G. C. (2023). Heat Tolerance of Urban Tree Species-A Review. *Urban Forestry & Urban Greening*, 128021.

Pitman, N. C., Widmer, J., Jenkins, C. N., Stocks, G., Seales, L., Paniagua, F., & Bruna, E. M. (2011). Volume and geographical distribution of ecological research in the Andes and the Amazon, 1995–2008. *Tropical Conservation Science*, *4*(1), 64-81.

Razgour, O., Forester, B., Taggart, J. B., Bekaert, M., Juste, J., Ibáñez, C., ... & Manel, S. (2019). Considering adaptive genetic variation in climate change vulnerability assessment reduces species range loss projections. *Proceedings of the National Academy of Sciences*, *116*(21), 10418-10423.

Socolar, J. B., Gilroy, J. J., Kunin, W. E., & Edwards, D. P. (2016). How should beta-diversity inform biodiversity conservation?. *Trends in ecology & evolution*, *31*(1), 67-80.

Tello, J. S., Myers, J. A., Macía, M. J., Fuentes, A. F., Cayola, L., Arellano, G., ... & Jørgensen, P. M. (2015). Elevational gradients in β-diversity reflect variation in the strength of local community assembly mechanisms across spatial scales. *PLoS One*, *10*(3), e0121458.

The World's Cities in 2018: Data Booklet (UN, 2018)

Tovar, C., Carril, A. F., Gutiérrez, A. G., Ahrends, A., Fita, L., Zaninelli, P., ... & Hollingsworth, P. M. (2022). Understanding climate change impacts on biome and plant distributions in the Andes: Challenges and opportunities. Journal of Biogeography, 49(8), 1420-1442.

Zhu, J., & Song, L. (2021). A review of ecological mechanisms for management practices of protective forests. *Journal of Forestry Research*, *32*(2), 435-448.

LIST OF ADDITIONAL PUBLICATIONS AS CO-AUTHOR DURING THE PH.D.

Ochoa-Beltrán, A., **Martínez-Villa, J. A.,** Kennedy, P. G., Salgado-Negret, B., & Duque, A. (2021). Plant Trait Assembly in Species-Rich Forests at Varying Elevations in the Northwest Andes of Colombia. *Land*, *10*(10), 1057. (co-advisor Master thesis)

Duque A, Peña MA, Cuesta F, González-Caro S, Kennedy P, Phillips OL, Calderón-Loor M, Blundo C, Carilla J, Cayola L, Farfán-Ríos W, Fuentes A, Grau R, Homeier J, Loza-Rivera MI, Malhi Y, Malizia A, Malizia L, **Martínez-Villa JA**, Myers JA, Osinaga-Acosta O, Peralvo M, Pinto E, Saatchi S, Silman M, Tello JS, Terán-Valdez A, Feeley KJ. Author Correction: Mature Andean forests as globally important carbon sinks and future carbon refuges. Nat Commun. 2021 Jun 8;12(1):3617. doi: 10.1038/s41467-021-23955-7. Erratum for: Nat Commun. 2021 Apr 9;12(1):2138. PMID: 34108485; PMCID: PMC8190032.

Feeley, K., **Martínez-Villa, J.A**, Perez, T., Silva Duque, A., Triviño Gonzalez, D., & Duque, A. (2020). The thermal tolerances, distributions, and performances of tropical montane tree species. *Frontiers in Forests and Global Change*, *3*, 25.